

# **T cell response to an MHC-II restricted epitope of rodent malaria**

**Matthias Hans Enders**

ORCID ID:

0000-0002-8296-3008

from Gera, Germany

Submitted in total fulfilment of the requirements of the joint degree of

Doctor of Philosophy (PhD)

of

The Medical Faculty

The Rheinische Friedrich-Wilhelms-Universität Bonn

and

The Department of Microbiology and Immunology,

The University of Melbourne

Melbourne/Bonn, 2022

Performed and approved by The Medical Faculty of The Rheinische Friedrich-Wilhelms-Universität Bonn and The University of Melbourne.

Supervisors:

1. Supervisor: Prof. William R. Heath, Ph.D., FAA (principal supervisor, Melbourne) The Department of Microbiology and Immunology, The University of Melbourne.
2. Supervisor: Prof. Dr. Elvira Mass, The LIMES Institute, The University of Bonn (principal supervisor, Bonn)

Date of submission: 24.11.2021

Date of oral examination: 13.01.2022

The Life & Medical Sciences Institute (LIMES) (University Bonn),

Director: Prof. Dr. Waldemar Kolanus

## **Table of Contents**

<b>Abbreviation .....</b>	<b>VI</b>
<b>List of Tables.....</b>	<b>XII</b>
<b>List of Figures .....</b>	<b>XIV</b>
<b>List of Videos .....</b>	<b>XVII</b>
<b>Abstract.....</b>	<b>XIX</b>
<b>Declaration.....</b>	<b>XXI</b>
<b>Acknowledgments .....</b>	<b>XXIII</b>
<b>List of publications.....</b>	<b>XXV</b>
<b>Chapter 1 Literature review .....</b>	<b>2</b>
1.1    Introduction .....	2
1.2 <i>Plasmodium</i> parasite life cycle .....	3
1.2.1    Pre-erythrocytic stage .....	4
1.3    Immune responses to <i>Plasmodium</i> spp. infection .....	10
1.3.1    Innate immune responses to <i>Plasmodium</i> spp. infection .....	10
1.3.2    T cell priming .....	15
1.3.3    Memory T cell development .....	22
1.4    The role of T cells in immunity against <i>Plasmodium</i> infection.....	29
1.4.1    The Role of CD8 T cells in immunity against <i>Plasmodium</i> liver-stage infection. ...	29
1.4.2    The role of CD4 T cells in immunity against <i>Plasmodium</i> liver-stage infection. ....	32
1.4.3    CD4 T cell mediated immune response to <i>Plasmodium</i> erythrocytic stage .....	35
1.5    Malaria Pathogenesis and naturally acquired immunity .....	42
1.6    Human anti-malaria vaccine approaches.....	48

1.6.1	Vaccines targeting the pre-erythrocytic stage of <i>Plasmodium</i> infection .....	48
1.6.2	Vaccines targeting the erythrocytic stage of <i>Plasmodium</i> infection .....	52
1.6.3	Vaccines targeting the transmission of <i>Plasmodium</i> parasites. ....	53
1.7	Research Aims .....	53
<b>Chapter 2 Material and Methods .....</b>		<b>58</b>
2.1	Materials .....	58
2.2	Methods .....	68
2.2.1	Mice .....	68
2.2.2	<i>Plasmodium</i> infections .....	68
2.2.3	Enrichment of CD4 or CD8 T cells .....	70
2.2.4	Dendritic cell isolation .....	71
2.2.5	<i>In vitro</i> differentiation of PbT-II and gDT-II cells .....	71
2.2.6	Adoptive cell transfer .....	72
2.2.7	Assessment of PbT-II activation and proliferation .....	72
2.2.8	Parabiotic mice .....	73
2.2.9	Intravital two-photon microscopy .....	73
2.2.10	Histology .....	74
2.2.11	Generation of <i>Plasmodium</i> -derived epitopes for LC-MS/MS analysis .....	75
2.2.12	Analysis of MHC bound epitopes by LC-MS/MS .....	75
2.2.13	$\alpha$ Clec9A vaccination .....	76
2.2.14	Cell culture .....	77
2.2.15	Preparation of mouse tissue for flow cytometric analysis .....	77
2.2.16	MHC-I and MHC-II Tetramer preparation and staining. ....	79
2.2.17	Elispot .....	80

2.2.18	Quantification of PbA liver parasite burden via real-time polymerase chain reaction (qPCR).....	81
2.1.1	RNA sequencing analyses.....	82
2.1.2	Statistical analysis.....	84
<b>Chapter 3 CD4 T cell response to a newly discovered <i>Plasmodium</i>-derived MHC-II epitope..</b>		<b>86</b>
3.1	Introduction .....	86
3.2	Results.....	88
3.2.1	CD4 T cell response to PbA infection .....	88
3.2.2	Minimal PbT-II epitope.....	95
3.2.3	PbT-II cell response to an antibody-based vaccine ( $\alpha$ -Clec9A-DIY).....	101
3.2.4	Endogenous CD4 T cell response to Hsp90 epitope.....	107
3.2.5	PbT-II cells can be differentiated into specific T helper subsets. ....	111
3.2.6	Expression of lineage-specific cytokines and surface markers after differentiation of PbT-II cells. ....	114
3.3	Discussion .....	118
<b>Chapter 4 Liver resident CD4 T cells in malaria.....</b>		<b>125</b>
4.1	Introduction .....	125
4.2	Results.....	127
4.2.1	Expression of T <sub>RM</sub> cell associated markers on PbT-II cells in the liver after RAS and $\alpha$ Clec9A-DIY vaccination.....	127
4.2.2	CD69 <sup>+</sup> memory PbT-II cells are resident in the liver after RAS vaccination .....	130
4.2.3	PbT-II T <sub>RM</sub> formation does not require cognate antigen expression in the liver. ....	134
4.2.4	CD4 T <sub>RM</sub> cells have a similar transcriptional signature to CD8 T <sub>RM</sub> cells in the liver. ....	137

4.2.5	Simultaneously priming of CD4 and CD8 T cell did not enhance liver T <sub>RM</sub> formation .....	149
4.2.6	The presence of Hsp90-restricted CD4 T cells does not enhance CD8 T <sub>RM</sub> formation after RAS vaccination.....	153
4.3	Discussion .....	158
<b>Chapter 5 The role of Hsp90-specific CD4 T cells in protection against <i>Plasmodium</i> infection</b>		<b>167</b>
5.1	Introduction .....	167
5.2	Results.....	169
5.2.1	Assessment of the protective capacity of Hsp90-specific CD4 T cells against <i>Plasmodium</i> liver-stage infection. ....	169
5.2.2	Assessment of the protective capacity of Hsp90-specific CD4 T cells against <i>Plasmodium</i> blood-stage infection.....	178
5.3	Discussion .....	189
<b>Chapter 6: General Discussion .....</b>		<b>200</b>
6.1	Context.....	200
6.2	Key findings.....	201
6.3	Are anti-malaria vaccines aiming to induce protective CD4 T cells an appropriate immunisation strategy? .....	203
6.3.1	Targeting CD4 T cells against blood-stage infection.....	203
6.3.2	Targeting CD4 T cells against <i>Plasmodium</i> liver stage infection.....	205
6.4	The importance of CD4 T <sub>RM</sub> cells in infectious diseases .....	210
6.4.1	CD4 T <sub>RM</sub> cells are involved in the defence mechanism against different pathogens .....	210
6.4.2	Can CD4 T <sub>RM</sub> cells be induced by vaccination? .....	211
6.4.3	What is the optimal vaccination protocol to induce CD4 T <sub>RM</sub> cells? .....	212
6.5	Concluding remarks .....	217

<b>References.....</b>	<b>218</b>
<b>Appendix .....</b>	<b>261</b>

**Abbreviation**

AA	amino acids
$\alpha$ GalCer	$\alpha$ -Galactosylceramide
APC	antigen-presenting cell
$\beta$ 2M	$\beta$ 2-microglobulin
B6	C57BL/6
Bcl6	B-cell Lymphoma 6
BSA	Bovine serum albumin fraction V
CAR	chimeric antigen receptor
CCR	CC-chemokine receptor
CD	cluster of differentiation
	cell traversal protein for ookinete and
CelTOS	sporozoite
ChAd	chimpanzee adenovirus
CHMI	controlled human malaria infection
CM	cerebral malaria
CpG	Cytosine-phosphate-Guanine
CSP	circumsporozoite protein
CTV	CellTrace Violet™
CXCR	C-X-C chemokine receptor
DC	dendritic cell
DEG	differential expressed gene
DEG	differently expressed gene
DMSO	Dimethyl Sulphoxide
DMXAA	5,6-dimethylxanthenone-4-acetic acid
DNA	desoxyribonucleic acid
DTR	diphtheria toxin receptor
e.g.	<i>exempli gratia</i>

## VII

ECM	experimental cerebral malaria
ELISpot	Enzyme-linked Immunospot
ESs	enrichment scores
FCS	fetal calf serum
Foxp	forkhead transcription factor
GAP	genetically attenuated parasites
GATA	GATA binding protein
GC	germinal centre
GFP	green fluorescent protein
GO	gene ontology
GSEA	geneset enrichment analysis
Gzmk	Granzyme K
HBSS	Hank's buffered salt solution
HLA	human leukocyte antigen
HPLC	high-performance liquid chromatography
HSP	heat shock protein
HSPG	heparan sulphate proteoglycans
HSV	herpes simplex virus
i.d.	intradermal
i.m.	intramuscular
i.n.	intranasal
i.v.	intravenous
ICAM	intercellular adhesion molecules
IFN	Interferon
Ifnar	interferon receptor alpha
Ig	immunoglobulin
IL	interleukin
iRBCs	infected red blood cells

## VIII

IRF3	interferon regulatory factor 3
IRF7	interferon regulatory factor 7
ISG	interferon stimulated genes
KC	Kupffer cell
KLRG1	Killer cell lectin like receptor subfamily G member
KO	knock out
LCMV	Lymphocytic choroimeningitis virus
LN	lymph node
LN	lymph node
LSEC	liver sinusoidal endothelial cells
LVS	live vaccine salmonella strain
M-CSF	macrophage colony-stimulating factor
mAb	monoclonal antibody
MACS	magnetic-activated cell sorting
MAVS	mitochondrial antiviralsignaling protein
MDA5	melanoma differntitaion-associated protein 5
ME	Multi-epitope string
MHC	major histocompatibility complex
MPECs	memory precursors effector cells
MSP	merozoite surface protein
MVA	modified vaccinia Ankara
NHP	non-human primates
NK	Natural killer
NKT	natural killer T cells
NO	nitric oxide
ODN	Oligodeoxynucleotides
OVA	Ovalbumin

P.	<i>Plasmodium</i>
PAMPS	Pathogen-associated molecular patterns
PbA	<i>Plasmodium berghei</i> ANKA
PbPL	phospholipase
Pch	<i>Plasmodium chabaudi</i>
PE	phycoerythrin
PfEMP1	<i>Plasmodium</i> erythrocytic membrane protein1
PMBC	peripheral blood mononuclear cell
Prf1	Perforin
PRR	pattern- recognition-receptor
PV	parasitophorous vacuole
qPCR	quantitative polymerase chain reaction
rAAV	recombinant adeno-associated virus
RAG	recombination-activating gene
RAS	radiation attenuated sporozoites
RBS	red blood cell
RNA	ribonucleic acid
ROR $\gamma$ T	RAR-related orphan receptor gamma
ROS	reactive oxygen species
RPL6	Ribosomal protein L6
RT	Room temperature
s.c.	subcutaneous
S1PR1	sphingosine-1-phosphate
sc	single cell
seq	sequencing
SLECS	short lived effector cells
SLO	secondary lymphoid organs

SLO	secondary lymphoid organs
SPECT2	Plasmodium perforin like protein
spz	sporozoite
STAT	signal transducer and activator of transcription
Tbet	T-box expressed in T cells
T <sub>CM</sub>	central memory T cell
TCR	T cell receptor
TDL	thoracic duct lymph
TDL	thoracic duct lymph
T <sub>EM</sub>	effector memory T cell
Tfh	T follicular helper
TGF	transforming growth factor
Th	T helper
TLR	toll-like receptor
TNF	tumour necrosis factor
T <sub>PM</sub>	peripheral memory T
Tr1	T regulatory type 1
TRAP	thrombospondin related anonymous protein
Treg	T regulatory helper cell
T <sub>RM</sub>	tissue-resident T cell
T <sub>SCM</sub>	memory T stem cells
VLA-1	very late antigen

WHO	World health organisation
WSV	whole sporozoite vaccine
WT	wild type

## List of Tables

<b>Table 2.1 List of antibodies and dyes.....</b>	<b>58</b>
<b>Table 2.2 List of antibodies for CD4 T cell enrichment .....</b>	<b>61</b>
<b>Table 2.3 List of antibodies for CD8 T cell enrichment .....</b>	<b>61</b>
<b>Table 2.4 List of mice strains used in this study.....</b>	<b>61</b>
<b>Table 2.5 List of cell lines used in this study.....</b>	<b>62</b>
<b>Table 2.6 Primers used for qPCR.....</b>	<b>63</b>
<b>Table 2.7 List of used Plasmodium species .....</b>	<b>63</b>
<b>Table 2.8 Different medias used in this study .....</b>	<b>63</b>
<b>Table 2.9 Peptides and recombinant proteins used for in vitro differentiation .....</b>	<b>64</b>
<b>Table 2.10 Antibodies used for in vitro differentiation .....</b>	<b>64</b>
<b>Table 2.11 Antibodies and detection reagents for Elispot assay .....</b>	<b>64</b>
<b>Table 2.12 List of enzymes used in this study.....</b>	<b>64</b>
<b>Table 2.13 Animal Serum .....</b>	<b>65</b>
<b>Table 2.14 Commercially available kits .....</b>	<b>65</b>
<b>Table 2.15 List of general chemicals and reagents.....</b>	<b>65</b>
<b>Table 2.16 Consumables.....</b>	<b>67</b>
<b>Table 2.17. List of R packages used in this study.....</b>	<b>83</b>
<b>Appendix Table 8.1. DEGs list of genes up or down-regulated in RAS generated liver PbT-II T<sub>RM</sub> cells versus RAS generated PbT-II T<sub>EM</sub> cells..</b>	<b>261</b>

<b>Appendix Table 8.2. DEGs list of genes up or down-regulated in <math>\alpha</math>Clec9A generated PbT-II T<sub>RM</sub> cells versus RAS generated PbT-II T<sub>RM</sub> cells from the liver. ....</b>	<b>265</b>
<b>Appendix Table 8.3. DEGs list of genes up or down-regulated in PbT-II Th1 T<sub>RM</sub> cells versus RAS generated PbT-II T<sub>RM</sub> cells from the liver.....</b>	<b>266</b>
<b>Appendix Table 8.4. DEGs list of genes up or down-regulated in PbT-II Th2 T<sub>RM</sub> cells versus RAS generated PbT-II T<sub>RM</sub> cells from the liver.....</b>	<b>267</b>
<b>Appendix Table 8.5. DEGs list of genes up or down-regulated in PbT-II Th1 T<sub>RM</sub> cells versus <math>\alpha</math>Clec9A-DIY generated PbT-II T<sub>RM</sub> cells from the liver. ....</b>	<b>269</b>
<b>Appendix Table 8.6. DEGs list of genes up or down-regulated in PbT-II Th2 T<sub>RM</sub> cells versus <math>\alpha</math>Clec9A-DIY generated PbT-II T<sub>RM</sub> cells from the liver. ....</b>	<b>271</b>
<b>Appendix Table 8.7. DEGs list of genes up or down-regulated in PbT-II Th2 T<sub>RM</sub> cells versus PbT-II Th2 T<sub>RM</sub> cells from the liver .....</b>	<b>273</b>

## List of Figures

<b>Figure 1.1 Plasmodium life cycle within the mammalian host.....</b>	<b>9</b>
<b>Figure 2.2. Differentiation and roles of CD4 T cells during Plasmodium infection.....</b>	<b>41</b>
<b>Figure 3.1. PbT-II cells form memory after PbA blood-stage infection. ....</b>	<b>89</b>
<b>Figure 3.2 PbT-II cells form memory after PbA radiation-attenuated sporozoite vaccination.....</b>	<b>92</b>
<b>Figure 3.3. Antigen is only available for about 7 days after administration of radiation-attenuated sporozoite (RAS).....</b>	<b>95</b>
<b>Figure 3.4. Discovery of the cognate peptide of PbT-II cells.....</b>	<b>97</b>
<b>Figure 3.5. Identification of the minimal epitope recognised by PbT-II cells. ....</b>	<b>101</b>
<b>Figure 3.6. Immunisation with an <math>\alpha</math>Clec9A construct targeting the DIY epitope induces expansion of PbT-II cells. ....</b>	<b>103</b>
<b>Figure 3.7. PbT-II cell response to <math>\alpha</math>Clec9A-DIY construct. ....</b>	<b>104</b>
<b>Figure 3.8. Visualisation of PbT-II cells in the liver after <math>\alpha</math>-Clec9A-DIY priming. ....</b>	<b>106</b>
<b>Figure 3.9. Detection of an endogenous CD4 T cell population reactive to the DIY epitope. ....</b>	<b>110</b>
<b>Figure 3.10. Induction of a specific endogenous CD4 T cell memory response to the DIY epitope.....</b>	<b>111</b>
<b>Figure 3.11. Th1 and Th2 in vitro differentiation of PbT-II cells. ....</b>	<b>113</b>
<b>Figure 3.12. Phenotypes of PbT-II cells generated after PbA iRBC infection, <math>\alpha</math>Clec9A-DIYpriming or in vitro differentiation. ....</b>	<b>117</b>

<b>Figure 4.1. Comparison of memory PbT-II cells population after <math>\alpha</math>Clec9A-DIY or RAS vaccination.</b>	129
<b>Figure 4.2. Homing and circulating pattern of Plasmodium-specific T cells after RAS vaccination.</b>	133
<b>Figure 4.3. In vitro polarized PbT-II Th1 and Th2 cells form T<sub>RM</sub> cells in the liver.</b>	136
<b>Figure 4.4. Differential gene expression by liver PbT-II T<sub>RM</sub> and T<sub>EM</sub> cells.</b>	139
<b>Figure 4.5. Shared liver resident core signature of CD4 and CD8 T<sub>RM</sub> cells.</b>	141
<b>Figure 4.6. Differential Gene Expression by liver PbT-II and PbT-I T<sub>RM</sub> cells.</b>	143
<b>Figure 4.7. Differential gene expression by lineage specific liver PbT-II T<sub>RM</sub> cells.</b>	146
<b>Figure 4.8. Differential Gene Expression by lineage specific liver PbT-II T<sub>RM</sub> cells.</b>	149
<b>Figure 4.9. Simultaneous priming of Plasmodium specific CD4 and CD8 T cells.</b>	152
<b>Figure 4.10. Single transcript expression in CD4 and CD8 liver T<sub>RM</sub> cells.</b>	156
<b>Figure 4.11. Sequential priming of Plasmodium specific CD4 and CD8 T cells.</b>	157
<b>Figure 5.1. Hsp90-specific CD4 T response to sporozoite infection as determined by liver-parasite burden.</b>	170
<b>Figure 5.2 PbT-II cells form cluster 24 h post sporozoite challenge.</b>	172

<b>Figure 5.3. Clustering can occur non-specifically and can involve macrophages.</b> .....	175
<b>Figure 5.4. OVA-specific CD4 T response to sporozoite infection determined by liver-parasite burden.</b> .....	177
<b>Figure 5.5. Hsp90-specific CD4 T cells induce partial immunity to blood-stage PbA infection, and ECM protection at an effector stage.</b> .....	180
<b>Figure 5.6 Hsp90-specific PbT-II CD4 T cells induce partial immunity to blood stage PbA infection, and ECM protection at a memory stage.</b> .....	183
<b>Figure 5.7 Protective capacity of PbT-II cells on blood stage Pch infection.</b> .....	187

## List of Videos

**2-photon intravital imaging Dataset (Video 8.1 to 8.7)** is accessible via <https://doi.org/10.22000/471> (The University of Bonn) or <https://cloudstor.aarnet.edu.au/plus/s/jf7sdvY4nYxpTvn> (The University of Melbourne).

**Appendix Video 8.1 Visualisation of PbT-II cells in the liver after  $\alpha$ -Clec9A-DIY priming. ....275**

**Appendix Video 8.2 Visualisation of PbT-II cells in the liver after  $\alpha$ -Clec9A-DIY priming and 24 h post sporozoite infection. ....275**

. (<https://cloudstor.aarnet.edu.au/plus/s/uXVIIIG1geKI7ory>)

**Appendix Video 8.3 Visualisation of PbT-II cells in the liver after  $\alpha$ -Clec9A-DIY priming and 48 h post sporozoite infection. ....276**

. (<https://cloudstor.aarnet.edu.au/plus/s/XZhmaK8rG1SoMsm>)

**Appendix Video 8.4, Visualisation of gDT-II cells in the liver after  $\alpha$ -Clec9A-DIY priming. ....276**

**Appendix Video 8.5 Visualisation of gDT-II cells in the liver after  $\alpha$ -Clec9A-DIY priming and 24 h post sporozoite infection. ....276**

**Appendix Video 8.6 Visualisation of Lysm.GFP cells in the liver. ....276**

(<https://cloudstor.aarnet.edu.au/plus/s/JQwsYZhBBDJiRGc>)

**Appendix Video 8.7 Visualisation of Lysm.GFP cells in the liver 24 h post spz challenge. ....276**

## Abstract

Malaria is caused by different *Plasmodium* species that can infect a variety of animals including humans and rodents. The life cycle of these parasites is complex and includes a liver stage followed by a blood-stage in their vertebrate hosts. While the host's immune response against each of these stages is incompletely understood, CD4 T cells are known to play an important role in immunity to *Plasmodium* infection during both stages. This project aims to examine the specific CD4 T cell response to a novel MHC II-restricted epitope in *Plasmodium* infection in C57BL/6 mice, and to characterise the protective capacity of these T cells. To this end, we made use of a recently generated TCR transgenic mouse line, termed PbT-II, which responds to a so far unknown *Plasmodium* derived epitope. In this project, the PbT-II epitope was identified as derived from heat shock protein 90, residues 484 to 496 (Hsp90<sub>484-496</sub> or abbreviated DIY). Different priming methods, such as injection of an anti-Clec9A antibody attached to the Hsp90 epitope ( $\alpha$ Clec9A-DIY), infection with *P. berghei* ANKA (PbA) infected red blood cells (iRBCs) or immunisation with radiation attenuated PbA sporozoites (RAS), were used to characterise PbT-II memory cell formation. Results revealed the formation of memory PbT-II cells expressing surface markers associated with central memory T cells (T<sub>CM</sub>), effector memory T cells (T<sub>EM</sub>) and tissue resident memory T cells (T<sub>RM</sub>). Given the importance of tissue-resident memory T cells in peripheral immunity, mainly studied in CD8 T cells, we focused our study on the formation and function of CD4 T<sub>RM</sub> cells in the liver. Parabiosis studies using RAS vaccinated mice confirmed the liver residency of a CD69<sup>+</sup> PbT-II cell population. Gene expression profile analysis revealed that these CD4 T cells expressed a core gene signature similar to that of CD8 resident memory T cells. Furthermore, differences in the gene expression profile of PbT-II T<sub>RM</sub> cells generated via different protocols, suggested lineage specific effector mechanisms, such as IL-4 production or perforin expression, for subsets of CD4 T<sub>RM</sub> cells in the liver.

As CD4 T cells can potentially act against both the liver and blood-stage of *Plasmodium* infection, we sought to investigate the protective potential of PbT-II effector and memory cells for both of these stages. While none of the PbT-II priming methods resulted in a reduction of liver parasite burden upon sporozoite infection, mice injected with large numbers of *in vitro* polarized PbT-II Th1 or Th2 cells showed reduced parasitemia after PbA blood-stage infection. Surprisingly, most of these mice were protected from experimental cerebral malaria (ECM), although they were not able to clear PbA blood-stage infection.

Altogether, these findings provide novel insight into the formation of *Plasmodium* specific CD4 memory T cells and their protective role in *Plasmodium* infection. PbT-II cells and their cognate antigen Hsp90 represent convenient tools to study antigen specific CD4 T cell responses against the liver and blood stages of *Plasmodium* infection.

## Declaration

The work that is presented in this thesis was conducted at the University of Melbourne in the laboratory Prof. William R. Heath PhD and at the University of Bonn in the laboratory of Prof. Dr. Elvira Mass. This project was funded by the National Health and Medical Research Council. Matthias Hans Enders was also supported by an Australian Government Research Training Program Scholarship from the University of Melbourne.

This is to certify that,

- (i) the thesis only comprises my original work towards the PhD except where indicated
- (ii) due acknowledgement has been made in the text to all other material used
- (iii) the thesis is less than 100,000 words in length, exclusive of tables, maps, bibliographies, and appendices.

Melbourne, 20. 07. 2021

Matthias Hans Enders

PREFACE

My contribution to the experiments within each chapter was as follows:

**Chapter 3:** 80 %

**Chapter 4:** 100 %

**Chapter 5:** 100 %

I acknowledge the important contribution of these people:

**Chapter3:**

Results Figure 3.4 and 3.5 Dr. Daniel Fernandez-Ruiz.

## **Acknowledgments**

The long journey leading to the work presented in this thesis was influenced by many people whom I would like to thank now.

To begin with, I would like to express my immense gratitude to my primary supervisor Bill Heath. Thank you for giving me a chance to join your group and leading my scientific development in the right direction. Thank you for leading my development to become a clearer communicator and especially delivering clearer writing.

Next I want to thank my co-supervisors at the University of Melbourne, Daniel Fernandez-Ruiz and Lynette Beattie. Both of you were so important for my development as an immunologist. I am very grateful to have learnt such a broad spectrum of new techniques from both of you. Equally important, I am grateful of all the emotional support and the encouragement I received from both of you over the past years, which have made my PhD enjoyable and enabled me to finish this thesis. Thank you.

Finally, I would like to express my gratitude to Elvira Mass, who spontaneously and unreluctantly took over my supervision in Bonn. Thank you for supporting me and my research throughout this period and for facilitating such incredible fast sample processing.

Furthermore, I want to thank all the members of the Heath laboratory for their help and support throughout the past years. All of you have made my PhD a great experience. Thank you, Lauren, for taking care of me in the first few weeks of my PhD and for showing me how to properly harvest organs without making a mess. Special thanks go to Sonia, who supported and sang with me throughout long experimental days and nights.

In addition, I want to thank the Mc Fadden laboratory and especially Anton for supplying the sporozoites, which were crucial for this study. Furthermore, a big thank you to Irene Caminschi and Mireille Lahoud for providing the novel vaccine reagents.

Special thanks go to my friends here in Melbourne, who have become so important to me over the past 4 years. I will miss the long evenings in the pub with beers, chips, a lot of fun and sometimes complaining about our work.

Lastly, I want to thank my family: Thank you, Katharina, for being such a good partner. I cannot describe how thankful I am for the past years. Without your emotional support and your help to free up writing time while you were taking care of Jonas, this thesis would probably never have been submitted.

Finally, a big thank you to my Mum Kerstin, my sister Katharina and my grandma Renate. I am really happy and thankful that we were able to hold such close contact despite the long distance and time difference. I am looking forward to seeing you soon.

## List of publications

Parts of the thesis are published in:

**ENDERS, M. H.**, BAYARSAIKHAN, G., GHILAS, S., CHUA, Y. C., MAY, R., DE MENEZES, M. N., GE, Z., TAN, P. S., COZIJNSEN, A., MOLLARD, V., YUI, K., MCFADDEN, G. I., LAHOUD, M. H., CAMINSCHI, I., PURCELL, A. W., SCHITTENHELM, R. B., BEATTIE, L., HEATH, W. R. & FERNANDEZ-RUIZ, D. 2021. *Plasmodium berghei* Hsp90 contains a natural immunogenic I-Ab-restricted antigen common to rodent and human Plasmodium species. *Current Research in Immunology*, 2, 79-92. ([10.1016/j.crimmu.2021.06.002](https://doi.org/10.1016/j.crimmu.2021.06.002))

HOCHHEISER, K., WIEDE, F., WAGNER, T., FREESTONE, D., **ENDERS, M. H.**, OLSHANSKY, M., RUSS, B., NUSSING, S., BAWDEN, E., BRAUN, A., BACHEM, A., GRESSIER, E., MCCONVILLE, R., PARK, S. L., JONES, C. M., DAVEY, G. M., GYORKI, D. E., TSCHARKE, D., PARISH, I. A., TURNER, S., HEROLD, M. J., TIGANIS, T., BEDOUI, S. & GEBHARDT, T. 2021. Ptpn2 and KLRG1 regulate the generation and function of tissue-resident memory CD8<sup>+</sup> T cells in skin. *J Exp Med*, 218. (<https://doi.org/10.1084/jem.20200940>)

GHILAS, S., **ENDERS, M. H.**, MAY, R., HOLZ, L. E., FERNANDEZ-RUIZ, D., COZIJNSEN, A., MOLLARD, V., COCKBURN, I. A., MCFADDEN, G. I., HEATH, W. R. & BEATTIE, L. 2021. Development of *Plasmodium*-specific liver-resident memory CD8(+) T cells after heat-killed sporozoite immunization in mice. *Eur J Immunol*, 51, 1153-1165. (<https://doi.org/10.1002/eji.202048757>)

GHILAS, S., VALENCIA-HERNANDEZ, A. M., **ENDERS, M. H.**, HEATH, W. R. & FERNANDEZ-RUIZ, D. 2020. Resident Memory T Cells and Their Role within the Liver. *Int J Mol Sci*, 21. (<https://doi.org/10.3390/ijms21228565>)

VALENCIA-HERNANDEZ, A. M., NG, W. Y., GHAZANFARI, N., GHILAS, S., DE MENEZES, M. N., HOLZ, L. E., HUANG, C., ENGLISH, K., NAUNG, M., TAN, P. S., TULLETT, K. M., STEINER, T. M., **ENDERS, M. H.**, BEATTIE, L., CHUA, Y. C., JONES, C. M., COZIJNSEN, A., MOLLARD, V., CAI, Y., BOWEN, D. G., PURCELL, A. W., LA GRUTA, N. L., VILLADANGOS, J. A., DE KONINGWARD, T., BARRY, A. E., BARCHET, W., COCKBURN, I. A., MCFADDEN, G. I., GRAS, S., LAHOUD, M. H., BERTOLINO, P., SCHITTENHELM, R. B., CAMINSCHI, I., HEATH, W. R. & FERNANDEZ-RUIZ, D. 2020. A Natural Peptide Antigen within the *Plasmodium* Ribosomal Protein RPL6 Confers Liver TRM Cell-Mediated Immunity against Malaria in Mice. *Cell Host Microbe*, 27, 950-962 e7. (<https://doi.org/10.1016/j.chom.2020.04.010>)

HOLZ, L. E., CHUA, Y. C., DE MENEZES, M. N., ANDERSON, R. J., DRAPER, S. L., COMPTON, B. J., CHAN, S. T. S., MATHEW, J., LI, J., KEDZIERSKI, L., WANG, Z., BEATTIE, L., **ENDERS, M. H.**, GHILAS, S., MAY, R., STEINER, T. M., LANGE, J., FERNANDEZ-RUIZ, D., VALENCIA-HERNANDEZ, A. M., OSMOND, T. L., FARRAND, K. J., SENEVIRATNA, R., ALMEIDA, C. F., TULLETT, K. M., BERTOLINO, P., BOWEN, D. G., COZIJNSEN, A., MOLLARD, V., MCFADDEN, G. I., CAMINSCHI, I., LAHOUD, M. H., KEDZIERSKA, K., TURNER, S. J., GODFREY, D. I., HERMANS, I. F., PAINTER, G. F. & HEATH, W. R. 2020. Glycolipid-peptide vaccination induces liver-resident memory CD8(+) T cells that protect against rodent malaria. *Sci Immunol*, 5. (<https://doi.org/10.1126/sciimmunol.aaz8035>)

FERNANDEZ-RUIZ, D., LAU, L. S., GHAZANFARI, N., JONES, C. M., NG, W. Y., DAVEY, G. M., BERTHOLD, D., HOLZ, L., KATO, Y., **ENDERS, M. H.**, BAYARSAIKHAN, G., HENDRIKS, S. H., LANSINK, L. I. M., ENGEL, J. A., SOON, M. S. F., JAMES, K. R., COZIJNSEN, A., MOLLARD, V., UBOLDI, A. D., TONKIN, C. J., DE KONING-WARD, T. F., GILSON, P. R., KAISHO, T., HAQUE, A., CRABB, B. S., CARBONE, F. R., MCFADDEN, G. I. & HEATH, W. R. 2017. Development of a Novel CD4+ TCR Transgenic Line That Reveals a Dominant Role for CD8+ Dendritic Cells and CD40 Signaling in the Generation of Helper and CTL Responses to Blood-Stage Malaria. *Journal of immunology (Baltimore, Md. : 1950)*, 199, 4165-4179. (<https://doi.org/10.4049/jimmunol.1700186>)

# **Chapter 1**

## **Literature review**

## Chapter 1 Literature review

### 1.1 Introduction

Malaria is a mosquito-borne disease caused by *Plasmodium* species, which are a protozoan parasite that can infect a variety of animals including humans and rodents (Cowman et al., 2016, Phillips et al., 2017, White et al., 2014). Six different *Plasmodium* species are described to cause malaria in humans. *Plasmodium falciparum* is considered the most prevalent species in the African and Eastern Mediterranean Regions, while *Plasmodium vivax* predominates in South-east Asia and South America. Other species, such as *P. ovale curtisi*, *P. ovale wallikeri*, and *P. malariae*, are much less common globally. However, in recent years *P. knowlesi*, a zoonosis from primates, has emerged as a local disease burden leading to severe infections in southeast Asia (Ahmed and Cox-Singh, 2015).

Globally, an estimated 229 million cases and around 409,000 deaths (2019) are caused by malaria annually (WHO, 2019). Most of these cases are reported in developing areas such as the African region (93 %) and South-East Asia (3.4 %). An estimated US\$ 2.7 billion were invested in efforts to control and eliminate malaria in 2018. Similarly, large investments in previous years led to an initial decrease in incidence from 71 to 57 cases per 1000 in at-risk populations between 2010 and 2014. Furthermore, the number of countries with less than 100 cases increased from 17 (2010) to 27 (2018). However, malaria disease's overall burden did not decrease significantly between 2014 and 2018, reflecting an emergence of drug-resistance in parasites and insecticide-resistance in mosquitoes. Recent modelling approaches also suggest that COVID-19 related disruption to malaria prevention activities, such as insecticide-treated nets and anti-malarial drug distribution, could double the number of malaria cases in 2020 in sub-Saharan Africa (Sherrard-Smith et al. 2020), further interfering with the

World Health Organisation's (WHO) goal of reducing malaria incidence by 90 % by the year 2030 (WHO, 2015).

A promising alternative to insecticides for targeting the mosquito vector or drugs for targeting the parasites is development of an effective vaccine. Vaccination aims to induce a long-lasting immune response preventing an individual from becoming infected by a specific pathogen. However, while some vaccination approaches against *Plasmodium* parasites, such as RTS,S, ChAd63-MVA and PfSPZ vaccine seemed promising at first, efficacy in field trials has been disappointing (RTS, 2015, Ewer et al., 2013, Seder et al., 2013, Partnership, 2015). This suggests that efficient vaccine development requires a better understanding of the host's immune response to *Plasmodium* infection.

## **1.2 *Plasmodium* parasite life cycle**

The *Plasmodium* parasite's complex lifecycle takes place in two different hosts, a female Anopheles mosquito and a vertebrate host. In both hosts, the parasite transits through individual cellular stages that allow the *Plasmodium* parasite to adapt to different organs and temperatures inside the hosts. There are two main phases inside a mammalian host, the pre-erythrocytic stage, and the disease-causing erythrocytic or blood stage.

## **1.2.1 Pre-erythrocytic stage**

### **1.2.1.1 Initial sporozoite inoculation**

During the blood meal of an infected female *Anopheles* mosquito, up to 1,300 *Plasmodium* parasites are released into the dermis of the host skin along with the mosquito's saliva (Medica and Sinnis, 2005). These parasites, termed 'sporozoites' actively move through the dermis until they reach a blood vessel, where they enter the circulation. Experimental mouse infection models with *P. berghei* ANKA (PbA) revealed that sporozoites require gliding motility for up to 30 minutes to enter the circulation if injected into the avascular dermal tissue (Vanderberg and Frevert, 2004). This active gliding depends on surface phospholipases, which breach host cell membranes during the migration stage (Bhanot et al., 2005).

Roughly 70 % of sporozoites that leave the bite area enter the host blood vessels, while the remaining 30 % invade the lymphatics, potentially becoming trapped in the draining lymph nodes (LN). In the LN, sporozoites may be phagocytosed by dendritic cells (DCs). PbA infection models have also shown that a small proportion of the parasites that migrate to lymphoid tissues develop into small exoerythrocytic forms, similar to the parasite inside a hepatocyte, and then eventually become degraded (Amino et al., 2006).

### **1.2.1.2 Liver structure**

The majority of sporozoites that enter the bloodstream reach the liver within minutes. The complex liver structure allows large volumes of blood to traverse through this organ. Inside the liver, nutrient-rich blood from the portal vein and oxygen-rich blood from the hepatic arteriole flow through small and highly branched capillaries, termed sinusoids, heading to the central vein,

eventually leading back to the heart (Wick et al., 2002). Sinusoids are unlike any other capillaries in solid organs, as the endothelial lining of the sinusoids is constituted by liver sinusoidal endothelial cells (LSECs). LSECs contain clustered fenestrations, known as sieve plates, that allow the exchange of small particles between the sinusoidal lumen and the space of Disse, a gap between LSECs and hepatocytes, which is formed by the lack of a basement membrane (Wisse et al., 1985, Warren et al., 2006). Inside this gap reside stellate cells, responsible for vitamin A storage and collagen secretion in the case of liver injury (Wake, 1971, de Leeuw et al., 1984). The outer layer of the sinusoids is formed by hepatocytes, the liver's main parenchymal tissue cell-type, and final targets of liver-stage *Plasmodium* parasites. The high vascularity of the liver and large surface area of sinusoids reduces the blood flow velocity inside the capillaries compared to other solid organs (McCuskey and Reilly, 1993). Additionally, liver resident macrophages, called Kupffer cells (KCs), can block sinusoids while patrolling, thereby further reducing the blood flow inside the liver (MacPhee et al., 1995).

### **1.2.1.3 Liver invasion**

The reduced blood flow in the liver facilitates interactions of sporozoites with the sinusoidal structures. These interactions depend on surface molecules derived from both host cells and sporozoites. One of the potentially best-studied surface molecules known to facilitate sporozoite arrest in the liver is the circumsporozoite protein (CSP). CSP, which densely coats the sporozoite surface, interacts with heparan sulphate proteoglycans (HSPGs) on liver cells and is considered the central receptors for attachment of *Plasmodium* parasites (Pinzon-Ortiz et al., 2001). Studies have shown that recombinant CSP binds to hepatocyte microvilli coated with HSPGs, within the space of Disse. However, HSPGs can also reach through endothelial fenestrations into the sinusoidal lumen leading to interaction with CSP and sporozoite arrest. (Wisse et al., 1985, Frevert et al., 1993, Cerami et al., 1992)

Upon sequestration in the liver sinusoids, sporozoites encounter two main cell types: KCs and endothelial cells. Studies using *in vitro* cultures of KCs and LSECs as well as *in vivo* 2-photon imaging showed that sporozoites mostly traverse through KCs to the space of Disse (Frevert et al., 2006). Interestingly, this invasion occurs independent of phagocytosis, but under the formation of a parasitophorous vacuole (PV) (Meis et al., 1983, Pradel and Frevert, 2001). Moreover, no colocalization with lysosome markers could be observed, so it is unlikely that the parasites are degraded inside the KCs. However, KC depletion studies, through clodronate liposomes, showed greater sporozoites infection levels in the absence of KCs, which indicated that traversing through KCs is not required for hepatocytes infection by sporozoites (Baer et al., 2007).

Once in the space of Disse, sporozoites infiltrate hepatocytes. To this end, the parasites breach the hepatocyte cell membrane, a process that induces micro lesions/injuries, which are rapidly repaired (Mota et al., 2001). Experimental mouse models using PbA sporozoite infections identified specific proteins involved in invading hepatocytes: SPECT2 (also known as *Plasmodium* perforin-like protein 1, PPLP1) and phospholipase (PbPL) are engaged in initial pore formation in the hepatocyte membrane (Vaughan et al., 1999, Ishino et al., 2005). Other proteins, such as cell traversal protein for ookinete and sporozoite (CelTOS), are essential for the movement through the hepatocyte cytosol (Kariu et al., 2006). Sporozoites migrate through several hepatocytes before invading the final hepatocytes in which a PV is formed and further differentiation begins (Mota et al., 2001, Silvie et al., 2003). So far, it is not fully understood why *Plasmodium* parasites migrate through different hepatocytes before starting further differentiation. Some studies suggest that migration activates exocytosis by sporozoites, resulting in membrane protein exposure on the sporozoites cell-surface and enhancing infection efficiency (Mota et al., 2002). Nevertheless, studies using sporozoites with a disrupted *spect* gene, which impairs the ability to migrate through hepatocytes, were still able to infect hepatocytes *in vitro*, indicating that migration might not be required to establish an infection (Mota et al., 2002, Ishino et al., 2004). One molecule important for hepatocyte invasion is thrombospondin-related anonymous protein (TRAP), which accumulates at the

parasite's apical end, contributing to tight interactions between the hepatocyte cell membrane and the sporozoite (Mota et al., 2002, Matuschewski et al., 2002).

Inside the final hepatocyte, *Plasmodium* parasites undergo several rounds of asexual proliferation for approximately 2 days in mice and up to 10 days in humans, resulting in a merozoite-filled vacuole called a schizont. Each schizont releases up to 40,000 merozoites into the blood circulation (Sturm, 2006). Reaching the blood, merozoites will invade erythrocytes within minutes.

Interestingly, *P. vivax* and *P. ovale* parasites have the potential to remain in the liver tissue in a dormant state termed hypnozoites, potentially leading to relapses months or years post the initial infection.

#### **1.2.1.4 Erythrocytic stage**

Once released into the blood, merozoites rapidly invade erythrocytes in a multi-step process, including pre-invasion, active invasion, and echinocytosis (Weiss et al., 2015). The initial step of invasion is mediated by the merozoite's low-affinity attachment to the erythrocytes, mediated by merozoite surface proteins (MSPs) (Holder and Blackman, 1994). The resulting interaction between surface molecules of both cells leads to the deformation of the erythrocyte cell membrane mediated by a parasite actomyosin motor (Weiss et al., 2015). After parasite attachment, the merozoite re-orientates so that the apical end faces the host membrane (Tham et al., 2012). An irreversible attachment of the merozoite to the erythrocyte is established through the formation of tight junctions. As a final step of invasion, the parasite is driven inside the host cell by actomyosin motor activity (Riglar et al., 2011). While entering the erythrocyte, lipid-rich content from the rhoptry, a secretory organelle of *Plasmodium* parasites, is secreted. Those lipids are involved in establishing a PV membrane, which surrounds and protects the blood-stage parasite (Riglar et al., 2011).

From within this vacuole, the parasite starts to export hundreds of proteins into the infected erythrocyte (Charpian and Przyborski, 2008, Maier et al., 2009).

To this end, a trafficking network is established inside the host-cell. One critical feature of this transport system are Maurer's clefts, membrane structures that bud from the parasitophorous membrane, facilitating protein transport throughout the host cell (Gruring et al., 2012). *P. falciparum* erythrocyte membrane protein 1 (PfEMP1) family members are the most extensively studied proteins exported to the *P. falciparum* infected host cell membrane. These proteins contain several adhesive domains, which allows the parasites to sequester in vasculature of several organs, thereby escaping splenic clearance (Nunes-Silva et al., 2015). Eventually, infected erythrocytes can block the vasculature in different organs, such as the brain and placenta, leading to the development of severe malaria-associated symptoms and fatal outcomes.

Simultaneously, merozoites mature through several differentiation stages. First, merozoites form a ring and start to enlarge their food vacuole, creating a trophozoite (Boddey and Cowman, 2013). At this stage, the parasite consumes a large amount of haemoglobin from the infected erythrocyte, resulting in the accumulation of hemozoin within the PV. Subsequently, a schizont is formed by nuclear divisions of the trophozoite. Finally, about 48 hours after infection of the initial erythrocyte, 16 -32 new *P. falciparum* merozoites are released into the bloodstream, rapidly infecting new erythrocytes.

Besides this asexual replication, a small proportion of merozoites differentiate into a long-lived, sexual form, termed gametocytes. If ingested by a mosquito, haploid male and female gametes fuse, generating zygotes inside the mosquito gut (Sinden, 1983). After further differentiation into oocysts, fresh sporozoites are formed. Finally, sporozoites migrate towards the salivary glands, resulting in a new transmission cycle if injected into the appropriate host (Vlachou et al., 2006, Josling and Llinas, 2015).

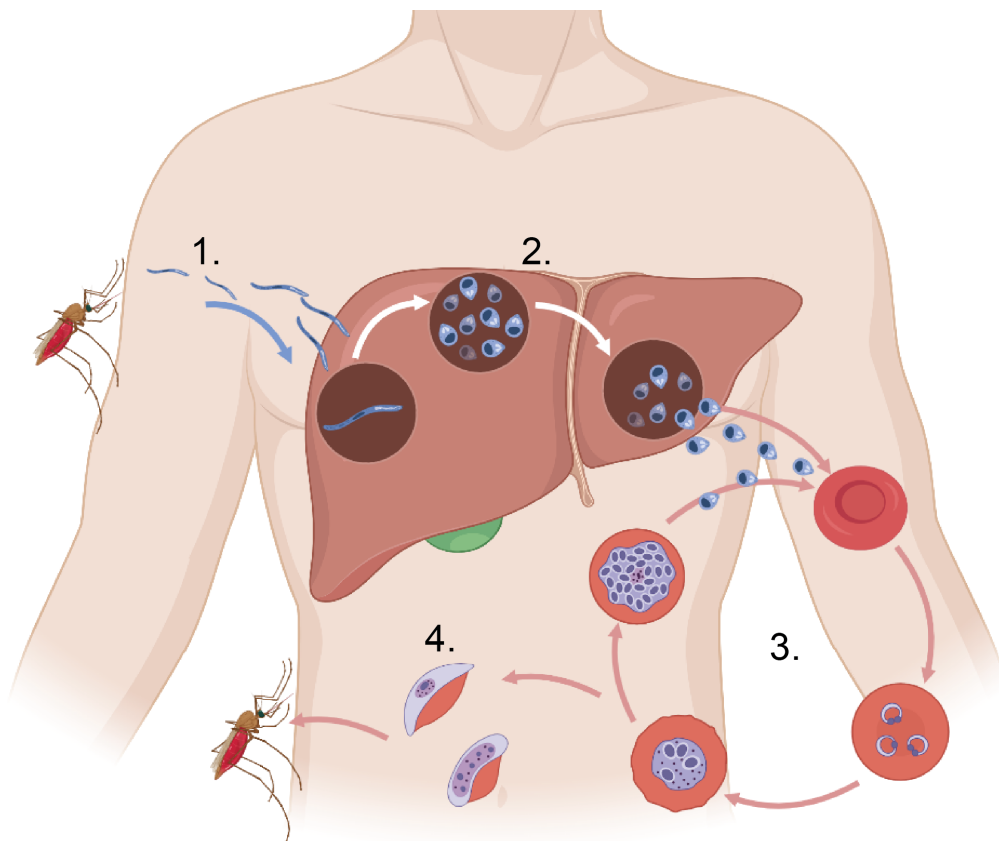


**Figure 1.1 *Plasmodium* life cycle within the mammalian host.**

(1) During the blood meal of a female infected *Anopheles* mosquito, sporozoites are released into the skin of the mammalian host. Within a few hours sporozoites migrate with the bloodstream towards the liver. (2) In the liver, sporozoites infiltrate the tissue by crossing the sinusoidal barrier towards the space of disse, most likely through KCs. Once they reach the space of disse, some sporozoites infiltrate hepatocytes. Within around 10 days, depending in the *Plasmodium* species, sporozoites differentiate into schizonts and begin to generate merozoites. Thereafter, thousands of merozoites are released into the blood stream, where they rapidly infect erythrocytes. (3) Inside red blood cells, merozoites undergo a series of asexual replication steps and duplicate once every 48 hours. The newly generated merozoites are then released into the blood stream, infecting new RBCs. This leads to a cyclic increase of parasitaemia inside the host. (4) Some merozoites differentiate into gametocytes, the sexual parasite stage. If taken up by a mosquito blood-meal, gametocytes develop into sporozoites inside the mosquito's gut, before they migrate to the salivary glands. With the next blood meal an infected mosquito can start a new cycle. Created with Biorender.com.

### **1.3 Immune responses to *Plasmodium* spp. infection**

The immune response to *Plasmodium* infection is multifaceted, with cells of the innate and adaptive immune systems working together to induce protection. Innate immunity responds rapidly, and in an antigen-independent manner, providing some level of initial parasite control and enabling the activation of adaptive immune cells. These latter cells, which include T and B cells, are highly specific and contribute to fighting established infections, as well as in generating immunological memory, ie. in mediating protracted protection against *Plasmodium* re-infection.

#### **1.3.1 Innate immune responses to *Plasmodium* spp. infection**

The pre-erythrocytic stage of *Plasmodium* spp. is clinically silent, but not immunologically inert. Upon natural, mosquito-transmitted infection, up to 1,300 sporozoites are inoculated into the dermis of the skin (Medica and Sinnis, 2005, Kebaier et al., 2009). Upon first exposure to these parasites, innate immune cells recognize invading sporozoites, potentially triggering an immune response (Roland et al., 2006, Stevenson and Riley, 2004). The fact that sporozoites have a short dwell time in the skin, blood, and the liver makes an adaptive immune response, which takes days to weeks to develop, unlikely to be effective during the primary infection (Ademokun and Dunn-Walters, 2010).

### 1.3.1.1 Innate immune response pre-erythrocytic *Plasmodium* parasite infection

The innate immune system evolved to recognize specific components derived from pathogens that distinguish them from host cells. This is achieved through pattern-recognition-receptors (PRRs) that sense various pathogen-derived molecules, including DNA, double or single-stranded RNA, peptidoglycans, and carbohydrates (Medzhitov and Janeway, 1997). PRRs are strategically expressed on the plasma membrane or in the cytoplasm of cells that are likely to be the first to encounter pathogens upon infections. The activation of PRR results in downstream signaling, often inducing direct effector functions.

Sporozoites that migrate into lymphoid organs, such as the skin draining LN, have been shown to be taken up by DCs, which can contribute to the activation of both innate and adaptive immune cells (Chakravarty et al., 2007). Once in the liver, hepatocytes can sense sporozoite infection through recognition of *Plasmodium* RNA using melanoma differentiation-associated protein 5 (MDA5). MDA5 binding to parasite-derived cytosolic RNA results in the activation of mitochondrial antiviral signalling protein (MAVS) (Liehl et al., 2014). MAVS activation leads to the induction of transcription factors Irf3/Irf7, which prompts a type I interferon (IFN) response in hepatocytes. This type I IFN response results in the induction of IFN-stimulated genes (ISGs) in an autocrine and paracrine fashion, thus also activating neighboring hepatocytes. Sporozoite infection of interferon receptor *alpha* I (*Ifnar1*) deficient mice resulted in elevated parasite loads in the liver compared to wild-type mice. Furthermore, wild-type mice treated with 5,6-dimethylxanthenone-4-acetic acid (DMXAA), 3h before infection, restricted parasite replication in the liver, compared to non-treated mice. DMXAA treatment induces the transcription factor Irf3, in a similar manner to that seen for MAVS activation, and results in the induction of a type I interferon response. DMXAA treatment of *IFNARI*<sup>-/-</sup> mice did not affect the liver-parasite burden (Liehl et al. 2014). These results indicate that a type-I interferon response, initiated by sporozoite infected hepatocytes, is one of the first defense mechanisms against

*Plasmodium* parasite liver infection. The same authors could show mice that received two consecutive sporozoite infections (day 0 and 2) had reduced liver parasite load, blood parasitemia, and improved survival compared to single infected mice (Liehl et al., 2015). This indicated that a pre-activated innate immune system enhanced immune responses against an immediate second *Plasmodium* infection. The same treatment of either IFNAR1<sup>-/-</sup> or IFN $\gamma$ <sup>-/-</sup> mice resulted in diminished protection, emphasizing a type I interferon and IFN- $\gamma$  mediated defense mechanism in response to liver-stage *Plasmodium* parasites, initiated by hepatocytes (Liehl et al. 2015).

Under steady-state conditions, 20-30 % of murine liver lymphocytes are natural killer T (NKT) cells (Bendelac et al., 1997). NKT cells express a semi-invariant T cell receptor (TCR) that comprises an invariant  $\alpha$  and a restricted  $\beta$  chain. With this TCR, NKT cells recognize glycolipids presented via a particular type of major histocompatibility (MHC) I like molecule termed CD1d (Godfrey and Kronenberg, 2004). One compound shown to induce strong NKT cell activation is a synthetic glycolipid, termed  $\alpha$ -galactosylceramide ( $\alpha$ -GalCer) (Hayakawa et al., 2004).  $\alpha$ GalCer was proven to form a complex with CD1d, which then binds to NKT cell TCR, inducing the activation of mouse and human NKT cells (Sidobre et al., 2002). Several immunological functions are attributed to NKT cells, such as specific antitumor responses and regulating the development of cellular immune response against *Toxoplasma gondii* infection (Nakagawa et al., 1998, Ronet et al., 2005). NKT cells can also play a role in immunity against *Plasmodium* liver-stage infection (Miller et al., 2014). After inoculation with *P.yoelli* sporozoites, NKT cells were recruited to the liver and were able to reduce the liver parasite burden. Interestingly, NKT cell numbers were decreased, and parasite burdens were increased in IFNAR ko mice, suggesting type I IFN dependent recruitment and defence mechanisms. Furthermore, mice treated with  $\alpha$ GalCer 2 days before *Plasmodium* challenge, displayed reduced liver-stage parasite burden (Gonzalez-Aseguinolaza et al., 2000). However, protection in CD1d KO mice, which lack NKT cells was not altered after radiation attenuated sporozoite (RAS) vaccination and sporozoite challenge one week later,

compared to that in wild-type (WT) mice (Romero et al., 2001). Thus, NKT cells only provide protection against *Plasmodium* infection if recently activated. In other settings, NKT cells have also been shown to provide help for adaptive immunity capable of controlling infection (Holz et al., 2020).

Another cell type potentially targeting the liver-stage of infection are NK cells. NK cells express multiple germ-line encoded cell surface receptors either having inhibitory or activating functions. These receptors allow NK cells to recognize infected or cancerous cells in an antigen and MHC independent manner (Lanier, 2005, Raulet et al., 2001, Ljunggren and Kärre, 1990). In murine malaria studies it was described that *P. yoelii* sporozoite infection led to a decrease of NK cells in the spleen and an increase in the liver (Roland et al., 2006). Furthermore, hepatic but not spleen-derived NK cells showed cytotoxic capacity against *P. yoelii* liver-stages *in vitro*.

### **1.3.1.2 Innate immune response to the erythrocytic-stage of *Plasmodium* infection**

Upon completion of their development in the liver, *Plasmodium* parasites infect red blood cells and are distributed throughout the circulation where they become accessible to a variety of immune cells. For example, upon encounter with *Plasmodium* iRBCs, NK cells are activated and start to express IFN- $\gamma$  (Artavanis-Tsakonas and Riley, 2002). IFN- $\gamma$  and cytotoxicity mediated by NK cells is IL-12 dependent and is essential for developing a protective immune response against *Plasmodium* blood-stage infection (Stevenson et al., 2001, Mohan K et al., 1997). The depletion of NK cells in C57BL/6 mice infected with non-lethal *P. chabaudi* (Pch) resulted in a rapid increase in parasitemia and a reduced capability to resolve infection compared to WT mice (Mohan K et al., 1997). Furthermore, NK cells isolated from human PMBCs are the first cells to respond to *P. falciparum* infected erythrocytes *in vitro* (Artavanis-Tsakonas and

Riley, 2002). This response is characterized by the rapid expression of IFN- $\gamma$  within 24 – 48 post stimulation. Other immune cells like  $\gamma\delta$ -T cells (48-72h) and  $\alpha\beta$  T cells (4-6 days) produced IFN- $\gamma$  at later times.

The clinical relevance of  $\gamma\delta$  T cells in the erythrocytic stage of *Plasmodium* infection has not been thoroughly evaluated. However, acute *P. falciparum* infection has been found to induce expansion of  $\gamma\delta$  T cells and secretion of large amounts of IFN- $\gamma$  (Hviid et al., 2001). Furthermore,  $\gamma\delta$  T cells were found to expand after resolution of acute Pch blood-stage infection and were essential in the control of parasite reoccurrence in the chronic phase of infection (Mamedov et al., 2018). In addition,  $\gamma\delta$ -T cell responses were linked to ECM development in an PbA blood-stage infection model (Yañez et al., 1999).

Macrophages can phagocytose *Plasmodium-infected* red blood cells in the absence of specific antibodies (Serghides et al., 2003). However, macrophages are more efficient at clearing *Plasmodium* iRBCs in conjunction with adaptive immunity. Opsonizing antibodies, secreted by B cells after Pch infection, mediated internalization of infected erythrocytes by macrophages more efficiently than without opsonizing antibodies (Mota et al., 1998). Furthermore, IFN- $\gamma$  secretion by CD4 T cells induced expression of anti-parasite molecules such as nitric oxide (NO) intermediates and reactive oxygen species (ROS) by macrophages, leading to *Plasmodium* parasite death inside the host cell (Su and Stevenson, 2000, Shear et al., 1989).

One of the most crucial cell types communicating between the innate and adaptive immune systems are DCs. Early studies showed that the binding of iRBCs by DCs can lead to reduced maturation of DCs and therefore impaired activation of the adaptive immune system (Urban et al., 1999). However, this was only the case when large numbers of iRBCs were cultured with small amounts of DCs (100 iRBCs: 1 DC), a lower dose of iRBCs (10 iRBCs: 1 DC) induced efficient maturation of DCs (Urban et al., 1999, Elliott et al., 2007). DC are activated by *Plasmodium-derived* pathogen-associated molecular patterns (PAMPs), which are molecular elements conserved across pathogens and

recognized by the immune system as foreign through certain protein families such as toll-like receptors (TLRs). This activation induces the up-regulation of co-stimulatory molecules such as CD83, CD86, and CD1a on human monocyte-derived DCs and the secretion of IL-12, a cytokine important for NK cell and T cell activation (Coban et al., 2002). One such *Plasmodium* derived PAMP was purified from merozoites (Wu et al., 2010, Gowda et al., 2011). The authors described a nucleosome-DNA complex as a major DC activating compound in *P. falciparum* blood-stage infection. This complex signalled TLR9 on DCs and led to the production of inflammatory cytokines such as IFN- $\gamma$ , TNF and IL-12. Such inflammatory cytokines are essential to activate other innate and adaptive immune cells. For example, DC activation is shown to induce NK cell function and, as such, depletion of DCs reduced NK cell-mediated IFN- $\gamma$  responses after PbA blood-stage infection (Ryg-Cornejo et al., 2013).

In addition to strong activation of the innate immune system, a robust adaptive immune response is essential to protect from a *Plasmodium* infection and re-infection. Thus, the next section will introduce the induction of adaptive immune responses against *Plasmodium* infections.

### 1.3.2 T cell priming

Conventional  $\alpha\beta$  T cells can be divided into two broad subsets of CD8 and CD4 T cells. Each T cell expresses a specific T cell receptor (TCR) consisting of an  $\alpha$  and a  $\beta$  chain. These TCRs can recognize peptides bound to major histocompatibility complex (MHC) molecules. Peptide fragments recognized by CD8 T cells are presented via MHC-I molecules on the cell surface of all nucleated cells. The TCR of CD4 T cells can bind to MHC-II molecules, which, unlike MHC-I molecules, are mainly expressed by specialized immune cells such as DCs, B cells, and macrophages. Those cells are commonly referred to as professional antigen-presenting cells (APCs). However, it was shown that non-

professional APCs can also be induced to express MHC-II molecules on the cell surface. For example, an IFN- $\gamma$  dependent upregulation of MHC-II molecules in brain microvascular cells of experimental cerebral malaria susceptible mice was observed (Monso-Hinard et al., 1997) . Similar, it was shown that in clinical hepatitis, hepatocytes expressed MHC-II molecules upon IFN- $\gamma$  stimulation, which in turn can stimulate CD4 T cell responses (Franco et al., 1988).

The origins of peptide fragments loaded onto either MHC-I or II molecules differ. Peptides derived from cytosolic molecules are typically loaded onto MHC-I molecules inside the endoplasmatic reticulum before they get presented on the cell surface (Purcell and Elliott, 2008). MHC-I molecules that do not bind to a peptide are unstable and unlikely to appear or be maintained on the cell surface (Townsend et al., 1989). On the other hand, MHC-II molecules are loaded with extracellular peptides generated in acidified endocytic vesicles (Watts, 1997). This suggests that MHC-I molecules present peptides of cytosolic pathogens, whereas MHC-II molecules contain peptides derived from extracellular pathogens. However, due to a process called “cross-presentation,” exogenous proteins can be introduced into the MHC-I loading machinery and be presented on MHC-I molecules by specialized APCs (Ackerman and Cresswell, 2004). In addition, autophagy, a process where portions of the cell’s own cytosol are taken up into specialized vesicles and degraded, enables cytosolic derived peptide fragments to be presented via MHC-II molecules (Dengjel et al., 2005). These mechanisms ensure the efficient initiation of specific immune responses against a wide variety of pathogens and malignant cells.

The length of peptides presented on MHC-I or II molecules differs. MHC-I molecules have a closed peptide-binding groove that stabilises the bound peptide at both ends (Bouvier and Wiley, 1994). Therefore, the variation in peptide length that can bind to MHC-I molecules is limited. In general, 8-10 amino acid long peptides are found inside the peptide-binding groove of MHC-I molecules (Van Bleek and Nathenson, 1990, Jardetzky et al., 1991). In contrast, MHC-II molecules have an open peptide binding groove allowing for longer peptides to be loaded into the MHC-II molecule binding groove (Fremont et al., 1998, Park et

al., 2003). Hydrogen bonds between the peptide and highly conserved amino acid residues within MHC-II molecules are responsible for stabilizing the MHC-II:peptide complex (McFarland et al., 1999, Landais et al., 2009, Holland et al., 2013).

The priming process of T cells mainly takes place in secondary lymphoid organs such as the spleen and lymph nodes (LN), where the density of APC and naïve T cells is high. DCs are the major APC population responsible for T cell priming. In general, DCs can be divided into monocyte derived DCs, plasmacytoid DCs and conventional DCs (cDCs) (Brown et al., 2019). Conventional DCs can be further divided into cDC type 1 (cDC1) and cDC type 2 (cDC2). Activation of T cells through TCR stimulation by peptide:MHC complexes and costimulatory signals results in their differentiation into effector T cells. Each effector T cell can undergo clonal expansion, a proliferation process that leads to an increased effector T cell pool with identical specificities. The now numerous effector T cells can re-enter the bloodstream through efferent lymphatics and be distributed throughout the body, where they seek and fight infection.

Upon intradermal *Plasmodium* sporozoite infection, CD8 T cell activation is first induced in the skin draining lymph node within 48 hours post-infection, but is not detectable in the spleen and liver (Chakravarty et al., 2007). Surgical removal of the draining LN prior to infection via a mosquito bite reduced the number of activated CD8 T cells in the liver by about 60 %. This suggests that the skin draining LN represents the primary site for CD8 T cell priming after *Plasmodium* mosquito bite infection. However, intravenous (i.v.) injection of live sporozoites or radiation attenuated sporozoites (RAS), used in experimental infection and vaccination models, demonstrated CD8 T cell priming in liver and spleen (Lau et al., 2014, Sano et al., 2001). Interestingly, RAS vaccination induces better CD8 T cell priming and memory formation compared to injection of heat-inactivated sporozoites (HKS) (Ghilas et al., 2021). Furthermore, co-administration of RAS and HKS could not rescue T cell priming and memory formation of a T cell population specific for an epitope only expressed by the HKS. Therefore, the authors argued that antigen is presented by a different subset of

APCs after RAS vaccination than after HKS. While the exact mechanism is not fully elucidated, activation of NKT cells enhanced T cell responses after HKS vaccination (Ghilas et al., 2021). This suggests that RAS vaccination may also induce NKT cells activation which, therefore, can lead to improved APC maturation and IL-4 and IL-12 production. Both cytokines were described to be essential for CD8 T cell activation and memory formation upon RAS vaccination (Carvalho et al., 2002, Jobe et al., 2009).

Immunofluorescence microscopy of the skin draining LN after intradermal sporozoite inoculation demonstrated cluster formation of antigen-specific CD8 T cells and CD8<sup>+</sup> cDCs (cDC1) (Radtke et al., 2015). As cDC1 have been described as the major APC facilitating cross-presentation, these data support the view that CD8 T cell priming was carried out by cDC1 during sporozoite infection (den Haan et al., 2000, Schnorrer et al., 2006, Radtke et al., 2015). Once activated, T cells can leave secondary lymphoid organs and migrate to the liver, where they detect infected hepatocytes through peptide:MHC presentation on the cell surface, and then kill infected cells without the need for APCs (Chakravarty et al., 2007, Balam et al., 2012). It remains unclear if CD4 T cells are primed in a similar way to CD8 T cells after sporozoite infection. However, it was shown that during *Plasmodium* infection the same DC subpopulation is required for efficient CD4 and CD8 T cell priming (Radtke et al., 2015, Borges da Silva et al., 2015). It is therefore likely, that the initial CD4 T cell priming also occurs in the skin draining LN.

After liver-stage infection, merozoites that enter the circulation and infect RBC are substantially different from sporozoites, making an array of new antigens available to the immune system. The Lack of MHC-I and II molecule expression on mature erythrocytes prevents T cells from directly responding to antigen on iRBCs. Nevertheless, robust CD8 T cell responses against *Plasmodium* blood-stage antigens are found in the spleen after blood-stage parasite exposure (Chandele et al., 2011, Lundie et al., 2008). Studies using transgenic CD8 T cells revealed CD8<sup>+</sup> (XCR1<sup>+</sup>) DCs (cDC1 DCs) were responsible for the activation of CD8 T cells during blood stage infection, via cross-presentation of antigen derived from *Plasmodium* erythrocytes (Lundie et

al., 2008, Miyakoda et al., 2008, Fernandez-Ruiz et al., 2016). The lack of MHC-I molecules on RBCs suggests that CD8 T cells cannot directly control *Plasmodium* blood-stage infection. However, a study using *P. yoelii* infections observed CD8 T cell dependent reduction of iRBCs in mice (Imai et al., 2010). Most likely, IFN- $\gamma$  secretion by CD8 T cells activated macrophages to kill *Plasmodium* iRBCs.

Compared to CD8 T cell activation, CD4 T cell priming is less well characterised. CD4 T cells undergo a specific differentiation process upon activation, resulting in different CD4 T cell lineages, each characterised by the expression of specific cytokines and transcription factors (TF) (Agarwal and Rao, 1998). Different factors such as cytokine milieu, the type of APC interacting with CD4 T cells, TCR signalling strength and co-stimulatory signals, determine CD4 T cell differentiation (Bajenoff et al., 2002, Eizenberg-Magar et al., 2017, Harpur et al., 2019, Tubo et al., 2013, Igyarto et al., 2011). cDC1 (lymphoid-related DCs) are believed to bias CD4 T cells differentiation towards a Th1 lineage due to high levels of IFN- $\gamma$  and IL-2 during T cell priming, while cDC2 (myeloid-related DCs) provide a cytokine milieu favouring Th2 differentiation (Pulendran et al., 1999, Gao et al., 2013).

Historically, naïve CD4<sup>+</sup> T cells were thought to give rise to either Th1 or Th2 cells upon activation. However, more recently it has become apparent that the CD4 T cell compartment is far more complex and consists of multiple different lineages, including follicular helper (Tfh), Th17 and regulatory T cell (Treg), to name some (Figure 1.2). Th1 cells are characterised by the expression of T-box transcription factor 21 (Tbet) and secretion of IFN- $\gamma$  and tumour necrosis factor (TNF) and are described to mainly play a role in the clearance of intracellular pathogens, whereas Th2 cells are characterised by the expression of GATA binding protein 3 (GATA3) and IL-4, IL-5 and IL-13 (Szabo et al., 2000, Zheng and Flavell, 1997). Interestingly, binding of GATA3 to the *Ifng* locus inhibits IFN- $\gamma$  expression, thereby suppressing the development of a Th1 phenotype (Jenner et al., 2009, Kishikawa et al., 2001, Chang and Aune, 2007). In contrast, Tbet expression by CD4 T cells inhibits the development of a Th2 phenotype by

binding to the *IL4* promoter, which abrogates IL-4 expression by CD4 T cells (Ansel et al., 2004, Jenner et al., 2009, Djuretic et al., 2007).

While Th2 cells were previously thought to be crucial for B cell activation and antibody maturation, it is now known that this function is mainly attributed to Tfh cells, expressing Bcl6 as their lineage marker TF (Hatzi et al., 2015). Tfh cells are described to be mainly located in secondary lymphoid organs, where they support germinal centre formation.

Another well characterised CD4 T cell lineage are Th17 cells, characterised by the expression of Ror $\gamma$ T, IL-17 and IL-22 (Ivanov et al., 2006, Liang et al., 2006). Th17 cells are mainly described to be involved in the immune response against fungi and extracellular bacteria.

Treg cells are the main immunosuppressive CD4 T cell subtype and can either be derived from the thymus (natural Treg, nTreg) or locally induced in the tissue (induced Treg, iTreg) (Lee and Lee, 2018). Tregs are known to suppress a variety of different immune cells through the secretion of immune suppressive cytokines such as IL-10 and IL-35 and consumption (and thereby depletion) of IL-2 (reviewed by (Schmidt et al., 2012)). Furthermore, Tregs are described to be able to directly kill effector cells through the secretion of perforin and Granzyme B.

It is unclear, whether CD4 T cells can recognize infected hepatocytes during the liver-stage of *Plasmodium* infection via MHC-II molecules. Under steady state conditions hepatocytes do not express MHC-II molecules, making them “invisible” for CD4 T cells (Franco et al., 1988). However, MHC-II expression by hepatocytes can be induced in an IFN $\gamma$  dependent manner. Sporozoite invasion results in the release of type-I interferons by hepatocytes, which in turn results in the induction of IFN- $\gamma$  (Liehl et al., 2014, Liehl et al., 2015). Theoretically, this local IFN- $\gamma$  response could result in the upregulation of MHC-II molecules on hepatocytes enabling CD4 T cells to recognize their cognate antigen on the infected cell surface. However, it is not known if this upregulation occurs.

*Plasmodium* specific CD4 T cells have also been shown to be primed in the spleen, similar to CD8 T cells. Increased colocalization of CD4 T cells and CD11c<sup>+</sup> DCs was found as early as 2 h post Pch infection in T cell-rich areas and the red pulp of the spleen (Borges da Silva et al., 2015). Furthermore, it was shown that CD11C<sup>high</sup> but not plasmacytoid DCs were able to phagocytose parasite and induce CD4 T cell activation (Voisine et al., 2010). Interestingly, a study investigating the role of CD11c<sup>+</sup> CD8<sup>+</sup> and CD8<sup>-</sup> DCs revealed that while both populations were able to induce IFN- $\gamma$  expression by CD4 T cells in response to Pch infection, CD8<sup>-</sup> DCs also induced CD4 T cell populations expressing IL-4 and IL-10 indicating the possibility of different DCs subset to induce different CD4 T cell lineages (Sponaas et al., 2006).

Not only can the specific DC subtype influence CD4 T cell lineage differentiation, also the way the antigen is delivered to and processed by DCs affects CD4 T cell priming and differentiation. cDC1 DCs express surface receptors such as Clec9A, DEC205, and Clec12A, which facilitate antigen uptake and processing (Jiang et al., 1995, Huysamen et al., 2008, Hutten et al., 2016). Targeting those receptors with an antibody carrying a specific T cell antigen can induce robust CD8 and CD4 T cell proliferation as well as humoral immunity (Lahoud et al., 2011). However, CD4 T cell responses differed depending on the targeted receptor. Delivering OVA antigen by targeting Clec9A receptor on CD8 $\alpha$ <sup>+</sup> DCs induced superior proliferation and maintenance of OT-II cells, compared to targeting DEC205 or Clec12A (Lahoud et al., 2011). Furthermore, targeting DEC-205 can skew CD4 T cell differentiation towards a regulatory phenotype, while Clec9A on CD8 $\alpha$ <sup>+</sup> DCs mostly led to Th1 and Tfh differentiation of CD4 T cells (Idoyaga et al., 2011, Lahoud et al., 2011). These reports showed that a monoclonal antibody targeting Clec9A induced the same CD4 phenotypes as PbA blood-stage infection in PbT-II cells (Idoyaga et al., 2011, Lahoud et al., 2011, Fernandez-Ruiz et al., 2017).

After T cell activation, differentiation and proliferation in response to an infection or vaccination, most effector T cells undergo cell death, leaving behind a small population of memory T cells. Those memory T cells are described to develop immediate effector functions in response to antigen encounter and are therefore better suited to prevent a re-infection. Therefore, the next chapter will give a brief overview of T cell memory formation and subpopulations.

### **1.3.3 Memory T cell development**

Effector T cells are a heterogeneous population and can be divided into KLRG1<sup>+</sup> CX3CR1<sup>+</sup>, S1PR1<sup>+</sup> short-lived effector cells (SLECs), and KLRG1<sup>-</sup>, IL-7R<sup>+</sup> memory precursor effector cells (MPECs) (Joshi et al., 2007, Kaech et al., 2003, Chandele et al., 2011, Jung et al., 2010, Gerlach et al., 2016). High numbers of SLECs form after T cell activation, but they rapidly decline in numbers after clearance of infection. MPECs, on the other hand, form at lower numbers but survive and develop into long-term memory T cells, which have the capacity to generate potent recall responses. However, it has to be noted that this classification of effector T cells into SLECs and MPECs is not exhaustive. An IL-7R<sup>+</sup>, KLRG1<sup>-</sup> phenotype cannot be exclusively used to define memory precursors, as not all IL-7R<sup>+</sup> cells are long-lived, and some KLRG1<sup>+</sup> T cells were found to persist into the memory phase (Lacombe et al., 2005, Olson et al., 2013, Martin et al., 2015). Furthermore, a recent study using a fate mapping system showed that some KLRG1<sup>+</sup> effector cells could switch off KLRG1 expression and give rise to memory cells, indicating a previously unappreciated degree of plasticity (Herndler-Brandstetter et al., 2018). Thus, the elements that determine T cell fate decision remain to be fully elucidated. Several factors, such as TCR signal duration and the inflammatory environment during T cell priming, have been shown to determine T cell fate (Joshi et al., 2007, Sarkar et al., 2008). Furthermore, asymmetric cell division of T cells is suggested to play a role in early T cell fate decisions (Chang and Aune, 2007). Within the first cell division, cells that derived from the proximal daughter T cell, in relation to the APC, showed

increased proliferation after primary infection and elevated downstream glycolysis metabolites, properties attributed to SLECs. In contrast, the distal daughter T cell displayed increased memory potential, recall responses, and higher dependency on lipid metabolism and therefore its respective daughter cells are better equipped to progress into the memory T cell pool (Borsa et al., 2019, Pollizzi et al., 2016, Verbist et al., 2016). Asymmetric cell division can be forced in CD8 T cells via a transient inhibition of the protein kinase mTOR, which has a central role regulation of cell growth and metabolism (Zoncu et al., 2011). This inhibition led to increased memory potential, recall response, and viral LCMV control in mice (Borsa et al., 2019). Further studies confirmed reduced mTOR signalling, and therefore expression of the transcription factor c-Myc, enhanced long-term survival by inducing anti-apoptotic molecules, increased response to secondary infection, and a shift to lipid metabolism in T cells (Pollizzi et al., 2016, Verbist et al., 2016). In addition, a study using a chronic *P.chabaudi* infection model described that once a memory precursor cell is formed a linear T cell memory differentiation occurs from central memory, early effector memory to late effector memory CD4 T cells (Stephens and Langhorne, 2010).

Establishment and long-term survival of MPECs and memory T cells depend on the cytokines IL-7 and IL-15 (Kaech et al., 2003, Surh and Sprent, 2008). After binding of these cytokines to their receptors on the T cell surface, intracellular signalling events result in the expression of anti-apoptotic molecules including Bcl2 and Mcl1. These molecules have been shown to promote memory formation and to prevent death of activated effector T cells (Rathmell et al., 2001, Opferman et al., 2003, Kondrack et al., 2003, Schluns et al., 2000, Yajima et al., 2006, Hildeman et al., 2002). Additionally, IL-15 induces a metabolic switch in T cells from glycolysis, characteristic for effector T cells, to fatty acid oxidation, associated with T cell memory formation (van der Windt et al., 2012). Fatty acid oxidation generates roughly 6 times more energy per unit of substrate weight than glycolysis and is crucial for memory T cell survival (Lodish et al., 2000). Studies using TRAF6 deficient T cells, which present defective mitochondrial fatty acid oxidation, demonstrated enhanced effector T cell contraction and lower memory potential, whereas the stimulation of fatty acid metabolism in these cells by a drug

that promoted AMP-activated kinases and circumvented TRAF6-dependency prevented these deleterious effects (Pearce et al., 2009). In addition to IL-15, IL-7 is thought to promote the metabolic switch from glycolysis to fatty acid oxidation. Most memory T cells arise from the IL-7R expressing subpopulation of effector T cells (Kaech et al., 2003). IL-7 signalling has been shown to induce the expression of aquaporin 9, which is a glycerol transporter that supports fatty acid uptake, thereby promoting fatty acid uptake and oxidation in CD8<sup>+</sup> T cells (Cui et al., 2015). The migration of MPECs to T cell areas in secondary lymphoid organs is facilitated by their expression of the chemokine receptor CCR7 which guides them along a CCL19 and CCL21 gradient (Hara et al., 2012). Within secondary lymphoid organs, T cells encounter IL-7, which is predominantly produced by stromal cells. Of note, epithelial cells in organs such as the skin and the intestine can also produce IL-7.

Memory T cells undergo homeostatic proliferation, which is important to sustain this population. IL-15 is shown to be involved in T memory cell homeostasis. For example, in the absence of IL-15, CD8<sup>+</sup> memory T cell number decline as basal CD8<sup>+</sup> T cell memory proliferation is impaired (Becker et al., 2002, Goldrath et al., 2002). Reliance on IL-15 for maintenance have been found in different subtypes of memory T cells (Holz et al., 2018, Herndler-Brandstetter et al., 2018). However, more recent studies indicate that IL-15 dependency might not be absolute for all CD8 memory T cells (Verbist et al., 2011, Schenkel et al., 2016).

Historically, memory T cells were classified into two subsets, CCR7<sup>+</sup> CD62L<sup>+</sup> central memory (T<sub>CM</sub>), and CCR7<sup>-</sup> CD62L<sup>-</sup> effector memory T (T<sub>EM</sub>) cells (Sallusto et al., 1999). CCR7 and CD62L are lymph node homing molecules essential for access into lymphoid tissues. T<sub>CM</sub> cells have been shown to migrate through lymphoid tissues, whereas T<sub>EM</sub> cells predominantly traffic through peripheral tissues and the blood (Sallusto et al., 1999, Masopust et al., 2001). However, recent work by Gerlach et al. described a higher complexity in T cell memory populations in mice. Based on the chemokine receptor CX3CR1 expression, three distinct memory populations could be discriminated. Besides

$T_{CM}$  (which are  $CX3CR1^-$ ) and  $T_{EM}$  ( $CX3CR1^{hi}$ ), a  $CX3CR1^{int}$  peripheral memory ( $T_{PM}$ ) cell population was described as the major migratory memory subsets in peripheral tissues, a role previously attributed to  $T_{EM}$  cells. The authors investigated migratory memory T cells in the thoracic duct lymph (TDL) after LCMV infection. In the TDL, migratory lymphocytes from tissues below the diaphragm and the left upper body accumulate on their way to the blood. Gerlach et al. found that  $T_{EM}$  cells dominated the peripheral blood, while  $T_{PM}$  cells represented the most abundant subset in TDL (Gerlach et al., 2016). In addition, LCMV infected mice were surgically joined to naïve mice, in a procedure termed parabiosis. Parabiotic mice establish a shared circulation, allowing hematopoietic cells to pass from one mouse to the other. Consistent with their previous findings,  $T_{EM}$  cells were the most abundant memory T cell population in the blood of naïve parabiotic mice. In the TDL of the naïve partner, however,  $T_{PM}$  outnumbered  $T_{EM}$  cells. The authors, therefore, concluded that  $T_{PM}$  and not  $T_{EM}$  cells, entered the peripheral tissues of the naïve parabiotic mouse and left through the afferent lymph resulting in the detected accumulation of  $T_{PM}$  cells in the TDL (Gerlach et al., 2016).

In humans and mice, another T memory subtype termed memory T stem cells ( $T_{SCM}$ ) was reported (Zhang et al., 2005, Gattinoni et al., 2011). Similar to naïve T cells but unlike other memory T cells,  $T_{SCM}$  cells express low levels of CD44 but high levels of CD62L.  $T_{SCM}$  can be further distinguished from other T cell subsets by the expression of CD122 and Bcl2 and, at least in mice, of Sca-1. Transcriptomic analyses of these cells indicated that  $T_{SCM}$  cells are the least differentiated memory subset population and can differentiate into SLECs,  $T_{EM}$ , and  $T_{CM}$ . Furthermore,  $T_{SCM}$  cells show higher levels of self-renewal, survival, and proliferation capacity than  $T_{EM}$  and  $T_{CM}$  cells (Zhang et al., 2005, Gattinoni et al., 2009, Gattinoni et al., 2011).

Finally, another memory T cell population that resides in peripheral tissues was described relatively recently. These cells, termed tissue-resident memory T cells ( $T_{RM}$ ), were first described in the skin, where they remained upon resolution of infection without recirculating, and efficiently controlled reinfection in a herpes simplex virus model (Gebhardt et al., 2009). Skin  $T_{RM}$  showed elevated

expression of CD69 and CD103 on the cell surface and lacked the expression of CD62L (Gebhardt et al., 2009). T<sub>RM</sub> cells have now been identified in most lymphoid and non-lymphoid tissues and have been recognised to represent the first line of defence towards pathogen reencounter in many infection models (Gebhardt et al., 2009, Teijaro et al., 2011, Schenkel and Masopust, 2014a, Fernandez-Ruiz et al., 2016).

### 1.3.3.1 Tissue resident memory T cells

Given that T<sub>RM</sub> cells represent the first line of defence against pathogen re-encounter and have a dominant role in peripheral immunity, these cells have received much attention in recent years (Gebhardt et al., 2009, Teijaro et al., 2011, Schenkel and Masopust, 2014a, Fernandez-Ruiz et al., 2016). The identification of T<sub>RM</sub> cells in mice and human has been challenging, however, as no surface marker that is exclusively expressed by T<sub>RM</sub> cells are known. One marker widely used as a starting point to dissect resident and circulatory memory T cell populations is CD69. Historically described as an early T cell activation marker, CD69 is upregulated on the surface of most but not all T<sub>RM</sub> cells (Steinert et al., 2015). CD69 expression leads to complex formation with sphingosine-1-phosphate receptor (S1PR1) on the cell plasma membrane. As S1PR1 mediates T cell egress from lymphoid tissues into the lymph and blood upon recognition of high sphingosine-1 phosphate (S1P) levels, S1PR1 complexation by CD69 blocks this function after entry into peripheral tissues, which, in the end, promotes tissue retention of CD69<sup>+</sup> T cells (Spiegel and Milstien, 2011, Mackay et al., 2015a). However, CD69 upregulation can also be induced by recent TCR stimulation and type I IFN (Shiow et al., 2006). Thus, CD69 alone cannot be used as a universal T<sub>RM</sub> cell marker.

A second widely used marker for T<sub>RM</sub> cells is the  $\alpha$  chain of the integrin  $\alpha$ E $\beta$ 7 (CD103). CD103 binds to E-cadherin expressed on epithelia cells, which can result in the retention of T cells in tissue (Cepek et al., 1994). While this

marker is broadly expressed on CD8 T<sub>RM</sub> cells in several non-lymphoid-tissues such as the brain, the skin, salivary glands, lung and tonsils in humans and mice, in other non-lymphoid organs, such as kidney and liver, as well as in lymphoid organs, such as spleen, bone marrow or lymph nodes, CD8 T<sub>RM</sub> cells do not express CD103 (Wakim et al., 2010, Mackay et al., 2013, Takamura et al., 2016, Kumar et al., 2017, Buggert et al., 2018, Schenkel and Masopust, 2014b, Fernandez-Ruiz et al., 2016). Adding to the complexity, expression of CD103 is generally less abundant on CD4 compared to CD8 T<sub>RM</sub> cells (Kumar et al., 2017, Smolders et al., 2018, Strutt et al., 2018, Romagnoli et al., 2017).

Thus, expression of either CD69, CD103 or both is not sufficient for the definite identification of T<sub>RM</sub> cells and additional markers are required to further distinguish circulatory and resident memory T cells in humans and mice (Gebhardt et al., 2009, Mackay et al., 2013, Cheuk et al., 2017, Kumar et al., 2018). Such T<sub>RM</sub> cells associated markers include CXCR6, PD-1, CD101 and CD49a, the latter of which interacts with CD29 to form the very late antigen 1 (VLA-1) capable of binding extracellular collagen and laminin and aiding tissue retention (Ray et al., 2004). Combinations of these markers are commonly used to identify T<sub>RM</sub> cell populations in different organs. In addition, Killer cell lectin like receptor subfamily G member (KLRG1) and CD62L, markers associated with T<sub>EM</sub> and T<sub>CM</sub> cells, respectively, are expressed at low levels on T<sub>RM</sub> cells and enable further separation of circulating and resident memory T cell populations (Casey et al., 2012, Kumar et al., 2017).

The diversity of expression patterns of surface markers associated with T<sub>RM</sub> cells complicates identification and comparison of T<sub>RM</sub> cells in different tissues. An alternative way to gain more comprehensive insights into T<sub>RM</sub> cell populations is the comparison of transcriptional profiles. By comparing mouse CD8 T<sub>RM</sub> cell microarray datasets from various tissues with circulatory T cell populations from the spleen, Mackay and co-authors defined a CD8 T<sub>RM</sub> cell core signature shared between T<sub>RM</sub> cells in lung, gut and skin after LCMV, influenza and HSV infection, respectively (Mackay et al., 2013). In a later study, the authors found a similar core signature shared by resident CD8 T cells in gut, skin and

liver after HSV or LCMV infection (Mackay et al., 2016). Interestingly, this core signature was also evident in liver NKT and liver resident NK cells but not circulatory NK cells isolated from the liver, which indicated that the identified transcriptional profile was not only shared between different CD8 T<sub>RM</sub> cells but represented a general residency signature. Furthermore, a shared transcriptional program was found in human lung derived CD4 and CD8 T<sub>RM</sub> cells, with a high correlation to already published mouse brain, lung and gut T<sub>RM</sub> microarray datasets (Kumar et al., 2017). Interestingly, this specific core signature was also expressed by human CD69<sup>+</sup> CD4 and CD8 memory T cell populations in the spleen, validating the existence of tissue resident memory T cells in human lymphoid and non-lymphoid organs, comparable to resident T cell populations in mice. Moreover, these studies confirmed previous findings of surface marker expression profiles of T<sub>RM</sub> cells, such as upregulation of CXCR6, CXCR3, and the reduced expression of T<sub>EM</sub> associated transcripts such as KLRG1, S1PR1 and S1PR5 (Mackay et al., 2016, Kumar et al., 2017).

While mRNA and protein expression profiles can readily be used to characterise different memory T cell populations, the ultimate proof of residency requires more definite experimental procedures. In experimental animal models, the residency of T cells can be determined by parabiosis, which requires the surgical union of the skin flank of two animals. This procedure results in a shared blood stream between both animals which allows determination of the distribution and migratory capacities of different memory cell populations (Jiang et al., 2012). As such, memory T cells that enter the circulation will reach an equilibrium between the host and the partner mouse, whereas memory T cells, that permanently remain in the tissues where they have formed (and are thus per definition T<sub>RM</sub> cells), will not be found in the joined partner mouse. With this method, tissue resident memory T cells were identified in several tissues, including in the lung, skin and liver (Teijaro et al., 2011, Steinert et al., 2015, Fernandez-Ruiz et al., 2016, Jiang et al., 2012). It was shown that liver CD8 T<sub>RM</sub> cells can be induced by systemic LCMV infection or RAS vaccination. Interestingly, unlike CD8 T<sub>RM</sub> cells from the skin that are shielded from the blood, liver CD8 T<sub>RM</sub> cells are exposed to the blood and patrol along sinusoids

(Fernandez-Ruiz et al., 2016). While most studies have focused on CD8 T<sub>RM</sub> cells and properties of CD4 T<sub>RM</sub> cells are less well understood, there is evidence that CD4 T cells form resident memory populations as well. For example, it was shown that liver homing T helper 1 CD4 T cells could mediate partial protection against *Salmonella* infection and their residency was suggested by parabiosis experiments (Benoun et al., 2018).

## **1.4 The role of T cells in immunity against *Plasmodium* infection**

### **1.4.1 The Role of CD8 T cells in immunity against *Plasmodium* liver-stage infection.**

Evidence that sterile immunity induced by RAS vaccination was mediated by CD8 T cells was first demonstrated in the 1980s by showing that protection was lost when CD8 T cells were depleted (Schofield et al., 1987). However, especially high numbers of these cells were suggested to be required to protect against *Plasmodium* infection (Schmidt et al., 2008, Schmidt et al., 2011). It was thought that this was due to the short time parasites remained in hepatocytes combined with the need to recognize and eliminate every infected hepatocyte to prevent the development of a blood-stage infection. Recently activated CD8 T cells can offer efficient protection against infection (Sano et al., 2001). Indeed, transfer of activated/memory CSP-specific CD8 T cells 24 h before sporozoite challenge, resulted in reduced parasite liver rRNA levels, while transfer of equal numbers of naïve CSP-specific CD8 T cells did not alter the parasite burden in the liver. Effector T cells are short lived and so is their protection capacity. However, memory T cells can provide long-term protection against pathogens expressing their cognate antigen and will rapidly gain effector functions upon antigen re-encounter (Lalvani et al., 1997). This makes memory T cells ideal candidates to prevent malaria infection through vaccination.

Of the three major types of memory T cells,  $T_{CM}$ ,  $T_{EM}$  and  $T_{RM}$ , there is little evidence supporting a major role of  $T_{CM}$  cells in protective immunity against malaria infection (Berenzon et al., 2003). PbA RAS vaccination of mice mainly induces  $T_{EM}$  cells (96 %) in the liver.  $T_{EM}$  cells induced by RAS vaccination circulate through the body, loaded with effector molecules to exert functions including cytokine production and lytic activity. The ratio of  $T_{CM}$  and  $T_{EM}$  cells seems to influence the ability of these cells to protect against *Plasmodium* infection (Schmidt et al., 2010). While BALB/c mice, which are described to generate a robust immune response against *Plasmodium* sporozoites infection, generate large numbers of CSP-specific  $T_{EM}$  cells after two doses of RAS vaccination, C57BL/6 (B6) mice are highly susceptible to sporozoite infection and are characterised by the induction of higher proportions of  $T_{CM}$  cells. Furthermore, immunisation of BALB/c mice with CSP peptide coated mature DCs, followed by a boosting with CSP expressing *Listeria monocytogenes* resulted in long-term protection in some mice (Schmidt et al., 2008). The authors suggested that protection in this system was mainly mediated  $T_{EM}$  cells, though at the time they were unaware of resident memory (Schmidt et al., 2010, Butler et al., 2010).

Recently, liver-resident memory CD8 T cells were identified, and shown to have a strong potential to protect against *Plasmodium* liver-stage infection in RAS vaccinated mice (Tse et al., 2013, Tse et al., 2014, Fernandez-Ruiz et al., 2016). It was shown that a specific population of CD8 T cells expressing high levels of CXCR6 formed after RAS vaccination and were crucial for protection against sporozoite infection (Tse et al., 2014). A later study, using TCR transgenic, *Plasmodium* specific CD8 T cells, confirmed, through parabiosis surgery, the resident character of  $CD69^+$ ,  $CXCR6^+$ ,  $CXCR3^+$  CD8  $T_{RM}$  cells in the liver after RAS vaccination (Fernandez-Ruiz et al., 2016). Those cells expressed low levels of KLRG1 and CD62L, which are markers related to circulatory memory cells, and shared a transcriptional signature with CD8  $T_{RM}$  cells from the lung, skin and the gut. Parabiosis experiments were performed to demonstrate the liver-residency of these memory CD8 T cells (Fernandez-Ruiz et al., 2016). This work also demonstrated that large numbers of *Plasmodium*-specific CD8 liver  $T_{RM}$  cells can be induced through administration of a three-component subunit vaccine,

termed “prime-and-trap”. In a first step, type 1 DCs (cDC1) are targeted with an  $\alpha$ Clec9A mAb, carrying a specific epitope (Caminschi et al., 2008, Lahoud et al., 2011, Fernandez-Ruiz et al., 2016). In addition, an oligodeoxynucleotide (ODN) adjuvant, CpG was injected. cDC1 are described as the major APCs responsible for T cell priming in *Plasmodium* infection and therefore an ideal target to induce CD8 T cell responses (Lau et al., 2014). CpG induces optimal CD8 T cell priming and liver-associated inflammation (Lahoud et al., 2011, Huang et al., 2013). The combination of both reagents, therefore, led to an optimal T cell activation and inflammatory environment in the liver, ideal for CD8 T<sub>RM</sub> formation (Holz et al., 2018, Mackay et al., 2012). A day after the priming step, a recombinant adeno-associated virus (rAAV) was injected. The rAAV was modified to induce the expression of the same specific CD8 T cell epitope in hepatocytes as used in the priming step. This step, “trapped” the freshly activated antigen-specific CD8 T cells in the liver, improving CD8 T<sub>RM</sub> cell formation (Fernandez-Ruiz et al., 2016). Vaccinated mice were efficiently protected against *Plasmodium* sporozoites, and depletion of CD8 T<sub>RM</sub> cells by injection of an anti-CXCR3 mAb abolished protection. In an additional study, Valencia-Hernandez and co-authors could induce sterile protection in some “prime-and-trap” vaccinated mice without the transfer of transgenic CD8 T cells, activating antigen-specific T cells within the endogenous T cell pool (Valencia-Hernandez et al., 2020). Unlike Fernandez-Ruiz et al., this study used a newly identified natural PbA derived peptide to activate endogenous *Plasmodium* specific CD8 T cell responses that had strong protective capacity (Valencia-Hernandez et al., 2020, Fernandez-Ruiz et al., 2016).

In addition, a self-adjuvating glycolipid-peptide vaccination strategy induced large numbers of malaria-specific CD8 T<sub>RM</sub> cells that provided sterile protection against *Plasmodium* liver-stage infection in mice (Holz et al., 2020). This experimental vaccine approach used  $\alpha$ GalCer linked to a specific peptide. Upon uptake of the conjugate by APCs,  $\alpha$ GalCer and the peptide are separated by cleavage. This results in the presentation of  $\alpha$ GalCer via CD1d to NKT cells and peptide via MHC-I molecules to CD8 T cells. Upon recognition of  $\alpha$ GalCer,

NKT cells activate APCs through CD40L and release soluble factors, which then enhances CD8 T cell activation, generation of large numbers of liver T<sub>RM</sub> cells, and protection against sporozoite infection (Hermans et al., 2003, Fujii et al., 2003, Holz et al., 2020).

These reports demonstrate that sterile protection against *Plasmodium* sporozoite infection can be achieved by CD8 liver T<sub>RM</sub> cell-based vaccination. However, limited knowledge of MHC-I epitopes protective against human malaria infection is a major challenge in the design of an efficient anti-malaria liver-stage vaccine. In addition, different HLA molecules can be expressed by humans, requiring several immunogenic epitopes to induce comprehensive protection.

#### **1.4.2 The role of CD4 T cells in immunity against *Plasmodium* liver-stage infection.**

The role of CD4 T cells in immunity against *Plasmodium* liver-stage infection is less clear than for CD8 T cells. In this context, a prominent role for CD4 T cells is to help B cells to generate protective, high affinity anti-sporozoite antibodies (Tam et al., 1990, Weiss et al., 1993). They may also provide help for CD8 T cell responses (Carvalho et al., 2002). In addition, several studies suggest CD4 T cells may contribute more directly to protection, but it is somewhat unclear whether this is via direct recognition of hepatocytes induced to express MHC-II molecules or via associated APC (Oliveira et al., 2008, Tsuji et al., 1990).

In an extensive study, Dolan and Hoffman examined protective capacity of immune cells induced by RAS vaccination in a variety of mice strains (Doolan and Hoffman, 2000). Antibody mediated CD8 T cell depletion after RAS vaccination abrogated protection in all tested mouse strains. However, protection was also abrogated after CD4 T cell depletion in C57BL6, B6x129, B10.D2, and a reduction of protection after CD4 T cell depletion was also detected in B10.BR, A/J<sup>d</sup> and B10.Q mice. In contrast, RAS vaccinated BALB/c mice depleted of CD4

T cells were still protected against *Plasmodium* liver-stage infection (Doolan and Hoffman, 2000). Therefore, the immunological background of mice used needs to be considered when defining the protective capacity of CD4 T cells.

In a different model, RAS vaccination of beta 2-microglobulin deficient ( $\beta_2M^{-/-}$ ) mice, on a BALB/c and B6 background, which fail to express stable MHC-I proteins and therefore lack CD8<sup>+</sup> T lymphocytes, conferred protection against PbA or *P. yoelii* sporozoite infection compared to WT (BALB/c, B6) mice (Oliveira et al., 2008). This protection was reduced when CD4 T cells were depleted in  $\beta_2M^{-/-}$  vaccinated mice prior to re-challenge. However, several doses and high numbers of RAS were required to induce sterile protection in these mice. In contrast to a study by Doolan and Hoffman, CD4 T cell depletion in RAS vaccinated WT B6 mice did not alter the protective capacity against *P. yoelii* liver-stage infection (Doolan and Hoffman, 2000, Oliveira et al., 2008). Therefore, CD8 T cell were still considered as the main protective cell type but CD4 T cell may induce sporozoite protective mechanisms in the absence of CD8 T cells.

Earlier studies identified a CD4 T cell population specific for the circumsporozoite protein (CSP) isolated from RAS vaccinated BALB/c mice (after two weekly immunisations for a month) (Tsuji et al., 1990). Adoptive transfer of these CSP-specific CD4 T cells into naïve BALB/c mice provided sterile-protection against PbA sporozoite challenge, but not against blood-stage infection. Furthermore, these CD4 T cells secrete IFN- $\gamma$  upon sporozoite and iRBCs stimulation, suggesting that their epitope is expressed during both stages of the parasite lifecycle. In addition, CSP-specific CD4 T cells were also detectable in volunteers immunised by multiple bites of irradiated *P. falciparum* infected mosquitos (Moreno et al., 1991). In this case, CD4 T cells did not only secrete IFN- $\gamma$  upon peptide restimulation, but also lysed CSP-peptide pulsed target cells in a cytotoxic assay. In humans, CS-specific CD4 T cell responses after RTS,S/AS02 vaccination correlated with higher protection to natural infection in individuals in The Gambia, West Africa (Reece et al., 2004). While these studies observed expression of IFN- $\gamma$  by CD4 T cells, suggesting a

dominate T helper 1 (Th1) CD4 subset was generated, no other memory subpopulations were analysed.

Besides the potential role for CD4 T cells in direct mediation of protection against sporozoite infection, other studies implied a role for CD4 T cells in promoting CD8 T cell-mediated sterile immunity after RAS vaccination (Weiss et al., 1993, Carvalho et al., 2002). Antibody-mediated depletion of CD4 T cells prior to RAS vaccination rendered mice susceptible to sporozoite challenge. However, mice depleted for CD4 T cells after immunization were still protected (Weiss et al., 1993). A later study by Carvalho et al. showed that CD4 T cell depletion two days before RAS immunization did not affect malaria-specific CD8 T cells proliferation capacity within the first 72 hours post vaccination (Carvalho et al., 2002). However, CD4 T cell depleted mice had reduced numbers of IFN- $\gamma$  producing malaria-specific endogenous and transgenic CD8 T cells as early as 4 days post immunization. This defect depended on STAT6 and IL-4, suggesting a role for T helper 2 (Th2) CD4 T cells after RAS vaccination in prompting a functional CD8 T cell response (Carvalho et al., 2002). In addition, the adoptive transfer of wildtype, but not IL-4 deficient, CD4 T cells into CD4 T cell depleted mice, rescued CD8 T cell responses after RAS vaccination. However, the authors did not show if IL-4 sustained proliferation of activated CD8 T cells or prevented cell death. Furthermore, it is not clear whether IL-4 acts directly on CD8 T cells or through other cells, such as antigen-presenting cells, which then influence CD8 T cell proliferation.

Collectively, these studies suggest a role of CD4 T cells in protective immunity against the pre-erythrocytic stage of *Plasmodium* infection. However, the mechanisms whereby CD4 T cells provide protection against *Plasmodium* sporozoite infection remain unclear. In particular, knowledge of the memory subpopulations and CD4 lineages that can lead to protective immunity, and the discovery of protective CD4 T cell epitopes, will provide new opportunities to harness these cells for protection through vaccination.

### 1.4.3 CD4 T cell mediated immune response to *Plasmodium* erythrocytic stage

Once *Plasmodium* parasites complete their development in the liver, they rapidly infect RBCs. Mature RBCs do not express MHC-I or MHC-II molecules and therefore cannot be recognized by CD4 or CD8 T cells. However, naïve T cells can be primed against *Plasmodium* blood-stage infection via APCs (Ing et al., 2006, Sponaas et al., 2006, Lundie et al., 2008). For example, splenic CD11c<sup>+</sup> DC activation, which resulted in IL-12 secretion, was observed in mice infected with Pch iRBCs, a non-lethal rodent *Plasmodium* species (Ing et al., 2006). IL-12 is known to induce T helper cell 1 (Th1) polarisation and IFN- $\gamma$  expression by CD4 T cells. Furthermore, it was shown that CD11c<sup>+</sup> CD8<sup>+</sup> and CD8<sup>-</sup> DCs were able to stimulate CD4 T cells to express IFN- $\gamma$  (Sponaas et al., 2006). However, only CD8<sup>-</sup> DCs were able to induce CD4 T cell populations that secreted IL-4 and IL-10 in response to antigen exposure, which suggested a T helper 2 (Th2) and regulatory T cell differentiation bias.

Further studies reported upregulation of MHC-II molecules and costimulatory signals such as CD40 and CD80 on DCs upon *P. yoelli* 17NL blood-stage infection in mice (Perry et al., 2004). This resulted in the activation of CD4 T cells, which in addition to IFN- $\gamma$ , produced IL-2 and TNF.

In mice, administration of IFN- $\gamma$  neutralizing monoclonal antibody (mAb) impaired control of blood-stage infection of several rodent *Plasmodium* species (Yoneto et al., 1999, Stevenson et al., 1990). Therefore, Th1 cells, as a major source of IFN- $\gamma$  upon parasite antigen re-stimulation, are thought to contribute to *Plasmodium* blood-stage control. In support of this view, Oakley et al. showed that mice deficient for the master regulator of Th1 cells, the transcription factor T-bet (*Tbx21*<sup>-/-</sup>), generated diminished numbers of IFN- $\gamma$ <sup>+</sup> CD4 T cells upon PbA blood-stage infection, compared to WT mice and this coincided with elevated parasitemia in *Tbx21*<sup>-/-</sup> mice (Oakley et al., 2013). Similar results were obtained infecting IL-12-deficient (*Il12*<sup>-/-</sup>) mice, which have impaired Th1 differentiation (Su

and Stevenson, 2000). Such mice had reduced numbers of IFN- $\gamma$  expressing CD4 T cells after infection with Pch. Together, these studies suggest that IFN- $\gamma$  secreting Th1 CD4 T cells have an important role in the control of *Plasmodium* blood-stage infection.

IFN $\gamma$  secretion by CD4 T cells is also reported to be involved in the induction of immunopathology. For example, *Tbx21*<sup>-/-</sup> mice were partially protected against the development of experimental cerebral malaria (ECM), a severe form of disease outcome (Oakley et al., 2013). Furthermore, IFN- $\gamma$  producing CD4 T cells accumulate in the spleen, lung and the brain after PbA blood-stage infection (Villegas-Mendez et al., 2012). These cells lead to ECM development through IFN- $\gamma$  secretion and increased accumulation of CD8 T cells in the brain. In contrast, PbA blood-stage infection of type I interferon deficient mice (IFN $\alpha$ R<sup>-/-</sup>), resulted in enhanced IFN- $\gamma$ , Tbet<sup>+</sup> (Th1) CD4 T cell responses, but an absence of ECM (Haque et al., 2011a). In this case, infection of IFN $\alpha$ R<sup>-/-</sup> mice was associated with enhanced control of PbA parasitemia. This suggests that Th1 cells have a critical function in *Plasmodium* blood-stage control, but the role of IFN- $\gamma$  produced by CD4 T cells in the induction of ECM is not fully elucidated.

CD4 T cell effector function against blood stage malaria can involve interactions with macrophages (Fontana et al., 2016, Su and Stevenson, 2000). CD4 T cell-derived IFN- $\gamma$  facilitates macrophage activation (Su and Stevenson, 2000). This stimulation leads to increased phagocytosis of iRBCs and enhanced production of reactive oxygen and nitrogen intermediates which can result in the killing of merozoites and parasites in RBCs (Shear et al., 1989, Su and Stevenson, 2000). In addition to IFN- $\gamma$ , Th1 cells are described to also express macrophage colony-stimulating factor (M-CSF), which is also known as CSF1 (Fontana et al., 2016). Experiments using M-CSF deficient CD4 T cells showed an enhanced loss of tissue-resident CD169<sup>+</sup> macrophages in the spleen after Pch infection (Fontana et al. 2016). Furthermore, these mice displayed reduced control of Pch blood-stage infection. Thus, the interaction between *Plasmodium*-

specific CD4 T cells and macrophages contribute to limiting *Plasmodium* blood-stage parasite growth.

Pch blood-stage infection can be divided into two distinct phases. The acute phase, where parasitemia peaks around day 10 post-infection, and a chronic phase, where low levels of parasites are detected up to 30 days post-infection (van der Heyde et al., 1997, Achtman et al., 2007). Following the induction of IFN- $\gamma$ <sup>+</sup> CD4 T cells in the acute phase of infection, IL-4 secreting CD4 T cells and large antibody responses could be detected in the chronic phase of Pch infection (Sponaas et al., 2006). The later response was historically attributed to Th2 cells helping B cell activation and antibody maturation to finally clear the Pch infection (Langhorne, 1989). The idea of Th2 cell induction during *Plasmodium* infection was strengthened by the observation that IL-4 secreting CD4 T cells and antibody responses were simultaneously detectable in *P. falciparum*-infected individuals (Troye-Blomberg et al., 1990). However, efficient IgG responses, and the control of Pch parasitemia was obtained in IL-4 deficient mice to a similar level compared to WT mice, arguing against this linkage (von der Weid et al., 1994). More recent studies linked follicular helper T (Tfh) cells to a protective B cell and antibody immune response that eventually clears Pch infection (Perez-Mazliah et al., 2017). In addition, single cell RNA sequencing (scRNA-seq) of CD4 T cells after Pch infection revealed a bifurcation between Th1 and Tfh cells as early as day 4 post infection, while no Th2 cells were detected (Lönnerberg et al., 2017). Tfh cells are characterised as a specialized CD4 T helper lineage expressing high levels of CXCR5 and providing help to B cells (Schaerli et al., 2000). Furthermore, the transcription factor Bcl6 is described at the master regulator of Tfh differentiation (Johnston et al., 2009). Pérez-Mazliah and co-authors showed that mice lacking Tfh cells, through a model allowing conditional deletion of Bcl6 in CD4 T cells (Bcl6<sup>fl/fl</sup> CD4-Cre<sup>+/-</sup> mice), displayed disrupted germinal centres (GC) and IgG formation (Perez-Mazliah et al., 2017). Furthermore, those mice were unable to eliminate the otherwise self-resolving infection. Contradicting the separation of Th1 and Tfh lineages, current research reveals IFN $\gamma$ <sup>+</sup>IL-21<sup>+</sup>CXCR5<sup>+</sup> Th1/Tfh hybrid cells form in human malaria patients

and during chronic Pch blood-stage infection in mice (Obeng-Adjei et al., 2015, Carpio et al., 2015). Carpio and co-authors could further show that Th1/Tfh cells strongly depended on Bcl6, Blimp-1, and STAT3 (Carpio et al., 2020). For example, STAT3 KO mice, which show stronger Th1-like (IFN $\gamma$ <sup>+</sup>IL21<sup>-</sup>CXCR5<sup>low</sup>) effector and memory T cell responses, were protected from re-infection, albeit having reduced antibody titres.

Conventional DCs are critical to induce Tfh cell activation and proliferation in *Plasmodium berghei* infection (Fernandez-Ruiz et al., 2017). In contrast, a study by Arroyo and Pepper, postulated B cells as the primary antigen presenting cells responsible for Tfh cell priming after *Plasmodium* blood-stage infection (Arroyo and Pepper, 2019). In this study, B cell deficient or depleted mice had reduced Tfh cell numbers as early as four days post *P. yoelii* infection, compared to WT mice. Furthermore, mice depleted of conventional DCs (cDCs) had similar Tfh numbers compared to WT mice post infection (Arroyo and Pepper, 2019). Both contradicting studies, used different approaches to deplete CD11c expressing DC (cDCs). Fernandez-Ruiz and co-authors used a system where all CD11c<sup>+</sup> cells are depleted by injection of diphtheria toxin (Fernandez-Ruiz et al., 2017). While CD11c is mainly expressed on cDCs, other cells such as activated B cells, T cells, NK and NKT cell are described to express CD11c (Hume, 2011, Rubtsov et al., 2011, Bennett and Clausen, 2007, van Rijt et al., 2005). Therefore, the reduced numbers of Tfh cells after CD11c<sup>+</sup> cell depletion could potentially be influenced by other cells. Arroyo and Pepper, used a more specific cDC deletion strategy (Arroyo and Pepper, 2019). In this system, administration of diphtheria toxin specifically depletes cDCs, but, of note, only 77 % of the cDC compartment was depleted. Therefore, it is possible that the remaining cDCs were sufficient to induce Tfh cells.

Other CD4 T cell subsets also form after *Plasmodium* infection. For example, IL-17<sup>+</sup> ROR $\gamma$ T<sup>+</sup> Th17 cells were shown to form after PbA, *P. yoelii* and Pch infection in mice and *P. vivax* infection in humans (Keswani and Bhattacharyya, 2014, Bueno et al., 2012). Antibody based neutralization of IL-17, a Th17 signature cytokine, post *P. yoelii* 17 XL infection, increased DCs numbers

as early as day 3, but these numbers declined rapidly with the progression of infection. Mice treated with anti-IL17 mAb expressed enhanced levels of MHC-II, CD80 and CD86, suggesting that DC maturation in the presence of Th17 cells is impaired during *Plasmodium* blood-stage infection (Chen et al., 2020). However, deficiency of IL17 did not alter the course of *Plasmodium* infection in mice (Mastelic et al., 2012, Chen et al., 2020).

The induction of immune regulatory CD4 T cells is well described in *Plasmodium* infection, and their regulatory functions can have a variety of effects (Jagannathan et al., 2014, Nie et al., 2007). They can limit immune-mediated pathology but also facilitate higher parasite burdens (Freitas do Rosario et al., 2012, Kurup et al., 2017). The best described regulatory T cells population are CD25<sup>high</sup> Foxp3<sup>+</sup> Treg cells. In *Plasmodium* infection, depletion of Tregs by administering of an anti-CD25 mAb prior to infection increased *Plasmodium* specific non-regulatory CD4 T cell responses and protected mice from the infection (Amante et al., 2007, Nie et al., 2007). However, anti-CD25 mAb treatment did not deplete all Tregs and was not exclusive for this cell type. Therefore, Foxp3-DTR mice were used to specifically deplete Tregs through administration of diphtheria toxin (Kurup et al., 2017). Specific depletion of Foxp3<sup>+</sup> lead to reduced *P. yoelii* blood-parasite burden compared to WT mice. In another study, depletion of Tregs, using the Foxp3-DTR approach, did not alter the blood-parasite levels after PbA infection (Haque et al., 2010). However, expansion of Foxp3<sup>+</sup> Tregs, through injection of IL-2, provided protection against the severe outcome of PbA infection.

Another described regulatory CD4 T cell subset in *Plasmodium* infection are T regulatory type 1 (Tr1) cells (Jagannathan et al., 2014). Tr1 cells are characterized by the co-expression of IFN- $\gamma$  and IL-10 and form early after blood stage *Plasmodium* infection. Unlike Tregs, Tr1 cells express Foxp3 only transiently upon activation (Levings et al., 2005). Type I Interferon responses in *P. yoelii* infection as well as IL-10 and IL-27 are described to favour Tr1 cell differentiation (Sukhbaatar et al., 2020, Zander et al., 2016, Loevenich et al.,

2017). Furthermore, studies using Pch infection in mice demonstrated that Tr1 cells are highly related and can directly derive from Th1 cells (Lönnerberg et al., 2017). Mice with elevated Tr1 cell numbers displayed suppression of inflammatory cytokines such as IFN- $\gamma$ , TNF, IL1 $\beta$ , IL-17 and IL-6, humoral immunity and elevated parasite burden (Couper et al., 2008, Montes de Oca et al., 2016, Zander et al., 2016). On the other side, Tr1 cell development was associated with protection against immune mediated tissue pathology in Pch infected mice (Freitas do Rosario et al., 2012). Furthermore, the frequency of Tr1 cells in children from Uganda was correlated with reduce risk of development of clinical malaria, although higher parasitemia was observed (Boyle et al., 2017).

Another regulatory CD4 T cell subtype, specialised in secretion of IL-27, was recently found to develop after PbA blood-stage infection (Kimura et al., 2016, Sukhbaatar et al., 2020). IL-27 secretion by CD4 T cells led to the suppression of IL-2 production by other CD4 T cells, a cytokine important for T cell differentiation. Reconstitution of T cell receptor beta chain (Tcr $\beta^{-/-}$ ) deficient mice with IL-27 deficient CD4 T cells resulted in reduced parasitemia and improved survival compared to mice reconstituted with wild type CD4 T cells (Kimura et al., 2016). It was further shown that IL-27 drives Tr1 differentiation and IL-10 production in a STAT3 dependent manner (Awasthi et al., 2007, Stumhofer et al., 2007). This suggests CD4 T cell-derived IL-27 has a deleterious, immune suppressive effect, rather than a protective role against blood-stage *Plasmodium* infection.

As shown above, CD4 T cells have multiple roles in the immune response towards *Plasmodium* blood-stage infection and modulate the overall outcome of disease. Induction of large numbers of CD4 T cells expressing Th1-like effector molecules can lower the overall parasite burden but may facilitate the development of immune-mediated pathology. On the other side, induction of a strong regulatory CD4 T cell response can dampen the development of an efficient immune response, resulting in elevated *Plasmodium* parasite burden but potentially reduced immune pathology. Therefore, inducing the appropriate CD4 T cell subpopulation, which protects from infection but also from the onset of

immune pathology, is critical for success of future CD4 T cell-based blood stage malaria vaccines.

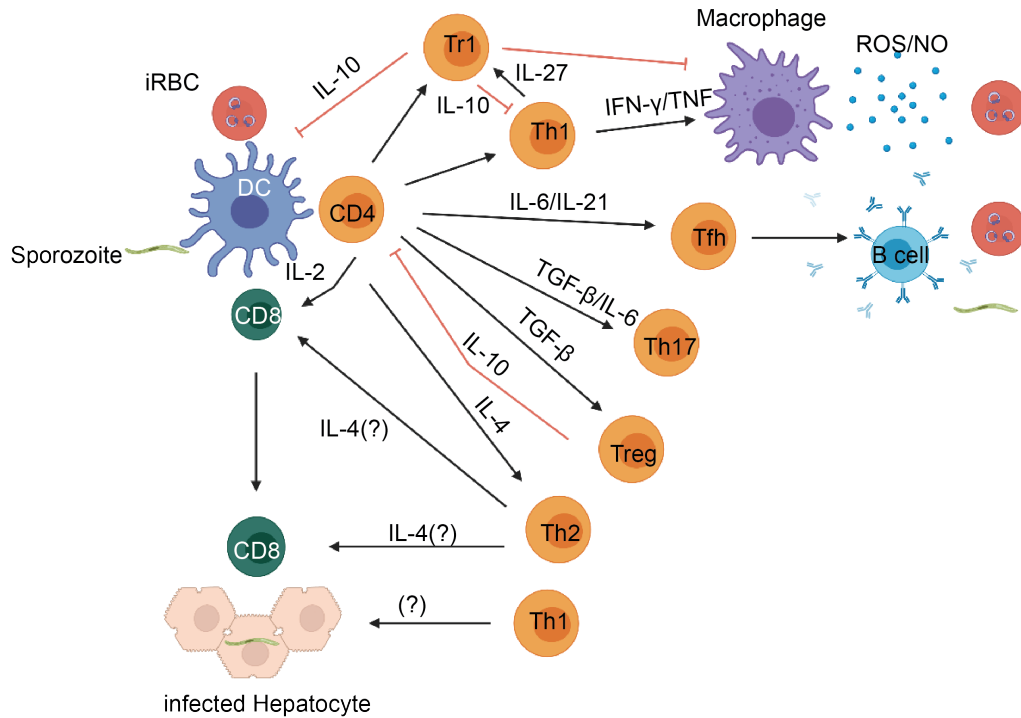


**Figure 1.2. Differentiation and roles of CD4 T cells during *Plasmodium* infection.**

Adapted from Kumar, 2019 (Kumar et al., 2019). DCs capture parasite derived molecules, which results in the release of different cytokines, including IL-12 or IL-6, IL-21 and IL-4. These cytokines, in combination with TCR stimulation, promote the expression of CD4 T cell lineage specific transcription factors that result in the differentiation into T helper (Th)1, T follicular helper (Tfh) and T helper (Th) 2 cell populations. Th1 cells can release pro-inflammatory cytokines, such as IFN $\gamma$  and TNF that stimulate macrophages to phagocytose infected red blood cells (iRBCs) and produce reactive oxygen and nitrogen intermediates (ROS and NO). Under the influence of IL-27 Th1 cells can also differentiate into type 1 regulatory (Tr1) cells that release IL-10 which suppresses ROS and NO production by macrophages as well as antigen presentation by DCs. Before Tr1 cell responses develop, FoxP3<sup>+</sup> CD4 T regulatory (Treg) cells can dampen immune responses in an early stage of *Plasmodium* infection. Treg cells either emerge from the thymus or can develop in the periphery upon IL-2 and TGF $\beta$  signalling. Tfh cells are essential for the selection and maturation process of B cells, immunoglobulin class switching and the development of high-affinity antibody responses. During the pre-erythrocytic stages of *Plasmodium* infection, CD8 T cells can migrate to the liver and recognize and kill infected hepatocytes potentially with the help of *Plasmodium*-specific CD4 T cell. Some reports suggested a Th1 cells can mediate protection against sporozoite infection

independent of CD8 T cell responses. Compared to Th1 and Tfh cells, Th2 and Th17 cell numbers are limited. Nevertheless, their existence has been reported in human and mice malaria studies. Created with Biorender.com.

## 1.5 Malaria Pathogenesis and naturally acquired immunity

Each *P. falciparum* iRBC releases around 16 new merozoites every 48h, leading to a rapid increase in blood parasitemia. During this process, ruptured RBCs can induce secretion of inflammatory cytokines by immune cells, leading to recurring high fever episodes and other malaria-related symptoms. After several replication rounds, *Plasmodium* blood-stage infection in malaria naïve individuals is accompanied by muscle pain, periodical fever, headache, and nausea. In contrast, the pre-erythrocytic stage of *Plasmodium* infections does not induce disease symptoms. If the infection is adequately treated, symptoms associated with blood stage infection decline within a few days, and re-occurring symptoms signify incomplete treatment, drug resistance of the parasite, or reinfection. In the case of *P. vivax* and potentially *P. ovale* infection, rising parasite levels after treatment can also result from reactivation of the dormant liver-resident parasite state (White, 2011, Richter et al., 2010). In sub-Saharan Africa, most deaths from *P. falciparum* infection occur in children under 5 years of age and are associated with symptoms such as severe anaemia, respiratory stress, acidosis, and cerebral malaria (CM) (Mackintosh et al., 2004, Wassmer et al., 2015).

*P. falciparum* induces cerebral malaria, a form of severe malaria with a poor prognosis. Infection with this parasite can lead to sequestration of mature-infected erythrocytes and platelets in the micro-vasculature of different organs (Taylor and Molyneux, 2015, Dorovini-Zis et al., 2011, Grau et al., 2003). This sequestration is mediated through the interaction of parasite-derived proteins such as *Plasmodium* erythrocytic membrane protein-1 (PfEMP-1), exposed on the cell surface of iRBCs, with host receptors such as intercellular adhesion

molecules-1 (ICAM-1), expressed by the endothelial lining (Chakravorty and Craig, 2005). These interactions can lead to blood vessel blockage, which is thought to impair perfusion and lead to damage in several organs such as the retina, and most dramatically, in the brain. The sequestration of iRBCs and platelets in the cerebral microvasculature is associated with coma and in some cases, death (Dorovini-Zis et al., 2011, Grau et al., 2003). In this pathological process, the blood-brain barrier loses its integrity, leading to brain swelling and inflammation (Dorovini-Zis et al., 2011, Greiner et al., 2015, Seydel et al., 2015, Brown et al., 1999). The importance of inflammatory changes in the brain tissue in the development of CM in humans is still under debate. While some studies find immune cell accumulation in the cerebral microvasculature, particularly in younger patients, others show the absence of inflammatory signs in brain tissue of patients who died in the acute phase of CM (Hochman et al., 2015, Grau et al., 2003). Those patients, however, show increased biomass of sequestered infected erythrocytes in the brain microvasculature (MacPherson et al., 1985, Pongponratn et al., 2003).

Animal models have been used to study this process in the controlled conditions of the laboratory. Similar to human CM, several studies confirmed the disruption of the blood-brain barrier, brain swelling, and vascular leakage at a time when ECM symptoms start to occur in PbA infected mice (Thumwood et al., 1988, Nacer et al., 2012, Ghazanfari et al., 2018). In these models, iRBCs and platelet sequestration in the cerebral vasculature is followed by the accumulation of monocytes, neutrophils, T cells, and natural killer cells resulting in an inflammatory environment leading to experimental cerebral malaria (ECM) (Ghazanfari et al., 2018, Belnoue et al., 2008, Hansen et al., 2007). Monocytes and NK cells contribute to the recruitment of T cells into the cerebral vascularity upon PbA blood-stage infection, as shown by depletion studies (Hansen et al., 2007, Pai et al., 2014, Swanson et al., 2016). In this model, CD8 T cells are described to be the central effector cell causing ECM. CD8 T cell depleted or deficient mice were not susceptible to experimental cerebral malaria after PbA infection (Henn et al., 1998, Yanez et al., 1996). Furthermore, the transfer of CD8<sup>+</sup> but not CD8<sup>-</sup> T cells, isolated from PbA infected mice, induced ECM in

otherwise ECM-resistant RAG2-KO mice (Nitcheu et al., 2003). It was shown that perforin and granzyme B, two well-characterized CD8 T cell effector molecules, are required by CD8 T cells to induce ECM (Nitcheu et al., 2003, Haque et al., 2011b). In addition, brain endothelial cells were described to phagocytose free merozoites and cross-present PbA derived epitopes upon IFN- $\gamma$  stimulation, making them susceptible to be killed by *Plasmodium*-specific CD8 T cells (Howland et al., 2015).

CD4 T cells, on the other hand, were mainly reported to facilitate ECM development by initiating CD8 T cell responses. For example, CD4 T cell deficient mice did not develop ECM after PbA infection. However, the depletion of CD4 T cells four days after infection did not alter the outcome of ECM (Belnoue et al., 2002, Boubou et al., 1999, Yanez et al., 1996, Swanson et al., 2016). Another study demonstrated that CD40 ligand deficient mice, where CD4 T cells are incapable of DC licensing, had impaired CD8 T cell proliferation (Fernandez-Ruiz et al., 2017). Five days after PbA blood-stage infection, reduced CD8 T cell responses were detectable in CD40L deficient mice, while the reconstitution of CD40L<sup>-/-</sup> mice with *Plasmodium*-specific CD4 T cells rescued CD8 T cell proliferation. In this study, CD40L<sup>-/-</sup> mice developed ECM 1-2 days later compared to WT or CD40L<sup>-/-</sup> mice injected *Plasmodium*-specific CD4 T cells. Therefore, CD8 T cells seem to be directly involved in ECM induction, while the role of CD4 T cells can be described as a helper function.

To this point, the validity of ECM as a model for human CM is still a matter of debate. Strong similarities exist between CM and ECM; however, human CM data mostly attribute CM to the sequestration of infected red blood-cells. In contrast, mouse models clearly show a critical role for immune responses in ECM development, although iRBC sequestration is also observed. The limited number of available post-mortem studies and the missing accessibility of human brain tissue in patients who survived CM hinders the evaluation of the role of human immune cells in the development of CM. However, recent studies confirmed an accumulation of CD8 T cells within the brain, potentially targeting the cerebrovasculature of CM patients (Barrera et al., 2019, Riggle et al., 2020).

However, differences in T cell frequency, reduced in CM, and compartmentalization, luminal and perivascular in ECM and CM, respectively could be detected. Therefore, further work is required to fully understand the mechanism of CM development in infected individuals. The dissection of this mechanism might potentially lead to new therapeutic approaches to reduce mortality.

Severe anaemia, another severe malaria pathology, is caused by the rupture of infected erythrocytes induced by the parasite and phagocytosis of infected and uninfected red blood cells in the spleen by macrophages (Buffet et al., 2011, Perkins et al., 2011). Uninfected red blood cells were demonstrated to have a reduced life span in a malaria-infected individuals compared to healthy individuals (Berkowitz, 1991). Potentially, reactive oxygen species produced during *Plasmodium* infection alter surface proteins on RBCs, making them susceptible to auto-antibodies and final clearance by macrophages (Jakobsen et al., 1995, Lutz et al., 1996). Furthermore, ROS causes cell membrane injury on infected and uninfected RBCs, triggering exposure of phosphatidyl serine and galactose residues. This leads to antibody independent phagocytosis and therefore increased red blood cell destruction in infected individuals (McGregor et al., 1968, Waitumbi et al., 2000).

Particularly in young children, severe anaemia can correlate with lethality. In addition, hypotension and the occlusion of the microcirculation can lead to a reduced supply of oxygen in some organs, inducing anaerobic glycolysis (English et al., 1997, Warrell et al., 1988). This metabolic shift, termed metabolic acidosis, results in the accumulation of organic acids in the blood, which can lower the pH of the blood, reducing the ability to exchange oxygen and carbon dioxide (Maitland and Newton, 2005). To compensate for the acidosis, patients develop accelerated breathing, a sign of respiratory distress. This distress can then result in organ failure and correlates with poor prognosis in infected individuals (Hanson et al., 2010, Marsh et al., 1995).

In pregnant women, infected red blood cells bind to chondroitin sulfate A, largely expressed in the placental endothelium. This occurs via PfEMP-1; a

parasite protein present on the cell-surface of *P. falciparum*-infected RBCs (Ndam and Deloron, 2007). This interaction leads to sequestration of iRBCs in the placenta, similar to CM, and accumulation of inflammatory immune cells and inflammation (Rogerson et al., 2003b, Rogerson et al., 2003a). This has a deleterious effect on the placenta, causing placental malaria (PM). High numbers of sequestered iRBCs lead to a thickened placenta, altering its function and providing insufficient nutrients to the foetus (Davison et al., 2000). In addition, elevated pro-inflammatory cytokines such as IFN- $\gamma$ , TNF, IL-1 $\beta$  and IL-2 are found locally in the placenta of infected women. These cytokines are described to enhance the phagocytic activity of macrophages and induce T cell proliferation (Suguitan et al., 2003, Fried et al., 1998). While these local responses are aimed at controlling infection in the placenta, the excess inflammation poses a risk for the pregnancy. In *Plasmodium* naïve women or women with their first pregnancy in endemic areas, the structural changes in the placenta associated with infection cause a higher risk of stillbirth (Reeder et al., 1999, Saba et al., 2008). However, multigravida women in endemic areas are less susceptible to severe pathology, due to the development of PfEMP1-specific antibodies (Duffy and Fried, 2003, Staalsoe et al., 2004). These antibodies can inhibit the adhesion of parasites and iRBCs to the placenta, which provides some protection against placental malaria's most severe outcome. Malaria infection in subsequent pregnancies still leads to low birth weight, maternal anaemia, and preterm delivery (McLean et al., 2015, Rogerson et al., 2018).

Interestingly, the passive transfer of maternal immunoglobulin (Ig) before birth and inhibitory factors in the breast milk protect children under 6 months of age against severe malaria (Snow et al., 1998, McGregor et al., 1970, Chizzolini et al., 1991) (Kassim et al., 2000). However, this early protection by maternal antibodies wanes within the first two years, as IgG Ab levels decline in the infant. As a consequence, children between 2 and 4 years old show increased morbidity and mortality compared to infants. Through several subsequent exposures to malaria, young children gradually develop anti-malaria antibodies, which enhance the protection against *Plasmodium* infection over time. For example, an

antibody study in Kenya revealed that children between the ages of 1 and 4 had the narrowest breadth of antibody responses and the lowest antibody titres compared to older children or adults (Dent et al., 2015). Beyond this age, individuals living in endemic areas developed an anti-malaria immune response that lowers the risk of severe malaria development. However, high parasitemia levels in the blood can still be found (Carneiro et al., 2010).

Adults living in high transmission endemic areas naturally acquire immunity that protects against clinical symptoms by controlling parasitemia (Owusu-Agyei et al., 2001, Baird et al., 2003). However, this clinical immunity is not long-lasting, and sterilizing immunity is never achieved (Doolan et al., 2009, Keegan and Dushoff, 2013). For example, in highly endemic areas that experienced a decline in transmission, an increase in the mean age of clinical malaria could be observed, indicating that natural immunity developed more slowly (Marsh and Kinyanjui, 2006). Furthermore, the onset of naturally acquired immunity from people living in low transmission areas is delayed compared to high endemic areas (Fowkes et al., 2016, Carneiro et al., 2010, Marsh and Kinyanjui, 2006). Therefore, the development and maintenance of naturally acquired immunity relies on repeated *Plasmodium* parasite exposure to prevent clinical symptoms.

The exact mechanisms by which naturally acquired immunity develop are not fully understood. Several reports described a correlation of IgG antibodies with reduced risk to develop severe malaria symptoms (Dodoo et al., 2001, Magistrado et al., 2007, Ofori et al., 2002, Yone et al., 2005). This correlation was supported in studies where immune adults were shown to control parasite growth when injected with blood-stage parasites (Bruce-Chwatt, 1962, Langhorne et al., 2008).

## 1.6 Human anti-malaria vaccine approaches

The severe outcomes of *Plasmodium* infection are terrible. While the *Plasmodium* blood-stage can be treated by drug administration, the development of drug resistance parasites is always a concern. An efficient, long-lasting anti-malaria vaccine, stopping symptoms onset and further transmission, would overcome periodical infection and drug treatment cycles and ultimately reduce malaria incidence globally. Currently, several vaccine strategies have been implemented in clinical trials targeting either *Plasmodium* gametocytes, the pre-erythrocytic or erythrocytic stage of infection. This section will introduce some vaccination approaches developed to protect against *Plasmodium* infection in humans.

### 1.6.1 Vaccines targeting the pre-erythrocytic stage of *Plasmodium* infection

Vaccines targeting the pre-erythrocytic stage of infection aim to eliminate infection before the blood-stage can be established. This strategy would prevent malaria-associated pathology and symptoms as well as further transmission. Different vaccine approaches have been used to induce pre-erythrocytic *Plasmodium* protection. Some vaccine strategies target specific *Plasmodium*-derived epitopes and are termed sub-unit vaccines. In contrast, whole sporozoite vaccines, are thought to induce an antigenically broader breadth of immunological responses in vaccinated individuals.

### 1.6.1.1 Sub-unit vaccines.

Currently, one of the most advanced human sub-unit malaria vaccine is RTS,S/AS01 (RTSS Clinical Trials Partnership, 2015). This vaccine consists of a virus-like particle containing several copies of a fragment of the *P. falciparum* CSP (PfCSP). This particle is fused to hepatitis B virus surface antigen and is administered with the liposomal adjuvant AS01 (RTSS Clinical Trials Partnership, 2015). RTS,S/AS01 induced partial clinical immunity during phase III clinical studies. Three doses of RTS,S/AS01, or control vaccine were administered to children (5-17 months of age) and infants (6-12 weeks of age) over a period of two years. Efficacy against clinical malaria in vaccinated children was 36 % and dropped to 26 % in young infants (RTSS Clinical Trials Partnership, 2015). In a follow-up study, at 7 years post-vaccination only 4.4 % of the children in this cohort were still protected (Olotu et al., 2016). Current studies attribute the protection of RTS,S/AS01 vaccination mainly to antibody. However, the induction of CD4 and CD8 T cells responses after RTS,S/AS01 vaccination is documented (White et al., 2013, Kester et al., 2009, Kazmin et al., 2017).

Another sub-unit human malaria vaccine uses a replication-deficient, recombinant chimpanzee adenovirus serotype 63 (ChAd63) as a priming reagent. ChAd63 was combined with a modified vaccinia Ankara (MVA) virus as a booster dose (Ewer et al., 2013, Ewer et al., 2015). The ChAd63-MVA viral particles express a multi-epitope string termed ME-TRAP, which includes the *P. falciparum* TRAP protein and a string of T and B cell epitopes derived from proteins expressed during the pre-erythrocytic stage of *Plasmodium* infection (Ewer et al., 2015, Gilbert et al., 1997).

In controlled human malaria infection, ChAd63-MVA vaccination induced sterile protection in about 20-25% of malaria naïve participants (Ewer et al., 2013). Furthermore, this vaccination approach reduced infection risk by about 67% for an 8-week follow-up period in Kenyan adults (Ogwang et al., 2015). However, no efficacy was observed in participants in Senegal (Mensah et al., 2016). Interestingly, unlike RTS,S/AS01, ChAd63-MVA is designed to generate

a robust CD8 T cell response against sporozoites and, indeed, protection correlated with peripheral CD8 T cell responses in vaccinated volunteers (Ewer et al., 2015, Gilbert et al., 1997).

#### **1.6.1.2 Whole Sporozoite vaccines (WSV)**

Another approach to induce protection against *Plasmodium* infection is the administration of whole sporozoite vaccines. This strategy overcomes the need-to-know immunogenic *Plasmodium* epitopes required to design sub-unit vaccines. Furthermore, WSV generates a more comprehensive immune response by using attenuated sporozoites or live sporozoites under drug treatment to prevent blood-stage infection. However, WSV faces many other challenges, such as large scale sporozoite production, cold temperature storage, and safety concerns about live sporozoites.

Initial studies, demonstrated that administration of radiation attenuated sporozoites (RAS) through mosquito bite infection has the potential to induce protection in humans (Clyde, 1990). However, protocols had to be developed to ensure the safe production of large numbers of RAS. One such RAS vaccine approach, termed "PfSPZ Vaccine" (*P. falciparum* sporozoite), requires injection of up to five doses of  $1.35 \times 10^5$  purified, aseptic, and cryopreserved radiation attenuated sporozoites (Seder et al., 2013). While four doses induced protection in only 33% of malaria naïve participants, 100 % of the enrolled individuals that received five doses of this vaccine were protected against sporozoites when challenged 3 weeks after the last immunization. Furthermore, 55 % of individuals remained protected 21 weeks after receiving four doses of  $2.7 \times 10^7$  RAS (Seder et al., 2013). However, the PfSPZ vaccine only showed about 51 % efficacy in clinical studies in endemic areas (Sissoko et al., 2017). A dose dependent increase in PfSPZ-specific antibodies and circulating T cells levels could be detected in vaccinated individuals (Seder et al., 2013). However, a vaccination study with non-human primates showed a 100-fold higher frequency of

*P. falciparum*-specific CD8 T cells in the liver than in the blood after PfSPZ vaccination (Ishizuka et al., 2016). This raised the possibility that the high numbers of *Plasmodium* specific CD8 T cells in the liver are responsible for the observed protection.

Another way to attenuate sporozoites is to induce specific deletions in the parasite genome. These genetically attenuated parasites (GAP) arrest during liver-stage development and do not proceed into a blood-stage infection. Sporozoite arrest in the liver could be observed in parasite strains in which distinct pre-erythrocytic genes were deleted: p52, p36, and sap1 (Mikolajczak et al., 2014). The so-termed PfGAP3KO parasite strain is shown to be safe and to induce inhibitory sporozoite-specific antibodies following mosquito bite infection in U.S. adults (Kublin et al., 2017). However, PfGAP3KO arrest early in the liver-stage development, which can result in reduced antigenic diversity and breadth of immunity. Therefore, current research focuses on developing late-arresting GAPs to overcome this limitation (Vaughan et al., 2018).

In the previous examples, attenuated sporozoites were used to induce protective immune responses against *Plasmodium* infection. An alternative vaccination strategy is injecting live sporozoites under drug treatment (chemoprophylaxis) to prevent progression to the blood-stage. This chemoprophylaxis and sporozoite immunization (CSP) allows for complete *Plasmodium* liver-stage development, potentially increasing the spectrum of exposed immunogenic antigens. In CHMI studies, CSP vaccination-induced 100 % protection in individuals 8 weeks after the final immunization, and 4 out of 6 participants were still protected 2 years after vaccination (Roestenberg et al., 2011). In a similar study, low numbers of live sporozoites (three doses of  $5.12 \times 10^4$  sporozoites), compared to vaccination with attenuated sporozoites (five doses of  $1.35 \times 10^5$  RAS), induced 100 % protection in volunteers (Mordmuller et al., 2017, Seder et al., 2013). In this study, several antibodies against *Plasmodium* liver-stage antigens were found in the serum of participants. Furthermore, the authors found a positive correlation between protection and induction of *P. falciparum*-specific CD4 memory T cells in volunteers (Mordmuller

et al., 2017). While these studies were performed with homologous sporozoite vaccination and infection, only 2 out of 10 and 1 out of 9 participants were protected against heterologous sporozoite challenge in vaccinated individuals (Walk et al., 2017).

### **1.6.2 Vaccines targeting the erythrocytic stage of *Plasmodium* infection**

While most of the vaccination approaches described so far target the pre-erythrocytic stage of *Plasmodium* infection, other vaccines approaches are designed to target the blood-stage of *Plasmodium* infection. Based on promising results in non-human primates, chemically attenuated *P. falciparum* blood-stage parasites were injected in a small cohort of malaria-naïve individuals (De et al., 2016, Stanisic et al., 2018). In the sera of participants, homologous and heterologous parasite reactive antibodies were detected, but further studies are required to examine the protective capacity (Stanisic et al., 2018).

A small experimental study in which volunteers were injected 4 times with ultra-low doses of around 30 viable *P. falciparum* infected RBCs, followed by drug treatment, resulted in sterile protection against blood-stage infection in 3 out of 4 malaria naïve volunteers (Pombo et al., 2002). Interestingly, no parasite-specific antibodies were detectable, and protection correlated with *Plasmodium* specific IFN $\gamma$ <sup>+</sup> CD4 and CD8 T cells.

Additional efforts have been made to develop blood-stage subunit vaccines to eliminate safety concerns related to the injection of live merozoites. The *P. falciparum* antigen RH5 was encoded into a ChAd and MVA complex, similar to the ChAd63-MVA malaria liver-stage vaccine approach described earlier (Payne et al., 2017, Ewer et al., 2015). RH5 is a novel *P. falciparum* parasite antigen shown to induce merozoite neutralizing Ab *in vitro* and *in vivo* in non-human primates studies (Douglas et al., 2011, Douglas et al., 2015, Illingworth et al., 2019). Initial studies in humans confirmed that RH5 specific Ab and T cell responses were generated in vaccinated participants. Furthermore, those Ab showed parasite growth inhibition in *in vitro* studies. Further studies are

necessary to determine this vaccine's protective capacity (Payne et al., 2017). In addition many other subunit vaccines targeting a variety of proteins expressed by iRBCs or merozoites are currently in clinical trials. Targeting proteins such as MSP3 (MSP3-LPS), subunit of trophozoite export protein (P27A), serine repeat antigen 5 (BK-SE26), AMA-1 (AMA-1 DiCo) and erythrocyte binding protein family member EBA-175 (EBA-175 RII NK) was proven to be safe to use in humans but with variable antibody titer responses leading to low protection efficacy (Sirima et al., 2007, Nebie et al., 2009, Steiner-Monard et al., 2019, Horii et al., 2010, Sirima et al., 2017, El Sahly et al., 2010).

### **1.6.3 Vaccines targeting the transmission of *Plasmodium* parasites.**

An alternative approach to stop *Plasmodium* transmission aims at targeting gametocytes, which mediate transmission through mosquitos. Specific epitopes expressed by gametocytes are targeted to attempt elimination of this parasite population. One such surface protein is Pfs25. In mouse studies, high Ab titers against Pfs25 could be generated, blocking further transmission (Kubler-Kielb et al., 2007). In preliminary humans trials, however, injection of soluble Pfs25 induced insufficient transmission-blocking activity (Miura et al., 2007, Wu et al., 2008, Radtke et al., 2017, Talaat et al., 2016). Furthermore, while such vaccines would progressively reduce malaria, they would not protect individuals from getting infected or developing malaria symptoms.

## **1.7 Research Aims**

Despite successful worldwide efforts to lower the incidence of malaria, this reduction has stalled in recent years. The emergence of drug and insecticide resistance makes it unlikely that malaria eradication will be achieved with current

strategies (WHO, 2019, WHO, 2015). Vaccination will be a significant step to a decisive decrease in infection numbers. A promising target for an anti-malaria vaccine is the liver-stage of *Plasmodium* infection. The elimination of parasites in the liver prevents blood-stage infection and, therefore, associated pathology as well as impeding disease transmission. While vaccines targeting the pre-erythrocytic stage have high efficacy in animal models and controlled human malaria trials with malaria naïve individuals, they show limited effectiveness in malaria-endemic areas (Butler et al., 2010, Clyde, 1990, Fernandez-Ruiz et al., 2016, Ishizuka et al., 2016, Mensah et al., 2016, Nussenzweig et al., 1967, Mordmuller et al., 2017, Seder et al., 2013, Tse et al., 2013, RTS, 2015, Ogwang et al., 2015, Sissoko et al., 2017). This suggests improvements to vaccination strategies are needed for effective deployment in Africa.

Most vaccine strategies targeting the pre-erythrocytic stage rely on the injection of either whole sporozoites or sub-unit vaccines. WSVs face major challenges, as large-scale sporozoite production is slow and cost intensive, WSVs require storage at cold temperatures and there are safety concerns with respect to complete inactivation. Sub-unit vaccines, which target specific *Plasmodium-derived* epitopes, can potentially overcome these challenges, in particular safety issues of delivering infectious sporozoites, if properly designed. However, only limited *Plasmodium-derived* immunogenic antigens have been described. For example, only three MHC-I restricted epitopes from PbA infection have so far been demonstrated to provide sterile protection against *Plasmodium* liver-stage infection in B6 mice (Hafalla et al., 2013, Pichugin et al., 2018, Valencia-Hernandez et al., 2020).

One study identified 14 MHC-II restricted epitopes obtained from PbA blood-stage infection of B6 mice (Draheim et al., 2017). Eight of these were associated with significant cytokine production in mice previously exposed to *Plasmodium* parasites, suggesting they are authentic antigens. Of these, the three most potent MHC-II restricted epitopes (ETRAM10.2, GAPDH, and EF1 $\alpha$ ) were responsible for one-third of total CD4 T cell response after PbA blood-stage infection, protection against sporozoite or blood-stage infection was not

investigated (Draheim et al., 2017). Our laboratory previously generated an MHC-II-restricted TCR transgenic mouse line, termed PbT-II, specific for a so far unknown *Plasmodium* epitope derived from PbA blood-stage infection (Fernandez-Ruiz et al., 2017). Interestingly, PbT-II cells were shown to respond by proliferation to various rodent blood-stage *Plasmodium* species as well as to human *P. falciparum*-infected red blood cells. Furthermore, PbT-II cells proliferated after vaccination of B6 mice with radiation attenuated sporozoites (RAS). Thus, this novel MHC-II restricted epitope is not only highly conserved throughout *Plasmodium* species but also proven to activate *Plasmodium*-specific CD4 T cells after inoculation of radiation attenuated sporozoites or blood-stage parasites. Given its conserved nature and presence throughout the life cycle this antigen appeared to be potentially valuable for vaccination studies. Thus, it became important to identify the *Plasmodium* epitope recognised by PbT-II T cells. Its identification would not only add to the limited number of immunogenic *Plasmodium*-specific CD4 T cell epitopes, but it would also allow the study of CD4 T cell responses to both *Plasmodium* liver and blood-stage infections. Identification of the epitope would also allow for assessment of its ability to generate long-lasting memory CD4 T cell responses, essential for any vaccination approach.

In many studies, the importance of T<sub>RM</sub> cells as the first line of defence against pathogens in several tissues has been demonstrated. It was explicitly shown that liver-resident CD8 T cells induced by RAS vaccination were essential to facilitate sterile-immunity against *Plasmodium* sporozoite infection in mice (Fernandez-Ruiz et al., 2016). Although it is not clear whether liver resident CD4 T cells form during *Plasmodium* infections, the formation of liver homing CD4 T cells in a salmonella vaccination study was shown (Benoun et al., 2018). Furthermore, CD4 T<sub>RM</sub> cells were documented to improve CD8 T<sub>RM</sub> cell formation in the lung and protection in an influenza infection model (Son et al., 2021). Thus, the identification of a *Plasmodium*-specific liver resident CD4 T cell population and determining their potential role in enhancing CD4 or CD8-mediated protection against sporozoite inoculation could fundamentally change the way liver-stage sub-unit vaccines are designed.

In addition, several studies have postulated a protective role for CD4 T cells towards liver- and blood-stage *Plasmodium* infection (Doolan and Hoffman, 2000, Oliveira et al., 2008, Fontana et al., 2016). However, it was not determined what MHC-II restricted epitopes induced protective CD4 T cell responses and how those responses could be harnessed to mediate protection. Thus, this project aimed to examine the protective capacity of T cells specific for the epitope recognised by PbT-II cells in their response to both liver and blood-stages of infection.

The aims of this project can be summarised as follows:

1. To identify the cognate antigen of PbT-II cells and characterize the development of CD4 T cell memory populations towards this MHC-II restricted epitope (Chapter 3).
2. To examine the existence of *Plasmodium*-specific liver-resident CD4 T cells after various activation methods and compare such cells to the well characterized CD8 T<sub>RM</sub> population in the liver (Chapter 4).
3. To determine the protective capacity of Hsp90-specific CD4 T cells towards *Plasmodium* liver- and blood-stage infection (Chapter 5).

## **Chapter 2**

### **Materials and Methods**

## Chapter 2 Material and Methods

### 2.1 Materials

**Table 2.1 List of antibodies and dyes.**

The table shows antibody name, fluorochrome, clone, company and dilution.

Name	Conjugate	Clone	Source	Cat. Number	Dilution
Bcl6	PerCPcy5.5	K112-91	BD Pharmingen™	562198	1:100
Bcl6	PerCP-eFluor 710	BCL-DWN	eBioscience™	46-5453-82	1:100
CD101	PE-Cy7	Moushi101	eBioscience™	25-1011-82	1:200
CD27	BV605	LG.3A10	BioLegend®	124233	1:200
CD38	eFLuor450	HIT2	eBioscience™	48-0389-42	1:400
CD4	APC	RM4-5	BD Pharmingen™	553051	1:400
CD4	PE	RM4-5	BD Pharmingen™	553049	1:400
CD4	BV604	RM4-5	BD Pharmingen™	563747	1:400
CD44	BV510	IM7	BD Horizon™	563114	1:200
CD44	AF700	IM7	eBioscience™	56-0441-82	1:200
CD45.1	AF700	A20	BD Pharmingen™	561235	1:100
CD45.2	PE-Cy7	104	BioLegend®	109830	1:100
CD45R (B220)	PerCP-Cy5.5	RA3-6B2	eBioscience™	45-0452-82	1:200
CD49a	BV711	Ha31/8	BD Horizon™	564863	1:200
CD62L	PerCP-Cy5.5	MEL-14	eBioscience™	45-0621-82	1:200
CD62L	BV605	MEL-15	BD Horizon™	563252	1:200

CD69	PE-Cy5	H1.2F3	eBioscience™	15-0691-82	1:200
CD69	BV605	H1.2F3	BioLegend®	104530	1:200
CD8	BV711	53-6.7	BioLegend®	100748	1:400
CD8	APC	53-6.7	BD Pharmingen™	553035	1:400
Cell trace violet™			Invitrogen™	C34557	0.5µl/ml
CX3CR1	APC	SA011F11	BioLegend®	149008	1:200
CX3CR1	PE/Dazzle™ 594	SA011F11	BioLegend®	149014	1:200
CXCR3 (CD183)	APC	CXCR3-173	eBioscience™	17-1831-82	1:200
CXCR3 (CD183)	BV605	CXCR3-173	BioLegend®	126523	1:200
CXCR5	Biotin	2G8	BD Pharmingen™	551960	1:200
F4/80	AF647	BM8	BioLegend®	123122	1:100
FC-block (CD16/CD31)			BD Pharmingen™	553142	1:200
FoxP3	eFluor® 450	FJK-16s	eBioscience™	48-5773-82	1:200
GATA-3	PE-Cy7	L50-8233	BD Pharmingen™	560405	1:100
Ghost Red Dye 780			Tonbo Biosciences	13-0865-T500	1:500
Hoechst 33258			ThermoFisher Scientific	H3569	5pg/ml
IFN-γ	PE-Cy7	XMG1.2	BD Pharmingen™	557649	1:100
IFN-γ	BV605	XMG1.2	BioLegend®	505839	1:100
IFN-γ	BV421	XMG1.2	BioLegend®	505829	1:100
IL-2	PE	JES6-1A12	BioLegend®	503702	1:100
IL-2	APC	JES6-5H4	BioLegend®	503810	1:100
IL-4	APC	11B11	eBioscience™	17-7041-81	1:100
IL-10	PE-Cy7	JES5-16E3	BioLegend®	505025	1:100

IL-13	PE	eBio13A	eBioscience™	12-7133-82	1:50
IL-17	APC	TC11-18H10.1	BioLegend®	506916	1:50
KLRG1	APC	2F1	Bioscience™	17-5863-82	1:200
KLRG1	BV605	2F1/KLRG1	BioLegend®	138419	1:200
LIVE/DEAD™ M Fixable Near-IR Dead Cell Stain Kit for 633 or 635 nm excitation			Invitrogen	L10119	1:400
Ly6C	BV785	HK1.4	BioLegend®	128041	1:200
NK-1.1	Percp-Cy5.5	PK136	BioLegend®	108728	1:200
P2X7/P2RX7	PE	HANO43	Novus Biologicals	NBP1-40894PE	1:200
PD1	PE-Cy7	29F.1A12	BioLegend®	135216	1:100
RoryT	APC	B2D	eBioscience™	17-698182	1:100
Streptavidin	PE		BD Pharmingen™	554061	1:200
Tbet	BV711	04-46	BD Horizon™	563320	1:100
Tbet	BV421	4B10	BioLegend®	644832	1:100
Tbet	PE	4B10	eBioscience™	12-5825-82	1:100
TNF	BV711	MP6-XT22	BioLegend®	506349	1:100
TNF	PE-Cy7	MP6-XT22	BD Pharmingen™	557644	1:100
TNF	BV421	MP6-XT22	BioLegend®	506328	1:100
Vα2	BV785	B20.1	BD OptiBuild™	743833	1:400
Vα2	PE-Cy7	B20.1	BD Pharmingen™	560624	1:400
Vα2	BV421	B20.1	BD Horizon™	562944	1:400
Vα3.2	APC	RR3-12	eBioscience™	17-5799-82	1:400
Vα8.3	PE	KT50	BioLegend®	125707	1:400

V $\beta$ 12	PE	MR11-1	BioLegend®	139704	1:400
--------------	----	--------	------------	--------	-------

**Table 2.2 List of antibodies for CD4 T cell enrichment**

Purified Rabbit anti-mouse	Clone
$\alpha$ -erythrocyte	Ter119
$\alpha$ -I-A/E	M5/114
$\alpha$ -CD8	53-6.7
$\alpha$ -GR-1	RB6-8C5
$\alpha$ -CD11b	M1/70
$\alpha$ -F4/80	BM8

**Table 2.3 List of antibodies for CD8 T cell enrichment**

Purified Rabbit anti-mouse	Clone
$\alpha$ -erythrocyte	Ter119
$\alpha$ -I-A/E	M5/114
$\alpha$ -CD4	GK1.5
$\alpha$ -GR-1	RB6-8C5
$\alpha$ -CD11b	M1/70
$\alpha$ -F4/80	BM8

All antibodies for CD4<sup>+</sup> and CD8<sup>+</sup> T cell enrichment were made by Recombinant antibody facility WEHI, Australia.

**Table 2.4 List of mice strains used in this study**

Strain	Description
C57BL/6 (B6)	Mice expressing MHC class I H-2 <sup>b</sup> and MHC class II I-A <sup>b</sup> and the congenic marker Ly5.2/CD45.2.
B6.SJL- <i>Ptprca<sup>a</sup>Pepcb<sup>b</sup></i> /BoyCrl	Mice expressing MHC class I H-2 <sup>b</sup> and MHC class II I-A <sup>b</sup> and the congenic marker Ly5.1/CD45.1.
PbT-I/uGFP	Mice generated on a B6 background expressing K <sup>b</sup> -restricted T cell receptor ( <i>V<math>\alpha</math>8.3 7 J<math>\alpha</math>11/V<math>\beta</math>10 D<math>\beta</math>2.1 J<math>\beta</math>2.2</i> ) specific for PbA blood-stage peptide and express

	green fluorescent protein (GFP) under the control of the ubiquitin C promotor.
PbT-II-157 (PbT-II)	Mice generated on a B6 background expressing I-A <sup>b</sup> -restricted T cell receptor (V $\alpha$ 2.7 J $\alpha$ 12/V $\beta$ 2 D $\beta$ 2.1 J $\beta$ 2.4) specific for PbA blood-stage infection derived epitope PbHsp90 <sub>(484-496)</sub> (DIYYITGESINAV)
PbT-II/uGFP	PbT-II mice that express a green fluorescent protein (GFP) under the control of the ubiquitin C promotor.
PbT-II/ubiTomato	PbT-II mice that express a red fluorescent protein (Tomato) under the control of the ubiquitin C promotor.
OT-II	Mice generated on a B6 background expressing CD4 <sup>+</sup> transgenic TCR (V $\alpha$ 2/ V $\beta$ 5) specific for an OVA derived epitope (OVA <sub>323-339</sub> )
OT-II/ ubiTomato/Ly5.1	OT-II mice expressing a green fluorescent protein (GFP) under the control of the ubiquitin C promotor and the congenic marker Ly5.1/CD45.1.
B6.gDT-II (gDT-II)	Mice generated on a B6 background expressing I-A <sup>b</sup> -restricted T cell receptor (V $\alpha$ 3.2 J $\alpha$ 16/V $\beta$ 2 D $\beta$ 2.1 J $\beta$ 2.1) specific for HSV-1-derived glycoprotein D peptide gD <sub>(315-327)</sub> ,
gDT-II $\times$ Ly5.1 (gDT-II.Ly5.1)	gDT-II mice expressing the congenic marker CD45.1.
gDT-II $\times$ B6.uGFP (gDT-II.uGFP)	gDT-II mice expressing a green fluorescent protein (GFP) under the control of the ubiquitin C promotor.
B6.Cd40L <sup>-/-</sup> (Cd40L <sup>-/-</sup> )	B6 mice that lack the expression of CD40L (CD154)

**Table 2.5 List of cell lines used in this study**

Cell line	Origin	Description	Source/References
B16.F1t3L cells	Mouse melanoma	Polyclonal B16.F10 cell line retrovirally transduced to express FMS-like tyrosine kinase 3ligand (Fit3L)	Mach et al., 2000

**Table 2.6 Primers used for qPCR**

<b>Oligo</b>	<b>Use in this study</b>
<b>Pb18SF</b>	AAGCATTAAATA AAGCGAATACAT CCTTAC
<b>Pb18SR</b>	GGAGATTGGTTT TGACGTTTATGT G
mBDNF	CTGGATGCCGC AAACATGTC
mBDNR	CTGCCGCTGTGA CCCACTC

**Table 2.7 List of used *Plasmodium* species**

<b>Species</b>	<b>Origin / Source</b>
<i>Plasmodium berghei</i> ANKA (PbA)	BEI Resources, MRA871
<i>Plasmodium chabaudi</i> AS (Pch)	Jean Langhorne (Spence et al., 2013)

**Table 2.8 Different medias used in this study**

<b>Media/solution</b>	<b>Source</b>
DMEM	Thermo Fisher Scientific
Hanks Buffered Salt Solution (HBSS)	Media Preparation Unit, Dept. Microbiology & Immunology, University of Melbourne, Australia.
KDS-RPMI	Media Preparation Unit, Dept. Microbiology & Immunology, University of Melbourne, Australia.
Phosphate Buffered Saline (PBS)	Media Preparation Unit, Dept. Microbiology & Immunology, University of Melbourne, Australia.
FACS buffer	PBS 5 % w/v BSA, EDTA 5mM

**Table 2.9 Peptides and recombinant proteins used for *in vitro* differentiation**

Peptides and recombinant proteins	Source
Recombinant human IL-2	Peprtech Inc., USA
Recombinant murine IFN $\gamma$	Peprtech Inc., USA
Recombinant murine IL-12 (p70)	BioLegend®
Recombinant murine IL-4	BioLegend®
Recombinant murine IL-6	BioLegend®
Recombinant murine TNF	Peprtech Inc., USA
gD <sub>(315-327)</sub> , Seq: IPPNWHIPSIQDA	Auspep, Australia.
PbHsp90 <sub>(484-496)</sub> Seq: DIYYITGESINAV	Auspep, Australia
OVA <sub>(323-339)</sub> Seq: ISQAVHAAHAEINEAGR	Auspep, Australia

**Table 2.10 Antibodies used for *in vitro* differentiation**

Antibodies	clone	Source
anti-IL-4	11B11	BIO X Cell
anti-IFN $\gamma$	XMG1.2	BIO X Cell

**Table 2.11 Antibodies and detection reagents for Elispot assay**

Antibodies	clone	Source
anti-IFN- $\gamma$ (capture)	AN-18	WEHI Antibody Services
biotin-conjugated anti-IFN- $\gamma$ (detection)	R4-6A2	WEHI Antibody Services
Streptavidin -HRP		MabTech
TMB Substrate		MabTech

**Table 2.12 List of enzymes used in this study**

Enzyme	Source
10X Trypsin/EDTA	Sigma Aldrich, USA
Heparin	Clifford Hallam

Collagenase 3	Worthington Biochemicals
DNase I	Roche Diagnostics

**Table 2.13 Animal Serum**

<b>Serum</b>	<b>Source</b>
Normal Donkey Serum	Jackson Immuno Research
Normal Mouse Serum	Jackson Immuno Research
Normal Rat Serum	Jackson Immuno Research

**Table 2.14 Commercially available kits**

<b>Kit</b>	<b>Source</b>
Cytofix/Cytoperm™ Fixation/Permeabilization Solution Kit	BD Biosciences
eBioscience™ Foxp3/ Transcription Factor Buffer Set	Invitrogen™
Fast SYBR™ Green Master Mix	Applied Biosystems™
<b>High-capacity cDNA Reverse Transcription Kit</b>	Thermo Fisher Scientific
<b>SensiMix™ SYBR® Hi-ROX Kit</b>	Meridian Bioscience™

**Table 2.15 List of general chemicals and reagents**

<b>Chemicals</b>	<b>Source</b>
2-β-mercaptoethanol	Sigma-Aldrich
Aceton	Chem-Supply, Australia
Acid Phenol:Chloroform pH4.5	Invitrogen™
Agarose	Sigma-Aldrich
Bovine Serum Albumin (BSA)	Sigma-Aldrich
Brefeldin A (BFA)	Sigma-Aldrich
Chloroquine diphosphate salt	Sigma-Aldrich

DETACHaBEAD Mouse CD4	Invitrogen
Dimethyl sulphoxide (DMSO)	Sigma-Aldrich
Dynabeads mouse CD4 (L3T4)	Invitrogen
EDTA, tetrasodium salt dihydrate	Sigma-Aldrich
Fetal calf serum (FCS)	CSL, Australia
Glycine	Carl Roth
Guanidine thiocyanate	Sigam-Aldrich
Hoechst 33258	ThermoFisher Scientific
Ionomycin	Sigma-Aldrich
Isoflurane	Cenvet, Australia
Ketamine	Parnell Laboratories, Australia
L-glutamine	Thermo Fisher Scientific
Lipopolysaccharide (LPS)	InvivoGen
N-Methylacetamide	Sigma-Aldrich
Nycodenz	Nycomed Pharma AS
Paraformaldehyde, EM grade, 16 %	Electron Microscopy Science, Australia
Percoll®	GE Health Care. Chicago, ILm USA
Penicillin	CSL
ProLong™ Gold Antifade Mountant	Life Technologies™
Propidium Iodide	Sigma-Aldrich
QIAzol™ Lysis Reagent	QIAGEN®
Red blood cell lysis buffer (Hybri-Max)	Sigma-Aldrich
<b>Serum-free Protein Block (DAKO)</b>	DAKO, Australia
SPHERO blank calibration beads (6.0-6.4 µm)	BD Pharmingen, USA
Streptomycin	Sigma-Aldrich,
Sucrose	Sigma-Aldrich
Tissue-Tek® Optical Cutting Temperature (O.C.T) compound	Dakura Finetek, USA
Tris	Carl Roth
Tween-20	Carl Roth
Ultrapure Dnase/Rnase free distilled water	Life Technologie, USA

**Table 2.16 Consumables**

<b>Consumable</b>	<b>Source</b>
10mL syringe	Terumo, Australia
18G needle	Terumo, Australia
1mL syringe	Terumo, Australia
21G needle	Terumo, Australia
24 well flat bottom plate	Corning, USA
26G needle	Terumo, Australia
30G syringe	BD Biosciences, USA
3mL syringe	Terumo, Australia
96 well f bottom plate (Clear plate, clear bottom)	Corning, USA
96 well round bottom plate (Clear plate, clear bottom)	Corning, USA
96-well plate LightCycler 480 (white)	Roche Life Sciences
Cell strainer, 70µm	Miltenyi Biotec, Germany
Electric shaver	Wahl, USA
Glass coverslips No 1.5 (24 × 50mm)	ProSciTech, Australia
Goat anti-rat IgG magnetic beads	Qiagen, Germany
Lacri-lube™ lubricating eye gel	Allergen Australia, Australia
Magnetic column	Life Technologies, USA
Metal sieve	Sefar Metal Mesh, Australia
MicroAmp optical 385-well reaction	Life Technologies, USA
Micropore™ surgical tape	3M, USA
MultiScreen-IP, clear Filter Plates	Merk
Pap pen	Daido Sangyo, Japan
Polypropylene round-bottom FACS tubes (5mL)	BD Biosciences, USA
Surgical blades	Livingstone, Australia
Sterile suture, Coated VICRYL 5-0	©Ethicon
Sterile suture, Prolene 3-0	©Ethicon

Vacuum grease Dow	Corning, USA
Veet™	Reckitt Benckiser, UK

## 2.2 Methods

### 2.2.1 Mice

Mice were maintained under Specific-pathogen-free (SPF) conditions at the Bioresource Facility (BRF) of the Department of Microbiology and Immunology, University of Melbourne. All transgenic strains were generated on a C57BL/6 (B6) background. Mice were housed with littermates of the same sex (up to 5 mice per box) and used for experiments between 6 to 12 weeks of age. Euthanasia was performed by carbon dioxide (CO<sub>2</sub>) administration at a fill rate of 1.6 g/l. Mice used for 2-photon intravital imaging were euthanised by cervical dislocation under isoflurane anaesthesia. All animal experiments were approved by the University of Melbourne Animal Ethics Committee. Animal ethics application numbers: 1814522, 20088, 1814660.

### 2.2.2 *Plasmodium* infections

#### 2.2.2.1 *Plasmodium* parasite infection

PbA sporozoites for liver-stage infection or RAS vaccination were obtained from the McFadden laboratory (The school of Biosciences, University of Melbourne). Sporozoites were either irradiated using 20,000 Rad or left untreated before being diluted in cold PBS. Between 500 and 50,000 sporozoites in a volume of 0.2 ml PBS were injected intravenously (i.v.) per mouse.

For blood-stage *Plasmodium* infection, donor mice were injected with frozen stabilates of blood stage parasites. After 3-7 (PbA) or 6-8 (Pch) days, donor mice were euthanised, cardiac bleeding was performed, parasitaemia was measured and recipient mice were injected i.v. with the indicated amount of PbA or Pch infected red blood cells (iRBC) diluted in 0.2 ml cold PBS. Parasitaemia was assessed by microscopic analysis of blood smears or by flow cytometry (see below).

#### **2.2.2.2 *Plasmodium* infection monitoring and treatment**

*Plasmodium* parasite infected mice were monitored daily. Mice were cured from PbA infection by intraperitoneal (i.p.) injections of 0.8 mg chloroquine for 5 consecutive days, starting on the 5th day post infection, followed by provision of drinking water containing 600 mg/l chloroquine for 3 additional days.

Untreated mice were assessed for parasitaemia from day 5 (PbA) or day 6 (Pch) by incubating ~2  $\mu$ l tail blood with a 5 pg/mL Hoechst 33258 solution in FACS buffer for 1 hour at 37°C. Parasite infected RBC were discriminated from uninfected RBC using a 405 violet laser and a 450/50 filter, using a Fortessa (BD Immunocytometry Systems, San Jose, CA, USA), and analysed through FACSDiva (BD Immunocytometry Systems) or Flowjo software (Tree Star, Ashland, OR, USA).

Untreated PbA infected mice were monitored daily for signs of experimental cerebral malaria (ECM). Mice were considered ECM positive, when symptoms, such as ataxia and paralyses, evaluated by inability to self-right, occurred. ECM positive mice were euthanized.

### 2.2.3 Enrichment of CD4 or CD8 T cells

Spleens and/or lymph nodes (LN) of B6, PbT-I, PbT-II or gDT-II mice were harvested into cold RPMI-10 (RPMI containing 10 % FCS, 2 mM L-glutamine, 5 mM HEPES and 50 mM 2-mercaptoethanol) and a single cell suspension was generated by passing organs through a sterile 70  $\mu$ m cell strainer. Cells were washed in RPMI-10, resuspended in RBC lysis buffer for 3 min and then washed again in RPMI-10. T cells were enriched by negative selection using magnetic beads. Briefly, cells were incubated for 30 min on ice with purified rat mAbs  $\alpha$ -Mac-1 (M1/70),  $\alpha$ -F4/80 (BM8),  $\alpha$ -erythrocyte (TER-119),  $\alpha$ -GR-1 (RB6-8C5),  $\alpha$ -I-A/E (M51/14) and  $\alpha$ -CD4(GK.15) or  $\alpha$ -CD8 (53-6.7), respectively. Cells were washed and then incubated for 20 min on a roller at 4 °C with goat  $\alpha$ -rat IgG-coupled magnetic beads, that were previously washed 3 times with RPMI-10. Following incubation, cells bound to beads were removed using a magnetic column and the supernatant was collected.

In addition, gDT-II cells were positively enriched using the Dynabeads® Mouse CD4 kit (L3T4) (Invitrogen). Dynabeads were added at a ratio of 1 bead: 1 cell and incubated for 20 min on a roller at 4 °C. The bead-cell solution was placed on a magnetic column and unbound cells were discarded. DETACHaBEAD (Invitrogen) was used, per manufacturer's instructions, to release CD4<sup>+</sup> T cells from beads. In Brief, 25  $\mu$ l, washed, anti-CD4 beads per 10<sup>7</sup> cells were incubated with cells (concentration 10<sup>7</sup> cells/ml) for 20 min at 4 °C under constant rolling. Next, 1-3 ml RPMI-2.5 was added to cells, and the tube was placed on a magnetic tube rack. Beads, cell mixture, was washed 3 times in RPMI-2.5. Once the supernatant was removed, the tube was removed from the magnet. Next, cells were resuspended in 300  $\mu$ l RPMI-2.5, and 30  $\mu$ l Detach-A-beads were added and incubated for 45 min at RT under constant rolling. After incubation, 2 ml RPMI-2.5 was added to cells, and the tube was placed on a magnet for 3-4 min. The supernatant was collected into a 50 ml tube, and beads

were washed 3 times, and the supernatant was collected in the same tube. Two samples were taken for enumeration and purity determination.

#### **2.2.4 Dendritic cell isolation**

Dendritic cells were purified from the spleens of naïve mice or mice subcutaneously (s.c.) injected with  $5 \times 10^6$  B16.F1t3L cells 8-10 days prior to harvest. Spleens were finely minced and digested in 1 mg/ml collagenase 3 (Worthington Biochemical Corporation, Lakewood, NJ, USA) and 20  $\mu$ g/ml DNase I (Roche Diagnostics Germany, Mannheim, Germany) under intermittent agitation for 20 min at RT. DC-T cell complexes were disrupted by adding EDTA (pH 7.2) to the digest to a final concentration of 7.9 mM and incubated for an additional 5 min. The suspension was filtered through a 70  $\mu$ m mesh and resuspended in 5 ml of 1.077 g/cm<sup>3</sup> isosmotic nycodenz medium (Nycomed Pharma AS, Oslo, Norway), and layered above 5 ml nycodenz medium, overlaid with 1-2 ml of FCS. Next, the gradient was centrifuged at 1,700 x g at 4 °C for 12 min. The DCs containing layer was resuspended in complete RPMI-10 medium before use in functional assays.

#### **2.2.5 *In vitro* differentiation of PbT-II and gDT-II cells**

$10^6$  PbT-II or gDT-II cells were cultured with  $10^7$  naïve DCs enriched as described above. Prior to co-culture, DCs were coated with 0.5 mg/ml Hsp90<sub>(484-496)</sub> or gD<sub>(315-327)</sub> peptide in RPMI-10 in the presence of 1  $\mu$ g/ml LPS for 30 min at 37°C. Polarization was performed for 4-5 days in a humidified incubator (37°C, 6.5 % CO<sub>2</sub>). Th1 polarization was induced by adding 1  $\mu$ g/ml LPS, 10 U/ml IL-2, 5  $\mu$ g/ml  $\alpha$ IL-4 and 5 ng/ml IL-12 to the culture. Th2 polarization was induced by adding 10 U/ml IL-2, 60 ng/ml IL-4 and 5  $\mu$ g/ml  $\alpha$ IFN- $\gamma$  to the culture. On day 3 of

culture 15 ml fresh RPMI-10, including specific polarization reagents, were added to the culture.

Prior to transfer, cells were washed 3 times with PBS, counted and their purity was analysed by staining with antibodies against, CD4, V $\alpha$ 2, V $\beta$ -12, V $\alpha$ 3.2, Tbet, Gata3, Ror $\gamma$ T or FoxP3.

### **2.2.6 Adoptive cell transfer**

A cell count was performed with a hemocytometer using trypan blue to exclude non-viable cells. Cell concentration was adjusted to required concentration and injected in a volume of 0.2 ml PBS vial tail vein.

### **2.2.7 Assessment of PbT-II activation and proliferation**

PbT-II cells enriched from the spleens and lymph nodes of PbT-II mice as described above were adjusted to  $10^7$  cells/mL in PBS containing 0.1 % BSA (Sigma). CellTrace™ violet was then used to label PbT-II cells: 40  $\mu$ L DMSO/vial were used to reconstitute the lyophilised CTV stock. Then, 0.5  $\mu$ L CTV per ml of cells were added, and cells were incubated for 10 min at 37°C, followed by two washes in RPMI containing 2.5 % FCS. For *in vivo* proliferation assays  $5 \times 10^4$  or  $5 \times 10^5$  CTV labelled cells were injected in a volume of 0.2 ml PBS via the tail vein. Mice were vaccinated one day later with  $\alpha$ Clec9A-DIY or  $5 \times 10^4$  RAS. In other experiments  $5 \times 10^5$  CTV labelled PbT-II cells were injected one day prior or 7 or 28 days post-vaccination with  $5 \times 10^4$  RAS. Spleens were harvested 4 days after  $\alpha$ Clec9A-DIY vaccination or 6 days after transfer into RAS vaccinated mice and cell numbers and CTV dilution were determined by flow cytometry.

For PbT-II activation assays, DC ( $6.5 \times 10^5$ ) were incubated with the indicated amounts of peptide, or with 6  $\mu$ l of each of the fractions generated by liquid chromatography, for 1 hour prior to adding  $5 \times 10^4$  CTV-coated PbT-I.GFP cells per well. CTV dilution and upregulation of CD69 were measured in PbT-II cells cocultured overnight with DC, using flow cytometry.

### **2.2.8 Parabiotic mice**

Surgery for generation of parabiotic mice was performed under sterile condition as described by Jiang et al. (Jiang et al. 2010). Briefly, vaccinated, age and weight matched mice were anaesthetised and shaved along the opposite lateral skin flanks. Skin was cleaned and disinfected with alcohol prep pads, and chlorhexidine followed by treatment with Betadine. Mirrored incisions were made on the skin flank of both mice, A non-absorbable 5-0 VICRYL thread was placed through olecranon and knee joints to secure legs. Surgical staples and absorbable 3-0 PROLENE sutures were used to conjoin the skin of the mice. Mice were monitored every hour for the first 8 h post surgery. On the following days, mice were monitored 3 times per day and from day 4 twice daily. Once mice reached day 14 post-surgery, monitoring was performed once daily. After 30 days, the blood, spleen and liver were harvested, processed and analysed by flow cytometry as described above. Animal ethic application number: 1814660.

### **2.2.9 Intravital two-photon microscopy**

Mice were anaesthetized with isoflurane (2.5 % for induction, 1-1.5 % for maintenance), vaporized in an 80:20 mixture of oxygen and air using a Tech 3 vaporizer (Surgivet). The abdomen was shaved and treated with hair removal cream. An incision was made to open the abdominal cavity using scissors and

forceps. Mice were placed on a custom-made imaging stage, and the left lateral lobe was rolled onto a stage using wet cotton swabs. The liver was surrounded with PBS-soaked gauze before a second stage with coverslip was laid on top of the liver. The stages were adjusted so that the liver tissue experienced only low pressure, before 38°C warm low melt agarose was injected between the two stages. Images were acquired with an upright FVMPE-RS multiphoton microscope (Olympus) with a 20x/1.0NA Water Immersion objective enclosed in a heated chamber maintained at 35°C. Fluorescence excitation was provided by Mai-Tai (690-1040nm) and InSight (680-1300) lasers and Galvano laser scanner (4fps). tdTomato was excited at 1100nm (InSight laser) and uGFP and collagen from the liver capsule visualized by via second harmonic generation (SHG) excited at 900/ 950nm (Mai-Tai laser). For four-dimensional data sets, three-dimensional stacks were captured. Raw imaging data were processed, and movies generated in Imaris 9 (Bitplane). Cell migration analyses were performed through automatic cell tracking aided by manual corrections.

### **2.2.10 Histology**

Organs were harvested in 2 % PFA and incubated at 4°C overnight before being extensively washed with PBS and dehydrated in 20 % sucrose in PBS for 8-12 h. Organs were embedded in O.C.T. and snap-frozen using liquid nitrogen. 10-12 µm-thick sections were cut on a Leica CM3050 cryostat (Leica) and air dried overnight. The dried sections were fixed in ice-cold acetone for 5 min and air-dried. With a PAP-pen, a hydrophobic barrier was drawn around each section and the sections rehydrated and blocked with Serum-Free Protein Block (DAKO) for 5 minutes. After washing the sections with PBS, staining was performed with PBS containing 2.5 % donkey serum and antibodies for 90-120 min at RT in a semi-humid chamber. Sections were washed 3 times with PBS for 3 min and mounted with ProLong® Gold Antifade Mountant (Thermo Fisher Scientific) and immediately analysed using a Zeiss LSM710 inverted confocal microscope.

### 2.2.11 Generation of *Plasmodium*-derived epitopes for LC-MS/MS analysis

*Plasmodium*-derived peptides were generated as described before by Valencia-Hernandez et al. (Valencia-Hernandez et al., 2020). B6 mice were s.c. injected with  $10^6$  B16.Fit3L and spleens were harvested 11 days later.  $2.22 \times 10^9$  splenic cells were co-cultured with  $19.88 \times 10^9$  blood-stage PbA parasites in complete RPMI-10 media for 8 h at 37 °C and 6.5 % CO<sub>2</sub>. The uninfected sample was generated by culturing  $1.66 \times 10^9$  splenic cells with  $57 \times 10^9$  RBC from uninfected B6 mice. Cells were then snap frozen prior to further analysis.

### 2.2.12 Analysis of MHC bound epitopes by LC-MS/MS

MHC class II bound peptides were isolated from DC by immunoaffinity chromatography and RP-HPLC (Enders et al., 2021). In brief, cells were lysed for 45 min in 0.5 % IGEPAL, 50 mM Tris-HCl pH 8.0, 150 mM NaCl and protease inhibitors at 4 °C. Next, lysates were cleared by ultracentrifugation at 40,000 g. By using the Y-3P mouse monoclonal antibody bound to protein A Sepharose MHC I-A<sup>b</sup> molecules were purified. Bound peptides were eluted under mild acetic conditions followed by a separation step on a 50 mm monolithic C18 reverse-phase high-performance liquid chromatography (HPLC) column (Chromolith SpeedROD) using an EttanLC HPLC system. 90 individual fractions could be collected and equidistantly pooled into 10 samples. Those samples were then vacuum concentrated and reconstituted to 15 µl with 0.1 % formic acid (FA).

Using a Dionex UltiMate 3000 RSLCnano system equipped with a Dionex UltiMate 3000 RS autosampler, the fractions were loaded via an Acclaim PepMap 100 trap column (100 µm x 2 cm, nanoViper, C18, 5 µm, 100 Å) onto an Acclaim PepMap RSLC analytical column (75 µm x 50 cm, nanoViper, C18, 2 µm, 100Å). Peptide separation was performed by an increasing concentrations of 80 % ACN / 0.1 % FA at a flow of 250 nl/min for 95 min and analyzed with a QExactive Plus

mass spectrometer. In each cycle, a full ms1 scan (resolution: 70.000; AGC target: 3e6; maximum IT: 50 ms; scan range: 375-1600 m/z) preceded up to 12 subsequent ms2 scans (resolution: 17.500; AGC target: 2e5; maximum IT: 150 ms; isolation window: 1.8 m/z; scan range: 200-2000 m/z; NCE: 27). To minimize repeated sequencing of the same peptides, the dynamic exclusion was set to 15 sec and the 'exclude isotopes' option was activated.

Acquired mass spectrometric .raw files were searched against a combined UniProtKB/SwissProt database containing both mouse and PbA protein sequences. To obtain peptide sequence information search engine Byonic (Protein Metrics) was used. Only peptides, below a threshold of a false discovery rate (FDR) of 5 % based on a decoy database were considered for further analysis.

### 2.2.13 $\alpha$ Clec9A vaccination

B6 mice were injected i.v. with the indicated doses of rat  $\alpha$ Clec9A mAb (clone 24/04-10B4) genetically fused to KDNQK**DIYYITGESINAVS**NSPFLEA, containing the *Pb*Hsp90<sub>484-496</sub> epitope (highlighted in bold) via a 4 Alanine linker to make the  $\alpha$ Clec9A-DIY mAb construct.  $\alpha$ Clec9A was injected with 5 nmol of a CpG oligonucleotide (CpG) generated by linking (5' to 3') CpG-2006 to CpG-21798 (Integrated DNA Technologies, Coralville, IA, USA).

### **2.2.14 Cell culture**

B16.Fit3L melanoma cell line was cultured in DMEM-10 media (DMEM media supplemented with 10 % fetal calf serum (FCS), 5 mM HEPES, 2 mM L-glutamine, 50 U/ml penicillin, 100 mg/ml streptomycin and 0.05 mM 2-mercaptoethanol) and maintained in a humidified incubator at 37 °C in 6.5 % CO<sub>2</sub>.

When cells reached 80-90% confluence, cells were passaged. Therefore, cells were washed with PBS and incubated with 2 ml 1 X Trypsin/EDTA for 3 min at 37 °C. Detached cells were transferred into 50 ml Falcon tube and centrifuged (1500 rpm, 5 min, 4°C). Cells were resuspended at 25 x 10<sup>6</sup> cells/ml and 100 µl (2.5 x 10<sup>6</sup> cells) were transferred into a new flask and incubated.

### **2.2.15 Preparation of mouse tissue for flow cytometric analysis**

Blood was sampled from the heart in 50-100 µl Heparin (200 U/ml) to prevent clotting. Blood was treated with red blood cell (RBC) lysis buffer twice for 5 min and washed once with FACS buffer.

Spleens and lymph nodes were harvested into cold RPMI-2.5 (RPMI containing 2.5 % FCS) and single cell suspensions were generated by pressing organs through a 70 µm sterile cell strainer. Next, cell suspensions were centrifuged at 1,600 rpm, 5 min, 4 °C and resuspended in 2 ml RBC lysis buffer for 2 min. FACS buffer was added to the cells and centrifuged at 1,600 rpm, 5 min, 4 °C. Half of the lymph node or 1/40th of the spleen were stained for flow cytometric analysis.

Livers were harvested into 10 ml cold RPMI-2.5 containing 50 µl heparin (200 U/ml) and single cell suspensions were generated by pressing organs through a 70 µm sterile cell strainer. Next, cell suspensions were centrifuged at 1,600 rpm, 10 min, 4 °C and resuspended in 10 ml isotonic Percoll® gradient

solution (35 %, room temperature (RT)). Cells were then centrifuged at 500g for 20 min at RT. The resulting pellet was resuspended in 20 ml RBC lysis buffer for 2 min. FACS buffer was added to cells and centrifuged at 1,600 rpm, 5 min, 4 °C. Cells were washed once with FACS buffer. 1/4 or the whole liver were stained for flow cytometric analysis.

For flow cytometric analyses samples were stained with specific surface marker antibodies (and in some experiments a fixable viability dye) in 50-100 µl of FACS buffer in polypropylene round bottom FACS tubes for ~30 min on ice in the dark.

For intracellular cytokine staining, cells were permeabilized and stained using a Fixation/Permeabilization kit (BD Biosciences) according to the manufacturer's instructions. In Brief, spleens were harvested in RPMI-10 and single cell suspensions were generated. CD4 T cell re-stimulation was performed in the presence of their specific peptide for a total of 5 hours at 37 °C in a humidified incubator. After 1 h of incubation 10 µg/ml Brefeldin A was added to the cultures. Next, cells were washed twice with 200 µl HBSS containing 10 µg/ml Brefeldin A and centrifuged at 1,600 rpm, 5 min, 4 °C. Surface staining was performed for 30 min on ice in HBSS containing 10 µg/ml Brefeldin A. After surface marker staining, cells were washed twice with 200 µl HBSS containing 10 µg/ml Brefeldin A and centrifuged at 1,600 rpm, 5 min, 4 °C. 100 µl of Cytofix/Cytoperm buffer were added per well and incubated for 20 min on ice before being washed twice with 200 µl Perm/Wash buffer per well. After a centrifugation step at 1,600 rpm, 5 min, 4 °C intracellular staining was performed in Perm/Wash buffer in the presence of CD16/CD32 (Fc Block, BD Pharmingen™) and rat serum (1:200) at 4 °C, overnight. The next day, samples were washed with 200 µl/well Perm/Wash buffer and centrifuged at 1,600 rpm, 5 min, 4 °C. Finally, cells were resuspended in 50 µl FACS buffer and analysed by flow cytometry.

For intracellular transcription factor staining, surface marker staining was performed in HBSS on single cell suspensions for 40 min on ice. Next, cells were washed twice in 150 µl FACS buffer per well and centrifuged at 1,600 rpm, 5 min,

4 °C, before cells were permeabilized using the FIX/Perm buffer of the eBioscience™ Foxp3/ Transcription Factor Buffer Set (Invitrogen™) for 40 min on ice. In the next step, samples were washed twice in Perm wash buffer, followed by centrifugation at 1,600 rpm, 5 min, 4 °C. Intra cellular staining was performed in 40 µl Ab cocktail per 10<sup>6</sup> cells at 4 °C, overnight. The next day, samples were washed with 200 µl/well Perm/Wash buffer and centrifuged at 1,600 rpm, 5 min, 4 °C. Finally, cells were resuspended in 50 µl FACS buffer and analysed by flow cytometry

A known number of SPHERO Blank Calibration Particles were added to each sample prior to analysis for enumeration. Samples were filtered through a 70 µm mesh and run on an LSRFortessa (BD Biosciences) or Aurora (Cytex™) and analysed using FlowJo software.

#### **2.2.16 MHC-I and MHC-II Tetramer preparation and staining.**

MHC-I Tetramers were freshly made one day prior to usage. Therefore, vials containing biotinylated monomers were thawed. At RT, 2 µl Streptavidin conjugated to PE or APC were added in 7 consecutive steps to the monomers. Between each step 5-6 min incubation time was granted. Tetramerised MHC-I molecules were used in a final concentration of 1:300 and incubated for 1 h at RT in the dark with corresponding samples.

MHC-II tetramers were provided by the Rossjohn laboratory (Monash University). 2-18 µg/ml MHC-II tetramer was incubated with cell suspension for 30, 90 or 180 min at 4 or 37°C in FACS buffer.

Following MHC-I or II tetramer staining, samples were stained for surface markers and analysed by flow cytometry as described above.

For some experiments, MHC-II tetramer-stained samples were enriched using anti-PE MicroBeads (Miltenyi Biotec) and MS columns (Miltenyi Biotec) per

manufacturer's instructions. In brief, MHC-II-PE stained samples were incubated with anti-PE microbeads on ice for 30 min. Samples were washed with FACS buffer and centrifuged at 1,600 rpm, 5 min, 4 °C. Samples were resuspended in FACS buffer and loaded on a buffer-equilibrated MS columns in a MACS-magnet. Columns were washed twice with FACS buffer, before being removed from the magnet. Magnetic bead-enriched cells were subsequently eluted from the column by adding FACS buffer. Cells were centrifuged at 1,600 rpm, 5 min, 4 °C, surface stained and analysed by flow cytometry.

### **2.2.17 Elispot**

Mice were injected with  $10^4$  PbA iRBC and cured by chloroquine treatment from day 5 post-infection, or injected with 2  $\mu$ g  $\alpha$ Clec9A-Hsp90 plus 5nmol CpG, 7 or 35 days before splenocytes were collected for ELISpot analysis (Enders et al., 2021). In brief, 0.45  $\mu$ m MultiScreen-IP sterile Filter Plates (Merck) were coated overnight with 3  $\mu$ g/mL IFN- $\gamma$  capture Ab (clone AN-18; WEHI Antibody Services) diluted in PBS and blocked with RPMI containing 10% FCS for 30 min at RT. Next,  $2 \times 10^5$  enriched CD4 T cells (day 7; as described above) or unenriched splenocytes containing  $2.5 \times 10^5$  CD4 T cells (day 35) from the spleens of immunized mice were plated and cultured 18 h at 37 °C and 5 % CO<sub>2</sub> in a humidified incubator in the presence of DIY peptide (PbHsp90<sub>484-496</sub>). As a negative control, cells were incubated either without any added peptide (day 7 samples) or HSV-1 peptide (gD<sub>315-327</sub>) (day 35 samples). Then, plates were incubated for 2 h with 1  $\mu$ g/mL biotin-conjugated detection mAb (clone R4-6A2; WEHI Antibody Services) in PBS containing 0.5 % FCS, followed by incubation with Streptavidin-HRP (MabTech, Stockholm, Sweden) for 1 h at RT and with TMB substrate (MabTech) for 15 min. Plates were washed 5 times after each incubation step with PBS. An AID ELISpot reader (Advanced Imaging Devices GmbH, Strassberg, Germany) was used to enumerate spots.

### 2.2.18 Quantification of PbA liver parasite burden via real-time polymerase chain reaction (qPCR)

Livers of mice were harvested into guanidinium Thiocyanate working solution (4 M Guanidinium Thiocyanate containing 0.5 % Sarkosyl, 25 mM Sodium Citratem 0,72 mM 2- $\beta$ -Mercaptoethanol) and homogenised for ~8 sec. on ice. Aliquots of 0.6 ml homogenized liver solution were mixed with 60  $\mu$ l 2 M Sodium acetate solution (pH 4). In a fume hood, 750  $\mu$ l acid phenol/chloroform solution was added and mixed. Then, samples were centrifuged (10 min, 4°C, 15,000 x g) and the upper aqueous phase transferred into fresh 1.5 ml Eppendorf tubes. 0.8-1 volume Isopropanol was added, mixed and placed at -20°C for RNA precipitation for a minimum of 1 h. Samples were centrifuged (20 min, 4°C, 15,000 x g) and the pellet washed with ~1 ml ice-cold Ethanol. Then pellet was air-dried for ~10 min and resuspended in 200  $\mu$ l Ultrapure Dnase/Rnase free distilled water. RNA integrity and concentration was measured using a TapeStation (Agilent).

cDNA was generated from 1  $\mu$ g total RNA using the High-capacity cDNA Reverse Transcription Kit. 20  $\mu$ l reactions were prepared following the manufactures's instructions.

Reverse transcription was performed with the following program:

1. 25 °C, 10 min
2. 37 °C, 120 min
3. 85 °C, 5 min
4. 4 °C hold

cDNA was diluted 1:4 in Ultrapure Dnase/Rnase free distilled water. SYBR Green Hi-rox Mastermix was used for qPCR analyses following the manufactures instructions, and results were analysed using a QuantStudio 7 Flex Real-Time PCR System (ThermoFisher Scientific) using a 384 well plate. Comparative C<sub>T</sub>

with 40 cycles were chosen.  $\Delta\Delta C_T$  values were determined and normalised against the mean of uninfected B6 mice.

### 2.1.1 RNA sequencing analyses

35 days post RAS vaccination,  $\alpha$ Clec9A-DIY vaccination or transfer of *in vitro* generated PbT-II Th1 or Th2 cells,  $\geq 15\,000$  specific CD4 or CD8 T cells were sorted directly into 500  $\mu$ l Quiazol and frozen at  $-80^\circ\text{C}$  or stored on dry ice. For each group, 5 technical replicates were performed. For each technical replicate 5 biological replicates were pooled.  $T_{EM}$  cells were defined as  $CD69^-CD62I^-$  T cells and  $T_{RM}$  cells were defined as  $CD69^+CD62I^-CXCR6^+$  T cells.

All analyses were performed in R version 3.5.3 using R-studio 1.2.1335. Transcript-level abundance was estimated by pseudoalignment tool *kalisto* to generate a normalized dataset under the use of the DESeq2 package using default parameters. All transcripts with a mean lower than 10 were excluded before performing DESeq2 analyses. DESeq2 computes a size factor by taking the median ratio of each sample over a pseudo sample. Unknown batch effects were adjusted from the normalized rlog transformed expression data by three surrogate variables identified by *sva* using the function `removeBatchEffect` from the *limma* package and modelled into the DESeq2 generated dataset (Sundararajan et al., 2019). Principal component analysis on all genes and hierarchical clustering on the 500 most variable DE genes was performed with default settings in PGS based on the p-values of the expression values of all samples across all conditions. The DESeq2 packages allow differential gene expression analyses (DGEA) via a negative binomial distribution model which uses variance-mean estimation for RNA-Seq data and the Wald test (Sundararajan et al., 2019). DE genes were defined by p-Value  $< 0.05$  and a  $|1.5\text{-fold change}|$  for the given comparisons if not specified otherwise in the figure legend.

Gene set enrichment analyses (GSEA) was performed by GSEA software (Broad Institute). Normalized Data of the DESeq2 analyses were used against published differently expressed Genes of *Plasmodium*-specific liver CD8 T<sub>RM</sub> and T<sub>EM</sub> cells (GSE71518) and known Genset of DEGs with a p-value of < 0.05 and |1.5-fold change|. Germutation for GSEA was set to 4000.

**Table 2.17. List of R packages used in this study.**

Package	version
tidyr	0.8.3
ggplot2	3.2.1
ggrepel	0.8.1
gplots	3.0.1.1
ggbeeswarm	0.6.0
hexbin	1.27.3
reshape2	1.4.3
factoextra	1.0.5
Hmisc	4.2-0
VennDiagram	1.6.20
openxlsx	4.1.0.1
BiocManager	1.30.4
rhdf5	2.26.2
clusterProfiler	3.10.1
DOSE	3.8.2
GSEABase	1.44.0
RColorBrewer	1.1-2
ComplexHeatmap	1.20.0
tximport	1.10.1
DESeq2	1.22.2
vsn	3.50.0
pheatmap	1.0.12
genefilter	1.64.0
biomaRt	2.38.0
limma	3.38.3
sva	3.30.1
IHW	1.10.1
org.Mm.eg.db	3.7.0
org.Hs.eg.db	3.7.0

Readxl	1.3.1
dplyr	0.83

### 2.1.2 Statistical analysis

Statistical analysis was performed using the Graphpad Prism 8 software. Data are shown as mean values  $\pm$  standard deviation (SD). The statistical tests used are indicated in the respective figure legends. P values of  $<0.05$  were considered as statistical significant. \*,  $P<0.05$ ; \*\*,  $P<0.01$ ; \*\*\*,  $P<0.001$ ; \*\*\*\*,  $P<0.0001$ . Statistical analyses of groups  $> 2$  were analysed by using a Kruskal-Wallis test with Dunn's multiple comparison post-test. Statistical comparisons of 2 groups were performed using two-tailed Mann-Whitney test. Differences in survival were analysed by performing pairwise comparisons between the different groups using log-rank tests and adjusting for multiple comparisons by a Bonferroni correction.

## Chapter 3

CD4 T cell response to a newly  
discovered *Plasmodium*-derived MHC-II  
epitope

## Chapter 3 CD4 T cell response to a newly discovered *Plasmodium*-derived MHC-II epitope

### 3.1 Introduction

CD4 T cells play a central role in the function of the adaptive immune system by providing help to both B cells for antibody production and DCs for induction of CD8 T cell expansion, differentiation, and effector functions. These functions are crucial for immunity against multiple pathogens, including *Plasmodium* species (Carvalho et al., 2002, Perez-Mazliah et al., 2017, Aloulou and Fazilleau, 2019). In mice, CD4 T cells were shown to contribute to liver- and blood-stage infection control after inoculation with different *Plasmodium* species and stages of the parasite life cycle (Doolan and Hoffman, 2000, Oliveira et al., 2008, Fernandez-Ruiz et al., 2017, Perez-Mazliah et al., 2017). For example, the transfer of MSP-1 specific CD4 T cells (B5 TCR Tg cells) was shown to protect RAG<sup>-/-</sup> mice from a lethal Pch infection (Stephens et al., 2005). However, limited knowledge of immunogenic MHC-II restricted *Plasmodium* antigens has precluded accurate dissection of the role of antigen-specific CD4 T cell responses against this parasite.

To address this issue, IA<sup>b</sup> restricted, *Plasmodium*-specific transgenic CD4 T cells, termed PbT-II cells, were developed in our laboratory (Fernandez-Ruiz et al., 2017). At the time of their generation, the *Plasmodium* epitope recognized by PbT-II cells was unknown. However, PbT-II cells were shown to proliferate in response to PbA, Pch, and human *P. falciparum* iRBCs, and after injection of radiation-attenuated PbA sporozoites (Fernandez-Ruiz et al., 2017). Furthermore, transfer of naïve PbT-II cells into CD40L<sup>-/-</sup> and RAG1<sup>-/-</sup> mice could rescue mice from an otherwise lethal Pch infection and thus showed the functionality of PbT-II cells in *Plasmodium* infection.

The apparent conservation of the PbT-II antigen throughout *Plasmodium* species and the demonstrated protective nature of PbT-II cells implied that the antigen recognised by these cells may have protective potential, prompting its identification. Knowledge of the PbT-II specific epitope would enable the study of endogenous CD4 T cell responses, a more physiological scenario than transgenic CD4 T cells.

This chapter examines the formation of *Plasmodium* specific CD4 memory T cell populations after *Plasmodium* liver- and blood-stage infection by studying transgenic PbT-II cells. Furthermore, the PbT-II cell-specific epitope, heat shock protein 90 (Hsp90), was identified and fused to a Clec9A specific antibody with the aim of targeting cDC1. This subunit vaccine was used to induce PbT-II and Hsp90-specific endogenous T cell populations in the liver and spleen. While circulating cells ( $T_{EM}$ ,  $T_{CM}$ ) were found in both liver and spleen, this chapter provides the first evidence of the induction of CD4  $T_{RM}$  cells in the liver after vaccination or *Plasmodium* parasite infection. Finally, induction of Th1 and Tfh helper PbT-II cells after  $\alpha$ Clec9A-targeted vaccination or PbA iRBCs infection is shown, matching findings from other studies using alternative antigens (Lahoud et al., 2011, Fernandez-Ruiz et al., 2017). To study the function of PbT-II cell responses with different helper lineages associated with *Plasmodium* infection, this chapter also describes the establishment of a PbT-II *in vitro* differentiation protocol.

## 3.2 Results

### 3.2.1 CD4 T cell response to PbA infection

#### 3.2.1.1 PbT-II response to blood-stage PbA infection

To investigate the response of malaria-specific CD4 T cells to *Plasmodium* infection, we took advantage of transgenic PbT-II T cells. These cells are responsive to a specific *Plasmodium* epitope that will be described later in this chapter. This study is mainly interested in two distinct organs: the liver, which is infected by sporozoites after the bite of an infected mosquito, and the spleen, as a lymphoid organ where T cell priming is documented (Borges da Silva et al., 2015). The initial expansion of effector T cells after an infection is followed by a rapid decline in cell numbers, leaving a small proportion of long-lived memory T cells. To investigate the quantitative response of PbT-II cells against PbA blood-stage infection,  $5 \times 10^4$  PbT-II cells were transferred into naïve B6 mice and one day later these mice were infected with  $10^4$  PbA iRBCs. To prevent a lethal outcome from PbA blood-stage infection, mice were treated with chloroquine from day 5 post-infection. Spleens and livers were harvested from groups of mice and PbT-II cells assessed by flow cytometry (Figure 3.1). 7 days post-infection around  $7 \times 10^5$  and  $2 \times 10^6$  PbT-II cells could be detected in the liver and spleen, respectively. After an additional week, 43.5 times fewer PbT-II cells were recovered from the liver and 16 times less from the spleen. By day 49, these numbers reduced to 5,500 and 45,500 PbT-II cells in the liver and spleen, respectively (Figure 3.1A).

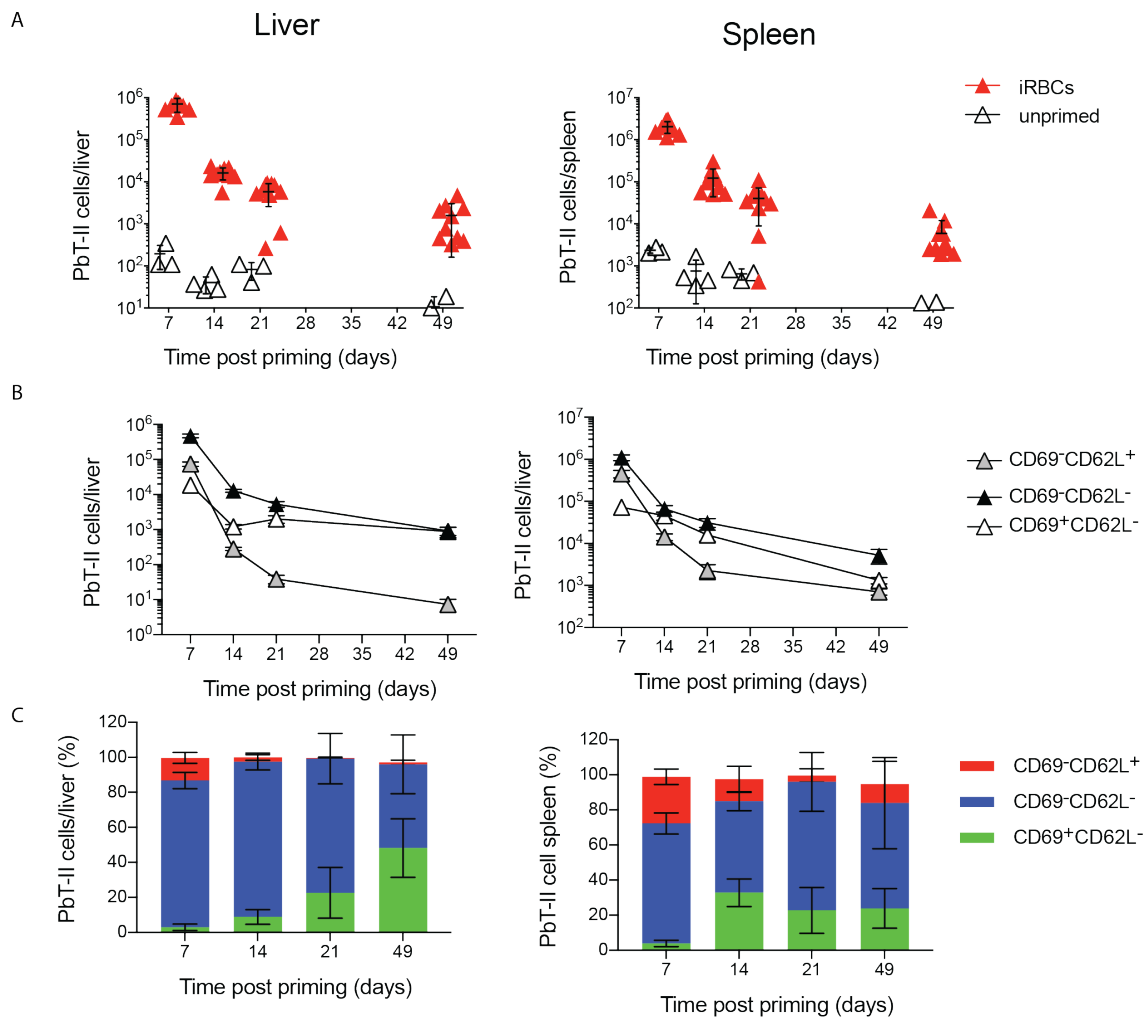


**Figure 3.1. PbT-II cells form memory after PbA blood-stage infection.**

$5 \times 10^4$  PbT-II.uGFP cells were transferred into naïve B6 mice and one day later these mice were infected with  $10^4$  PbA iRBCs (i.v.). Chloroquine treatment was performed from day 5 post-infection to prevent lethal infection. On day 7, 14, 21 and 49 after infection, liver (left) and spleen (right) were harvested and PbT-II cell numbers were determined by flow cytometry by gating on live, CD4<sup>+</sup>, V $\alpha$ 2<sup>+</sup>, GFP<sup>+</sup>, CD44<sup>hi</sup> cells (closed triangles). Naïve PbT-II cell numbers of (live, CD4<sup>+</sup>, V $\alpha$ 2<sup>+</sup>, GFP<sup>+</sup>) uninfected control groups were also included (open triangles). **A.** Total PbT-II cell numbers per organ. Each symbol represents an individual mouse. **B, C.** Analysis of the number (**B**) and proportion (**C**) of PbT-II T cell subsets in the liver (left) and spleen (right) at different time points post-challenge based on expression of CD69 and CD62L. The experiment was performed twice for a total of 10 mice per group.

The memory pool is of special interest in the context of vaccine development due to its faster and stronger recall response. In general, the T cell memory pool can be divided into three different subsets, which can be distinguished by the surface expression of CD69 and CD62L:  $T_{CM}$  cells lack the expression of CD69 but express CD62L and circulate between lymphoid organs.  $CD69^-CD62L^-$   $T_{EM}$  cells can circulate between lymphoid organs and peripheral tissues via the blood. The recently described  $T_{RM}$  cells express CD69 but lack CD62L expression and remain in peripheral tissues without re-circulating through the blood. While these markers act as a guide to phenotype, more extensive marker analysis is required to definitively identify subsets. In addition, early in the response antigen-stimulated T cells may express CD69 as a consequence of antigen recognition, making distinction of  $T_{RM}$  from  $T_{EM}$  somewhat problematic for the first 2 weeks. While  $CD4^+$   $T_{CM}$  and  $T_{EM}$  have been well described, little is known about tissue-resident  $CD4$  T cells in the liver, especially in the context of *Plasmodium* infection. To understand  $CD4$  memory T cell differentiation in *Plasmodium* infection, expression of CD69 and CD62L were analysed in the liver and spleen over the course of the experiment. In the liver, 80 % of PbT-II cells were  $CD69^-CD62L^-$  for the first two weeks after infection, matching with an effector or  $T_{EM}$  phenotype. Nevertheless, a decline from  $7 \times 10^5$  at day 7 to 1,500  $CD69^-CD62L^-$  cells at 49 days post-infection was evident. While  $CD69^-CD62L^-$  negative cells dominated the effector response,  $CD69^+CD62L^-$  T cells represented about 50 % of PbT-II cells 7 weeks post-infection, suggesting a gradual increase in the frequency of  $CD4$  T cells with a  $T_{RM}$  cell phenotype. After an early drop of CD69 expressing cells from almost 19,000 to 1,200 PbT-II cells in the liver over the first two weeks, the decline was less pronounced up to day 49 when average of 900 cells could still be detected (Figure 3.1B, C). This suggests superior survival of  $CD69^+CD62L^-$   $T_{RM}$ -like PbT-II cells compared to  $T_{EM}$  or  $T_{CM}$  cells in the liver after PbA blood-stage infection. However, it should be noted that the expression of CD69 early in infection can be explained by recent activation and does not necessarily correlate with a tissue-resident phenotype. A thorough investigation of the properties of the  $CD62L^-CD69^+$  T cells in the liver will be discussed in chapter 4.

In the spleen, CD69<sup>-</sup>CD62L<sup>-</sup> PbT-II cells represented the main PbT-II cell population, with over 50 % of this phenotype present throughout the experiment. Nevertheless, there was a rapid contraction from over  $10^6$  to  $5 \times 10^4$  PbT-II cells within 7 weeks post-infection. CD69<sup>+</sup>CD62L<sup>-</sup> PbT-II cells dropped from 70,000 to 1,300 cells per spleen between day 7 to day 49 post-infection, while PbT-II cells expressing CD69<sup>-</sup>CD62L<sup>+</sup> showed a reduction from 14,000 to 700 cells (Figure 3.1B, C). Thus, compared to the liver, T<sub>EM</sub> and T<sub>CM</sub> PbT-II cells in the spleen showed a less pronounced contraction, whereas T<sub>RM</sub>-like cells did not seem to be retained to the same level as in the liver. Together, these data show, that memory T cells form in the liver and spleen after *Plasmodium* infection and indicate preferential retention/survival of CD69<sup>+</sup> potentially T<sub>RM</sub>-like PbT-II in the liver.

### 3.2.1.2 PbT-II response to liver-stage PbA infection

After identifying a memory PbT-II response to blood-stage PbA infection, we investigated the potential of memory development to liver-stage infection. Sporozoite infection of hepatocytes in the liver leads to local inflammation and a type I IFN responses (Liehl et al., 2015, Liehl et al., 2014). This property and altered antigen availability in the liver compared to blood-stage infection will potentially change the CD4 T cell response. To isolate the liver-stage from the blood-stage, irradiation attenuated sporozoites (RAS) were used to prevent the parasites from fully developing in the liver and then proceeding to blood-stage infection.  $5 \times 10^4$  RAS were injected into naïve B6 mice one day after the transfer of PbT-II cells. These mice were then left for various times before assessing the spleen and liver for PbT-II cell numbers and phenotype by flow cytometry (Figure 3.2). Eight days post-RAS priming,  $4 \times 10^5$  PbT-II cells were detected in the liver, which was followed by a 2.5-fold reduction in cell numbers by day 22. Further reduction in PbT-II cell numbers was seen at day 50 post priming, where  $4 \times 10^3$  cells could be detected in the liver (Figure 3.2A). A similar decline in PbT-II cell

numbers was found in the spleen between day 8 and 50 post-priming (Figure 3.2A).

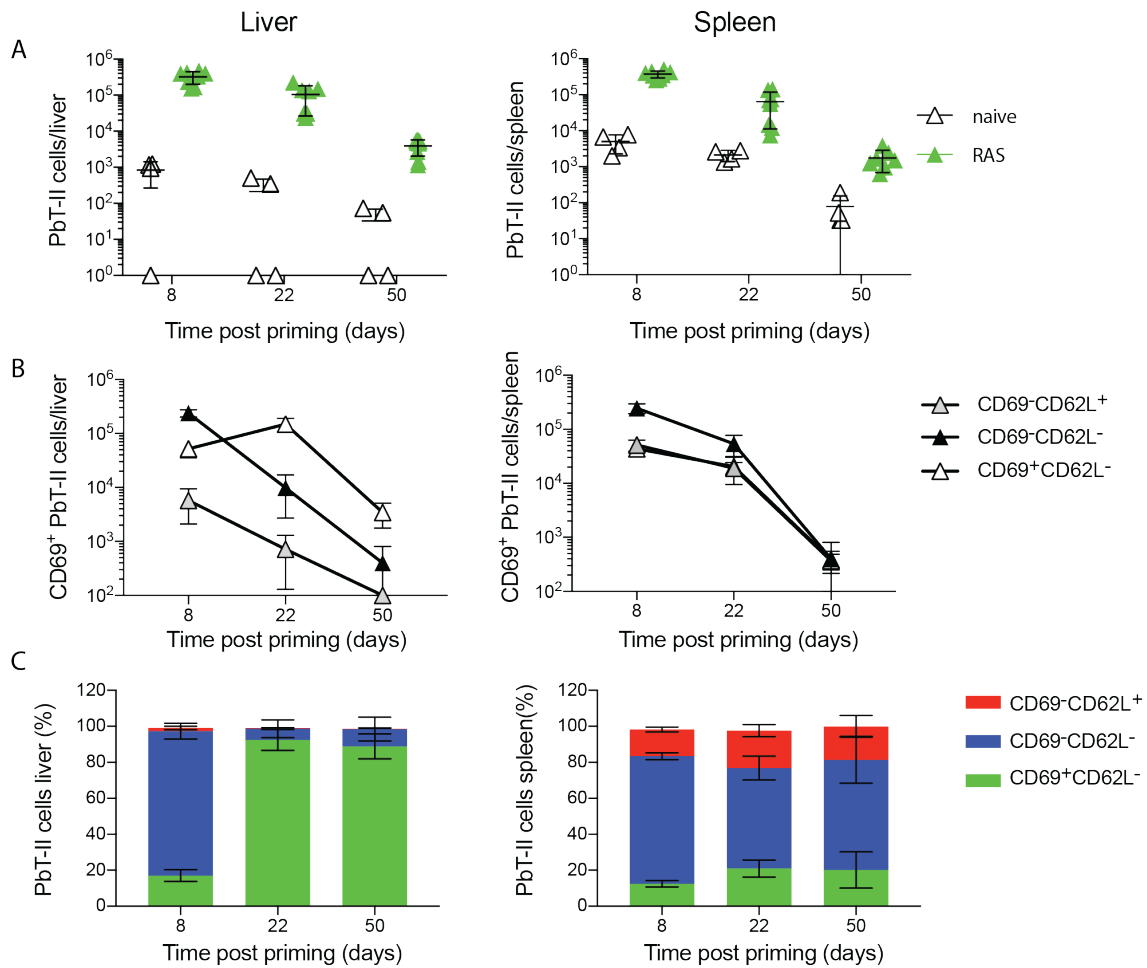


**Figure 3.2 PbT-II cells form memory after PbA radiation-attenuated sporozoite vaccination.**

$5 \times 10^4$  PbT-II.uGFP cells were transferred into naïve B6 mice and one day later these mice were vaccinated with  $5 \times 10^4$  PbA RAS (i.v.). On day 8, 22, and 50 after vaccination, liver (left) and spleen (right) were harvested and PbT-II cell numbers were determined by flow cytometry, gating on live, CD4+, V $\alpha$ 2+, GFP+, CD44<sup>hi</sup> cells (closed triangles). Naïve PbT-II cell numbers of (live, CD4+, V $\alpha$ 2+, GFP+) uninfected control groups were also included (open triangles). **A.** Total PbT-II cell numbers per organ. Each symbol represents an individual mouse. **B.** **C.** Analysis of the number (**B**) and proportion (**C**) of PbT-II T cell subsets in the liver (left) and spleen (right) at different time points post-priming based on expression of CD69 and CD62L. The experiment was performed twice for a total of 7-8 mice per group.

Next, T cell subpopulations, distinguished by their expression of CD69 and CD62L were examined. CD69<sup>-</sup>CD62L<sup>+</sup> T<sub>CM</sub> PbT-II cells in the liver represented the smallest subset over the duration of the experiment. At day 8 post-RAS inoculation, CD69<sup>-</sup>CD62L<sup>-</sup> PbT-II cells represented the dominant subset of PbT-II cells, but these cells rapidly declined in numbers over the experimental period until around 400 PbT-II T<sub>EM</sub> were recovered at day 50 post RAS priming. Interestingly, while CD69<sup>+</sup>CD62L<sup>-</sup> T<sub>RM</sub>-like PbT-II cells made up only 17 % of PbT-II cells in the liver at day 8 post-priming, they represented around 90 % of all PbT-II cells at days 22 and 50, with around  $3 \times 10^3$  cells still present at the latter time point (Figure 3.2B, C). Therefore, CD69<sup>+</sup>CD62L<sup>-</sup> T<sub>RM</sub>-like PbT-II cells are the dominant memory T cell type in the liver after RAS vaccination.

In the spleen, CD69<sup>-</sup>CD62L<sup>-</sup> PbT-II cells represented the major T cell population, with over 50 % at all times tested. CD69<sup>+</sup>CD62L<sup>-</sup> and CD69<sup>-</sup>CD62L<sup>+</sup> PbT-II cells displayed similar expansion and contraction profiles with T cell numbers from an average of  $5 \times 10^4$  at day 8 to around 400 cells at day 50 post priming in the spleen and each represented around 15 – 20 % of the PbT-II cell population in this organ. Thus, T<sub>EM</sub>-like PbT-II cells dominate the memory pool in the spleen, whereas cells with a T<sub>RM</sub>-like phenotype dominate the memory pool in the liver after RAS-priming (Figure 3.2B, C).

CD69 is also known to be an early activation marker and presentation of retained RAS antigens could potentially lead to elevated CD69 on PbT-II cells in the liver, especially at early time points. If this were the case, cells that appear to be T<sub>RM</sub>-like may in fact be activated effectors responding to antigen. To investigate the antigen availability at different times after RAS injection, an *in vivo* proliferation assay was performed. To this end, CellTrace Violet™ (CTV) labelled PbT-II cells were injected into mice either before or 7 to 28 days after RAS vaccination. CTV binds to the cell surface membrane and is diluted with each proliferation step. Therefore, reduction or loss of CTV signal on labelled cells shows proliferation and thus antigen encounter after cell transfer. As seen in Figure 3.3, injection of CTV labelled PbT-II cells one day before RAS priming (day 0 group) led to a complete loss of CTV signal of PbT-II cells in the liver 5 days

post-RAS injection, indicating that these cells proliferated heavily in response to antigen. Similarly, in the spleen, over 90 % of PbT-II cells had a reduced CTV signal after 5 days when injected before priming. Transfer of cells one week after RAS inoculation (day 7 group) resulted in 50 % divided PbT-II cells in both the liver and the spleen, indicating that antigen was still present, albeit at lower levels. In contrast, less than 5 % of CTV labelled PbT-II cells injected 28 days post priming showed signs of proliferation (CTV dilution) in either organ, reflecting the same proliferation capacity as PbT-II cells injected into naïve mice (Figure 3.3) and suggesting an absence of antigen at this stage. This implied that the CD69<sup>+</sup> PbT-II cells in the liver 50 days post-RAS injection did not express CD69 as a consequence of recent antigen encounter but were more likely of a T<sub>RM</sub> phenotype.

Together, these data showed that *Plasmodium*-specific CD4 T cell memory formed after RAS vaccination. Similar to *Plasmodium* blood-stage infection, CD69<sup>-</sup>CD62L<sup>-</sup> T<sub>EM</sub> cells were the dominant T cell population in the spleen, but PbA liver stage infection induced a far greater proportion of CD69<sup>+</sup>CD62L<sup>-</sup> T<sub>RM</sub>-like PbT-II cells in the liver.

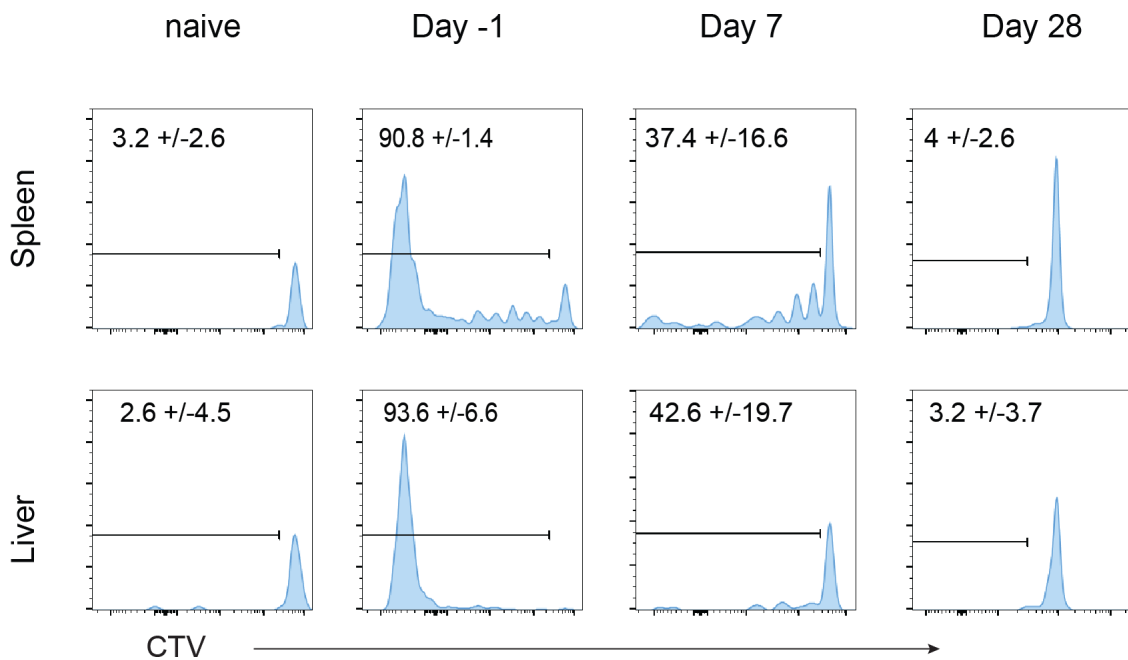


**Figure 3.3. Antigen is only available for about 7 days after administration of radiation-attenuated sporozoite (RAS).**

B6 mice were vaccinated with  $5 \times 10^4$  RAS (i.v.). Either one day prior or 7 or 28 days post vaccination,  $5 \times 10^5$  CTV labelled PbT-II.uGFP cells were adoptively transferred. Spleen (upper) and liver (lower) were harvest 6 days post PbT-II cell transfer and CTV staining was assessed for dividing cells by flow cytometry after gating on CD4+, V $\alpha$ 2+, GFP+, cells. The experiment was performed twice for a total of 6 mice per group.

### 3.2.2 Minimal PbT-II epitope.

As shown so far, PbT-II cells can respond to either blood-stage or liver-stage *Plasmodium* infection. We wanted to take advantage of this responsiveness to design a non-infective reagent that could potentially be used as a vaccine candidate against any of these stages. In order to do this, the specific *Plasmodium* epitope recognized by PbT-II cells needed to be identified. To do this, Dr. Daniel Fernandez-Ruiz adopted an *in vitro* culture system whereby DCs were incubated with blood-stage *Plasmodium* parasites to enable their uptake, processing, and presentation of immunopeptides via MHC-II molecules. DCs were cultured with PbA infected red blood cells for 8 hours and snap frozen. Peptides were then dissociated from MHC-peptide complexes and separated by

reverse-phase high-performance liquid chromatography (HPLC). Subsequently, mass spectrometric analyses of the eluants were performed, identifying 75 different peptides that were mapped to *Plasmodium* proteins. To determine whether PbT-II cells responded to any of these peptides, splenocytes were extracted from PbT-II mice infected for 8 days with blood-stage PbA parasites and were incubated *in vitro* with the peptides. The expression of IFN- $\gamma$  and TNF by PbT-II CD4 T cells was determined by flow cytometric analyses. A single peptide, number 58 (NQKDIYYITGESINAVS), was found to induce IFN- $\gamma$  expression in CD4 T cells above background levels (Figure 3.4A). This was also true for TNF, although background levels were somewhat raised for some of the peptides (Figure 3.4B). Peptide mapping revealed that Peptide 58 originated from the heat shock protein 90 (Hsp90) of PbA. Hsp90, one of the most abundant chaperones, is expressed throughout the *Plasmodium* lifecycle in the mammalian host (Howick et al., 2019). Therefore, it represented an interesting candidate for further investigation.

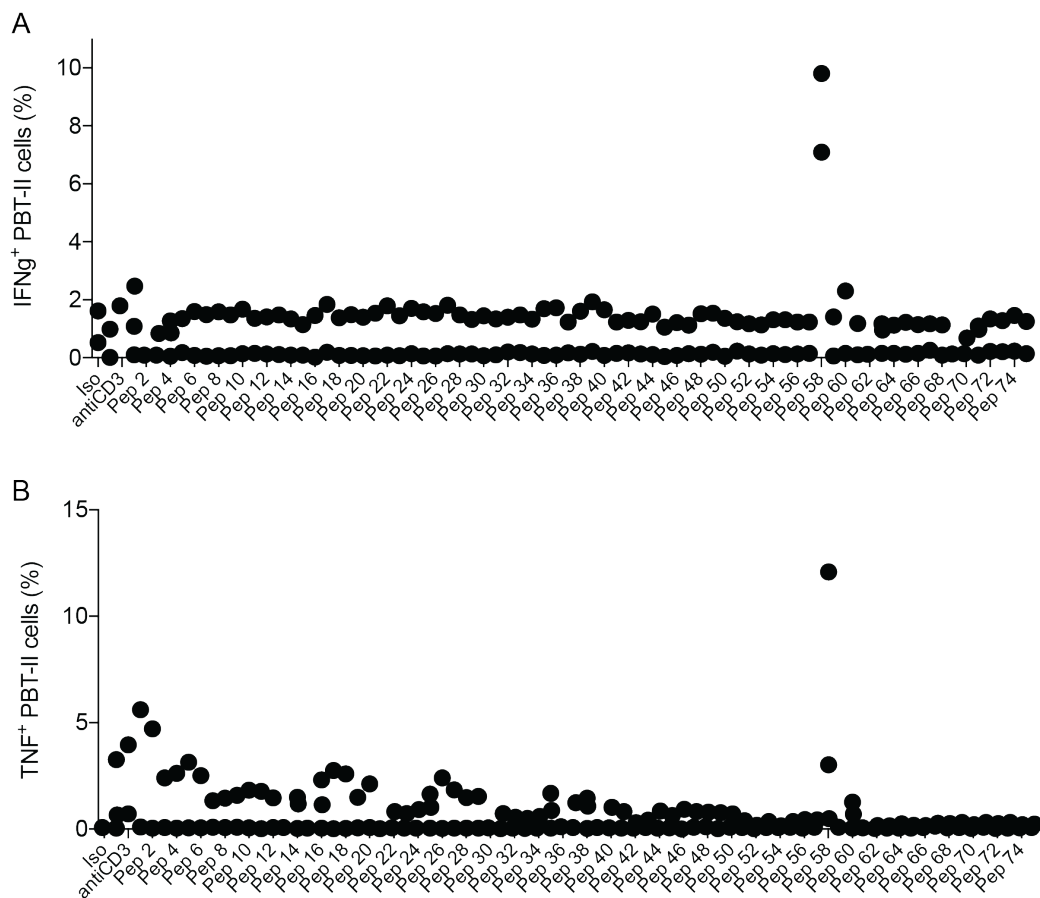


### Figure 3.4. Discovery of the cognate peptide of PbT-II cells.

**A.** PbT-II.GFP mice were infected with  $10^4$  PbA iRBC (i.v.) and treated with chloroquine from day 4. 8 days post-infection, intracellular staining was performed on splenocytes 5 h post-incubation in presence of brefeldin A and candidate peptides at a concentration of  $2.5 \mu\text{M}$ . PbT-II cells were identified by the expression of CD4,  $V\alpha 2$ , and GFP and the expression of IFN- $\gamma$  or TNF was examined. **A.** Percentages of IFN- $\gamma$ <sup>+</sup> PbT-II cells. **B.** Percentages of TNF<sup>+</sup> PbT-II cells. Data were pooled from two independent experiments. Peptide discovery experiments performed by Dr. Daniel Fernandez-Ruiz.

Based on these results, the minimal epitope of PbT-II cells was determined. The minimal epitope is the shortest peptide sequence recognized by T cells that leads to activation and cytokine production and is of crucial importance for the development of immune-intervention strategies. Peptide presentation to CD4 T cell is mediated via MHC-II molecules expressed on the cell surface of APCs. Unlike MHC-I molecules, which present peptides with a length of 8-10 residues,

MHC-II molecules have an open binding groove and accommodate peptides of 13-17 residues, that protrude from the molecule (Bouvier and Wiley, 1994, Rudensky et al., 1991). To identify the PbT-II minimal epitope, N-terminal or C-terminal-shortened variants of peptide 58 were incubated with naïve PbT-II cells overnight, and CD69 upregulation was measured by flow cytometry (Figure 3.5). PbT-II cells incubated with the full-length peptide, NQKDIYYITGESINAVS, showed CD69 upregulation in 93 % of PbT-II cells at 20  $\mu$ M peptide concentration. High CD69 expression was achieved in around 90 % of PbT-II cells with peptide concentrations above 0.16  $\mu$ M (Figure 3.5A, B).

Sequential removal of the three first N-terminal amino acids (NQKDIYYITGESINAVS) did not affect the CD69 expression of PbT-II cells compared to the full-length sequence (Figure 3.5A). Removing two additional amino acids (NQKDIYYITGESINAVS) led to similar CD69 expression, compared to the full-length peptide, at high peptide concentrations (20-4  $\mu$ M) but was reduced by 10 % at peptide concentration below 0.8  $\mu$ M. Removal of the following amino acid, tyrosine (Y), (NQKDIYYITGESINAVS) reduced PbT-II cell activation by about 15 % versus the full-length sequence, at 20 and 4  $\mu$ M. Furthermore, CD69 expression of PbT-II cells was markedly lower after incubation with a peptide missing the first seven amino acids (NQKDIYYITGESINAVS) (Figure 3.5A).

Next, C-terminal shortened variants of Hsp90 peptide (NQKDIYYITGESINAVS) were tested. The C-terminal flanking amino acid, serine (S), from the YYITGESINAVS sequence was not required to induce full CD69 upregulation in PbT-II cells. However, the loss of valine (V), from the YYITGESINAVS sequence, reduced CD69 expression by about 15 % at 20  $\mu$ M and responses were no longer detectable after incubation with less than 0.032  $\mu$ M peptide (Figure 3.5B). Interestingly, the removal of the C-terminal valine (YYITGESINAV) could be rescued by re-introducing N-terminal Aspartic acid (D) and Isoleucine (I) (DIYYITGESINA), and incubation with the peptide variant DIYYITGESINAV could fully activate PbT-II cells compared to the full-length peptide (Figure 3.5B).

Finally, Hsp90 peptide variants longer than the full peptide (NQKDIYYITGESINAVS) were tested for their PbT-II stimulatory capacity. Addition of four amino acids residues on the C-terminus of peptide 58 also resulted in maximal CD69 upregulation by PbT-II cells (Figure 3.5C). As it was already shown that PbT-II cells proliferate in response to *in vitro* incubation with *P. falciparum* iRBCs, we wanted to investigate if the equivalent *P. falciparum* Hsp90 epitope could stimulate PbT-II cells. The first N-terminus residue between the *P. falciparum* ortholog of the PbA Hsp90 differ by the change from aspartic acid (D) in PbA to glutamic acid (E). Incubation of PbT-II cells with both peptide versions showed an equal upregulation of CD69 (Figure 3.5C).

Thus, we reasoned that the minimal epitope for maximal stimulation of PbT-II cells was DIYYIGESINAV, and the minimal epitope to get any response was YYITGESINA (Figure 3.5). Based on these results, the DIYYIGESINAV epitope, termed hereafter DIY, derived from Hsp90 was further investigated as a potential novel CD4 T cell vaccine target.

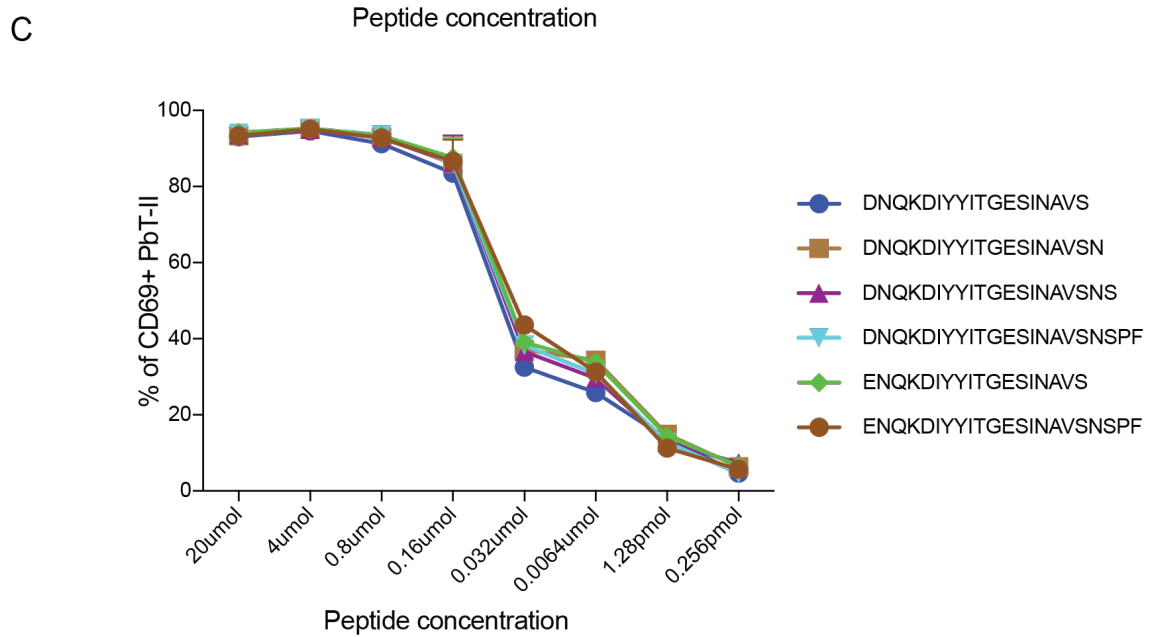
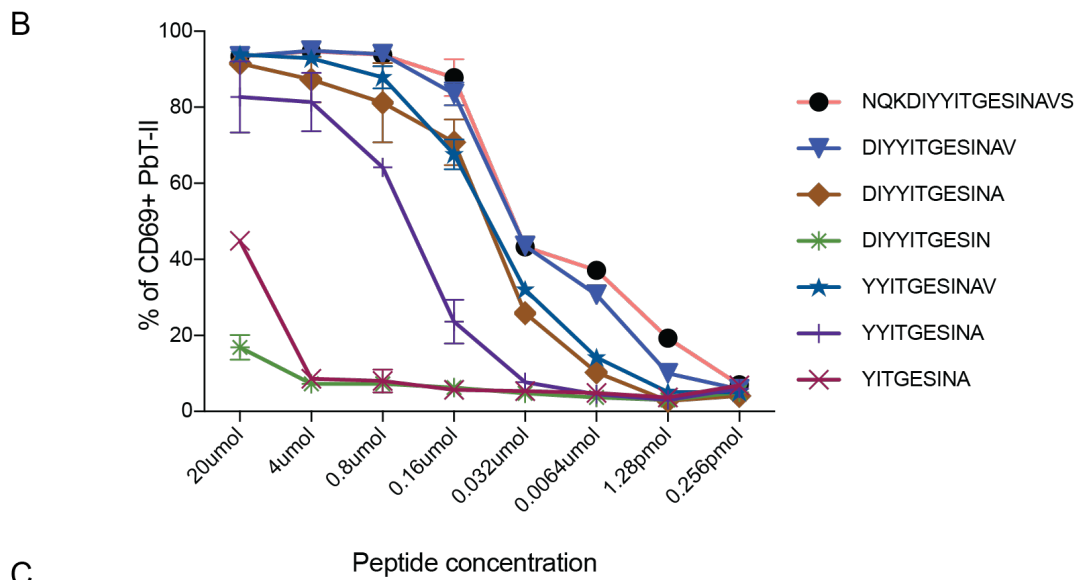
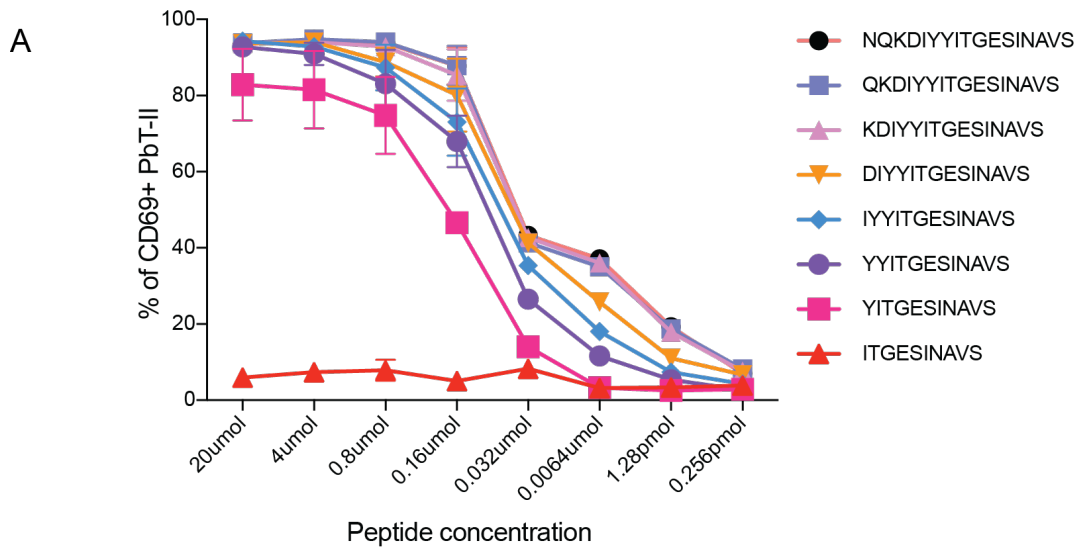


**Figure 3.5. Identification of the minimal epitope recognised by PbT-II cells.** Naïve splenocytes from PbT-II.GFP mice were cultured overnight with the specified amounts of the indicated peptides, after which the expression of CD69 was measured by flow cytometry. **A.** DNQKDIYYITGESINAVS variants shortened from N-terminus. **B.** DNQKDIYYITGESINAVS variants shortened from C-terminus. **C.** peptide variants with additional amino acids on N and C-terminus. Data were pooled from two independent experiments. Minimal peptide discovery experiments performed by Dr. Daniel Fernandez-Ruiz.

### 3.2.3 PbT-II cell response to an antibody-based vaccine ( $\alpha$ -Clec9A-DIY)

As shown above, PbT-II cells can be activated and form a memory population after exposure to *Plasmodium* parasites. Furthermore, incubation with Hsp90 derived epitopes leads to activation and cytokine release. Previous work on PbT-II cells had shown that CD8 $\alpha^+$ , XCR1 $^+$  DCs were the major APC responsible for priming of an immune response against PbA blood-stage infection (Fernandez-Ruiz et al., 2017). Those CD8 $\alpha^+$  DCs express various surface receptors such as Clec9A, DEC-205, and Clec12A, which have previously been successfully used to deliver Ag to these DCs for efficient T cell priming (Lahoud et al., 2009, Lahoud et al., 2011). Targeting the same DC subset via distinct receptors can generate divergent immune responses due to different properties of these receptors. For example, targeting DEC205 to induce an antigen-specific CD4 T cell response can cause the formation of regulatory T cells while targeting Clec9A induces an Ag-specific CD4 T cell response biased towards a Tfh phenotype (Lahoud et al., 2011). Furthermore, targeting Ag to Clec9A was also shown to be more efficient in inducing Ag-specific CD4 T cell proliferation and total numbers compared to targeting the same Ag to Clec12A or DEC205.

Therefore, we decided to test whether linking the PbT-II epitope to a Clec9A-specific monoclonal antibody (mAb) would result in the priming of PbT-II cells. To achieve this goal, the PbT-II epitope and some surrounding sequence (KDNQKDIYYITGESINAVSNSPFLEA) was genetically fused to the heavy chain

of a mAb specific for Clec9A. This antibody-based priming reagent, named hereafter  $\alpha$ -Clec9A-DIY, was then examined for its capacity to induce PbT-II cell activation and memory formation. First, the optimal dose of  $\alpha$ -Clec9A-DIY to induce PbT-II activation was determined. Titrated amounts of  $\alpha$ -Clec9A-DIY were injected into naive B6 mice one day after the transfer of  $5 \times 10^5$  naïve PbT-II cells. Earlier studies had shown that CpG improves priming, therefore CpG was included as an adjuvant (Sparwasser et al., 1998). Around  $10^6$  PbT-II cells could be detected in the spleen 4 days after injection of  $0.5 \mu\text{g}$   $\alpha$ -Clec9A-DIY and  $5 \text{ nmol}$  CpG (Figure 3.6A). Increased antibody concentration led to a dose dependent increase in cell-numbers, which resulted in the generation of three times higher average PbT-II cell numbers with  $4 \mu\text{g}$   $\alpha$ -Clec9A-DIY and CpG (Figure 3.6A). While an adjuvant, such as CpG, is necessary to induce activation and proliferation of CD8 T cells after  $\alpha$ -Clec9A priming, CD4 T cells can proliferate after  $\alpha$ -Clec9A injection in the absence of adjuvants (Lahoud et al., 2011). To test whether this was the case in the present system, different amounts of  $\alpha$ -Clec9A-DIY were injected with or without CpG into B6 mice one day after transfer of PbT-II cells (Figure 3.6B). At low Ab doses, the administration of CpG adjuvant appeared to improve PbT-II cell expansion (x5), but no significant difference was reached. At high Ab doses, an effect of CpG adjuvant was less evident.

In summary, the injection of  $\alpha$ Clec9A-DIY with or without CpG induced PbT-II cell proliferation. PbT-II cell numbers reached a plateau at  $0.5\mu\text{g}$   $\alpha$ Clec9A mAb (with CpG) or  $8\mu\text{g}$  (without CpG) in this experiment. To ensure maximal expansion of PbT-II T cells, we decided to use  $2$  to  $8 \mu\text{g}$   $\alpha$ Clec9A-DIY and  $5 \text{ nmol}$  CpG in further experiments.

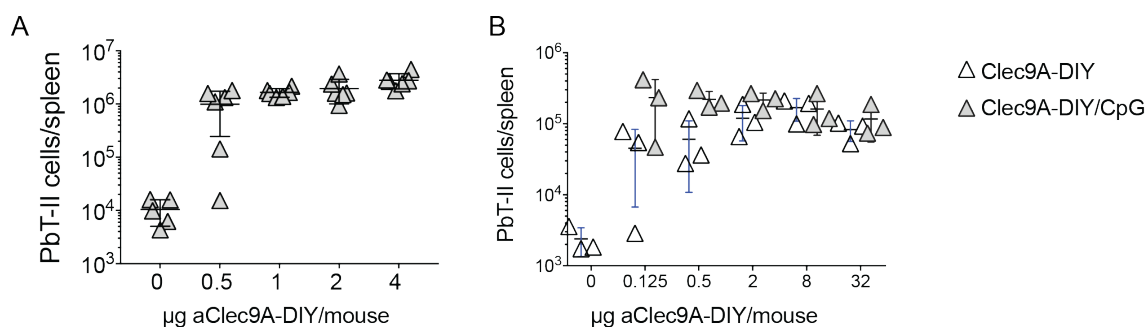


**Figure 3.6. Immunisation with an  $\alpha$ Clec9A construct targeting the DIY epitope induces expansion of PbT-II cells.**

**A, B.** Mice received (A)  $5 \times 10^5$  or (B)  $5 \times 10^4$  CTV-labelled PbT-II.GFP cells and the next day were injected with indicated amounts of  $\alpha$ Clec9A-DIY, with or without 5 nmol CpG adjuvant. PbT-II cells were quantified in the spleen 4 days after immunisation (live, CD4+, V $\alpha$ 2+, GFP+). The experiment was performed (A) two times for a total of 6 mice per group or (B) once with a total of 3 mice per group. (\* $p < 0.05$ ; \*\* $p < 0.01$ ; \*\*\* $p < 0.001$ ; \*\*\*\* $p < 0.0001$ , n.s.  $> 0.05$ , two-tailed Mann-Whitney test)

After the optimal dose of  $\alpha$ -Clec9A-DIY was determined, we investigated the potential of this reagent to induce the generation of PbT-II cell memory populations.  $5 \times 10^4$  PbT-II cells were injected into naïve B6 mice and one day later these mice were primed with 8  $\mu$ g  $\alpha$ -Clec9A-DIY in the presence of CpG. Numbers of PbT-II cells were examined in the liver and the spleen on days 7, 14, 21, and 49 after immunization (Figure 3.7). PbT-II cell numbers in the liver peaked at around day 7 with an average of  $3 \times 10^6$  cells. 6 weeks later, around  $1.4 \times 10^5$  PbT-II cells were still present in the livers of vaccinated mice. In the spleen, the highest PbT-II cell numbers were detected on days 7 and 14. Compared to the liver, the contraction phase of PbT-II cells in the spleen was delayed by around a week. At the day 49 time point,  $6 \times 10^5$  PbT-II cells could be recovered from the spleens of  $\alpha$ Clec9A-DIY primed mice. Compared to blood- and liver-stage *Plasmodium* infection,  $\alpha$ -Clec9A priming could induce substantially higher numbers of effector and memory PbT-II cells in the liver and spleen.

As the nature of memory T cell formation depends on the priming method, PbT-II cell memory subpopulations, defined by expression of CD69 and CD62L, were investigated.

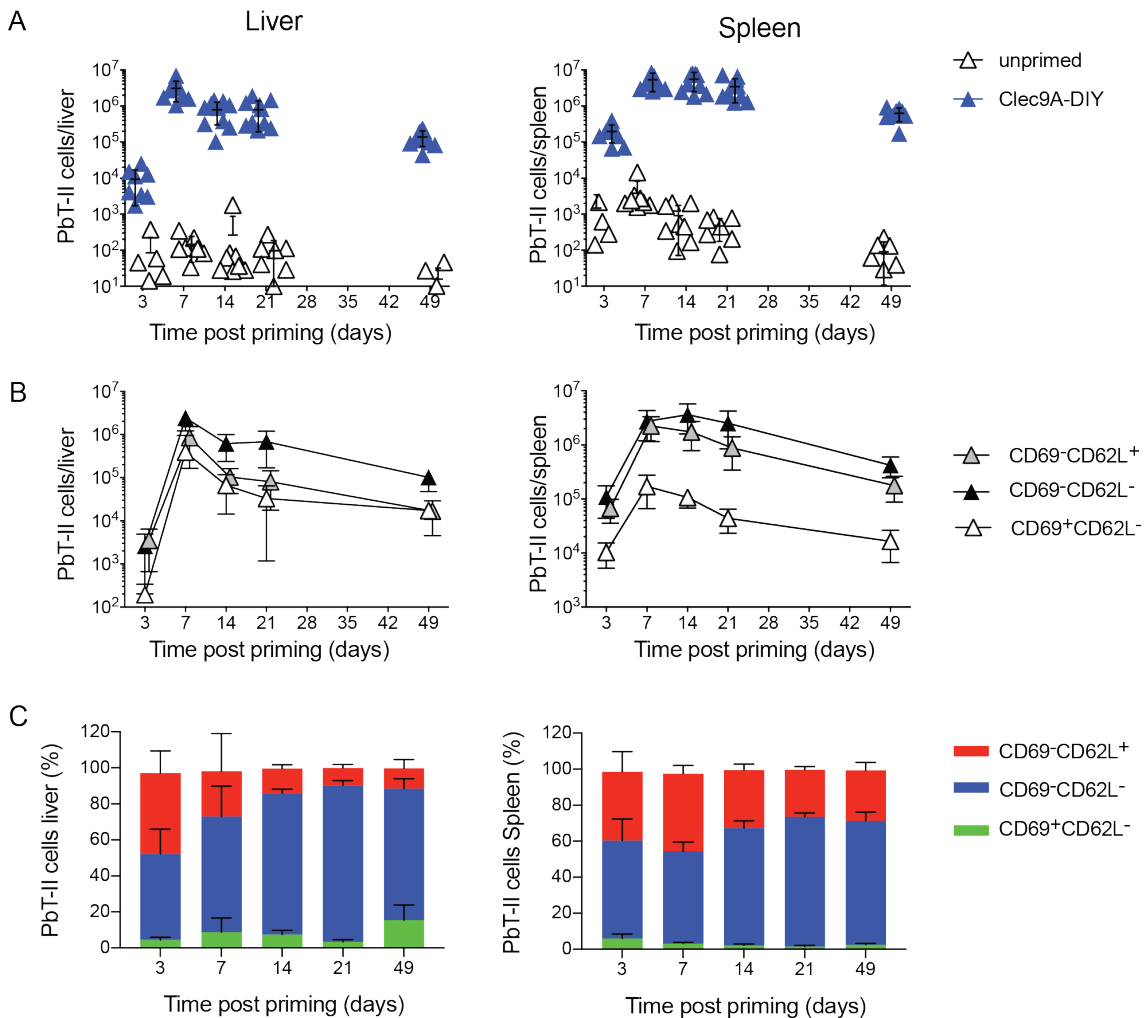


**Figure 3.7. PbT-II cell response to  $\alpha$ Clec9A-DIY construct.**

$5 \times 10^4$  PbT-II.uGFP cells were transferred into naïve B6 mice and one day later mice were injected (i.v.) with  $8 \mu\text{g}$   $\alpha$ Clec9A-DIY and  $5 \text{ nmol}$  CpG. On day 7, 14, 21 and 49 after priming, liver (left) and spleen (right) were harvested and PbT-II cell numbers were determined by flow cytometry by gating on live, CD4<sup>+</sup>, V $\alpha$ 2<sup>+</sup>, GFP<sup>+</sup>, CD44<sup>hi</sup> cells (closed triangles). Naïve PbT-II cell numbers of (live, CD4<sup>+</sup>, V $\alpha$ 2<sup>+</sup>, GFP<sup>+</sup>) uninfected control groups were also included (open triangles). **A.** Total PbT-II cell numbers per organ. Each symbol represents an individual mouse. **B, C.** Analysis of the number (**B**) and proportion (**C**) of PbT-II T cell subsets in the liver (left) and spleen (right) at different time points post-challenge based on expression of CD69 and CD62L. The experiment was performed twice for a total of 10 mice per group.

CD69<sup>-</sup>CD62L<sup>-</sup> PbT-II cells represented the major PbT-II cell population throughout the time course in both liver and spleen (Figure 3.7B, C). At day 49 post-vaccination,  $4 \times 10^5$  and  $10^5$  CD69<sup>-</sup>CD62L<sup>-</sup> PbT-II cells could be detected in the spleen and the liver, respectively. Interestingly, CD69<sup>+</sup>CD62L<sup>-</sup> PbT-II cells (T<sub>RM</sub>) made up 20 % of the total PbT-II cells in the liver at day 49 and represented only 2.5 % of PbT-II cells in the spleen. However, similar CD69<sup>+</sup>CD62L<sup>-</sup> PbT-II cell total numbers of around  $1.7 \times 10^4$  cells were found in both organs 49 days post-immunisation. CD69<sup>+</sup>CD62L<sup>-</sup> PbT-II cells were the PbT-II subpopulation with the lowest rate of decline (1.9-fold) compared to CD69<sup>-</sup>CD62L<sup>-</sup> T<sub>EM</sub> (6.7-fold) and CD69<sup>-</sup>CD62L<sup>+</sup> T<sub>CM</sub> (4.8-fold) cells between day 21 and 49 post  $\alpha$ Clec9A-DIY priming (Figure 3.7B, C).

In general,  $\alpha$ -Clec9A-DIY priming induced extensive PbT-II cell expansion, predominantly generating large numbers of CD69<sup>-</sup>CD62L<sup>-</sup> T<sub>EM</sub> like cells in the liver and spleen. Proportionally, PbT-II cells generated by  $\alpha$ -Clec9A-DIY priming formed larger memory cell populations ( $1.4 \times 10^5$  cells; liver and  $6 \times 10^5$  cells; spleen) 49 days post priming compared to those generated after PbA RAS ( $4 \times 10^3$  cells; liver and  $2 \times 10^3$  cells; spleen) or blood-stage infection ( $5.5 \times 10^3$  cells; liver and  $4.55 \times 10^4$  cells; spleen). Therefore, the mode of CD4 T cell activation influenced the magnitude of the resulting T cell response but also changed the survival and composition of T cell memory subpopulations. Of note, experiments were started on the same day but flow cytometry analyses were performed on different days. This and the fact that, especially in the unprimed mice, only low numbers of PbT-II cells were detectable, can result in variations in total PbT-II cell numbers per organ.

Cell numbers and phenotypes are essential to understand the features of the immune responses to infections. However, the localization of those cells in relation to the pathogen or activation site can also give valuable insights. To explore spatial aspects of the immune response, tdTomato expressing mice were injected with  $5 \times 10^4$  PbT-II.uGFP cells one day before  $\alpha$ -Clec9A-DIY priming, and 2-photon intravital imaging was performed 14 days later. This analysis revealed three distinct types of PbT-II cell behaviour in the liver. Some PbT-II

cells patrolled the sinusoids. Others showed no sign of movement throughout the imaging period of 30-60 minutes. A third group of PbT-II rapidly moved through the sinusoids, essentially moving with blood flow, and were only detectable for 1-3 frames before leaving the imaging field (Figure 3.8A, Appendix Video 8.1). Computational analyses revealed an average velocity of 8  $\mu\text{m}/\text{min}$  for patrolling PbT-II cells (Figure 3.8B), which represents a similar velocity to that reported for CD8 T cells patrolling the liver sinusoids, i.e. 10  $\mu\text{m}/\text{min}$  (Fernandez-Ruiz et al., 2016). Due to the higher speed of the rapidly moving PbT-II cells briefly visible in the liver, these cells could not be included in the analysis. So far, no correlations between the behaviour of the various groups of PbT-II cell and  $T_{EM}$ ,  $T_{RM}$ ,  $T_{CM}$  subpopulations can be drawn, but the patrolling cells are reminiscent of liver CD8  $T_{RM}$  cells (Fernandez-Ruiz et al., 2016). Further 2-photon intravital imaging of sporozoite infected mice might shed additional light on the PbT-II cell response to liver-stage infection and will be discussed in chapter 5.

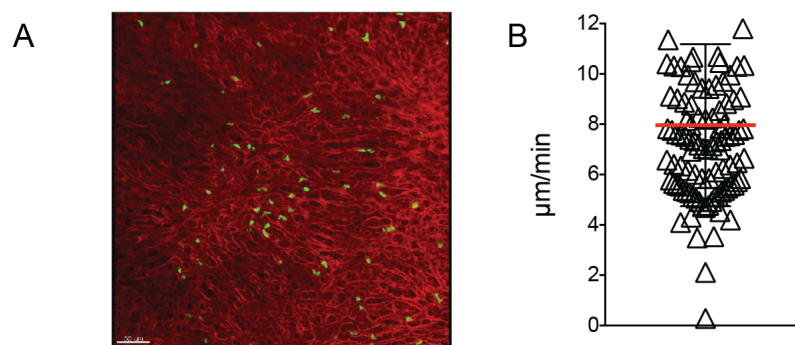


**Figure 3.8. Visualisation of PbT-II cells in the liver after  $\alpha$ -Clec9A-DIY priming.**

$5 \times 10^4$  PbT-II.uGFP cells were transferred into tdTomato mice one day prior to administration of  $2\mu\text{g}$   $\alpha$ Clec9A-DYI and 5 nmol CpG-combo. 14 days later mice underwent a surgical procedure to gain access to the liver and 2 photon-intravital imaging was performed. **A.** Representative image of the liver structure (red) and PbT-II cells (green) 14 days post-priming. **B.** Speed data of PbT-II cells were analysed from 30-40 min time-lapse series using IMARIS software. Data were pooled from 3 independent images of  $n = 6$  mice.

### 3.2.4 Endogenous CD4 T cell response to Hsp90 epitope

To make use of the newly detected MHC-II restricted PbA epitope as a potential vaccine-candidate, it was important to know whether there was an endogenous response to this epitope, as so far, we had only examined responses by transgenic PbT-II cells. Therefore, in collaboration with Dr Hugh Reid from Prof Rossjohn's laboratory, an MHC-II tetramer was generated, carrying the Hsp90 epitope, to detect endogenous CD4 T cells.

To determine the ideal MHC-II tetramer staining condition, splenocytes from naïve PbT-II mice were incubated for up to 180 min, at 4 or 37°C with different concentration of the specific MHC-II tetramer (IA<sup>b</sup>-Hsp90) and assayed by flow cytometry. As seen in Figure 3.9, a high concentration (18 µg/ml) of IA<sup>b</sup>-Hsp90 resulted in the highest proportion of MHC-II tetramer positive CD4 T cells. In addition, 37°C improved the staining efficiency at lower MHC-II tetramer concentrations and shorter incubation times (Figure 3.9A, B). Based on this analysis, IA<sup>b</sup>-Hsp90 staining was routinely performed at 37°C for 30 min with 18 µg/ml MHC-II tetramer per sample.

Utilising the MHC-II tetramer staining conditions, the formation of endogenous Hsp90 specific CD4 T cell populations was investigated after PbA blood-stage infection (Figure 3.9C, D). Seven days post-infection, around  $2 \times 10^3$  and  $2 \times 10^4$  IA<sup>b</sup>-Hsp90<sup>+</sup> CD4 T cells could be detected in the liver and spleen, respectively. However, by day 14 and 21 no differences between infected and naïve mice could be detected by IA<sup>b</sup>-Hsp90 staining. This suggested T cell numbers reduced rapidly to low levels, below detection by this approach.

As shown in the previous chapter,  $\alpha$ -Clec9A-DIY priming induced more extensive PbT-II memory cell formation compared to blood-stage infection. To determine if  $\alpha$ -Clec9A-DIY priming also induced higher numbers of endogenous DIY-specific T cells, naïve mice were primed with 8 µg  $\alpha$ Clec9A-DIY and 5 nmol CpG. Around  $6 \times 10^3$  cells were detected in the liver and  $5 \times 10^4$  cells in the

spleen 7 days post-priming (Figure 3.9E, F). While IA<sup>b</sup>-Hsp90<sup>+</sup> CD4 T cells could be detected at later time points, high background staining and low separation of MHC-II tetramer positive and negative cells complicated interpretation (Figure 3.9G). To try to better separate specific cells from background staining, enrichment (MACS) of tetramer<sup>+</sup> cells from the spleens of mice 7 days post-PbA blood-stage infection was performed. This approach uses magnetic beads to enrich for MHC-tetramer-stained cells. After splenocytes were labelled with IA<sup>b</sup>-Hsp90 tetramer conjugated to phycoerythrin (PE), the samples were incubated with anti-PE beads and placed on a magnet. After washing out unlabelled cells, enriched and unenriched samples were examined by flow cytometry (Figure 3.9H). The enriched sample showed better separation between IA<sup>b</sup>-Hsp90 positive and negative populations compared to an unenriched sample (Figure 3.9D, E). Based on this analysis, MACS enrichment appeared to be a promising technique to quantitate Hsp90 reactive CD4 T cells. However, the limited availability of IA<sup>b</sup>-PbHsp90 tetramer reagent and the high enrichment cost meant that an alternative approach was sort, i.e. Enzyme-Linked Immunospot (ELISpot) assays, to examine memory responses by endogenous Hsp90-specific CD4 T cells.

The ELISpot assay is a highly sensitive technique for the detection of cytokine secreting cells. To identify endogenous Hsp90 specific memory CD4 T cells, mice were either vaccinated with  $\alpha$ Clec9a-DIY or infected with PbA iRBCs. 35 days later, spleen and liver lymphocytes were used for the IFN- $\gamma$  ELISpot assay. An anti-IFN- $\gamma$  mAb was used to detect IFN- $\gamma$  producing cells in response to the Hsp90 epitope. In the spleen, 480 and 157 cells per million plated cells secreted IFN- $\gamma$  in response to the DIY epitope after priming with  $\alpha$ Clec9A-DIY or *Plasmodium* infection, respectively (Figure 3.10A). In the liver, IFN- $\gamma$  producing cells, above background level, were only detectable after  $\alpha$ Clec9A-DIY vaccination (Figure 3.10B). These data show that an endogenous Hsp90 specific memory CD4 T cell population formed after  $\alpha$ Clec9A priming and *Plasmodium* blood-stage infection. Furthermore, as previous experiments indicated (Figure 3.1 and Figure 3.6), where transgenic PbT-II cells were used,  $\alpha$ Clec9A-DIY

vaccination induced a larger endogenous Hsp90-specific CD4 T cell population compared to iRBC infection. It should be mentioned that not all cells secrete IFN- $\gamma$ . Therefore, unlike MHC-II tetramers, where all Hsp90 specific CD4 T cells can be identified, only a subpopulation of Hsp90 specific cells were detected by the ELISpot assay. Nevertheless, the observed induction of endogenous CD4 T cells reactive to the DIY epitope, strengthened the view that Hsp90 can be used as a potential CD4 T cell antigen for vaccination.

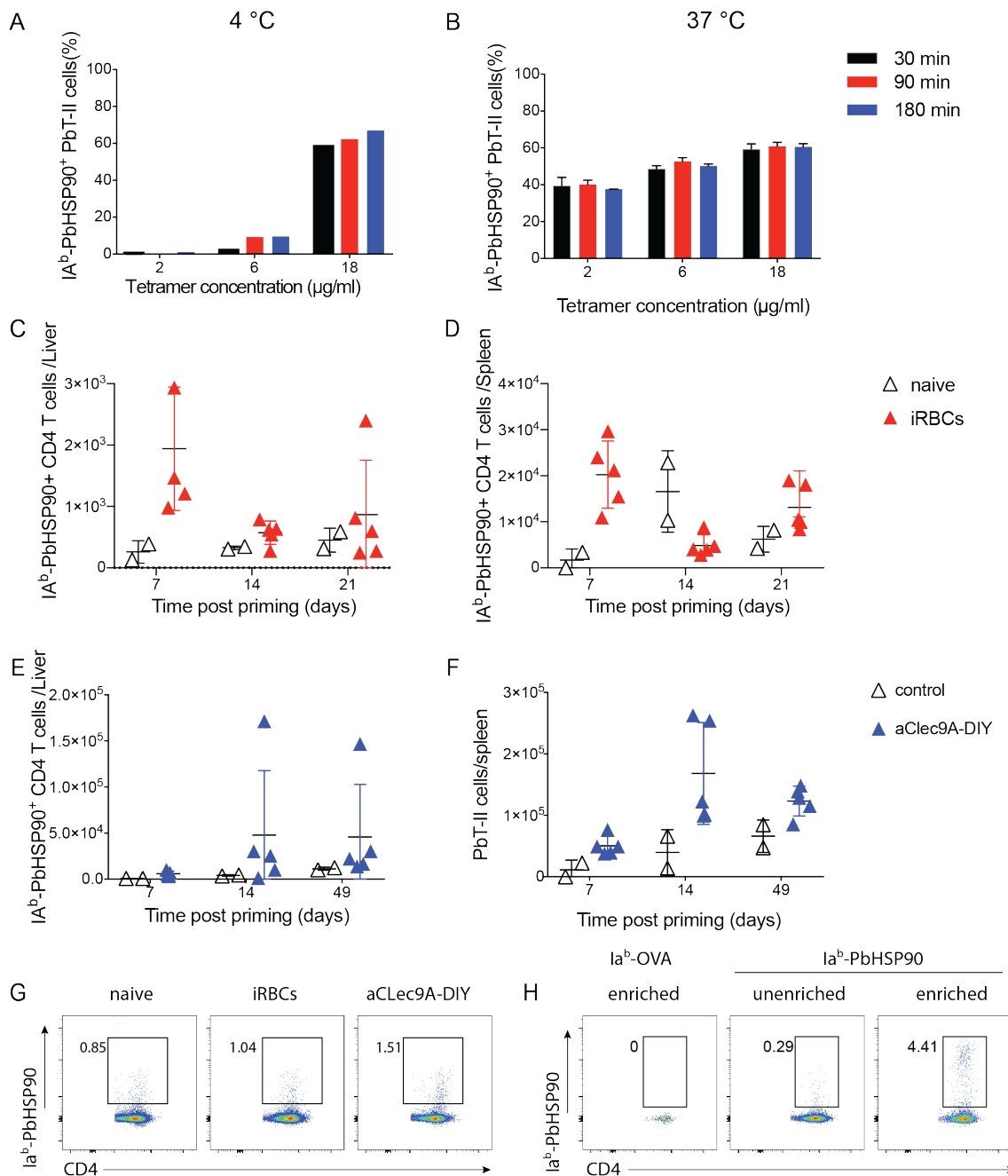


**Figure 3.9. Detection of an endogenous CD4 T cell population reactive to the DIY epitope.**

**A, B.** Titration of IA<sup>b</sup>-HSP90 Tetramer using naïve PbT-II spleen cells. Staining was performed with an MHC-II tetramer concentration between 2-18 μg/ml for 30, 90 or 180 min at 4 (**A**) or 37°C (**B**). Data represent two independent experiments with a total of 3 PbT-II mice **C-H**. B6 mice were infected with (**C, D**) 10<sup>4</sup> PbA iRBCs and cured from day 5 of infection or (**E, F**) vaccinated with 2 μg αClec9A-DIY and 5 nmol CpG. Liver (**C, E**) and spleen (**D, F**) were harvest 7 to 21 days post priming and IA<sup>b</sup>-Hsp90 staining was performed at 37 degree and 18 μg/ml for 30 min. **G.**

Representative dot plots from B and C, 7 days post infection or immunisation. (\* $p < 0.05$ ; \*\* $p < 0.01$ ; \*\*\* $p < 0.001$ ; \*\*\*\* $p < 0.0001$ ; n.s.  $> 0.05$ ; two-tailed Mann-Whitney test). Data represent single experiments with a total of 4-5 mice **E**. Representative dot plots after Magnetic-activated cell sorting enrichment (MACS) (right) or unenriched (middle) of IA<sup>b</sup>-HSP90 stained spleen cells of B6 mouse 7 days post infection with  $10^4$  PbA iRBCs. IA<sup>b</sup>-HSP90<sup>+</sup> CD4 T cells were defined as CD4<sup>+</sup>, CD62L<sup>-</sup>, B220<sup>-</sup>, NK1.1<sup>-</sup>, IA<sup>b</sup><sup>+</sup> cells.

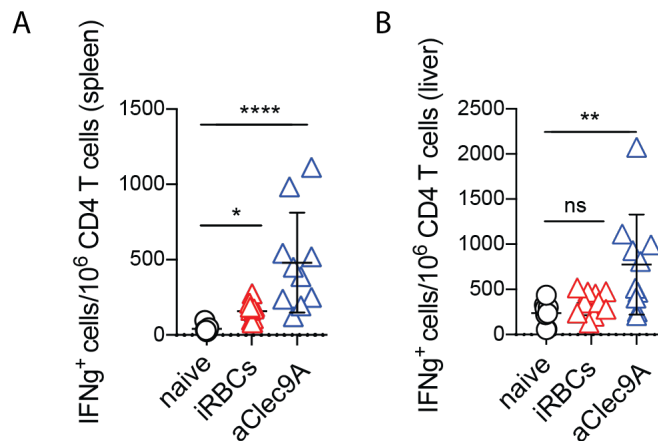


**Figure 3.10. Induction of an endogenous CD4 T cell memory response to the DIY epitope**

Mice were infected with  $10^4$  PbA iRBCs and cured from day 5, or vaccinated with  $2 \mu\text{g}$   $\alpha$ Clec9A-DIY and  $5 \text{ nmol}$  CpG. **A, B.** 35 days after infection or vaccination, spleen (**A**) or liver (**B**) derived lymphocytes (including  $2.5 \times 10^5$  CD4 T cells/well) were restimulated *in vitro* with the DIY peptide and an ELISpot assay was performed to detect IFN- $\gamma$  producing cells. (\* $p < 0.05$ ; \*\* $p < 0.01$ ; \*\*\* $p < 0.001$ ; \*\*\*\* $p < 0.0001$ ; n.s.  $> 0.05$ ; Kruskal-Wallis followed by Dunn's Multiple Comparisons test). Data were pooled from 2 independent experiments with a total of 10 mice per group.

### 3.2.5 PbT-II cells can be differentiated into specific T helper subsets.

Different CD4 T cell lineages can mediate different effector functions, e.g. Th1 cells activate macrophages, whereas Tfh cells primarily induce B cell maturation and antibody class switching (Fontana et al., 2016, Perez-Mazliah et al., 2017). The composition of the CD4 T cell pool in terms of T cell lineages depends on the nature of the infection. PbA blood-stage infection induces Th1 and Tfh cells, whereas Th2 responses are undetectable (Fernandez-Ruiz et al., 2017). However, Th2 cells have been reported to play a role in *Plasmodium* infection (Taylor-Robinson et al., 1993). Furthermore, IL-4, secreted by Th2 cells,

was described to be crucial for CD8 T cell responses to sporozoite infection, which is why we aimed to investigate the protective capacity of this particular CD4 lineage (Carvalho et al., 2002). To overcome limitations arising from *in vivo* differentiation and mixed CD4 T cell pools, an *in vitro* polarization assay was established that aimed to generate large numbers of pure PbT-II Th1 or Th2 cells (Figure 3.11). This technique allowed for examination of lineage-specific differences in memory CD4 T cell formation and responses to *Plasmodium* infection.

To achieve CD4 T cell differentiation, PbT-II cells were co-cultured with DIY-peptide pulsed DCs for 4-5 days under Th1 or Th2 polarising conditions (Figure 3.11A, Chapter 2.2.7). Th1 polarizing conditions led to stable expression of the Th1 differentiation transcription factor Tbet in over 90 % of PbT-II cells (Figure 3.11B). In contrast, under Th2 polarizing conditions most PbT-II cells expressed Gata3, the transcription factor responsible for Th2 differentiation (Figure 3.11B). A low proportion of Th1 or Th2 differentiated PbT-II cells expressed the transcription factors Ror $\gamma$ T while none expressed FoxP3, which relate to Th17 and Treg differentiation, respectively (Figure 3.11B). This data showed that PbT-II cells can be efficiently differentiated into the Th1 and Th2 lineages with very low levels of cross contamination of Th17 differentiated cells.

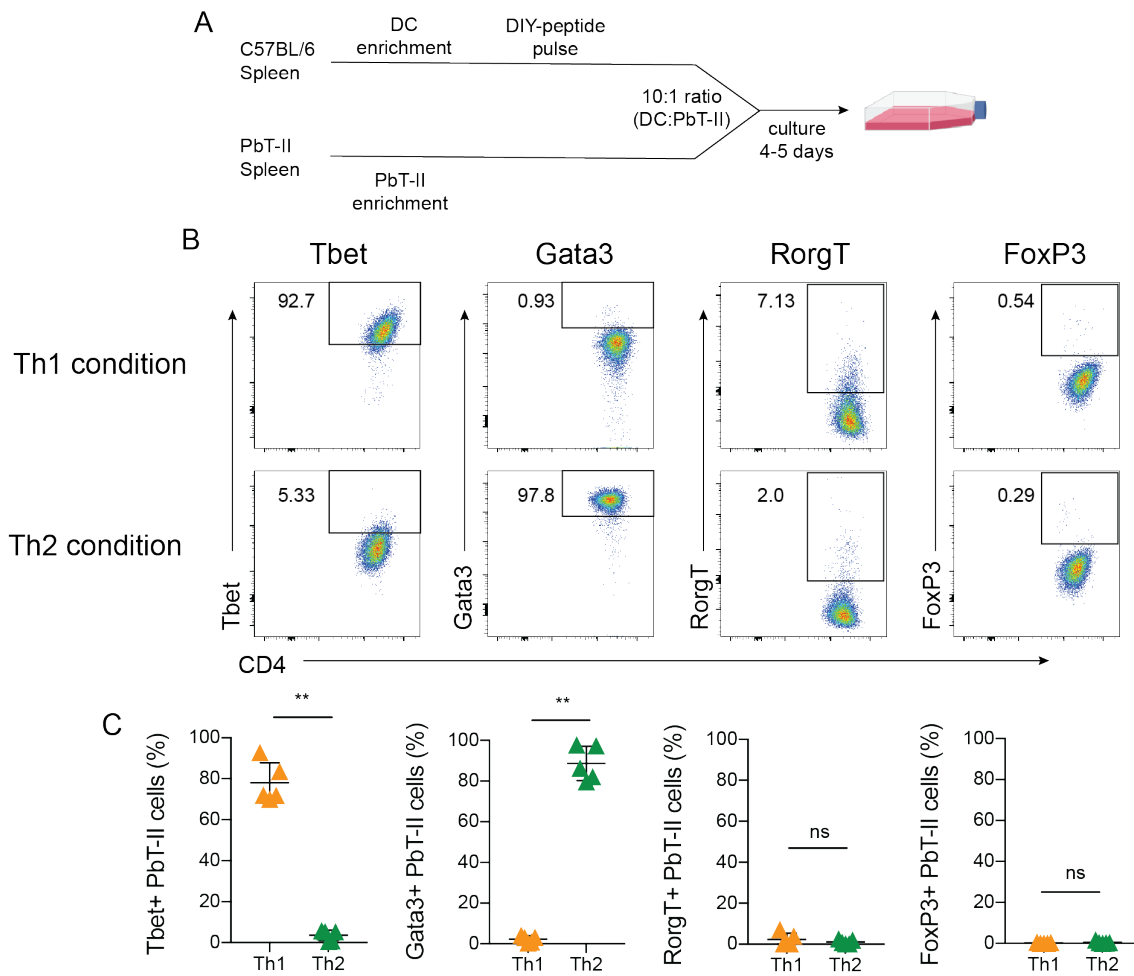


**Figure 3.11. Th1 and Th2 *in vitro* differentiation of PbT-II cells.**

$10^6$  purified, naïve PbT-II cells were co-cultured with  $10^7$  DIY-peptide pulsed dendritic cells for 5 days under Th1 or Th2 polarization condition (Chapter 2.2.7). Expression of the transcription factors Tbet, Gata3, Ror $\gamma$ T and FoxP3 were examined by flow cytometry 5 days after the initiation of cultures. **A.** Experimental scheme. **B.** Representative dot plots for data in C, by gating on live, CD4<sup>+</sup>, V $\alpha$ 2<sup>+</sup>, GFP<sup>+</sup> cells. **C.** Percentage of transcriptions factor positive cells. (\*\* $p < 0.001$ ; ns, not significant; two-tailed Mann-Whitney test. Data were pooled from 2 independent experiments with total of 5 different flask per group.

### 3.2.6 Expression of lineage-specific cytokines and surface markers after differentiation of PbT-II cells.

Priming induced by the injection of the mAb  $\alpha$ Clec9A was previously shown to induce IFN- $\gamma$  producing CD4 T cells (Th1 cells) as well as Tfh cells (Kato et al., 2015). Similarly, a previous study using PbA blood-stage infection showed that PbT-II cells differentiated into Th1 as well as Tfh cells (Fernandez-Ruiz et al., 2017). To validate previous reports, PbT-II cells were phenotyped for their specific CD4 T cell lineage by investigating cytokine expression. To do this, mice were injected iv with either PbA iRBCs or  $\alpha$ Clec9A-DIY one day after transfer of PbT-II cells. Seven days post-priming, splenic PbT-II cells were re-stimulated *in vitro* with DIY peptide and examined for cytokine production (Figure 3.12). After blood-stage *Plasmodium* infection, 51.6 % of PbT-II cells produced IFN- $\gamma$  and around 13 % also expressed TNF and can therefore be considered as Th1 cells (Figure 3.12A-C). After,  $\alpha$ Clec9A-DIY priming and re-stimulation, 40 % of the PbT-II cells expressed IFN- $\gamma$ . These cells also expressed TNF (17 %) and low levels of IL-2 (22 %), the latter of which was not detectable in iRBCs primed PbT-II cells. While a low level of IL-10 expression was also detectable after blood-stage infection or  $\alpha$ Clec9A-DIY priming, none of the other cytokines that were tested were detectable (Figure 3.12A-C). Therefore, PbA blood-stage infection, as well as  $\alpha$ Clec9A-DIY priming, led to Th1 differentiation of PbT-II cells early after infection or priming (Figure 3.12A, B). The induction of Tfh cells after *Plasmodium* blood-stage infection or  $\alpha$ -Clec9A-DIY immunisation was investigated by examining the expression of PD1 and CXCR5, markers of Tfh cells. However, PD1 staining was faint, therefore we first examined CXCR5 expression alone. PbA blood-stage and  $\alpha$ Clec9A-DIY priming induced the upregulation of CXCR5 in 36.6 % and 69.8 % of PbT-II cells, respectively (Figure 3.12D-F). Although PD1 staining was low, its expression could be observed after both priming methods relative to the lack of expression seen for Th1 or Th2 cells-differentiated PbT-II cells. However,  $\alpha$ -Clec9a-DIY activated PbT-II cells showed

greater expression of PD1 than PbT-II cells from mice infected with PbA iRBCs (Figure 3.12D, F). In line with previous reports, this data demonstrates that *Plasmodium* blood-stage infection and  $\alpha$ -Clec9A priming induced differentiation towards Th1 and Tfh cells.

As shown in Figure 3.11 PbT-II cells could be differentiated into Th1 and Th2 cells, but it was unclear if these cells remained in their specific differentiation state. Therefore, PbT-II cells previously differentiated into Th1 and Th2 cells were examined for cytokine production, 7 days after transfer into mice. Most splenic PbT-II Th1 cells expressed IFN- $\gamma$  (71.2 %) and TNF (90 %) (Figure 12A-C). Furthermore, the majority of Th2 differentiated PbT-II cells expressed IL-4 (54.6 %) and/or IL-13 (64.2 %), hallmark cytokines for Th2 CD4 T cells. In addition, Th1 and Th2 differentiated PbT-II cells showed a higher proportion of IL-2-expressing cells compared to  $\alpha$ -Clec9-DIY primed PbT-II cells. Other than the hallmark cytokines for Th1 and Th2 lineage and IL-2, no other cytokine expression was detectable (Figure 3.12A-C). In addition, no staining for Tfh surface markers CXCR5 and PD-1 was observed in PbT-II Th1 or Th2 cells (Figure 3.12D-F). This indicated that both Th1 and Th2 differentiated PbT-II cells did not differentiate into other CD4 lineages, for at least 7 days after transfer into naïve mice.

In Summary, PbT-II cells differentiate into Tfh and Th1 CD4 T cell lineages after PbA blood-stage infection and  $\alpha$ -Clec9A-DIY priming, with  $\alpha$ Clec9A priming favouring the Tfh phenotype. Furthermore, *in vitro* differentiated Th1 and Th2 PbT-II cells remained stable in their specific T helper lineages for at least 7 days after adoptive cell transfer.

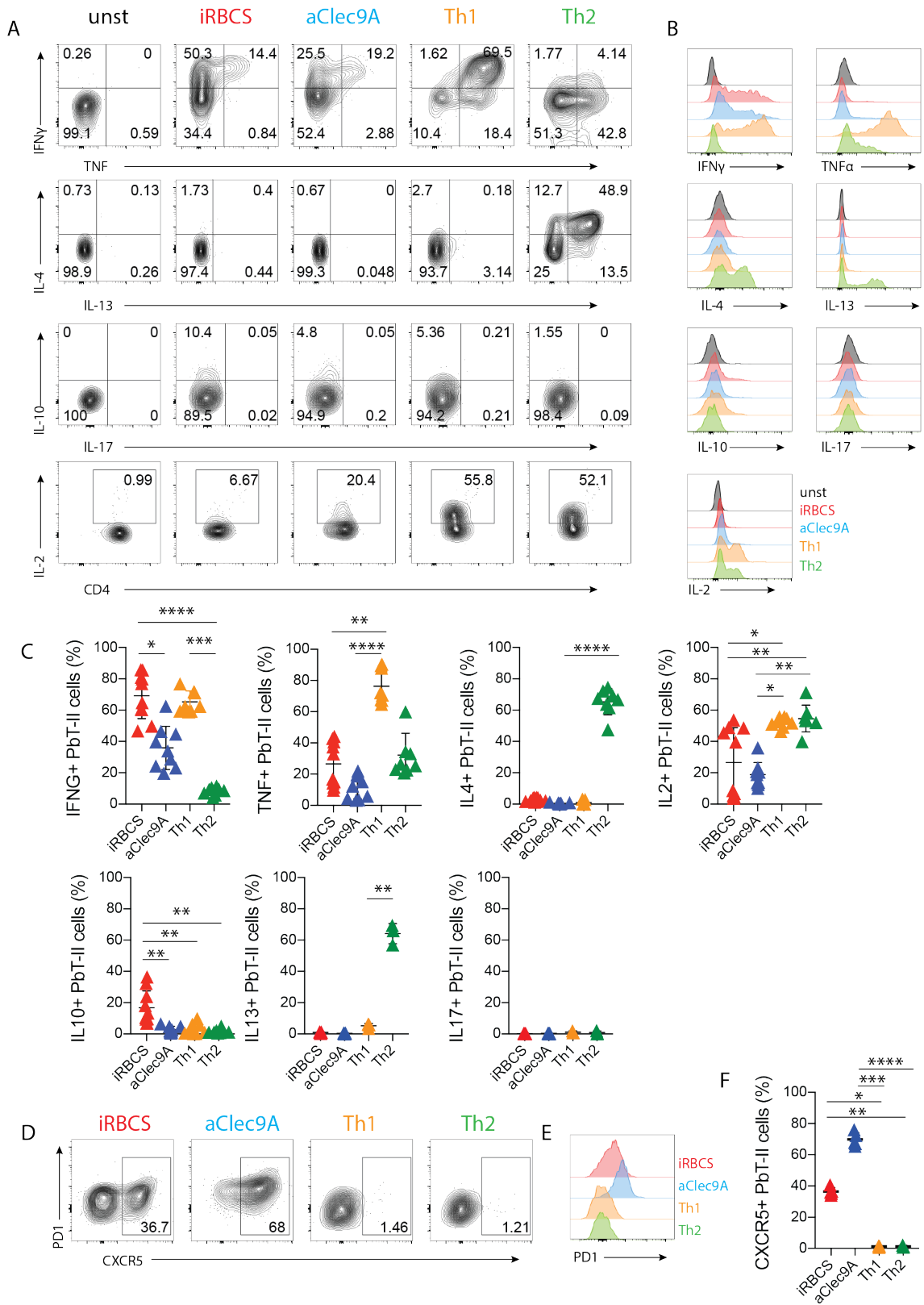


**Figure 3.12. Phenotypes of PbT-II cells generated after PbA iRBC infection,  $\alpha$ Clec9A-DIY priming or *in vitro* differentiation.**

Naïve mice received  $5 \times 10^4$  PbT-II.GFP cells and, one day later, were infected with  $10^4$  PbA iRBC or primed with  $2 \mu\text{g}$   $\alpha$ Clec9A-DIY and 5 nmol CpG. Additional mice received  $2 \times 10^6$  *in vitro* polarised PbT-II Th1 or Th2 cells. **A-C.** 7 days post infection, immunisation or adoptive cell transfer, spleen cells were recovered and IFN- $\gamma$ , TNF, IL-4, IL-13, IL-10, IL-17 and IL-2 production by PbT-II cells was determined by intracellular staining 5 h post-incubation with brefeldin A and DIY peptide. **A.** Representative dot plots. **B.** Representative histograms. **C.** Percentages of PbT-II cells expressing the indicated cytokines. **D-F.** Additional unstimulated samples were stained for PD1 and CXCR5 expression **D.** Representative contour plots. **E.** Representative histograms for PD1 expression. **F.** Proportions of CXCR5<sup>+</sup> cells. **A, B** are representative for the data shown in **C**. **D, E** are representative for the data shown in **F**. **C, F** were pooled from 2 independent experiments. IL-17 and IL-13 expression was examined in a single experiment. Each experiment included 3-5 mice per group. (\* $p < 0.05$ ; \*\* $p < 0.01$ ; \*\*\* $p < 0.001$ ; \*\*\*\* $p < 0.0001$ ; n.s.  $> 0.05$ ; Kruskal-Wallis followed by Dunn's Multiple Comparisons test)

### 3.3 Discussion

Induction of memory T cell populations is crucial to protect against experimental *Plasmodium* infection by vaccination (Doolan and Hoffman, 2000, Schmidt et al., 2010, Butler et al., 2010, Fernandez-Ruiz et al., 2016). However, only limited numbers of immunogenic MHC-I or MHC-II restricted epitopes are described that can potentially be harnessed for use as vaccine targets (Hafalla et al., 2013, Pichugin et al., 2018, Valencia-Hernandez et al., 2020, Draheim et al., 2017). This chapter aimed to characterise the formation of memory CD4 T cells specific to a so far unknown PbA derived MHC-II restricted epitope, after *Plasmodium* infection or vaccination.

To investigate the formation of *Plasmodium*-specific memory CD4 T cells, a T cell receptor (TCR) transgenic CD4 T cell line, termed PbT-II, was used. Previous work showed that PbT-II cells responded by proliferation after iRBCs infection with various rodent *Plasmodium* species and after PbA RAS immunisation (Fernandez-Ruiz et al., 2017). In line with the latter study, PbT-II cells were found to proliferate and form a memory PbT-II cell population, which was still detectable 50 days after RAS immunisation. In addition, PbT-II memory cells were generated in response to PbA iRBCs infection and their numbers exceeded those generated by RAS vaccination. Both immunization methods induced memory PbT-II cell populations consisting of T<sub>EM</sub>, T<sub>CM</sub>, and T<sub>RM</sub>-like cells based on the expression of CD69 and CD62L, similar to CD8 memory T cells found after RAS vaccination in liver and spleen (Schmidt et al., 2010, Fernandez-Ruiz et al., 2016). As RAS-induced CD8 memory T cells can protect against *Plasmodium* liver stage infection in different mouse strains, we hypothesised that, similarly, the generation of large numbers of memory CD4 T cells might also protect against infection (Doolan and Hoffman, 2000). However, it was essential to identify the cognate antigen of PbT-II cells to allow us to utilise these cells and their cognate antigen for vaccination studies against *Plasmodium* blood and liver-stage infection.

The immunogenic epitope of Hsp90-peptide responsible for PbT-II cell activation was identified as an 18-mer peptide (DNQKDIYYITGESINAVS) eluted from MHC-II molecules (IA<sup>b</sup>) of DCs after PbA iRBCs exposure. Unlike MHC-I molecules, which have a stabilised binding groove, allowing peptide fragments of 8-10 amino acids to bind, MHC-II molecules have an open binding groove allowing larger peptides to bind to the cleft with protruding amino acids at both sides (Bouvier and Wiley, 1994, Van Bleek and Nathenson, 1990, Jardetzky et al., 1991, Fremont et al., 1998, Park et al., 2003, Hunt et al., 1992, Brown et al., 1993). While peptides are stabilised by hydrogen bonds between peptide and amino acids within the binding cleft, the primary binding site is a 9-mer core (McFarland et al., 1999, Landais et al., 2009, Holland et al., 2013). This 9-mer core is flexible and can allow the same peptide to bind in different MHC-II molecule registers, hence using alternative 9-mer cores (McFarland et al., 1999). However, protruding residues, flanking the 9-mer core, can also influence the MHC-II-peptide binding stability, TCR interaction and MHC-II affinity (McFarland et al., 1999, Landais et al., 2009, Nelson et al., 1994, Holland et al., 2013). Therefore, it was necessary to determine the minimal epitope within PbHsp90. YITGESINA was the minimal epitope to activate PbT-II cells, as further reduction of either C or N terminal amino acids led to a drastic loss in T cell activation. However, maximal PbT-II cell stimulation was achieved by a 14-mer (DIYYITGESINAVS), that included additional amino acids on both sides of the 9-mer core. Interestingly, additional amino acids on either the N or C terminus of this 14-mer that generated the original 18-mer peptide did not increase PbT-II cell stimulation, suggesting that these extra residues that protrude from the MHC-II binding cleft might not be involved in interactions with either MHC-II or the TCR. As longer peptides associated with MHC-II can be digested in acidified endocytic vesicles to form shorter versions, it is possible that the eluted long peptide version and other long versions were shortened by DCs before being presented on the MHC-II molecule to PbT-II cells (Watts, 1997).

Previous work revealed that PbT-II cells proliferate in response to *in vitro* incubation with *P. falciparum* iRBCs (Fernandez-Ruiz et al., 2017). In line with this finding, a similar sequence to DIY is found in *P. falciparum*, with only one

residue differing in this species, i.e. the initial D being E. It was, therefore, no surprise that this residue variation, well outside the 9-mer core peptide, did not affect immunogenicity. As PbT-II cells were also shown to proliferate after *P. yoelii* 17XNL, *P. chabaudi* AS, *P. berghei* NK65 iRBCs infection, the use of the Hsp90 epitope enables study of CD4 T cell responses to multiple *Plasmodium* species (Fernandez-Ruiz et al., 2017).

Hsp90 is commonly found in the cytoplasm of *P. falciparum* parasites (Pallavi et al., 2010, Echeverria et al., 2005, Banumathy et al., 2003). However, unlike other commonly expressed heat shock proteins, Hsp90 is not found in the exportome of infected red blood cells (Sargeant et al., 2006). Nevertheless, Hsp90 can be presented to CD4 T cells via MHC-II molecules as APCs can phagocytose parasites and present internal proteins (Fernandez-Ruiz et al., 2017, Arroyo and Pepper, 2019). While the cytosolic character of Hsp90 prevents it from being targeted by humoral responses, Hsp90-specific CD4 T cells can activate B cells of other specificities to mediate isotype class switching and high-affinity antibodies that eventually clear the infection (Fernandez-Ruiz et al., 2017, Kawabe et al., 1994). This was shown by the use of CD40L<sup>-/-</sup> mice, where endogenous CD4 T cells were unable to provide help for B cells (Fernandez-Ruiz et al., 2017). PbT-II transfer prior to Pch infection rescued the otherwise lethal infection and partially restored Pch specific humoral responses.

Additional MHC-II restricted *Plasmodium* epitopes have been described. For example, Draheim and colleagues identified 14 different MHC-II restricted PbA specific epitopes obtained from PbA blood stage infection (Draheim et al., 2017). While Hsp90 was not identified in this study, 8 of the 14 epitopes induced significant IFN- $\gamma$  and TNF expression in CD4 T cells from PbA iRBC infected mice. Unlike Hsp90, two of the three most dominant peptides (ETRAPM, MSP1) identified in this study are only expressed by PbA but not expressed by Pch blood-stage parasites. Furthermore, it is not clear whether those epitopes are also expressed in sporozoites and thus can induce CD4 T cell responses that target the liver stage of infection (Draheim et al., 2017).

The highly conserved nature of Hsp90 and the fact that memory T cell formation can be induced in responses against liver and blood-stage parasites makes this epitope a suitable candidate for vaccine studies to generate memory CD4 T cell responses against both infectious *Plasmodium* stages. However, to induce CD4 T cell activation and proliferation, a cognate antigen has to be presented via MHC-II molecules expressed by APCs. In PbA iRBCs infection, CD8<sup>+</sup> DCs were shown to be the dominant DC population responsible for PbT-II cell priming (Fernandez-Ruiz et al., 2017). These CD8<sup>+</sup> DCs can be specifically targeted with antigen by a monoclonal antibody (mAb) against the surface C-type lectin-like molecule Clec9A, which is expressed on mouse CD8<sup>+</sup> DCs and human BDCA-3<sup>+</sup> DCs (Caminschi et al., 2008, Huysamen et al., 2008). mAbs targeting the Clec9A receptor ( $\alpha$ Clec9A), fused to specific epitopes, induced strong humoral, CD4, and CD8 T cell responses in mice and strong humoral responses in non-human primates (Idoyaga et al., 2011, Li et al., 2015). CD4 T cell responses induced by  $\alpha$ Clec9A treatment are characterised by strong Tfh and moderate Th1 formation, reflecting CD4 T cell lineages found to be generated after *Plasmodium* iRBCs infection (Lahoud et al., 2011, Lönnberg et al., 2017, Fernandez-Ruiz et al., 2017). As  $\alpha$ Clec9A subunit vaccination was shown to induce potent CD4 T cell activation, an  $\alpha$ Clec9A subunit vaccine carrying the Hsp90 epitope ( $\alpha$ Clec9A-DIY) was designed to induce PbT-II cell activation (Lahoud et al., 2011, Kato et al., 2015). In line with previous studies, injection of this construct resulted in the differentiation of Tfh and Th1 PbT-II cells (Lahoud et al., 2011, Kato et al., 2015). Interestingly,  $\alpha$ Clec9A-DIY vaccination induced memory PbT-II cell responses exceeding those seen after RAS vaccination or PbA iRBCs infection. While the amount of cognate antigen injected can be precisely defined for  $\alpha$ Clec9A targeting, it is not known how much cognate PbT-II antigen is available after RAS vaccination or PbA iRBCs infection. This discrepancy in antigen availability might be one factor leading to different sizes of PbT-II memory cell pools. RAS parasites that infiltrate the hepatocytes might be “shielded” from CD4 T cell recognition, as hepatocytes do not express MHC-II molecules under steady state-conditions, which would result in low antigen availability for CD4 T cells (Franco et al., 1988). The reduced PbT-II memory cell

formation after RAS compared to  $\alpha$ Clec9A-DIY vaccination could therefore be due to antigen availability. However, iRBCs can be phagocytosed by macrophages and DCs, which can present cognate antigen via MHC-II molecules. Rising parasitaemia after iRBCs infection before drug treatment most likely led to high antigen availability, suggesting that other mechanisms might contribute to the different magnitudes of CD4 T cell memory responses. One likely explanation for reduced PbT-II cell memory formation after PbA iRBCs infection is the induction of regulatory mechanisms. It was previously shown that IL-27 secreting CD4 T cells were induced after PbA iRBCs infection (Kimura et al., 2016). The secretion of IL-27 led to a reduced IL-2 production by CD4 T cells that did not secrete IL-27 (Kimura et al., 2016, Sukhbaatar et al., 2020). While our study did not investigate the production of IL-27, we found that IL-2 secretion by PbT-II effector cells generated after PbA iRBCs infection was reduced compared to  $\alpha$ Clec9A-DIY vaccination. As IL-2 is a crucial cytokine for T cell differentiation and survival, IL-27 producing CD4 T cells induced by PbA iRBCs infection could have led to reduced expression of IL-2 by PbT-II effector cells and therefore reduced formation of effector and memory T cells (Kelly et al., 2002). Furthermore, IL-2 production by PbT-II cells after  $\alpha$ Clec9A-DIY vaccination was reduced compared to in vitro differentiated PbT-II Th1 and Th2 cells. Interestingly, a study published by Attridge et. al linked one of the Tfh key cytokines, IL-21, with active reduction of CD4 T cell derived IL-2 in cell cultures (Attridge et al., 2012). It is therefore possible, that Tfh cells expressed large amounts of IL-21 after  $\alpha$ Clec9A-DIY priming which therefore limited the ability of PbT-II cells to express IL-2. However, IL-21 levels of PbT-II cells after  $\alpha$ Clec9A-DIY priming were not analysed in this study and will need to be evaluated.

As vaccines must ultimately induce endogenous memory T cell responses, the finding that we were able to induce endogenous Hsp90-reactive CD4 memory cells after  $\alpha$ Clec9A-DIY vaccination supports the potential of this vaccination strategy. However, the induced endogenous IFN- $\gamma$ <sup>+</sup> memory CD4 T cell response was relatively small compared to that seen for PbT-II cells. This difference was

most likely because  $5 \times 10^4$  PbT-II cells were injected before vaccination or infection, which is a relatively large number compared to endogenous precursor populations. For example, it has been shown that naive CD4 T cell precursors vary from 20-200 cells per naive mouse (Moon et al., 2007). It was further suggested that the size of the CD4 precursor T cell population could directly influence the number of induced memory T cells in humans (Kwok et al., 2012). Determining the number of Hsp90 restricted precursor cells may be useful to provide an estimate of the maximal amount of endogenous Hsp90-restricted memory that can be induced through vaccination. It is worth noting that  $\alpha$ Clec9A vaccination and PbA iRBCs infection induce both IFN- $\gamma$  secreting Th1 cells as well as a significant number of Tfh cells that do not express IFN- $\gamma$ . Therefore, the endogenous memory CD4 T cell pool reactive to the Hsp90 epitope will be larger than that measured simply by detecting IFN- $\gamma$  producing CD4 T cells. It would therefore be useful to investigate the formation of endogenous Hsp90-reactive memory T cells based on additional cytokines also expressed by other CD4 T cell lineages such as TNF, IL-4 and IL-21, in future experiments. Furthermore, IA<sup>b</sup>-HSP90 tetramer staining showed high background staining, which made evaluation of endogenous Hsp90-restricted CD4 T cells challenging. However, based on IA<sup>b</sup>-HSP90 staining and ELISpot assays, the overall expansion of endogenous Hsp90-restricted CD4 T cells seems limited compared to endogenous CD4 T cell responses for PEPCK, an MHC-II restricted epitope presented during *L. major* infection (Mou et al., 2015).

In Summary, the identification of Hsp90 as the cognate antigen of PbT-II cells added this immunogenic peptide to a small list of known MHC-II restricted *Plasmodium-derived* epitopes. This knowledge allowed us to generate an  $\alpha$ Clec9A-targeted vaccine that induced PbT-II and endogenous CD4 memory T cell responses that were larger than those induced by PbA iRBCs infection or RAS vaccination. This epitope, combined with the  $\alpha$ Clec9A vaccination approach, represent ideal tools to investigate the role of HSP90-specific CD4 T cells in protection against *Plasmodium* blood and liver stage infection.

## **Chapter 4**

# **Liver resident CD4 T cells in malaria.**

## Chapter 4 Liver resident CD4 T cells in malaria.

### 4.1 Introduction

Tissue-resident memory T cells ( $T_{RM}$ ) represent the first line of defence against pathogen re-encounter and have gained a lot of interest in the past decade.  $T_{RM}$  cells are found in virtually every organ and form after pathogen encounters, including viral, bacterial, and parasite infections.

A well-established method to determine residency of immune cells is parabiosis (Jiang et al., 2012). For parabiosis, two animals are surgically joined which, over time, leads to a shared blood supply between the two parabionts. This linkage allows circulatory cells to reach an equilibrium in both parabionts, while resident cells remain in the host tissue and do not recirculate. They are therefore only found in the parabiont partner in which they originated. Using this method, it was demonstrated that  $T_{RM}$  cells exist in most organs, including lung, kidney and small intestine (Steinert et al., 2015). Furthermore, it was shown that  $CD69^+$  CD8 T cells found in the liver after RAS vaccination represented  $T_{RM}$  cells (Fernandez-Ruiz et al., 2016). Interestingly, different experimental vaccination approaches induced  $T_{RM}$  cells in the lung, genital tract and the liver (Wakim et al., 2015, Shin and Iwasaki, 2012, Fernandez-Ruiz et al., 2016, Gola et al., 2018, Benoun et al., 2018). In line with this, a subunit  $\alpha$ Clec9A approach, as shown above, induced long-lasting protection against sporozoite infection and this protection was shown to be mediated by *Plasmodium* specific CD8  $T_{RM}$  cells (Fernandez-Ruiz et al., 2016, Valencia-Hernandez et al., 2020).

In many tissues,  $T_{RM}$  cells express CD69 and this is therefore a useful marker to distinguish resident and circulatory T cell memory populations. However,  $CD69^-$  tissue-resident CD8 T cells have been described in some organs, such as in salivary glands and in the female reproductive tract (Steinert et al., 2015). CD69 is thus an insufficient marker to unequivocally define  $T_{RM}$  T cells, and additional markers are required to accurately identify this T cell memory

population. Recent work has identified C-X-C chemokine receptor type 6 (CXCR6) expression on T<sub>RM</sub> cells as part of a core cluster of upregulated markers on CD69<sup>+</sup> CD8 T<sub>RM</sub> cells in mice and humans (Mackay et al., 2013, Kumar et al., 2017, Fernandez-Ruiz et al., 2016, Tse et al., 2014, Hombrink et al., 2016). Other markers associated with effector memory T cells such as CX3 chemokine receptor 1 (CX3CR1) and Killer cell lectin-like receptor subfamily G member 1 (KLRG1) are downregulated in T<sub>RM</sub> cells and also contribute to this T<sub>RM</sub> core signature (Kumar et al., 2017, Mackay et al., 2013, Fernandez-Ruiz et al., 2016). Therefore, multi-panel staining protocols are required to specifically distinguish T<sub>RM</sub> cells.

In contrast to CD8 T<sub>RM</sub> cells, CD4 T<sub>RM</sub> cells have not been studied in the same detail. Nevertheless, CD4 T<sub>RM</sub> cells are found in several tissues such as lung, gut and the genital tract after viral or bacterial infections (Strutt et al., 2018, Iijima, 2014, Smith et al., 2018, Romagnoli et al., 2017). Moreover, a previous study confirmed a resident CD4 T cell phenotype homing to the liver after *salmonella* infection (Benoun et al., 2018). However, *Plasmodium*-specific CD4 T<sub>RM</sub> cells in the liver and their potential role during sporozoite infection have not been described. In this work, by utilising PbT-II cells, the formation of resident CD4 T cells in the liver after RAS vaccination was examined using parabiosis. In addition, alternative CD4 T cell activation methods, such as  $\alpha$ Clec9A vaccination and *in vitro* polarization of PbT-II cells, which induced Th1, Th2 and Tfh PbT-II cells, were used to examine differences in CD4 liver T<sub>RM</sub> formation and gene expression.

CD4 T<sub>RM</sub> cells were shown to attract CD8 T<sub>RM</sub> cells into the lung tissue by secreting IFN- $\gamma$  or IL-21, in an influenza infection model (Laidlaw et al., 2014, Son et al., 2021). Hypothetically, a *Plasmodium*-specific CD4 T<sub>RM</sub> cell population, secreting IFN- $\gamma$  or IL-21 could therefore increase CD8 T cell accumulation in the liver for conversion into T<sub>RM</sub> cells after vaccination. Thus, the potential capacity of Tfh, Th1, or Th2 T<sub>RM</sub> PbT-II cells to enhance CD8 T<sub>RM</sub> cell formation in the liver and improve protection against sporozoite challenge was also examined.

## 4.2 Results

### 4.2.1 Expression of T<sub>RM</sub> cell associated markers on PbT-II cells in the liver after RAS and $\alpha$ Clec9A-DIY vaccination.

As shown in Chapter 3,  $\alpha$ Clec9A-DIY and RAS vaccination induced the formation of memory PbT-II cells in the liver and spleen and all three memory subsets, CD69<sup>-</sup>CD62L<sup>+</sup> T<sub>CM</sub>, CD69<sup>-</sup>CD62L<sup>-</sup> T<sub>EM</sub>, and CD69<sup>+</sup>CD62L<sup>-</sup> T<sub>RM</sub>-like cells, could be detected.

To compare the relative capacity of these two vaccination strategies to generate CD4<sup>+</sup> liver T<sub>RM</sub> cells, 5 x 10<sup>4</sup> PbT-II cells were injected into naïve B6 mice. One day later, these mice received either 2  $\mu$ g  $\alpha$ Clec9A-DIY + 5 nmol CpG or 5 x 10<sup>4</sup> RAS intravenously. 28 days after vaccination, the livers and spleens were harvested, and the total PbT-II cell numbers were examined by flow cytometry (Figure 4.1 A, B). Confirming our previous results,  $\alpha$ Clec9A priming induced significantly larger numbers of memory PbT-II cells in both tissues compared to RAS vaccination. Given the protective capacity of liver resident CD8 T cells against liver-stage *Plasmodium* infection, we then further investigated the existence and function of liver-resident CD4 T cells in *Plasmodium* infections (Fernandez-Ruiz et al., 2016). CD69 expression was used as a starting point to discriminate potential CD4 T<sub>RM</sub> cells from other PbT-II memory cells in the liver. 28 days post-RAS injection, a larger proportion of PbT-II cells expressing CD69 were generated than induced by  $\alpha$ Clec9A-DIY priming (Figure 4.1A, C), but numerically,  $\alpha$ Clec9A-DIY priming induced a greater number of these cells (Figure 4.1D). As mentioned earlier, CD69 is also upregulated on recently activated T cells. However, it is unlikely that the observed CD69 expression in this experiment was due to recent antigen exposure. As shown in the previous chapter, naïve PbT-II cells did not proliferate when injected into mice 28 days

post-RAS vaccination, demonstrating that there was unlikely to be any antigen left in the liver or spleen at this time point (Figure 3.3).

To further characterise the CD69<sup>+</sup> PbT-II cells detected in the liver, CXCR6 expression, a marker associated with tissue resident cells, was examined (Mackay et al., 2013, Fernandez-Ruiz et al., 2016) (Figure 4.1E). Indeed, CXCR6 expression was abundant in almost all CD69<sup>+</sup>CD62L<sup>-</sup> PbT-II cells 28 days after RAS vaccination (91.4 %), or  $\alpha$ Clec9A-DIY (87.8 %) priming and these cells lacked the expression of either KLRG1 or CX3CR1, which are associated with the T<sub>EM</sub> phenotype (Figure 4.1E). An additional marker associated with T<sub>RM</sub> cells, Immunoglobulin superfamily member 2 (CD101), was expressed at higher levels on CD69<sup>+</sup>CD62L<sup>-</sup> PbT-II cells after RAS vaccination compared to  $\alpha$ Clec9A treatment (Figure 4.1F) (Park et al., 2018). These results suggested that a population of CD4 T<sub>RM</sub>-like cells formed in the liver after both RAS and  $\alpha$ Clec9A-DIY vaccination.

While liver CD69<sup>+</sup>CD62L<sup>-</sup> PbT-II memory T cells showed similar CXCR6<sup>+</sup>, KLRG1<sup>-</sup> and CX3CR1<sup>-</sup> expression profiles independently of the activation method (RAS or  $\alpha$ Clec9A-DIY), different expression profiles of these markers were observed in the CD69<sup>-</sup>CD62L<sup>-</sup> T<sub>EM</sub> cells. Based on the expression of CX3CR1 and CXCR6, three populations could be identified in the liver after RAS vaccination: CXCR6<sup>+</sup>CX3CR1<sup>-</sup> (36.1 %), CXCR6<sup>-</sup>CX3CR1<sup>+</sup> (36 %) and CXCR6<sup>-</sup>CX3CR1<sup>-</sup> (24.9 %) (Figure 4.1E).  $\alpha$ Clec9A priming induced CXCR6<sup>+</sup>CX3CR1<sup>-</sup> (12 %), CXCR6<sup>-</sup>CX3CR1<sup>+</sup> (16 %), and CXCR6<sup>-</sup>CX3CR1<sup>-</sup> (63.1 %) PbT-II cells, as well as a fourth population expressing both CX3CR1 and CXCR6 (8.9 %) (Figure 4.1E). Additionally, none of the T<sub>EM</sub> PbT-II cells showed expression of CD101, and 35.7 % and 10 % of these cells expressed KLRG1 after RAS or  $\alpha$ Clec9A-DIY vaccination, respectively. This suggested that T<sub>EM</sub> PbT-II cells have a higher heterogeneity compared to T<sub>RM</sub>-like PbT-II cells in the liver based on the markers used here.

In summary, CD69<sup>+</sup>CD62L<sup>-</sup> memory PbT-II cells in the liver expressed the T<sub>RM</sub> marker CXCR6 and lacked expression of the T<sub>EM</sub> markers CX3CR1 and KLRG1. This resembled the expression profile of CD8 T<sub>RM</sub> cells in different

tissues such as the lung and liver and supported our hypothesis of the existence of resident memory CD4 T cells in the liver (Mackay et al., 2013, Fernandez-Ruiz et al., 2016, Hombrink et al., 2016, Tse et al., 2014). However, phenotypic characterisation by itself was not sufficient to prove the existence of CD4 T<sub>RM</sub> cells. While CD69<sup>+</sup>CD62L<sup>-</sup> PbT-II cells were always generated, independently of the vaccination method, their proportion was highly dependent on the type of priming. RAS vaccination, as described in the previous chapter, was overall less potent than  $\alpha$ Clec9A-DIY in inducing memory PbT-II cells, but almost exclusively induced CD69<sup>+</sup>CXCR6<sup>+</sup>CD62L<sup>-</sup>CX3CR1<sup>-</sup>KLRG1<sup>-</sup> T<sub>RM</sub>-like cells. In contrast, CD69<sup>-</sup>CD62L<sup>-</sup>CXCR6<sup>-</sup>CX3CR1<sup>-</sup> PbT-II cells (T<sub>EM</sub>) were the dominant memory population generated after  $\alpha$ Clec9A-DIY priming.

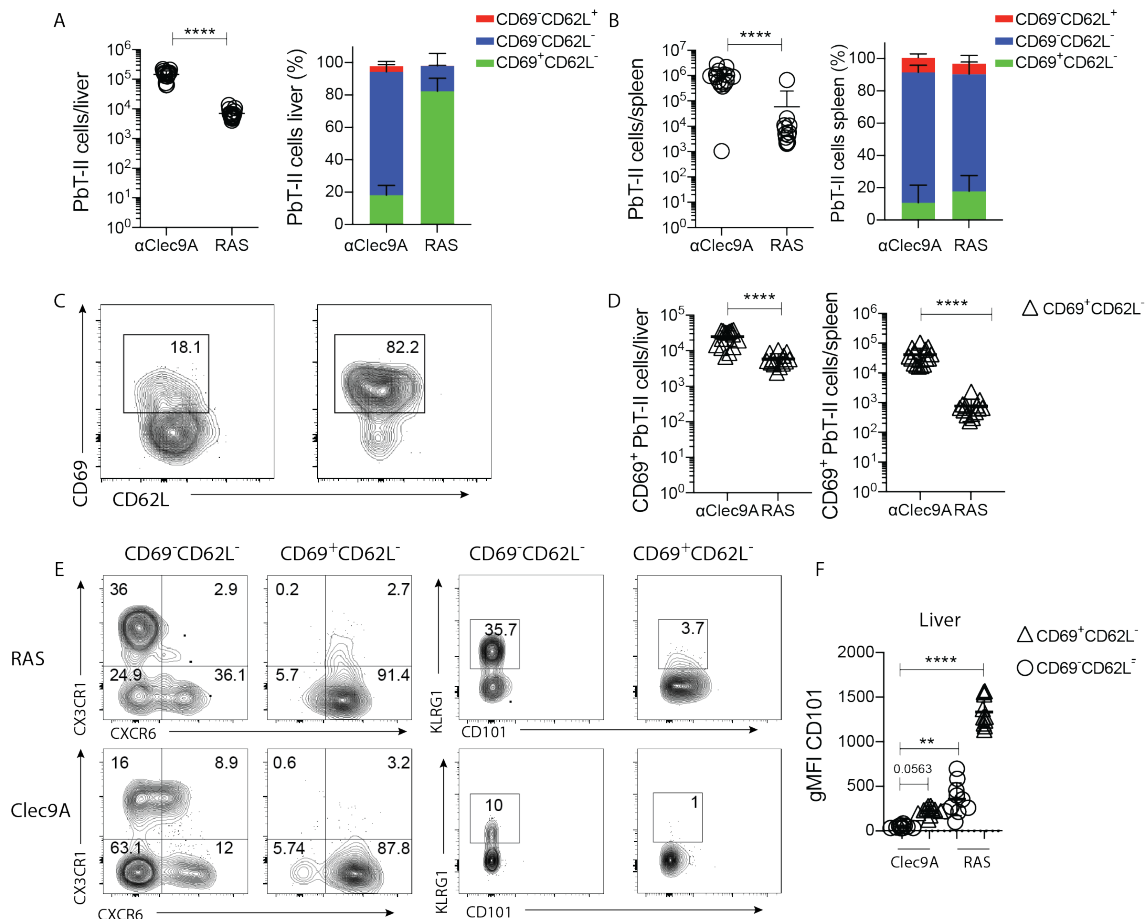


**Figure 4.1. Comparison of memory PbT-II cells population after  $\alpha$ Clec9A-DIY or RAS vaccination.**

B6 mice received  $5 \times 10^4$  PbT-II.uGFP cells one day prior to priming with either  $2 \mu\text{g}$   $\alpha\text{Clec9A-DIY}$  and  $5 \text{ nM}$  CpG-combo or  $5 \times 10^4$  radiated attenuated PbA sporozoites. **A, B.** Total PbT-II numbers (left) and CD69, CD62L expression distribution (right) was determined by flow cytometry of **(A)** liver and **(B)** spleen 28 days post priming. **C.** Expression profile and **D.** total number of CD69<sup>+</sup> PbT-II cells. (\*\*\*\* $p < 0.0001$ , two-tailed Mann-Whitney test). **E.** Surface marker expression and **F.** mean fluorescence intensity of CD101 from CD69<sup>+</sup>CD62L<sup>-</sup> and CD69<sup>-</sup>CD62L<sup>-</sup> liver PbT-II cells. (\*\*\*\* $p < 0.0001$ , \*\* $p < 0.001$  Kruskal-Wallis test following Dunn's multiple comparison test). PbT-II cells are defined as live, CD4<sup>+</sup>, V $\alpha$ 2<sup>+</sup>, GFP<sup>+</sup>, CD44<sup>hi</sup>. Data were pooled from 2 independent experiments with total of 10 mice per group.

#### **4.2.2 CD69<sup>+</sup> memory PbT-II cells are resident in the liver after RAS vaccination**

So far, it was shown that RAS and  $\alpha\text{Clec9A-DIY}$  vaccination induced a subpopulation of PbT-II cells in the liver that expressed T<sub>RM</sub> cell associated surface markers (Figure 4.1). However, the resident nature of these cells cannot be clearly determined based on surface marker expression. Parabiosis experiments were therefore performed to investigate the circulatory capacity of the different PbT-II memory cell subpopulations generated by RAS vaccination. B6 mice, either expressing the congenic marker Ly5.1 or Ly5.2, were vaccinated with  $5 \times 10^4$  RAS. One day prior to this vaccination, B6.Ly5.2 mice were also injected with  $5 \times 10^4$  naïve PbT-II cells. 35 days post-vaccination, after formation of T cell memory, pairs of B6.Ly5.1 and B6.Ly5.2 mice were surgical joined via their flank skin (Jiang et al., 2012). This process leads to a spontaneous joining of the blood-vessels of both mice within about two weeks of surgery, which leads to a shared bloodstream. Any circulating cell populations are thereafter found in both parabionts, while tissue-resident cells remain in the mouse where they were originally formed. In this analysis, we waited 30 days after surgery, before harvesting the blood, liver and spleens of these parabionts to investigate memory T cell distribution by flow cytometry (Figure 4.2A).

A successful parabiosis experiment requires efficient blood circulation between both parabionts. To prove an established shared bloodstream, the distribution of Ly5.1<sup>+</sup> and Ly5.2<sup>+</sup> CD4 T cells in the blood of both parabionts was investigated. As seen in Figure 4.2B and C a similar distribution of CD4 T cells expressing either Ly5.1 or Ly5.2 were found in the B6.Ly5.1 and B6.Ly5.2 mice. Thus, the blood of both mice in every pair was sufficiently mixed 30 days post-surgery and the parabiosis surgery could be regarded as successful.

Next, as a control for our methodology, the distribution of CD8 memory T cells in the liver was examined. CD8 T<sub>RM</sub> cells have been demonstrated to form after RAS vaccination and identification of resident and circulatory *Plasmodium*-specific CD8 T cells in our model would further validate the success of the present parabiosis surgery (Fernandez-Ruiz et al., 2016). Previous work from our group used *Plasmodium*-specific transgenic CD8 T cells (PbT-I cells) to describe CD8 T<sub>RM</sub> formation after RAS vaccination (Fernandez-Ruiz et al., 2016). Here, an MHC-I tetramer that was able to detect *Plasmodium*-specific endogenous CD8 T cells specific for the parasite protein RPL6 was used. Via this strategy, two populations of *Plasmodium*-specific CD8 memory T cells were found in the liver of vaccinated mice, CD69<sup>+</sup>CD62L<sup>-</sup> T<sub>RM</sub> and CD69<sup>-</sup>CD62L<sup>-</sup> T<sub>EM</sub> cells (Figure 4.2D). *Plasmodium*-specific CD8 T<sub>EM</sub> cells, expressing either Ly5.1 or Ly5.2 were found in similar numbers in the liver of both parabiotic mice (Figure 4.2D, E), as expected for circulating cells. In contrast, around 90 % of CD69<sup>+</sup> RPL6-specific MHC-I tetramer<sup>+</sup> liver CD8 T cells expressed the same congenic marker as the mouse they were recovered from. This indicated that CD69<sup>+</sup> *Plasmodium*-specific CD8 T<sub>RM</sub> cells were largely retained in the liver where they had originally formed and did not recirculate. These results confirmed that this experiment could distinguish between circulating and resident memory T cells in the liver. Furthermore, an endogenous *Plasmodium*-specific CD8 T<sub>RM</sub> cell population was found, which extended previous results that used RAS vaccination and transgenic PbT-I T cells (Fernandez-Ruiz et al., 2016).

Next, the circulating properties of CD4 memory subpopulations in the liver were examined. In mice that received PbT-II cells prior to vaccination, almost all

liver-associated PbT-II cells had a CD69<sup>+</sup>CD62L<sup>-</sup> T<sub>RM</sub> phenotype (Figure 4.2F). Over 95 % of total liver CD69<sup>+</sup>CD62L<sup>-</sup> PbT-II cells were recovered from the mice in which they were originally formed (i.e. B6.Ly5.2 mice) (Figure 4.2G, H). In contrast CD69<sup>-</sup>CD62L<sup>-</sup> T<sub>EM</sub> PbT-II cells were found in equal distribution and numbers in the livers of both mice. This demonstrated that CD69<sup>+</sup>CD62L<sup>-</sup> PbT-II cells formed after RAS vaccination remained in the liver where they formed for at least 30 days. These cells will therefore now be considered resident and termed CD4<sup>+</sup> T<sub>RM</sub> cells. As expected, CD69<sup>-</sup>CD62L<sup>-</sup> T<sub>EM</sub> PbT-II cells were found to circulate. Like the liver, a population of CD69<sup>+</sup>CD62L<sup>-</sup> PbT-II memory cells could be identified in the spleen, which seemed to be not in equilibrium within the circulation and could therefore be considered as T<sub>RM</sub> cells. However, the relatively small number of CD69<sup>+</sup>CD62L<sup>-</sup> PbT-II memory cells recovered from the spleen suggests further investigation is required to draw definitive conclusions.

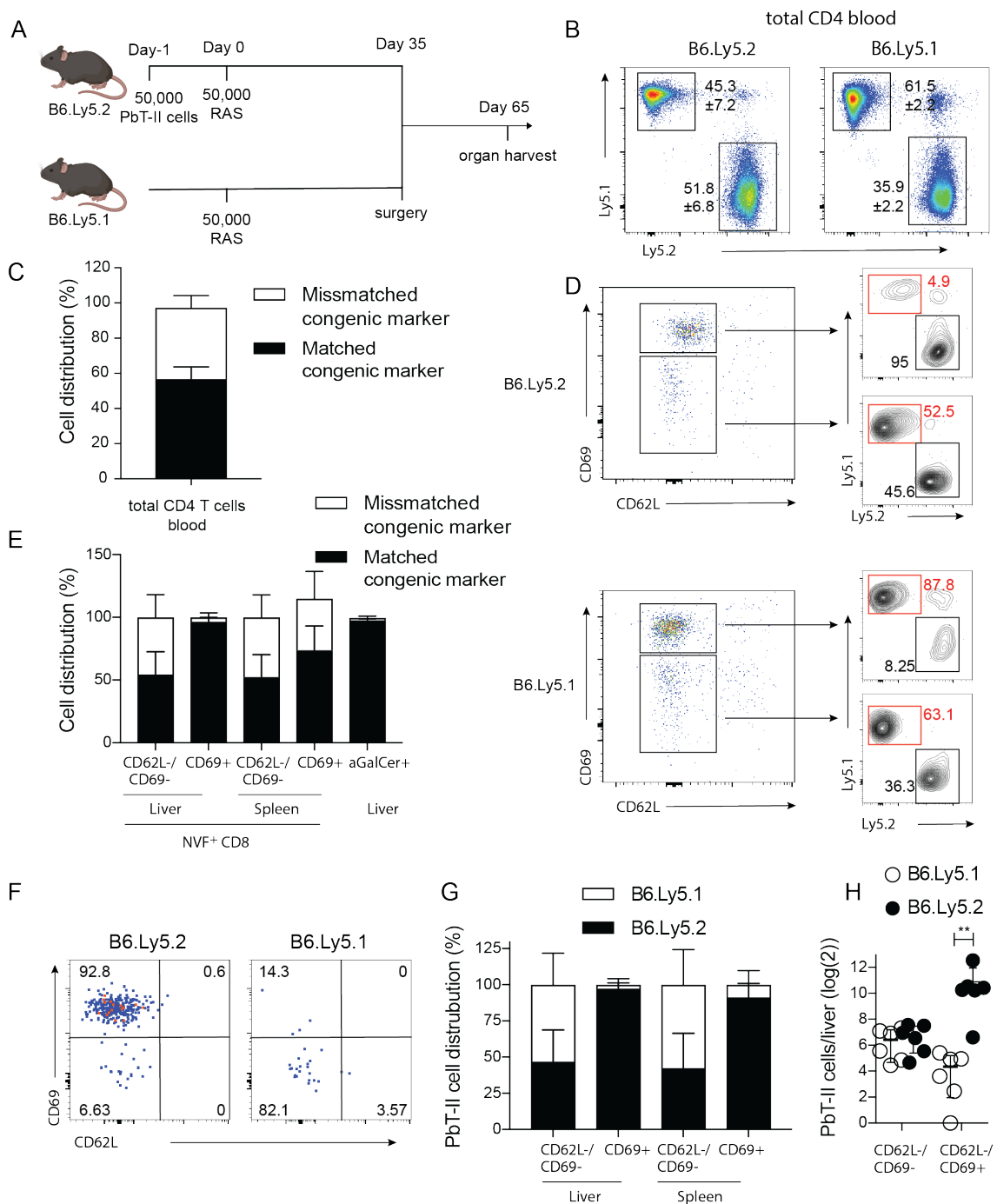


**Figure 4.2. Homing and circulating pattern of Plasmodium-specific T cells after RAS vaccination.**

B6.Ly5.1 and Ly5.2 mice were vaccinated with  $5 \times 10^4$  PbA RAS. One day prior to vaccination, B6.Ly5.2 mice received  $5 \times 10^4$  PbT-II.uGFP cells. 35 days post-vaccination, mice were surgically joined on the skin flank to allow sharing of their blood circulation. After an additional 30 days, T cell distribution in the liver, spleen and blood of both parabionts was analysed by flow cytometry. **A.** Experimental scheme. **B.** Total blood CD4 T cells distribution between parabionts **C.** Ly5.1 and Ly5.2 expression profile of total blood CD4 T cells. **D.** CD69, CD62L, Ly5.1 and Ly5.2 expression profile of NVF-specific CD8 memory T cells in the liver. **E.** NVF-

specific CD8 memory T cells and NKT cell distribution between parabionts. **F.** Distribution of liver PbT-II cells revealed by expression of CD62L and CD69 on PbT-II cells. **G.** PbT-II cells distribution between parabionts. **H.** Total numbers of liver T<sub>EM</sub> and T<sub>RM</sub> PbT-II cells. (\*\*p < 0.01, two-tailed Mann-Whitney test). Data were pooled from two independent experiments with a total of 6 pairs.

#### **4.2.3 PbT-II T<sub>RM</sub> formation does not require cognate antigen expression in the liver.**

Compared to  $\alpha$ CLec9A-DIY vaccination, RAS vaccination favoured PbT-II cell differentiation towards a liver-resident phenotype (Figure 4.1). As RAS infiltrate hepatocytes, *Plasmodium* derived antigen is potentially presented within the liver to PbT-II cells. It is therefore possible that local antigen presentation enhanced CD4 T<sub>RM</sub> cell formation in the liver. *In vitro* activation and adoptive transfer of antigen-specific CD8 T cells was previously shown to lead to the spontaneous formation of CD8 T<sub>RM</sub> cells in the liver (Holz et al., 2018). Therefore, we wondered whether similar transfer of activated CD4 T cells would lead to liver T<sub>RM</sub> cell formation. To address this question, PbT-II cells were activated with antigen *in vitro* under conditions to induce differentiation into Th1 or Th2 cells and then these cells were injected into naïve mice and assessed for the formation of liver T<sub>RM</sub> cells after 35 days *in vivo*. In this case, cognate antigen was not available for recognition by T cells after their transfer *in vivo*. Both Th1 and Th2 PbT-II cells were able to form T<sub>RM</sub> cells in the liver as determined by expression of CD69 and lack of CD62L (Figure 4.3A-C). Interestingly, while the same number of each helper type of PbT-II cells were transferred, more Th2 cells were recovered from the liver compared to Th1 cells (Figure 4.3A). Furthermore, around 80 % of PbT-II Th2 cells differentiated into a CD4 T<sub>RM</sub> phenotype, whereas only 20 % of the Th1 cells formed this phenotype (Figure 4.3B). Both Th1 and Th2 populations of CD69<sup>+</sup>CD62L<sup>-</sup> PbT-II cells expressed other markers consistent with a T<sub>RM</sub> phenotype, e.g. CXCR6 and P2RX7 (Figure 4.3G). While most PbT-II Th2 (83.72 %) lacked expression of Ly6C, around 60 % of Th1 cells expressed this marker

(Figure 4.3G). Ly6C is usually expressed on T<sub>CM</sub> but not T<sub>RM</sub> cells and mediates homing to the lymph nodes (Hanninen et al., 2011).

In contrast to observations in the liver, more PbT-II Th1 cells were recovered from the spleen compared to Th2 cells (Figure 4.3D). In both groups, T<sub>EM</sub> cells were the dominant PbT-II cell phenotype followed by T<sub>CM</sub> and then T<sub>RM</sub>-like cells, suggesting that CD4 T cell residence in secondary-lymphoid organs is less pronounced.

CD4 T cell lineages are described to have plasticity that allows differentiation from one lineage to another upon exposure to specific stimuli (Hegazy et al., 2010, Bending et al., 2009). To determine whether *in vitro* differentiated PbT-II Th1 and Th2 cells remained stable in their specific CD4 T cell lineage for some time after transfer, the production of key cytokines, IFN- $\gamma$  and IL-4, was examined by peptide restimulation of recovered PbT-II cells 35 days after transfer. This revealed that a proportion of Th1 cells expressed IFN- $\gamma$  and that none expressed IL-4, while over 60% of Th2-differentiated PbT-II cells still expressed IL-4 but not IFN- $\gamma$  (Figure 4.3I, J). Therefore, PbT-II Th1 and Th2 cells stayed relatively stable in their CD4 specific lineage under steady-state conditions.

In summary, these results indicate that, like liver CD8 T<sub>RM</sub> cells, formation of liver CD4 T<sub>RM</sub> cell does not require cognate antigen presentation in the liver. However, differences in the quantity of T<sub>RM</sub> cell formation could be observed between distinct CD4 helper phenotypes, with Th2 cells favouring T<sub>RM</sub> cell differentiation.

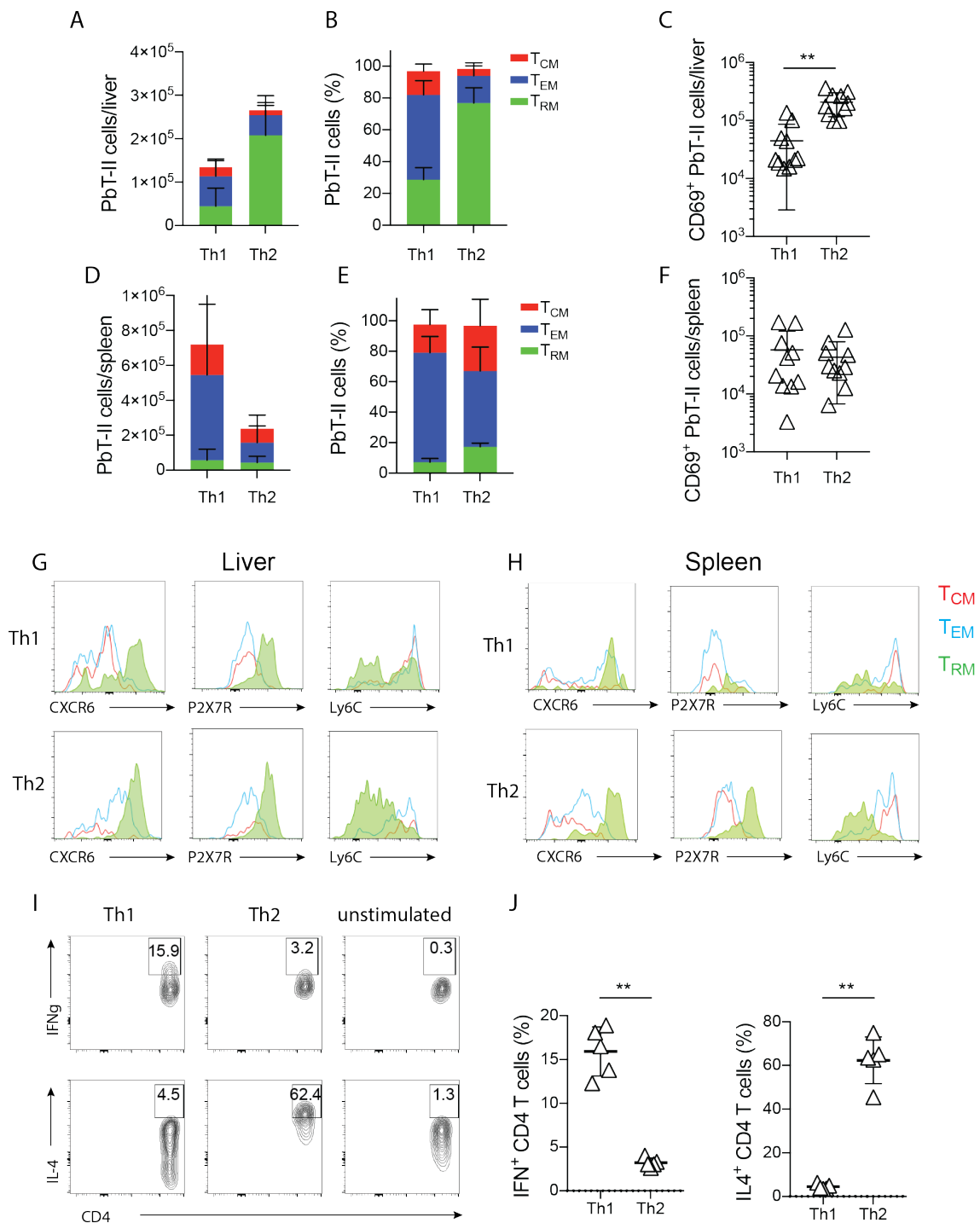


**Figure 4.3. *In vitro* polarized PbT-II Th1 and Th2 cells form T<sub>RM</sub> cells in the liver.**

10<sup>7</sup> *in vitro* differentiated PbT-II Th1 and Th2 cells were injected into naïve B6 mice. 35 days later liver (**A-C**) and spleen (**D-F**) were harvested and PbT-II cell memory numbers were determined by flow cytometry by gating on live, CD4<sup>+</sup>, Vα2<sup>+</sup>, GFP<sup>+</sup>, CD44<sup>hi</sup> cells. Memory PbT-II cell subsets were identified by the expression of CD62L and CD69. PbT-II T<sub>RM</sub> cells were considered as

CD69<sup>+</sup>CD62L<sup>-</sup>, T<sub>EM</sub> cells as CD69<sup>-</sup>CD62L<sup>-</sup> and T<sub>CM</sub> cells as CD69<sup>-</sup>CD62L<sup>+</sup>. Total number (**A, D**) and proportion (**B, E**) of liver (**A, B**) and spleen (**D, E**) memory PbT-II cell subsets as identified by the expression of CD69 and CD62L **C, F**. Total numbers of CD69<sup>+</sup>CD62L<sup>-</sup> PbT-II cells from the liver (**C**) and spleen (**F**). (\*\*p < 0.01; n.s.> 0.05; two-tailed Mann-Whitney test) **G, H**. Expression profile of T<sub>RM</sub> associated surface marker (CXCR6, P2XR7, Ly6C) by PbT-II T<sub>RM</sub>, T<sub>CM</sub> and T<sub>EM</sub>. Data were pooled from 2 independent experiments with a total of 10 mice per group. (**I, J**) Some splenocytes recovered on day 35 post-cell transfer were re-stimulated with DIY-peptide in the presence of Brefeldin A for 5 hours and analysed for IFN- $\gamma$  and IL-4 expression by flow cytometry. **I**. Representative Flowcytometry profile, **J**. proportion of cytokine producing PbT-II cells. (\*\*p < 0.01; n.s.> 0.05; two-tailed Mann-Whitney test). Single experiment with 5 mice per group.

#### **4.2.4 CD4 T<sub>RM</sub> cells have a similar transcriptional signature to CD8 T<sub>RM</sub> cells in the liver.**

To this point, it had been shown that liver resident PbT-II cells could be generated after RAS or  $\alpha$ Clec9A-DIY vaccination and could form spontaneously after transfer of *in vitro* polarized PbT-II Th1 and Th2 cells. However, little had been done to characterise these T<sub>RM</sub> cell populations generated by different methods. Therefore, to examine population differences, RNA sequencing (RNAseq) was performed. First, CD69<sup>+</sup>CXCR6<sup>+</sup> T<sub>RM</sub> and CD69<sup>-</sup>CD62L<sup>-</sup> T<sub>EM</sub> PbT-II cells were analysed 35 days after RAS vaccination. This analysis revealed 295 differently expressed genes (DEGs) with 215 DEGs upregulated and 80 downregulated in T<sub>RM</sub> cells (Figure 4.4A, B, Appendix Table 8.1). Within the 295 DEGs we observed upregulation of various T<sub>RM</sub> associated genes including Cxcr3, Cxcr6 and P2rx7, and downregulation of various T<sub>EM</sub> associated genes including S1pr5, Klr1 and S1pr1 (Figure 4.4B, Appendix Table 8.1). Further analysis of the 295 DEGs using the Gene Ontology-term (GO) analyses suggested that CD4 T<sub>RM</sub> cells generated more effector proteins and cytokines, such as IFN- $\gamma$ , and developed more prominent cell activation and differentiation responses compared to T<sub>EM</sub> cells (Figure 4.4C). This suggests that CD4 T<sub>RM</sub> cells are poised to elicit more potent effector mechanisms than CD4 T<sub>EM</sub> cells.

Interestingly, while IFN- $\gamma$  production indicates Th1 differentiation, the IL-4 production pathway was also elevated in PbT-II T<sub>RM</sub> cells compared to T<sub>EM</sub> cells. As IL-4 production is considered a key cytokine for Th2 differentiated CD4 T cells, these results suggest that RAS vaccination induces T<sub>RM</sub> cells of both the Th1 and Th2 lineages (Figure 4.4C). However, this result should be validated by investigating GATA3 and Tbet expression or cytokine release by PbT-II cells after RAS vaccination.

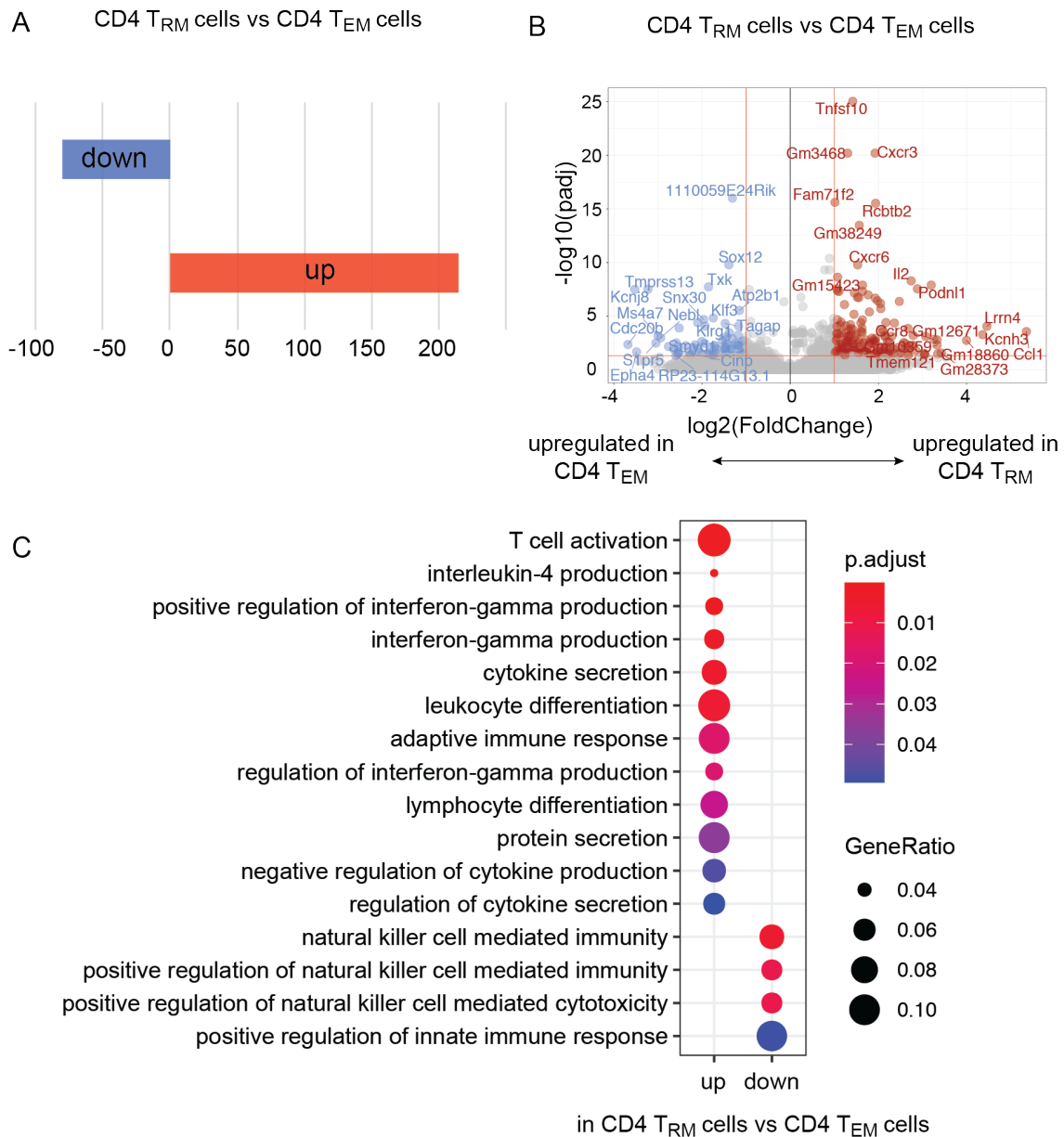


**Figure 4.4. Differential gene expression by liver PbT-II T<sub>RM</sub> and T<sub>EM</sub> cells.** B6 mice received  $5 \times 10^4$  naïve PbT-II.uGFP cells and were vaccinated with  $5 \times 10^4$  RAS one day later. 35 days after vaccination, memory GFP<sup>+</sup>CD44<sup>hi</sup> PbT-II cells were sorted from the liver (either CD69<sup>+</sup>CXCR6<sup>+</sup> T<sub>RM</sub> or CD69<sup>-</sup>CD62L<sup>-</sup> T<sub>EM</sub>) and analysed for gene expression by RNAseq. **A.** Number of differentially expressed genes (DEGs) by PbT-II liver T<sub>RM</sub> and T<sub>EM</sub> cells ( $\geq 1.5$  fold change, independent hypothesis weighting adjusted p value of  $<0.05$ ). **B.** Volcano plot of DEGs **C.** Gene ontology analysis of terms up or down regulated in CD4 T<sub>RM</sub> cells compared to T<sub>EM</sub> cells from the liver (adjusted p value of  $<0.05$ , Cluster size  $> 5$  DEGs).

CD8 liver T<sub>RM</sub> cells have been shown to form after RAS vaccination, and it was of interest to compare these cells to CD4 liver T<sub>RM</sub> cells (Fernandez-Ruiz et al., 2016). Therefore, *Plasmodium*-specific liver CD8 (PbT-I) T<sub>RM</sub> and T<sub>EM</sub> cells were obtained 35 days after RAS immunisation and included in the RNAseq analyses together with PbT-II T<sub>RM</sub> cells. Using a liver resident cell core signature published by Mackay and colleagues, we compared the gene signatures of CD8 T<sub>RM</sub> and T<sub>EM</sub> cells after RAS vaccination to those for CD4 T<sub>RM</sub> and T<sub>EM</sub> cells generated by either RAS or  $\alpha$ Clec9A vaccination (Mackay et al., 2016). PbT-II Th1 and Th2 liver T<sub>RM</sub> cells were also included in the RNAseq analysis to allow the investigation of Th lineage specific differences. As displayed in the heatmap in Figure 4.5A, the gene cluster typically upregulated in CD8 T<sub>RM</sub> cells, including *Xcl1* and *Cxcr6* was also upregulated in each CD4 T<sub>RM</sub> cell population relative to CD4 or CD8 T<sub>EM</sub> cells. Furthermore, genes displaying low expression in liver-resident CD8 T cells, were also downregulated in CD4 T<sub>RM</sub> cells. This showed that liver CD4 T<sub>RM</sub> cells, independently of the priming method used, expressed the same core gene signature as liver CD8 T<sub>RM</sub> cells (Figure 4.5A). However, as this core signature only included 29 DEGs, geneset enrichment analysis (GSEA) was used to investigate similarities between CD4 and CD8 T<sub>RM</sub> cells in relation to the complete data set. To do this, liver PbT-II CD4 T<sub>RM</sub> generated after RAS or  $\alpha$ Clec9A-DIY vaccination or via transfer of Th1 and Th2 cells were compared for gene expression to a previously published dataset for CD8 liver T<sub>RM</sub> cells generated after RAS vaccination (Fernandez-Ruiz et al., 2016). As seen in Figure 4.5B, C, all CD4 PbT-II liver T<sub>RM</sub> cell populations showed strong similarities to CD8 T<sub>RM</sub> cells (Figure 4.5B, C).

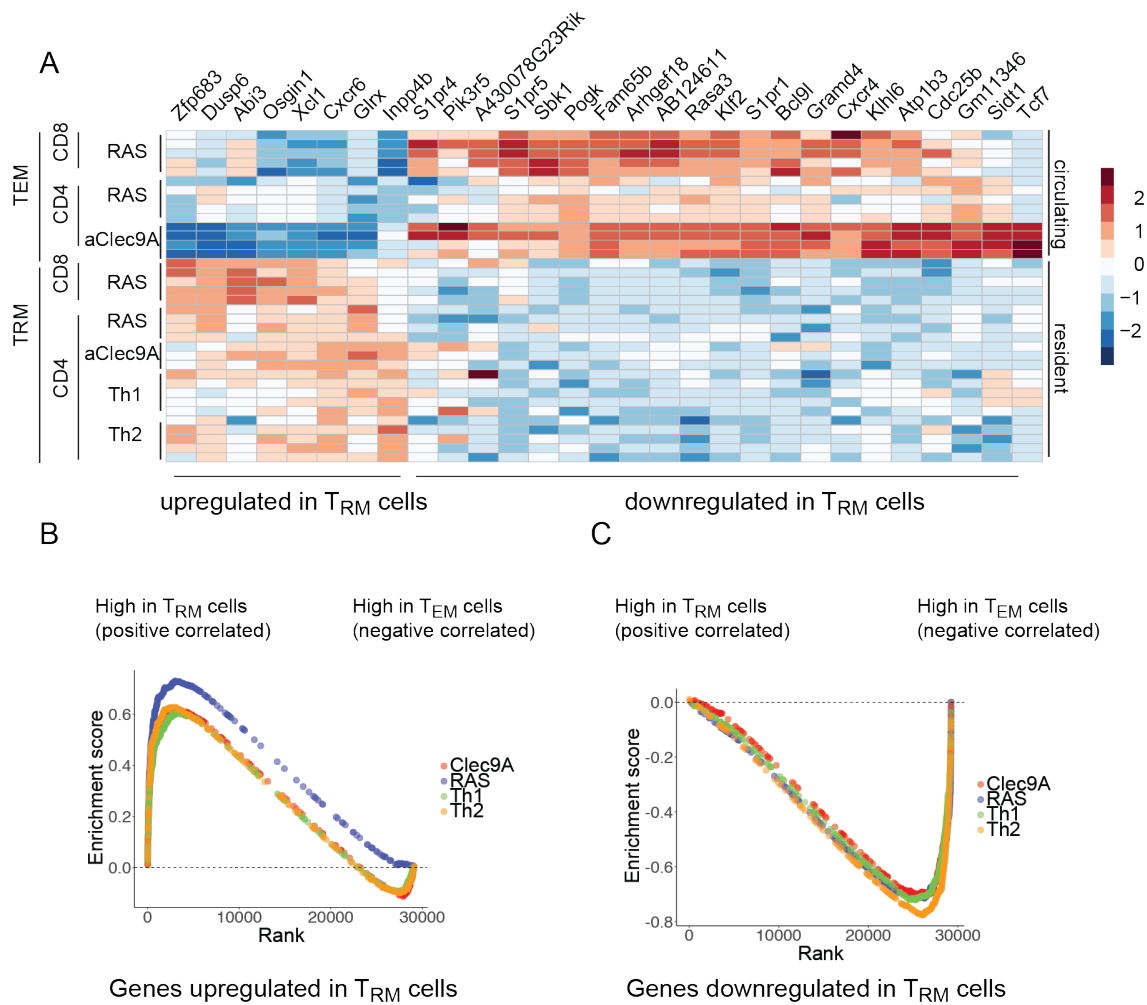


**Figure 4.5. Shared liver resident core signature of CD4 and CD8  $T_{RM}$  cells.**

B6 mice received  $5 \times 10^4$  naïve PbT-II.uGFP or PbT-I.uGFP cells and were vaccinated with  $5 \times 10^4$  RAS or  $2 \mu\text{g}$   $\alpha\text{Clec9a}$ -DIY and 5nmol CpG one day later. Additional mice received  $10^7$  *in vitro* polarized PbT-II Th1 or Th2 cells. 35 days after vaccination or cell transfer, memory GFP<sup>+</sup>CD44<sup>hi</sup> PbT-II and PbT-I cells were sorted from the liver (either CD69<sup>+</sup>CXCR6<sup>+</sup>  $T_{RM}$  or CD69<sup>-</sup>CD62L<sup>-</sup>  $T_{EM}$  cells) and analysed for gene expression by RNAseq. **A**. Expression profile of liver resident core signature genes published by (Mackay et al., 2016) **B, C**. Gene set enrichment analyses of genes upregulated (**B**) or downregulated (**C**) in CD8  $T_{RM}$  cells from published CD8  $T_{RM}$  microarray dataset (Fernandez-Ruiz et al., 2016). False discovery rate  $q$  value (FDR) of the enrichment scores (ESs) of upregulated (**B**) or downregulated (**C**) expression gene sets from CD8  $T_{RM}$  cells were all 0.0000. ESs were considered significant when FDR < 0.05. All data were derived from a single experiment with 3-5 samples per group with 5 mice per sample.

After it was shown that liver CD4 and CD8 T<sub>RM</sub> cells expressed a similar transcriptional core signature, we investigated differently expressed genes between CD4 T<sub>RM</sub> (PbT-II cells) and CD8 T<sub>RM</sub> (PbT-I cells) cells after RAS vaccination. 375 genes were upregulated and 166 were found to be expressed at lower levels in CD4 T<sub>RM</sub> cells (Figure 4.6A). However, many of these DEG appeared to be related to the different origins of these cells as, for example, CD4 and CD8 $\alpha$  were within these genes as were several genes related to T cell receptor transcripts of PbT-II and PbT-I cells (Figure 4.6B). The plethora of differentially expressed genes between CD4 and CD8 T cells made the analysis of transcriptional differences between CD4 and CD8 T<sub>RM</sub> at a single gene level difficult. Therefore, we took a broader approach and performed GO-term analyses, which classifies genes into clusters rather than comparing single genes. As seen in Figure 4.6C CD4 T<sub>RM</sub> cell expressed genes associated with enhanced chemotaxis, migration and proliferation. On the opposite side, GO-terms associated with cytotoxicity and cell killing were upregulated in CD8 T<sub>RM</sub> cells (Figure 4.6C). These findings suggest CD4 T<sub>RM</sub> cells might have a higher potential to recruit cells and to proliferate while CD8 T<sub>RM</sub> cells have higher cytotoxic capacities.

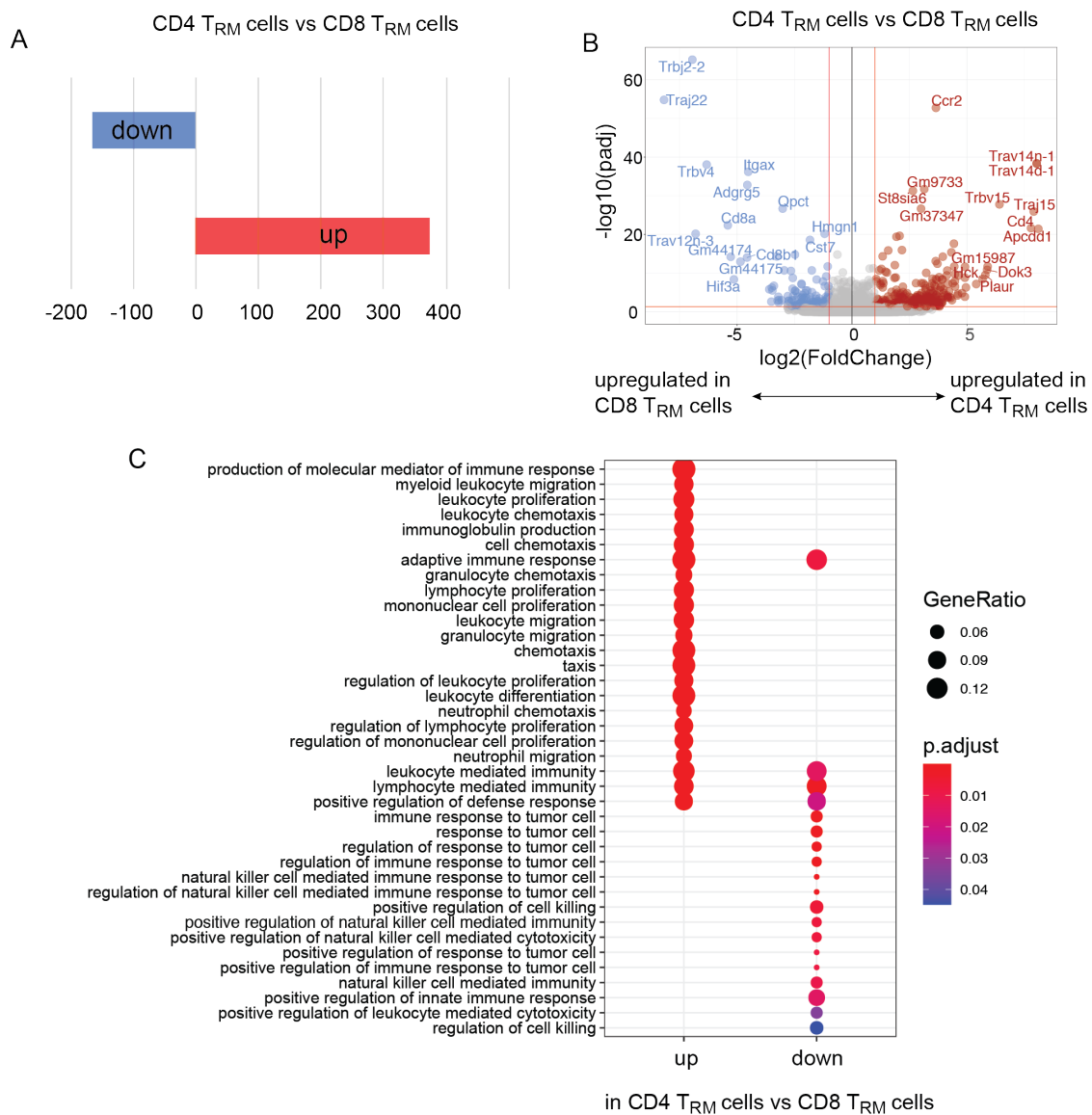


**Figure 4.6. Differential Gene Expression by liver PbT-II and PbT-I T<sub>RM</sub> cells.** Differential gene expression was examined for PbT-II and PbT-I T<sub>RM</sub> cell population generated as in Figure 4.5. **A.** Number of differentially expressed genes (DEGs) by CD4 and CD8 liver T<sub>RM</sub> cells ( $\geq 1.5$  fold change, independent hypothesis weighting adjusted p value of  $<0.05$ ) **B** Volcano plot of DEGs. **C.** Gene ontology analyses of terms up or down regulated in CD4 T<sub>RM</sub> cells compared to CD8 T<sub>RM</sub> cells from the liver (adjusted p value of  $<0.05$ , Cluster size  $\geq 4$  DEGs).

Despite the similarity in the core gene signature of CD4 and CD8 T<sub>RM</sub> T cells, and overall similar gene expression between T<sub>RM</sub> cells, it was important to determine whether CD4 T<sub>RM</sub> cells generated via different activation methods differed in gene expression. To assess this question, gene expression by CD4 T<sub>RM</sub> cells generated after RAS or  $\alpha$ Clec9A-DIY vaccination or those derived from PbT-II Th1 and Th2 cells were compared (Figure 4.7). As expected, principal component analyses of CD4 T<sub>RM</sub> and T<sub>EM</sub> cells from the liver showed that all CD4 T<sub>RM</sub> cells, regardless of their activation method, clustered together and apart from T<sub>EM</sub> cells (Figure 4.7A). To examine differences between the CD4 T<sub>RM</sub> cell populations, CD4 PbT-II T<sub>RM</sub> cells generated after RAS were compared with  $\alpha$ Clec9A-DIY, Th1 and Th2 PbT-II CD4 liver T<sub>RM</sub> cells in more detail. As seen in Figure 4.7B, 61, 118 and 135 genes were differently expressed between  $\alpha$ Clec9A, Th1 and Th2 T<sub>RM</sub> cells compared to RAS-induced PbT-II T<sub>RM</sub> cells, respectively (Figure 4.7B, Appendix Table 8.2, Appendix Table 8.3, Appendix Table 8.4). Interestingly, the 61 DEGs between  $\alpha$ Clec9A-DIY and RAS CD4 T<sub>RM</sub> cells were enriched in pathways related to T cell/lymphocyte activation and differentiation, which were upregulated in  $\alpha$ Clec9A CD4 T<sub>RM</sub> cells (Figure 4.7C). In contrast, RAS CD4 T<sub>RM</sub> cells showed cell proliferation pathways were enriched. In addition, RAS CD4 T<sub>RM</sub> seemed to have a higher responsiveness to chemokines or to facilitate chemotaxis compared to previously *in vitro* polarized Th1 or Th2 T<sub>RM</sub>. However, no upregulated GO-terms were found in those analyses with the set parameters (Figure 4.7D, E). These analyses suggested that differences exist between CD4 T<sub>RM</sub> populations, which may vary in their responsiveness to, or the secretion of, cytokines and proteins which may lead to different protective capacities against infection.

After comparison of PbT-II T<sub>RM</sub> cells generated by the “gold standard” vaccination approach RAS, with the novel  $\alpha$ Clec9A-DIY approach, and with lineage specific Th1 and Th2 PbT-II T<sub>RM</sub> cells, we investigated transcriptional differences between  $\alpha$ Clec9A-DIY vaccinated and lineage specific Th1 and Th2 PbT-II T<sub>RM</sub> cells, focusing on potential effector mechanisms. Transcripts that are described to be associated with regulatory CD4 T cell differentiation, such as

FoxP3 and Lag3, were upregulated in  $\alpha$ Clec9A-DIY generated CD4 T<sub>RM</sub> cells compared to Th1 and Th2 T<sub>RM</sub> cells (Figure 4.8A, C, Appendix Table 8.5, Appendix Table 8.6). In line with this finding, GO-term analysis revealed that negative regulation of immune system processes were upregulated in  $\alpha$ Clec9A-DIY generated PbT-II T<sub>RM</sub> cells compared to Th1 T<sub>RM</sub> cells (Figure 4.8B). In contrast, Granzyme K (Gzmk) and Perforin (Prf1) were upregulated in  $\alpha$ Clec9A generated PbT-II T<sub>RM</sub> cells compared to Th2 PbT-II T<sub>RM</sub> cells, indicating a superior cytotoxic function of these cells (Figure 4.8C).

Finally, differences between Th1 and Th2 PbT-II T<sub>RM</sub> cells were examined. As expected, GO-term analyses showed strong upregulation of type 2 immune responses in PbT-II Th2 T<sub>RM</sub> cells, while PbT-II Th1 cells were associated with positive regulation of defence responses. Furthermore, PbT-II Th2 T<sub>RM</sub> cells had a greater ability to regulate cell secretion and myeloid differentiation (Figure 4.8E).

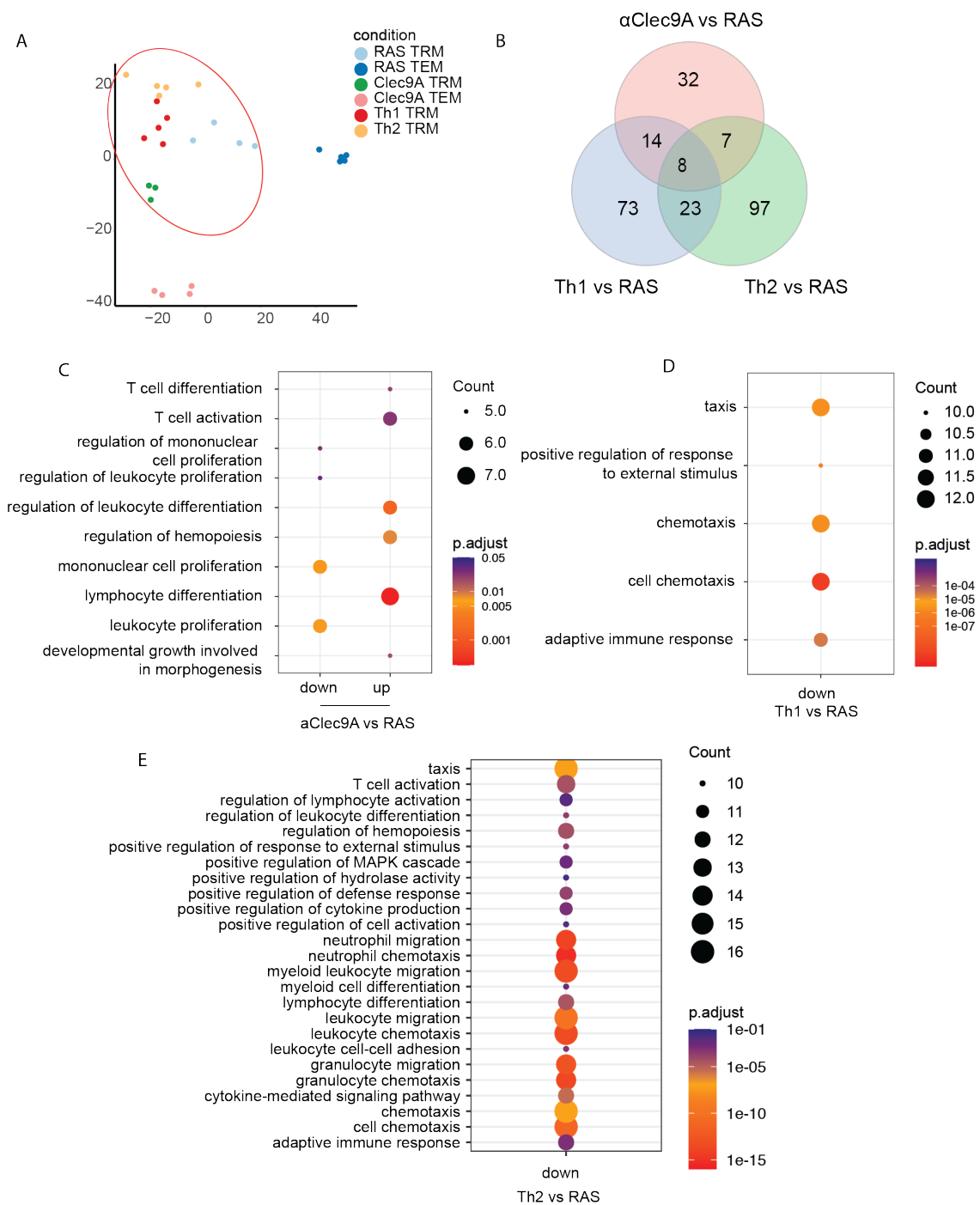


**Figure 4.7. Differential gene expression by lineage specific liver PbT-II T<sub>RM</sub> cells.**

Differential gene expression was examined for PbT-II T<sub>RM</sub> and T<sub>EM</sub> cell populations generated as in Figure 4.5. **A.** Principal component analysis (PCA). **B.** Venn diagram of DEGs of Th1, Th2 or  $\alpha$ Clec9A-DIY generated T<sub>RM</sub> cells compared to RAS vaccination generated T<sub>RM</sub> cells ( $\geq 1.5$  fold change, independent hypothesis weighting adjusted p value of  $<0.05$ ), **C.** Gene ontology analyses between  $\alpha$ Clec9A and RAS immunisation generated liver T<sub>RM</sub> cells

(adjusted p value of  $<0.05$ , Cluster size  $> 4$  DEGs). **D, E.** Gene ontology analyses between PbT-II Th1 (D) and Th2 (E) and RAS immunisation generated liver T<sub>RM</sub> cells (adjusted p value of  $<0.05$ , Cluster size  $> 8$  DEGs).

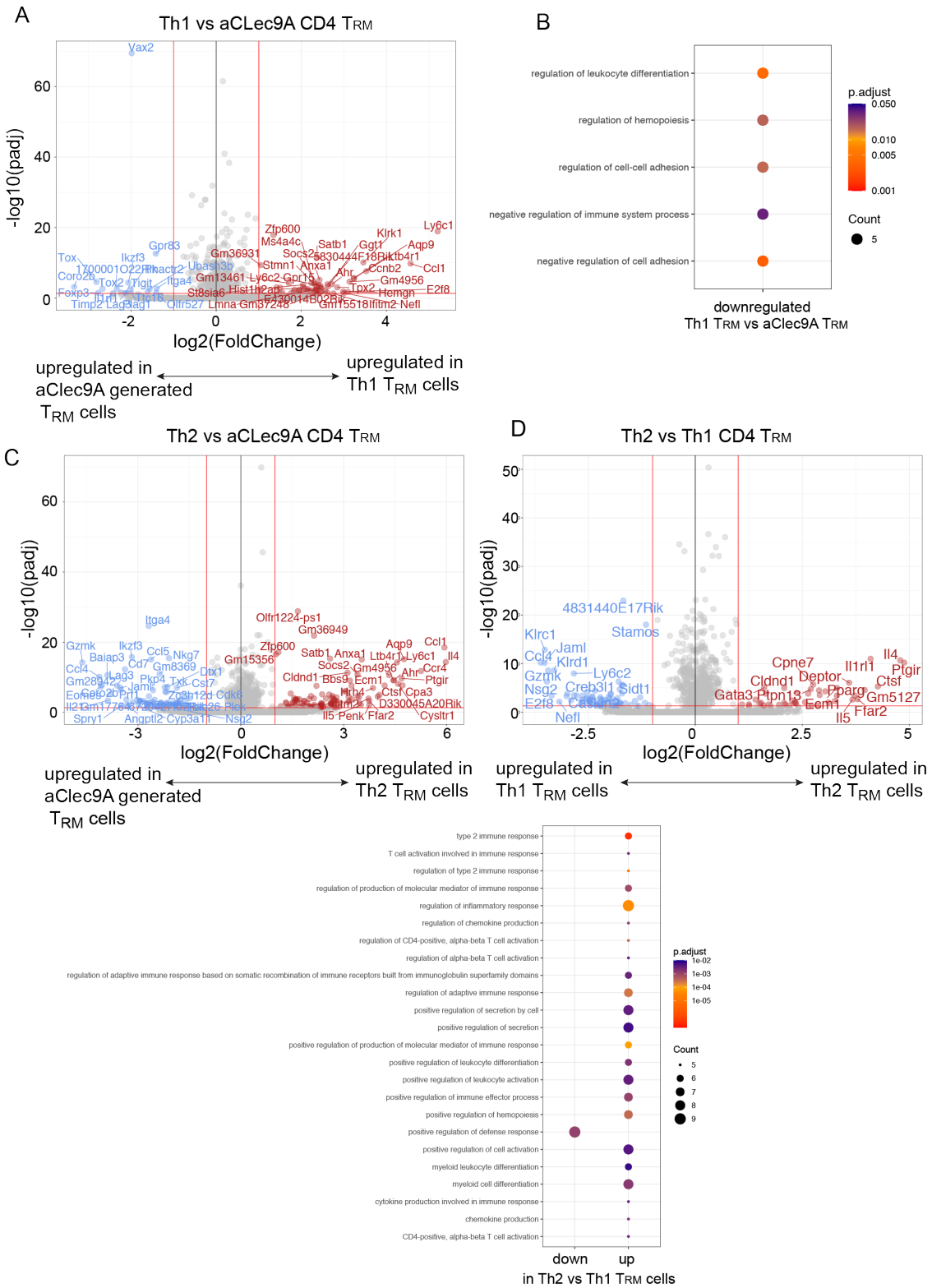


**Figure 4.8. Differential Gene Expression by lineage specific liver PbT-II T<sub>RM</sub> cells.**

Differential gene expression was examined for PbT-II T<sub>RM</sub> cell populations generated as in Figure 4.5. **A, B.** Comparison of Th1 vs.  $\alpha$ Clec9A-DIY generated PbT-II T<sub>RM</sub> cells. **C.** Comparison of Th2 vs.  $\alpha$ Clec9A-DIY generated PbT-II T<sub>RM</sub> cells. **D, E.** Comparison of Th2 vs. Th1 generated PbT-II T<sub>RM</sub> cells. **A, C, D.** Volcano plot of DEGs ( $\geq 1.5$  fold change, independent hypothesis weighting adjusted p value of  $<0.05$ ). **B, E.** GO-term analyses (adjusted p value of  $<0.05$ , Cluster size  $> 4$  DEGs).

**4.2.5 Simultaneously priming of CD4 and CD8 T cell did not enhance liver T<sub>RM</sub> formation**

CD4 T cells are crucial for DC activation which in turn mediates efficient CD8 T cell priming (Smith et al., 2004). In the absence of proper CD4 T cell responses, the development of CD8 T cell response against liver stage *Plasmodium* infection was impaired (Weiss et al., 1993, Carvalho et al., 2002). Furthermore, in an influenza infection model, the presence of CD4 T cells in the lungs improved the formation of CD103<sup>+</sup>CD69<sup>+</sup> CD8 T<sub>RM</sub> cells in this organ (Laidlaw et al., 2014). Therefore, it was of interest to investigate if the presence of Hsp90-restricted CD4 T cells enhanced the formation of *Plasmodium*-specific CD8 T<sub>RM</sub> cells in the liver. Our first approach to test the influence of CD4 T cells was to simultaneously prime *Plasmodium*-specific CD4 and CD8 T cells. For stimulation of CD4 T cells we used  $\alpha$ Clec9A-DIY, whereas for stimulation of CD8 T cells we used  $\alpha$ Clec9A-TRAP. The latter contains an MHC-I restricted epitope derived from thrombospondin-related anonymous protein (TRAP), a protein that accumulates at the parasite's apical end upon hepatocyte invasion (Mota et al., 2002, Matuschewski et al., 2002). This epitope was shown to induce TRAP-specific T cells responses and can act as a liver-stage target mediating partial protection (Bhardwaj et al., 2003, Valencia-Hernandez et al., 2020). By using an MHC-I tetramer carrying the TRAP epitope, endogenous TRAP-specific CD8 T cells can be enumerated by flow cytometry. To prime CD8 and CD4 T cells simultaneously, we generated an  $\alpha$ Clec9A mAb carrying both the DIY epitope,

on the  $\alpha$ Clec9A heavy chain and the TRAP epitope on the light chain ( $\alpha$ Clec9A-DIY/TRAP). Three groups of mice were examined in this experiment. Each group was adoptively transferred with  $5 \times 10^4$  PbT-II.uGFP cells to ensure the presence of a robust helper response. Mice were primed with either  $\alpha$ Clec9A-DIY,  $\alpha$ Clec9A-DIY/TRAP or  $\alpha$ Clec9A-TRAP. The latter two groups were also injected with a liver-tropic recombinant adeno-associated virus that expressed the TRAP epitope (rAAV-SAL), which was previously shown to enhance CD8 T<sub>RM</sub> formation by trapping recently activated CD8 T cells in the liver (Valencia-Hernandez et al., 2020). 35 days post-vaccination, the number of PbT-II cells and TRAP-specific CD8 T cells were determined in the spleen and the liver of the relevant groups (Figure 4.9A-D). No difference was observed in the number of memory PbT-II cells that formed in mice vaccinated with  $\alpha$ Clec9A mAb carrying the DIY and the TRAP epitope compared to the DIY epitope alone (Figure 4.9A, B). This control showed that simultaneous priming of *Plasmodium* restricted CD4 and CD8 T cells did not alter CD4 T<sub>RM</sub> cell formation. Importantly, while a drop in total TRAP-specific CD8 memory T cells was apparent, the reduction in liver T<sub>RM</sub> cells was not significant (Figure 4.9C, D). These results suggest that simultaneous priming of CD4 and CD8 T cells does not enhance formation of *Plasmodium*-specific CD8 liver T<sub>RM</sub> cells.

In the absence of CD4 T cell help during CD8 T cell priming, CD8 T cells can display reduced cytotoxic function, shown by lower granzyme B levels (Laidlaw et al., 2014). It is therefore possible that higher availability of CD4 T cells during CD8 T cell priming may lead to higher cytotoxicity of CD8 memory T cells and better protection against sporozoite infection after RAS vaccination. To investigate differences in protective capacity, mice were vaccinated with  $\alpha$ Clec9A-DIY,  $\alpha$ Clec9A-TRAP, or  $\alpha$ Clec9A-DIY/TRAP and infected with 200 sporozoites 35 days later. Parasitemia was determined from day 6 post-infection by flow cytometric analyses. As expected, mice that were vaccinated with  $\alpha$ Clec9A-TRAP had a reduced blood-parasite burden compared to naïve infected mice (Figure 4.9E). Mice that received the  $\alpha$ Clec9A-DIY/TRAP vaccine did not show a greater reduction in parasitemia (Figure 4.9E). Therefore, simultaneous

priming of *Plasmodium*-specific CD4 and CD8 T cells did not appear to improve elimination of sporozoite infected hepatocytes compared to  $\alpha$ Clec9A-TRAP vaccination. Interestingly, two mice of the  $\alpha$ Clec9A-DIY/TRAP vaccination group did not develop any detectable parasitaemia, implying that all sporozoites were killed in the liver (Figure 4.9F). Such protection was not seen using  $\alpha$ Clec9A-TRAP alone, raising the possibility that the combination may be more protective, but given the small number of mice achieving sterile immunity with the dual vaccine, we would need to test very large numbers of mice to assess whether this difference can reach significance.  $\alpha$ Clec9A-DIY vaccination did not influence parasitemia levels, which suggested that the previously described drop in parasitemia was due to response of TRAP-specific CD8 T cells and not PbT-II cells (Figure 4.9E).

In Summary, simultaneous priming of *Plasmodium*-specific CD4 and CD8 T cells did not enhance the formation of CD8 memory T cells in the liver, nor significantly increase the protective capacity of CD8 T<sub>RM</sub> cells against *Plasmodium* sporozoite infection.

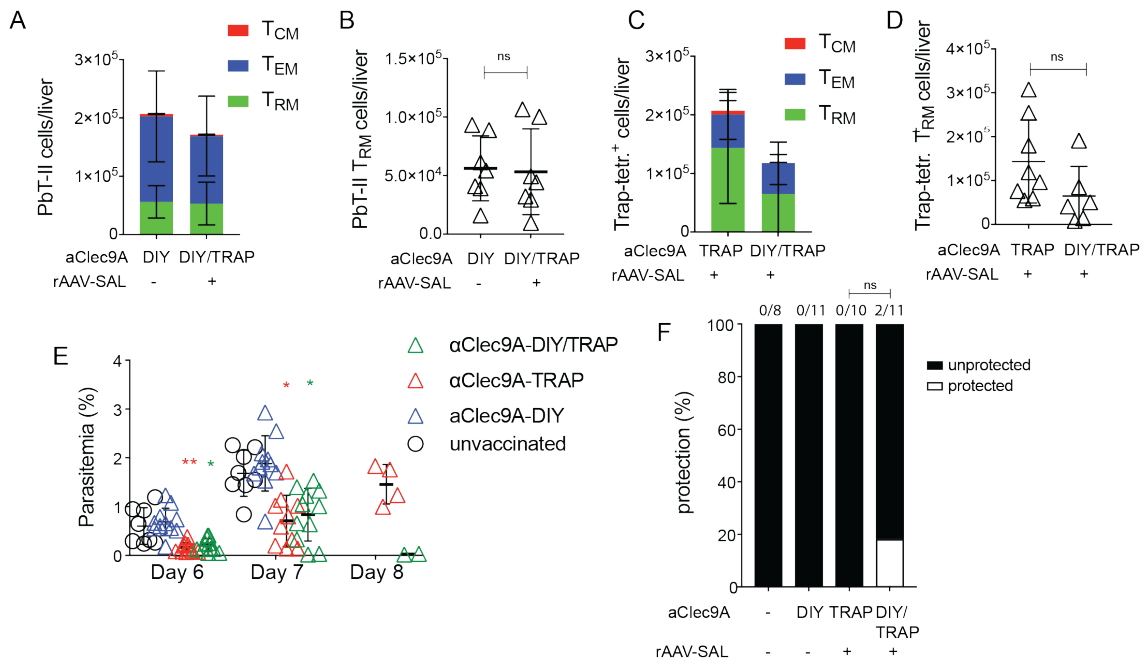


**Figure 4.9. Simultaneous priming of *Plasmodium* specific CD4 and CD8 T cells.**

B6 mice received  $5 \times 10^4$  PbT-II.uGFP cells and were vaccinated with either  $8 \mu\text{g}$   $\alpha\text{Clec9A-DIY}$ ,  $\alpha\text{Clec9A-DIY/TRAP}$  or  $\alpha\text{Clec9A-TRAP}$  and  $5\text{nmol}$  CpG. One day later, mice were vaccinated with  $\alpha\text{Clec9A-DIY/TRAP}$  or  $\alpha\text{Clec9A-TRAP}$  received  $10^9$  vgc of rAAV-SAL. 35 days post-vaccination, mice were assessed for total PbT-II (**A**) (live,  $\text{CD4}^+$ ,  $\text{V}\alpha 2^+$ ,  $\text{GFP}^+$ ,  $\text{CD44}^{\text{hi}}$ ) or Trap-tetramer+ (**C**) (live,  $\text{CD8}^+$ ,  $\text{CD44}^{\text{hi}}$ ) T cell numbers and  $\text{CD69}^+\text{CD62L}^-$  PbT-II (**B**) and Trap-tetramer+ (**D**)  $\text{T}_{\text{RM}}$  cell numbers in the liver. 35 days post-vaccination mice were challenged with 200 live PbA sporozoites and parasitaemia (**E**) and protection (**F**) of infected mice was determined. **A-E**. Data pooled from 2 independent experiments with a total of 6 mice per group. **B, D**.  $**p < 0.01$ , two-tailed Mann-Whitney test. **E**. ( $****p < 0.0001$ ,  $**p < 0.001$  Kruskal-Wallis test following Dunn's multiple comparison test) **F**. Data pooled from 2 independent experiments with a total of 8-11 mice per group.  $*p < 0.05$ ;  $**p < 0.01$ ;  $***p < 0.001$ ; ns, not significant; Fisher's exact test.

#### 4.2.6 The presence of Hsp90-restricted CD4 T cells does not enhance CD8 T<sub>RM</sub> formation after RAS vaccination.

For RAS vaccination, the presence of CD4 T cells in the priming phase is essential for generation of protective *Plasmodium*-specific CD8 T cells, as depletion of CD4 T cells before vaccination abrogated protection by these cells (Weiss et al., 1993). Furthermore, two studies suggested the importance of CD4 T cells in CD8 T<sub>RM</sub> cell development by showing that blocking IL-21 expressed by Tfh and depletion of CD4 T cells that mainly expressed IFN- $\gamma$  reduced CD8 T<sub>RM</sub> cell numbers and viral clearance in the lung (Laidlaw et al., 2014, Son et al., 2021). Thus, IFN $\gamma$  and IL21 expression by PbT-II cells might enhance CD8 T<sub>RM</sub> formation in the liver after RAS vaccination. IFN- $\gamma$  secretion by PbT-II Th1 and  $\alpha$ Clec9A-DIY primed PbT-II cells was shown in Figure 3.12, indicating this function was available to help CD8 T cells. To assess the availability of IL-21, we investigated the potential of PbT-II T<sub>RM</sub> cells to produce this cytokine. IL-21 expression levels were investigated in the RNA.seq dataset described earlier (Chapter 4.2.4). As expected, PbT-II T<sub>RM</sub> cells induced by  $\alpha$ Clec9A-DIY priming, which produce Tfh cells, generated IL-21 transcripts (Figure 4.10A) (Nurieva et al., 2008). In contrast, those produced by RAS vaccination or through Th1 or Th2 differentiation showed little evidence of *Il21* transcript expression (Figure 4.10A). Of relevance, however, CD8 T<sub>RM</sub> cells showed elevated levels of *Il21r*, which should enable CD8 liver T<sub>RM</sub> cells to directly respond to IL-21 secreted by PbT-II T<sub>RM</sub> cells generated by  $\alpha$ Clec9A-DIY priming (Figure 4.10B). This result showed that PbT-II T<sub>RM</sub> cells generated by  $\alpha$ Clec9A-DIY immunisation have the potential to support CD8 T<sub>RM</sub> formation after RAS vaccination in the liver via IL-21 and IL-21R signalling.

In addition to IL-21, IL-4 secreted by *Plasmodium*-specific CD4 T cells is essential for efficient CD8 T cells priming during RAS vaccination (Carvalho et al., 2002). Moreover, IL-4 receptor (IL-4R) expression by CD8 T cells is required for the generation of a protective CD8 memory T cell population against

*Plasmodium* infection (Morrot et al., 2005). However, these studies did not specifically investigate CD8 T<sub>RM</sub> populations, as the importance of CD8 T<sub>RM</sub> in the protection of liver-stage *Plasmodium* infection was not known at the time. It is therefore possible that observed effects of IL-4 secretion by CD4 T cells and the requirement for IL4R expression by CD8 memory T cells was CD8 T<sub>RM</sub> cell related. However, IL-4 might only be required in the priming phase but not for the formation of CD8 T<sub>RM</sub> cells. Thus, the expression of IL4 and IL4-receptor by CD4 and CD8 T<sub>RM</sub> cells was investigated. As already shown in chapter 3, PbT-II Th2 cells released IL-4 upon restimulation. Moreover, RNAseq data revealed that Th2 differentiation and RAS vaccination induced elevated *Il4* expression levels by PbT-II T<sub>RM</sub> compared to Th1 and  $\alpha$ Clec9A-DIY induced T<sub>RM</sub> cells (Figure 4.10C). To directly sense IL-4, CD8 T<sub>RM</sub> cells require the expression of IL4R. As seen in Figure 4.10D, no differences in *Il4r* expression levels was found between CD8 T<sub>RM</sub> cells generated after RAS vaccination compared to CD4 T<sub>RM</sub> cells generated under the same conditions (Figure 4.10D). However, a study by Fernandez-Ruiz and co-authors showed a that liver CD8 T<sub>RM</sub> cells had higher expression of IL-4R on the cell surface compared to CD8 T<sub>EM</sub> cells (Fernandez-Ruiz et al., 2016). This suggests, that CD8 T<sub>RM</sub> in the liver sense IL-4.

Based on these results, we investigated whether an established population of Tfh, Th1 or Th2 PbT-II cells could enhance CD8 T<sub>RM</sub> formation in the liver after RAS vaccination. To achieve this goal, mice were vaccinated with  $\alpha$ Clec9A-DIY, which induced a strong Tfh cell responses, or were injected with PbT-II Th1 or Th2 polarized cells. Two weeks later, mice were immunized with  $5 \times 10^4$  RAS, and PbT-II and CD8 T<sub>RM</sub> cell numbers determined by flow cytometry 35 days later. After RAS vaccination, similar PbT-II cell numbers were found in mice given  $\alpha$ Clec9A vaccination or transferred with PbT-II Th1 cells, but the transfer of PbT-II Th2 polarised cells yielded an enhanced number of PbT-II cells (Figure 4.11B, C). To examine CD8 T cells responses, an MHC-I tetramer was used to detect TRAP-specific CD8 T cells (Figure 4.11D, E). No differences in TRAP-specific total T cells or T<sub>RM</sub> CD8 T cell numbers were detectable in the liver. This suggested that none of the PbT-II cell lineages investigated in this experiment

enhanced the formation of *Plasmodium*-specific CD8 T<sub>RM</sub> cells in the liver after RAS vaccination. However, previous research examining lung resident CD8 T cells after influenza infection revealed that IL-21 produced by CD4 T cells helps establish CD8 T<sub>RM</sub> cells restricted to the nucleoprotein but not to the polymerase peptide from the influenza virus (Son et al., 2021). It was, therefore, possible that a different specificity of CD8 T<sub>RM</sub> cells in the liver are directed into a T<sub>RM</sub> phenotype in the presence of PbT-II cells. To investigate this possibility, a second tetramer was used to stain for NVF specific CD8 T cells. NVF is an abbreviation for a recently described CD8 T cell epitope derived from *P. berghei* ribosomal protein L6 (RPL6), which is expressed in all stages of the parasite life cycle (Valencia-Hernandez et al., 2020). Examination of the NVF-specific response revealed that, similar to TRAP-specific CD8 T cells, addition of the various PbT-II helper populations did not affect either total NVF-specific CD8 T cell numbers or T<sub>RM</sub> cell numbers in the liver after RAS vaccination (Figure 4.11F, G). Therefore, a pre-formed Hsp90 restricted T<sub>fh</sub>, Th1, or Th2 CD4 T cell population did not enhance CD8 T cell or CD8 T<sub>RM</sub> cell formation in the liver after RAS vaccination.

In summary, it was shown here that Hsp90-specific CD4 T<sub>RM</sub> cells form in the liver after RAS and  $\alpha$ Clec9a-DIY vaccination. In addition, Hsp90-specific liver T<sub>RM</sub> cells do not require cognate antigen expression in the liver and can form spontaneously from *in vitro* differentiated PbT-II cells. Hsp90-restricted CD4 liver T<sub>RM</sub> cells resemble *Plasmodium*-specific CD8 liver T<sub>RM</sub> cells in their gene expression, sharing a liver-resident core gene signature independently of the priming method used for their generation. However, CD4 T<sub>RM</sub> cells generated via different activation methods or differentiation protocols displayed different gene expression profiles in terms of effector molecules, indicating that they might mediate distinct immune responses during *Plasmodium* infections. In contrast to recent studies with influenza-specific CD4 T<sub>RM</sub> cells in the lung, which suggested a role for CD4 T cells in promoting CD8 T<sub>RM</sub> recruitment, Hsp90-specific CD4 T

cells did not improve CD8 T<sub>RM</sub> generation after vaccination with RAS (Son et al., 2021).

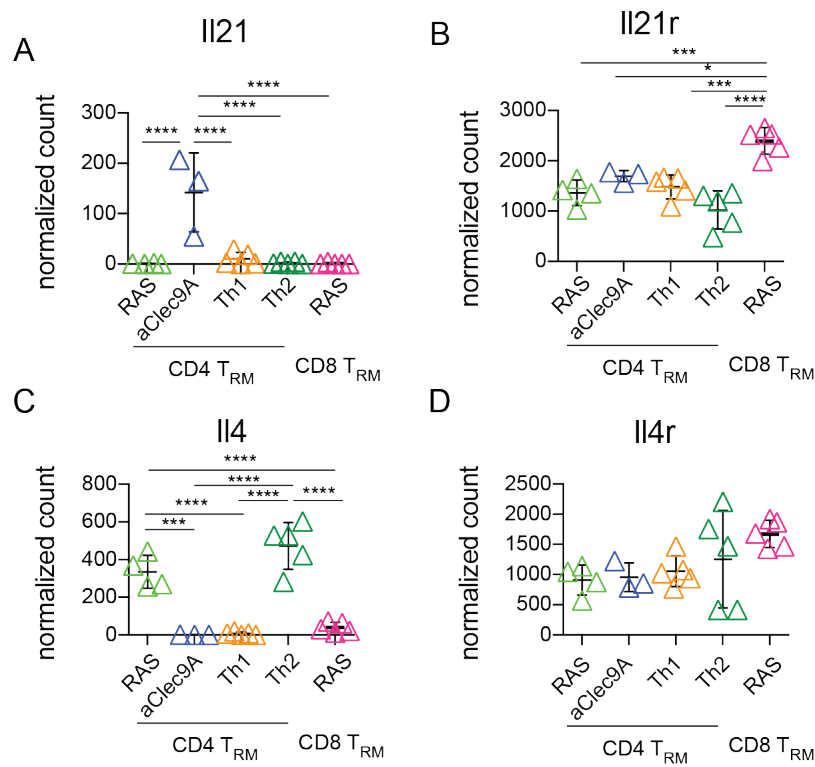


**Figure 4.10. Single transcript expression in CD4 and CD8 liver T<sub>RM</sub> cells.**

B6 mice received  $5 \times 10^4$  naïve PbT-II.uGFP or PbT-I.uGFP cells and were vaccinated with  $5 \times 10^4$  RAS or  $2 \mu\text{g}$   $\alpha\text{Clec9a-DIY}$  and  $5\text{nmol}$  CpG one day later. Additional mice received  $10^7$  *in vitro* polarized PbT-II Th1 or Th2 cells. 35 days after vaccination or cell transfer, memory GFP<sup>+</sup>CD44<sup>hi</sup>CD69<sup>+</sup>CXCR6<sup>+</sup> T<sub>RM</sub> PbT-II and PbT-I cells were sorted from the liver and analysed for gene expression by RNAseq. **A-D.** Transcriptional expression of genes potentially correlated to enhanced CD8 T<sub>RM</sub> cell formation. (\*p < 0.05; \*\*p < 0.01; \*\*\*p < 0.001; \*\*\*\*p < 0.0001, n.s. > 0.05, Ordinary one-way ANOVA followed by Turkey's multiple comparison test.

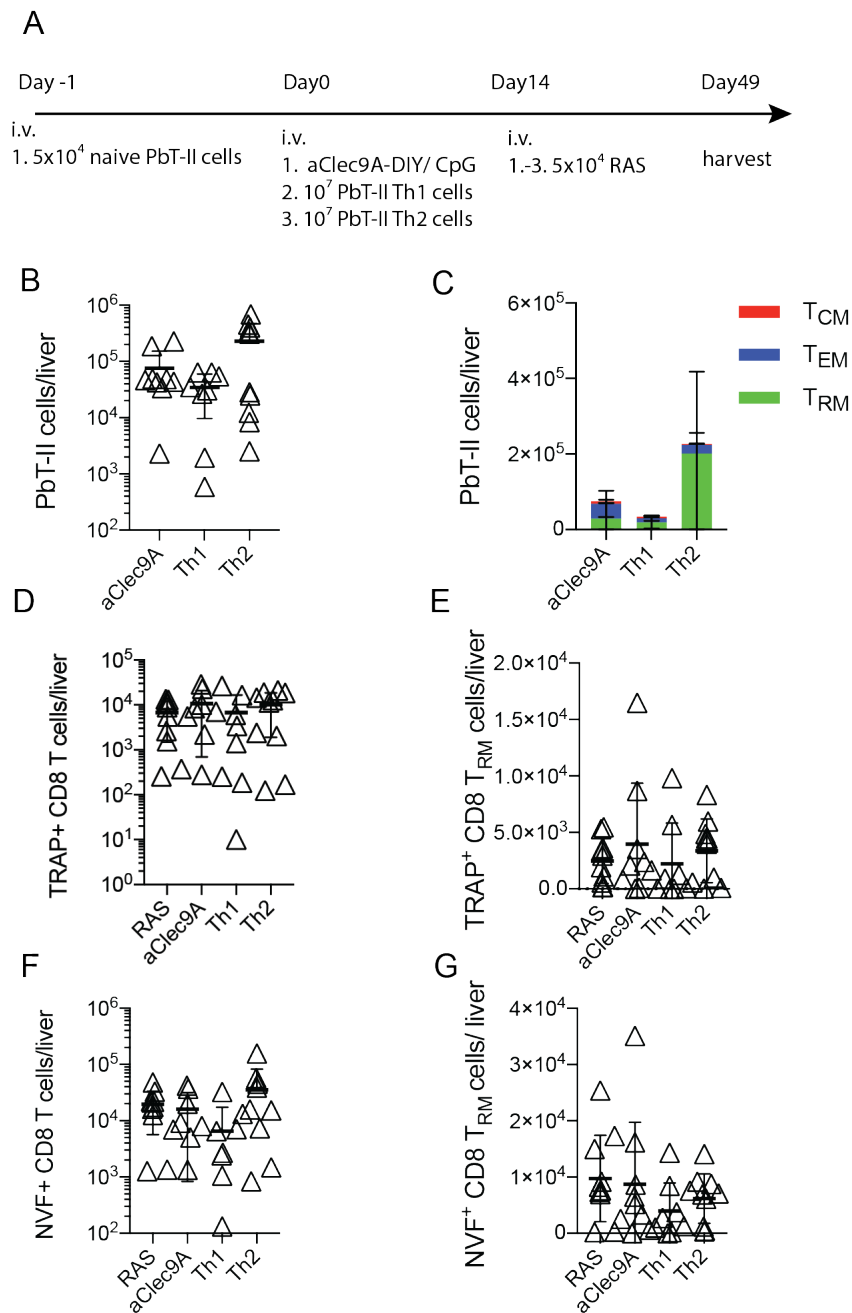


**Figure 4.11. Sequential priming of *Plasmodium* specific CD4 and CD8 T cells.**

B6 mice received  $5 \times 10^4$  PbT-II.uGFP cells and were vaccinated with either  $2 \mu\text{g}$   $\alpha$ Clec9A-DIY and 5nmol CpG or were injected with  $10^7$  *in vitro* polarized PbT-II Th1 or Th2 cells. 14 days post priming or cell transfer, mice were vaccinated with  $5 \times 10^4$  PbA RAS. After an additional 35 days, mice were assessed for total PbT-II T cells, PbT-II memory T cell subsets, or CD8+ TRAP-specific or NVF-specific T cells by flow cytometry analyses. Data pooled from 2 independent experiments with a total of 10 mice per group. (\*\*\*\* $p < 0.0001$ , \*\* $p < 0.001$  Kruskal-Wallis test following Dunn's multiple comparison test).

### 4.3 Discussion

In this chapter, parabiosis was used to show that RAS vaccination led to the generation of two distinct CD4<sup>+</sup> memory T cell populations: a population of effector memory T cells ( $T_{EM}$ ) that recirculated in the blood and a population of resident memory T cells ( $T_{RM}$ ) that remained permanently within the liver. The PbT-II  $T_{RM}$  cells in the liver expressed typical  $T_{RM}$  cell-associated markers such as CD69, CXCR6, and CXCR3 and lacked expression of the  $T_{EM}$  associated marker KLRG1 (Fernandez-Ruiz et al., 2016, Benoun et al., 2018, Kumar et al., 2017). Furthermore, gene expression profiles of liver CD4  $T_{RM}$  cells were highly correlated with those of RAS-generated CD8 liver  $T_{RM}$  cells (Fernandez-Ruiz et al., 2016). In addition, liver PbT-II (CD4)  $T_{RM}$  expressed genes associated with a recently published core signature of skin and gut CD8  $T_{RM}$  cells and liver-resident CD8 T cells, NKT and NK cells (Mackay et al., 2016).

Although we recovered most CD69<sup>+</sup> PbT-II  $T_{RM}$  cells from the parental liver 30 days after parabiotic surgery, strongly implicating a liver-resident population, we could recover a small number of CD69<sup>+</sup> PbT-II cells in the liver of the naïve parabiotic partner. This suggested that some CD4  $T_{RM}$ -like cells had entered the circulation and subsequently infiltrated the liver of the parabiotic partner. This is consistent with evidence that  $T_{RM}$  cells, when isolated from an organ and transferred into a naïve host, preferentially re-home to the same organ. For example, a previous report showed that lung derived influenza-specific memory CD4 T cells accumulated in the lung when transferred into naïve mice, while spleen derived memory CD4 T cells were distributed in several organs including in the spleen, lung and liver (Teijaro et al., 2011). In addition, RAS generated liver CD8  $T_{RM}$  cells preferentially homed back to the liver but not lungs, brain or spleen after transfer into naïve mice, suggesting that tissue-specific homing can be imprinted in memory T cells (Fernandez-Ruiz et al., 2016).

One potential mechanism that might have led to egress of T<sub>RM</sub> cells from the parental liver after parabiotic surgery is local re-activation (Fonseca et al., 2020). It was recently shown that local reactivation of CD8 T<sub>RM</sub> cells led to an egress of these cells into the circulation. Upon tissue entry those reactivated CD8 T<sub>RM</sub>-like cells preferentially re-acquired T<sub>RM</sub> cell characteristics (Fonseca et al., 2020). Therefore, small populations of PbT-II T<sub>RM</sub> cells could have been reactivated by persistent Ag in the liver, left the parental liver and homed to the parabiotic partner's liver. However, we found little evidence for persisting Ag at day 30 post RAS vaccination (Chapter 3). It is therefore unlikely that reactivation caused the appearance of CD69<sup>+</sup> PbT-II cells in the parabiotic partner liver.

In addition to showing that CD4 PbT-II cells could form liver resident memory after RAS vaccination, we validated conclusions drawn from earlier work showing that transgenic CD8 PbT-I T cells specific for RPL6 could also form residence under these circumstances (Valencia-Hernandez et al., 2020, Fernandez-Ruiz et al., 2016). Here we extended these finding to endogenous CD8 T cells using an MHC-I tetramer to detect RLP6-specific CD8 T cells.

After providing evidence for the existence of *Plasmodium*-specific liver CD4 T<sub>RM</sub> cells, we aimed to identify factors that might enforce their formation. The formation of PbT-II T<sub>RM</sub> cells in the liver did not require cognate antigen expression in the liver, with T<sub>RM</sub> cells forming spontaneously after adoptive transfer of *in vitro* activated and polarized PbT-II cells. This finding is consistent with a previous study showing that CD8 T<sub>RM</sub> cells can form independently of antigen expression in the liver (Holz et al., 2018). However, the ability of activated PbT-II T cells to spontaneously form T<sub>RM</sub> cells did not exclude the possibility that cognate antigen stimulation within the liver might enhance CD4 T<sub>RM</sub> cell formation. RAS vaccination, which potentially leads to antigen presentation by hepatocytes, favoured T<sub>RM</sub> cell differentiation compared to  $\alpha$ Clec9A-DIY vaccination. As shown for *Plasmodium*-specific CD8 T cells, CD8 T<sub>RM</sub> cell formation was improved by combining the  $\alpha$ Clec9A subunit vaccine with injection of a recombinant adeno-associated virus (rAAV) that enabled expression of the cognate antigen in the liver. This strategy generated higher CD8 T<sub>RM</sub> cell numbers

than  $\alpha$ Clec9A vaccination alone, suggesting local antigen recognition favours CD8 T<sub>RM</sub> formation (Fernandez-Ruiz et al., 2016, Valencia-Hernandez et al., 2020). Future studies are required to determine whether similar mechanisms contribute to CD4 T<sub>RM</sub> cell development. The generation of a DIY epitope-expressing rAAV, and then combining this stimulus with  $\alpha$ Clec9A-DIY/CpG vaccination, would test whether antigen expression in the liver supports CD4 T<sub>RM</sub> formation.

In addition to local antigen availability, other factors might influence CD4 T<sub>RM</sub> differentiation. It was observed that Th2 cells are more prone to differentiate into T<sub>RM</sub> cells when compared to Th1 cells. Th1 and Th2 T cell differentiation is characterised by expression of T-box transcription factor 21 (Tbet) and GATA binding protein 3 (GATA3), respectively, which orchestrate differentiation by binding to specific regulatory elements enhancing or diminishing expression of lineage-specific key cytokines (Jenner et al., 2009). Tbet binds to a regulatory element of the *Ifng* locus, resulting in histone modification and *Ifng* transcription (Wilson et al., 2009, Lee et al., 2004, Shnyreva et al., 2004). In contrast, by binding to the *Il4* promoter, Tbet silences *Il4* transcription (Ansel et al., 2004, Jenner et al., 2009, Djuretic et al., 2007). GATA3 acts in opposition to Tbet. GATA3 binds to multiple-locus sites of *Il4*, *Il5*, and *Il13* and enhances transcription of these genes, while binding of GATA3 to the *Ifng* locus results in the recruitment of repressive complexes, thereby reducing IFN- $\gamma$  expression (Jenner et al., 2009, Chang and Aune, 2007, Kishikawa et al., 2001).

Early high Tbet expression is also observed in CD8 T cells in the skin after HSV infection (Mackay et al., 2015b). However, Tbet expression decreased over time in the process of CD8 T<sub>RM</sub> differentiation in lung or skin (Laidlaw et al., 2014, Mackay et al., 2015b). Furthermore, forced Tbet expression led to reduced CD103<sup>+</sup> CD8 T<sub>RM</sub> cell accumulation in the skin at an early memory time point, indicating that the timing or magnitude of Tbet expression is crucial for optimal T<sub>RM</sub> cell differentiation (Mackay et al., 2015b). It is therefore possible that high expression of Tbet by PbT-II Th1 cells reduced the ability of these cells to differentiate into T<sub>RM</sub> cells. Interestingly, Eomes, which also belongs to the T-box

transcription factor family, was downregulated in PbT-II Th2 liver T<sub>RM</sub> cells compared to PbT-II Th1 T<sub>RM</sub> cells or PbT-II T<sub>RM</sub> cells generated after  $\alpha$ Clec9A-DIY vaccination. In a similar fashion to Tbet expression, Eomes is usually downregulated in the process of CD8 T<sub>RM</sub> formation, with forced expression of Eomes causing reduced numbers of CD8 T<sub>RM</sub> cells in the skin (Mackay et al., 2015b). Therefore, both Tbet and Eomes, which are expressed at higher levels in Th1 compared to Th2 PbT-II cells, might reduce the ability of PbT-II Th1 cells or PbT-II cells generated after  $\alpha$ Clec9A-DIY vaccination to transition into a T<sub>RM</sub> cell phenotype in the liver. One mediator to induce early Tbet upregulation, in CD8 T cells *in vitro* cultures, is IL-12 (Takemoto et al., 2006). In our experimental model, IL-12, amongst other reagents, was utilized to polarise PbT-II cells towards a Th1 phenotype *in vitro*. Furthermore, CpG treatment, as used during  $\alpha$ Clec9A-DIY immunisation, was reported to induce IL-12 secretion by APCs (Krieg et al., 1998, Halpern et al., 1996). Therefore, prolonged Tbet expression in PbT-II cells induced by IL-12 stimulation, during *in vitro* polarisation or  $\alpha$ Clec9A-DIY vaccination, may limit their capacity to differentiate into T<sub>RM</sub> cells. It has previously been shown that Eomes is suppressed in CD8 T cells cultured with IL-12 and upregulated in the presence of IL-4 (Takemoto et al., 2006). It is thus likely that IL-12 and IL-4 also influence Eomes expression in CD4 T cells. Eomes expression is associated with induction of long-lived T cell memory, while high Tbet expression is common in short-lived effector T cells (Joshi et al., 2007). Perhaps, early Eomes expression could further provide PbT-II Th2 cells with long-term survival while Tbet expression by PbT-II Th1 may favour short-lived effector T cell differentiation (Joshi et al., 2007, Mackay et al., 2015b). Interestingly, PbT-II Th2 T<sub>RM</sub> cells, induced in the presence of IL-4, had lower Eomes expression levels than PbT-II Th1 cells at a memory time point. It is possible that transient Eomes expression was induced early by IL-4 in Th2 polarization conditions but downregulated over time in the process of differentiation towards memory T cells, as observed for CD8 T cells (Mackay et al., 2015b). It would be interesting to determine the expression levels of Tbet and Eomes by PbT-II Th1 and Th2 cells over time after transfer to determine the role of those two transcription factors during CD4 T<sub>RM</sub> cell development. Manipulation

of Tbet or Eomes expression with different adjuvants during vaccination could bias CD4 memory differentiation towards a specific memory subpopulation, which might influence control of *Plasmodium* liver-stage infection. It is worth noting, however, that the negative roles of prolonged Tbet and Eomes expression in the formation of CD8 T<sub>RM</sub> cells was only described for CD103<sup>+</sup> T<sub>RM</sub> cells, which rely on IL-15 and transforming growth factor (TGF)- $\beta$  signalling (Mackay et al., 2015b). It is currently unclear whether liver CD4 T<sub>RM</sub> cells require the same molecular pathways as CD8 T<sub>RM</sub> cells. Liver CD4 T<sub>RM</sub> cells commonly do not express CD103, and it is also unknown whether CD4 T<sub>RM</sub> cell formation in the liver depends on IL15 or TGF- $\beta$  signalling (Benoun et al., 2018). Nevertheless, the generation of lung resident CD4 T cells and liver resident CD8 T cells was shown to be directly linked to IL-15 signalling. Whether IL-15 signalling is also important for the formation of liver-resident CD4 T cells requires further studies.

An additional cytokine worth investigating for its potential role in liver T<sub>RM</sub> cell formation is IL-4. We found that *in vitro* polarisation of PbT-II into Th2 cells, in the presence of IL-4, IL-2 and IFN $\gamma$  blocking antibody ( $\alpha$ IFN- $\gamma$ ), favoured liver T<sub>RM</sub> cell formation when compared to Th1 polarising conditions (IL-12, IL-2, LPS and  $\alpha$ -IL4). Furthermore, our analyses revealed that IL-4 was upregulated in CD4 T<sub>RM</sub> cells generated after RAS compared to those generated by  $\alpha$ Clec9A-DIY immunisation. As RAS vaccination favoured induction of PbT-II T<sub>RM</sub> cells whereas  $\alpha$ Clec9a-DIY vaccination favoured T<sub>EM</sub> cells, we hypothesise that an autocrine IL-4 stimulation could potentially favour T<sub>RM</sub> cell formation in the liver. Furthermore, upregulation of IL-4 and IL-4 production pathways were found in RAS-generated PbT-II T<sub>RM</sub> cells compared to T<sub>EM</sub> cells, further strengthening the hypothesis that IL-4 might be necessary for CD4 T<sub>RM</sub> formation or maintenance but not for T<sub>EM</sub> cells. Additional preliminary data showed that PbT-II cells *in vitro* activated in the presence of recombinant IL-4, IL-2 and Hsp90 peptide, led to enhanced liver and lung PbT-II T<sub>RM</sub> cell formation after adoptive transfer compared to PbT-II cells activated without IL-4 (Personal communication Dr. Daniel Fernandez-Ruiz). This showed that the presence of IL-4 indeed favours PbT-II T<sub>RM</sub> cell formation and might be a useful supplement for vaccines aiming

to induce large liver CD4 T<sub>RM</sub> cell populations. Administration of recombinant IL-4 or the use of an adjuvant inducing IL-4 secreting CD4 T cells, such as aluminium hydroxide, might thus improve PbT-II T<sub>RM</sub> cell formation after  $\alpha$ Clec9A-DIY immunisation (Sokolovska et al., 2007).

While little is known about the role of IL-4 in CD4 T<sub>RM</sub> cell biology, several studies on CD8 T cells support a crucial function for this cytokine in CD8 T cell responses in the liver. It was previously reported that CD8 T cell responses induced by RAS immunisation are dependent on IL-4 (Carvalho et al., 2002). In addition, IL-4 receptor expression by memory CD8 T cells was shown to be essential for protective immunity to sporozoite infection (Morrot et al., 2005). While it is now known that CD8 T<sub>RM</sub> cells are the main memory subset responsible for protection against sporozoite infection, the existence of T<sub>RM</sub> cells was not known at the time of these studies. This raises the question whether the findings in these earlier studies were a consequence of IL-4 dependence in liver CD8 T<sub>RM</sub> cells. The observation that addition of PbT-II Th2 cells, prone to release IL-4, did not enhance induction of *Plasmodium*-specific CD8 T<sub>RM</sub> cell responses upon RAS vaccination, questions this conclusion. However, there are two potential explanations for the lack of effect of PbT-II Th2 cells here. Firstly, IL-4 secretion may already have been optimal as we observed that IL-4 was upregulated in PbT-II T<sub>RM</sub> cells after RAS vaccination. Thus, RAS vaccination clearly induces CD4 T cells that make IL-4. Secondly, it is not clear whether PbT-II cells recognised their cognate antigen in the liver, which would be essential to stimulate release of IL-4. Nevertheless, preliminary data showed that *in vitro* activation of CD8 T cells in the presence of recombinant IL-4 was able to improve liver CD8 T<sub>RM</sub> cell formation (Personal communication Dr. Daniel Fernandez-Ruiz). It is therefore likely, that an anti-malaria vaccine, designed to induce IL-4 or administration of IL-4 during the priming phase will enhance the formation of CD4 and CD8 T<sub>RM</sub> cells in the liver, potentially leading to improved protection against sporozoite infection.

In addition to IL-4, IL-13 was highly expressed by Th2 PbT-II cells and might therefore be capable of improving tissue-resident memory T cell formation.

Interestingly, IL-13 receptor complex and IL-4 receptor complex share the IL-4Ra subunit and binding of either IL-13 or IL-4 can induce similar downstream signalling pathways. However, the IL-13Ra subunit is not commonly expressed on T cells, resulting in only IL-4 being potent enough to induce Th2 cell differentiation. Therefore, IL-13 might indirectly influence T cell differentiation and therefore T<sub>RM</sub> cells formation, but this requires further investigation.

In addition to IL-4-producing CD4 T cells, those secreting IFN- $\gamma$  and IL-21 have been shown to promote CD103<sup>+</sup> CD8 T<sub>RM</sub> cell recruitment into the lung (Laidlaw et al., 2014, Son et al., 2021). In our study, liver CD8 T<sub>RM</sub> formation was not elevated in the presence of *in vitro* differentiated PbT-II Th1 cells or  $\alpha$ Clec9A-DIY generated Th1 and Tfh cells, despite their potential for IFN- $\gamma$  or IL-21 secretion. PbT-II Th1 and Tfh might not be locally activated to secrete cytokines due to insufficient MHC-II expression by hepatocytes, or because Hsp90 may not be expressed at sufficient levels in the liver after RAS vaccination (Franco et al., 1988). Furthermore, IFN- $\gamma$  or IL-21 secretion by endogenous CD4 T cells upon RAS vaccination may have already been optimal for the generation of potent CD8 T<sub>RM</sub> cells responses, potentially explaining the lack of elevated CD8 T<sub>RM</sub> formation in the liver. Furthermore, while previous studies investigated CD8 T<sub>RM</sub> cell recruitment in the absence of IFN- $\gamma$  and IL-21, they did not determine the effect of elevating cytokine levels above natural endogenous levels (Laidlaw et al., 2014, Son et al., 2021). Potentially, endogenous levels of IFN- $\gamma$  or IL-21 after  $\alpha$ Clec9A or RAS vaccination are sufficient for CD8 T<sub>RM</sub> recruitment and formation in our experimental design, without a benefit of additional cytokine producing PbT-II cells. Alternatively, liver CD103<sup>-</sup> CD8 T<sub>RM</sub> cells, unlike CD103<sup>+</sup> T<sub>RM</sub> cells in the lung, might not require IL-21 or IFN- $\gamma$  for recruitment into the tissue.

The identification of *Plasmodium*-specific liver resident CD4 T cells opens new possibilities to design efficient vaccine strategies. As memory T cell numbers declined over time and higher *Plasmodium*-specific CD8 T<sub>RM</sub> cell numbers correlated with better protection against sporozoite infection, mechanisms and factors for improving CD4 and CD8 T<sub>RM</sub> cell numbers, such as IL-4, may lead to prolonged protection against *Plasmodium* infection (Fernandez-Ruiz et al.,

2016). If such mechanisms can be incorporated or targeted in an anti-malaria vaccine and potentially other vaccines that target T cell responses in the liver, this could potentially improve liver-specific vaccines in humans.

## **Chapter 5**

# **The role of Hsp90-specific CD4 T cells in protection against *Plasmodium* infection**

## Chapter 5 The role of Hsp90-specific CD4 T cells in protection against *Plasmodium* infection

### 5.1 Introduction

CD4 T cells have been found to be involved in the defence response against *Plasmodium* mediated liver and blood-stage infection, and also in the development of malaria-associated pathology (Doolan and Hoffman, 2000, Oliveira et al., 2008, Tsuji et al., 1990, Su and Stevenson, 2000, Perez-Mazliah et al., 2017, Oakley et al., 2013). CD4 T cells show a high degree of plasticity and, as such, different CD4 T cell lineages can influence the outcome of a *Plasmodium* infection (Tsuji et al., 1990, Kurup et al., 2017, Couper et al., 2008). For example, regulatory T cells, such as Tregs and Tr1 cells, can reduce the risk of developing pathology but also decrease the control of parasite growth (Kurup et al., 2017, Zander et al., 2016, Haque et al., 2010, Freitas do Rosario et al., 2012). On the other hand, Th1 CD4 T cells are associated with immune pathology, such as ECM in mice, but contribute to the control of liver and blood-stage parasites (Fontana et al., 2016, Oakley et al., 2013). The ideal CD4 T cell-based vaccine would induce cells that provide sterile protection but are not involved in immune pathology. One way to achieve this is to eliminate sporozoite-infected hepatocytes before parasites can progress to the blood-stage, as the pre-erythrocytic stages are not associated with pathology. While tissue resident memory CD8 T cells are known to be highly protective against *Plasmodium* sporozoite infection, only limited data is available for CD4 T cells directly killing infected hepatocytes (Fernandez-Ruiz et al., 2016, Doolan and Hoffman, 2000, Tsuji et al., 1990, Oliveira et al., 2008). In such studies, repeated RAS vaccination with large doses of RAS still only induced limited protection against sporozoite challenge in mice that lacked CD8 T cells (Oliveira et al., 2008). CD4 T cells are required for the generation of protective CD8 T cell responses after RAS

vaccination and a combination of CD4 and CD8 T cell responses have been suggested to strengthen the immune response against *Plasmodium* sporozoite infection (Carvalho et al., 2002).

Due to its disappointing results in the field, RAS vaccination might not be feasible for broad application in malaria endemic areas (Sissoko et al., 2017). The use of a subunit vaccine, such as the  $\alpha$ Cle9A-based vaccine described here, might be an alternative for future vaccination strategies. Thus, we investigated its potential to induce CD4 T cell-mediated protection against the liver-stage of infection.

Previous studies have shown that Hsp90-specific CD4 T cells can rescue CD40L<sup>-/-</sup> mice from Pch blood-stage infection, which is lethal in these KO mice (Fernandez-Ruiz et al., 2017). Furthermore, transfer of naïve PbT-II cells could delay the severe outcome of Pch blood-stage infection in RAG1KO mice. In CD40L<sup>-/-</sup> mice, CD4 T cells are not able to activate DC or B cells via CD40, while RAG1KO mice lack mature B or T cells. Therefore, both models added PbT-II cells to an impaired CD4 T cell response, to rescued CD4 T cell activity. However, it was not yet investigated whether adding PbT-II cells to a normal B6 repertoire could improve protection against *Plasmodium* infection.

The identification of the PbT-II restricted antigen, as described in Chapter 3, allowed us to *in vitro* activate and polarize PbT-II cells into different CD4 T cell lineages. This provided the opportunity to study CD4 T cell lineage specific differences in protection against liver and blood-stage *Plasmodium* infection. Furthermore, an  $\alpha$ Clec9A vaccine was designed and evaluated for its specific protective capacity against *Plasmodium* infection.

## 5.2 Results

### 5.2.1 Assessment of the protective capacity of Hsp90-specific CD4 T cells against *Plasmodium* liver-stage infection.

The previous chapters have shown that Hsp90-specific memory CD4 T cell populations form after vaccination or *Plasmodium* infection. However, it was unclear whether these cells could protect against infection. Here, the protective capacity of Hsp90-specific CD4 T cells against liver stage *Plasmodium* infection was investigated. To test the protective capacity of memory cells of Hsp90-specificity, B6 mice were either adoptively transferred with  $5 \times 10^4$  naive PbT-II cells and then vaccinated with  $\alpha$ Clec9A-DIY or were injected with  $10^7$  *in vitro* differentiated PbT-II Th1 or Th2 cells and challenged with  $10^4$  PbA spz 35 days later. In addition, as a non-specific control, a group of mice received *in vitro* differentiated gDT-II Th1 cells, which are specific for an epitope derived from HSV-1 glycoprotein D and cannot respond to *Plasmodium* (Bedoui et al., 2009). At 42 h post challenge, the livers were harvested and parasite RNA was quantified by qPCR analysis. Vaccination, or transfer of large numbers of *in vitro* activated cells, did not reduce the liver parasite burden (Figure 5.1A). These findings strongly suggest that Hsp90-specific memory cells are unable to eliminate infection in hepatocytes. One possible explanation was that memory T cell numbers were not sufficient to provide protection against sporozoite infection. Therefore, it was tested whether similar groups of mice were protected against sporozoite infection when challenged early after vaccination or adoptive transfer, prior to significant contraction of the effector T cell pool. To this end, naïve mice were adoptively transferred with  $5 \times 10^4$  naive PbT-I cells and vaccinated with  $\alpha$ Clec9A-DIY and then left 14 days before challenge with  $10^3$  sporozoites. At the same time, naïve mice were injected with PbT-II Th1 or Th2 cells and challenged one day post transfer. As seen in Figure 5.1B no differences in liver parasite burden could be detected between untreated naïve mice and mice vaccinated

with  $\alpha$ Clec9A-DIY or injected with PbT-II Th1 or Th2 cells. This finding further supported the view that PbT-II cells were not able to eliminate sporozoite infected hepatocytes.

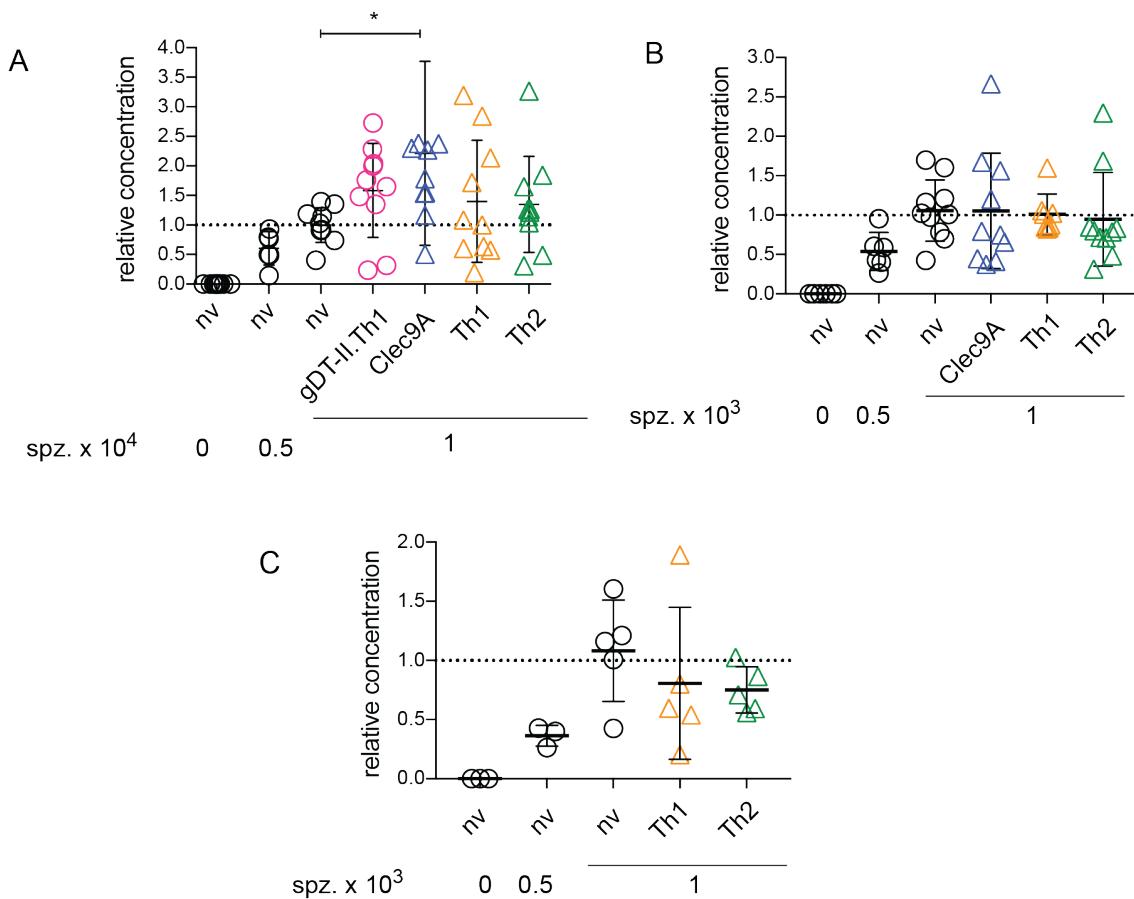


**Figure 5.1. Hsp90-specific CD4 T response to sporozoite infection as determined by liver-parasite burden.**

Protective capacity of  $\alpha$ Clec9A-DIY vaccination or *in vitro* differentiated Th1 or Th2 Hsp90-specific PbT-II CD4 T cells against PbA sporozoite infection. **A-C.** Mice received  $5 \times 10^4$  PbT-II cells and were vaccinated with  $2 \mu\text{g}$   $\alpha$ Clec9A-DIY and 5 nmol CpG one day later or received  $2 \times 10^6$  (**B**) or  $10^7$  (**A, C**) *in vitro* activated Th1 or Th2 polarised PbT-II cells or gDT-II (**C**) cells.  $\alpha$ Clec9A-DIY vaccinated mice were challenged with  $10^3$  (**B, C**) or  $10^4$  (**D**) sporozoites, 14 (**B, C**) or 35 (**A**) days post-vaccination. Mice that received *in vitro* activated cells were challenged with  $10^3$  (**B, C**) or  $10^4$  (**A**) sporozoites, one (**B, C**) or 35 (**A**) days post cell transfer. Livers were harvested 42-43 h post infection. **A, C.** Data were pooled from two independent experiments with a total of 8-10 mice per group. **B.** One experiment with a total of 5 mice per group. Data was normalized to naïve mice infected with  $10^3$  (**B, C**) or  $10^4$  (**A**) sporozoites. Relative concentration based on the mean of spz infected livers of untreated mice. Statistical comparison performed Kruskal-

Wallis test followed by Dunn's multiple comparison test. \*, $P < 0.05$ ; \*\*, $P < 0.01$ ; \*\*\*, $P < 0.001$ ; \*\*\*\*,  $P < 0.0001$ ; n.s., not significant.

Again, we reasoned that PbT-II cell numbers in this experiment may still be too low to significantly eliminate liver stage parasites. Therefore,  $10^7$  instead of  $2 \times 10^6$  *in vitro* differentiated PbT-II Th1 or Th2 cells were injected one day prior to sporozoite challenge. However, as seen in Figure 5.1C the transfer of  $10^7$  Th1 or Th2 PbT-II cells still did not significantly reduce liver-parasite burden (Figure 5.1C). This suggested two main possibilities: either effector CD4 T cells cannot mediate protection regardless of their specificity or the Hsp90-epitope, recognised by PbT-II cells, is not a good target for control of liver-stage parasites. It has to be noted, though, that not all possible differentiation phenotypes e.g. Th17, could be tested.

While PbT-II cells were not able to eliminate parasites in the liver, they responded to RAS vaccination by proliferation and therefore might be able to sense sporozoite infection and, or the damage that was mediated by infiltrating parasites (Figure 3.3)(Fernandez-Ruiz et al., 2017). To assess this possibility, we undertook live imaging analyses of PbT-II cells in the liver. tdTomato mice, which expressed a red fluorescence protein in the membrane of all cells, were vaccinated with  $\alpha$ Clec9A-DIY one day after the transfer of naïve PbT-II cells expressing green fluorescence protein (GFP). 14 days later, mice were challenged with  $1.5 \times 10^4$  spz and 2-photon intravital imaging was performed on the liver 24 to 48 h later (Figure 5.2, Appendix Video 8.2). As described in a previous chapter (Chapter 3.2), three distinct PbT-II cell phenotypes could be observed, i.e. patrolling cells, cells that flowed through the liver sinusoids, and cells that did not move over the period of imaging. Imaging of infected mice at 24 h post-challenge showed that PbT-II cells formed clusters inside the liver tissue, which were not observed in unchallenged mice or at 48 h post infection (Figure 5.2A-C, Appendix Video 8.3). Sporozoite challenge resulted in a decrease in the velocity of PbT-II cells after 24 h (Figure 5.2D). Similar proportions of patrolling

PbT-II cells were found in challenged mice, compared to unchallenged controls, or to mice imaged 48 h post challenge (Figure 5.2E). Thus, cluster formation occurs around 24 h post-infection but is short-lived, as no clusters were observed 48 h post-infection. Formation of clusters, potentially as a consequence of antigen recognition in the liver, was consistent with a previous report demonstrating the capacity of PbT-II cells to proliferate in response to RAS vaccination (Fernandez-Ruiz et al., 2017).

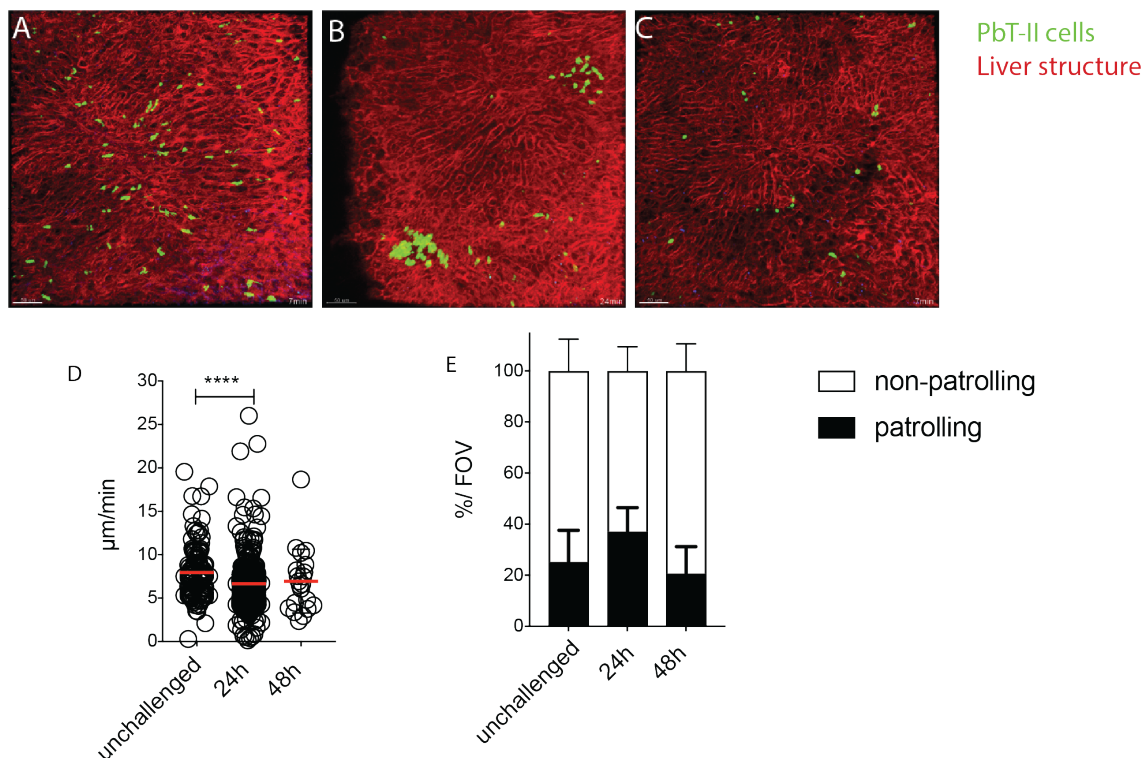


**Figure 5.2 PbT-II cells form clusters 24 h after sporozoite challenge.** 2-Photon intravital liver imaging after  $\alpha$ Clec9A-DIY vaccination. TdTomato mice received  $5 \times 10^4$  PbT-II.uGFP cells and were vaccinated with  $2 \mu\text{g}$   $\alpha$ Clec9A-DIY +  $5 \text{ nmol}$  CpG. 14 days later mice were either left uninfected (**A**) or challenged with  $1.5 \times 10^4$  sporozoites (**B**, **C**). At approximately 24 h (**B**) and 48 h (**C**) post sporozoite infection, surgery was performed to gain access to the liver and 2-photon intravital imaging was performed. **A-C**. Representative single frames from intravital imaging of PbT-II cells (green) within the liver structure (red). **D**. Mean velocity of individual PbT-II cells. **E**. Proportion of patrolling and non-patrolling PbT-II cells in the liver per field of view. Data was pooled from 3 independent experiments with a total of 6 mice per group and 2 - 3 movies per mouse. Statistical comparison performed Kruskal-Wallis test followed by Dunn's multiple comparison test. \*,  $P < 0.05$ ; \*\*,  $P < 0.01$ ; \*\*\*,  $P < 0.001$ ; \*\*\*\*,  $P < 0.0001$ ; n.s., not significant.

Like PbT-II cells, CD8 T cells have been reported to form clusters in the liver after sporozoite infection (Akbari et al., 2018). However, antigen specific and non-specific CD8 T cells were found in these clusters. Therefore, the formation of PbT-II cell clusters in the liver after sporozoite challenge could potentially be driven independently of antigen. The inability of PbT-II cells to reduce liver-parasite burden supports this concept. To determine whether the observed cluster formation was antigen-specific, mice received non-malaria specific gDT-II.GFP cells (specific for HSV-1 glycoprotein D) and were vaccinated with  $\alpha$ Clec9A-D3 (carrying the gDT-II restricted epitope), one day later. After 14 days, mice were challenged with sporozoites, and gDT-II cluster formation was investigated by 2-photon intravital imaging at 24 h post challenge (Figure 5.3). While no clusters were found in unchallenged mice, infected mice showed gDT-II cell clusters 24 h after sporozoite inoculation, indicating that cluster formation could occur independently of antigen recognition (Figure 5.3A, B, Appendix Video 8.4, Appendix 8.5). KC are liver resident macrophages described as a potential first entry point for sporozoites (Frevert et al., 2006). As it is well described that CD4 T cells interact with macrophages during a *Plasmodium* blood-stage infection, it was important to determine whether this also occurred during liver-stage infection (Fontana et al., 2016, Su and Stevenson, 2000, Shear et al., 1989). In addition, CD11c<sup>+</sup> cells in the liver, which represent subpopulations of KCs and dendritic cells, have been described to be crucial for the formation of CD8 T cell clusters in the liver after sporozoite infection (Akbari et al., 2018). As a first approach in order to image macrophage interactions with CD4 T cells, LysM.GFP mice were injected with PbT-II.ubTomato cells and vaccinated with  $\alpha$ Clec9A-DIY. LysM.GFP mice express GFP under the Lysozyme M promoter, which is mainly active in macrophages and neutrophils within the liver. 24 h after sporozoite challenge 2-photon intravital imaging revealed cluster formation of LysM<sup>+</sup> cells, similar to that observed for PbT-II cells in the liver (Figure 5.3C,D, Appendix Video 8.6, Appendix 8.7). However, no PbT-II.ubTomato cells could be found, which suggested that these cells were rejected by the LysM.GFP recipients. Thus, no conclusion could be drawn about co-clustering of CD4 T cells and macrophages in this setting. To resolve this question, a different approach

was undertaken and histological analyses of PbT-II cells and F4/80<sup>+</sup> cells were performed on livers of B6 mice that had been  $\alpha$ Clec9A-DIY vaccinated and sporozoite challenged 24 h or 36 h before organs were harvested. F4/80 is a well-defined marker for KC. As seen in Figure 5.3E, PbT-II cells in the liver co-clustered with F4/80 expressing cells after sporozoite challenge, indicating that PbT-II cells co-clustered with macrophages after sporozoite challenge. Furthermore, DAPI staining in liver tissue 36 h post-infection revealed an accumulation of cell nuclei within close distance to the PbT-II cell cluster. This suggests that in addition to PbT-II cells and KCs, other cell types were also included in these clusters. It should be noted, that no images of naïve mice were taken, as no clustering in those mice could be observed.

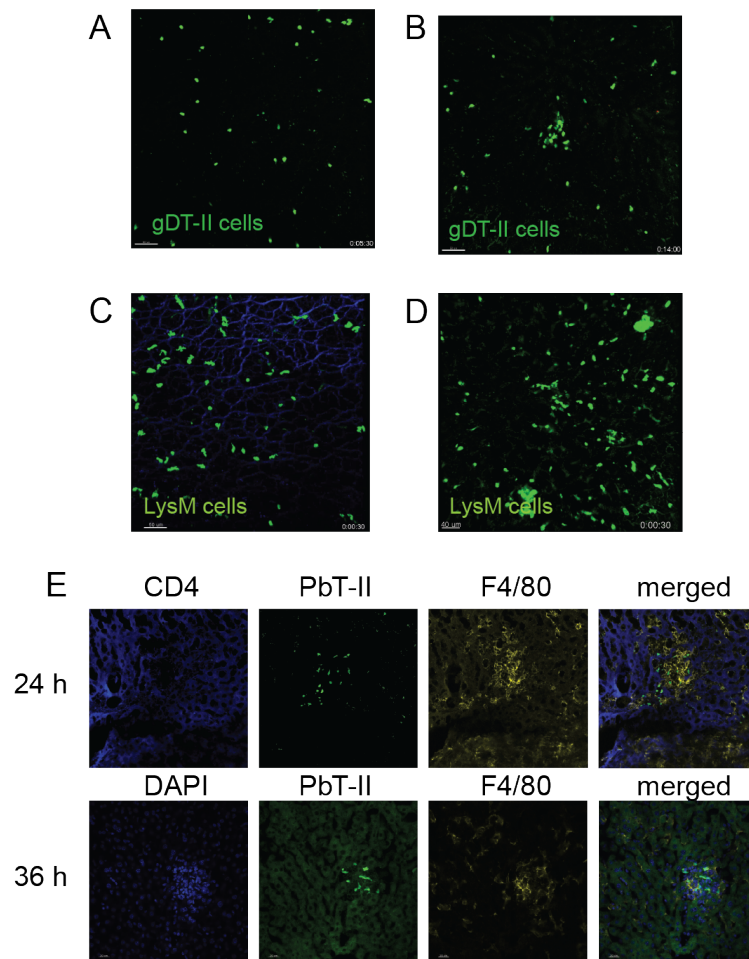


**Figure 5.3. Clustering can occur non-specifically and can involve macrophages.**

**A, B.** Mice received  $5 \times 10^4$  gDT-II.uGFP cells and were vaccinated with  $2 \mu\text{g}$   $\alpha\text{Clec9A-D3}$  +  $5 \text{ nmol}$  CpG. 14 days later, mice were either left uninfected (**A**) or challenged with  $10^4$  sporozoites (**B**). 24 h (**B**) after sporozoite infection, mice underwent surgery to gain access to the liver and 2-photon intravital imaging was performed. **C, D.** LysM.GFP mice received  $5 \times 10^4$  PbT-II.ubTomato cells and were vaccinated with  $2 \mu\text{g}$   $\alpha\text{Clec9A-DIY}$  +  $5 \text{ nmol}$  CpG one day later. 14 days later, mice were challenged with  $10^4$  sporozoites (**D**) or left unchallenged (**C**). 24 h later LysM.GFP mice underwent surgery to gain access to the liver and 2-photon intravital imaging was performed. Data represent one single experiment with 2 mice per group. **D.** B6 mice received  $5 \times 10^4$  PbT-II.uGFP cells and were vaccinated with  $2 \mu\text{g}$   $\alpha\text{Clec9A-DIY}$  +  $5 \text{ nmol}$  CpG. 14 days later, mice were challenged with  $10^4$  sporozoites. 24 h (upper panel) or 36 h (lower panel) post sporozoite infection, livers were harvested and prepared for histology analysis. Data represent a single experiment with 2 mice per group.

So far, it has been shown that PbT-II cells form clusters in the liver within 24 h of sporozoite challenge, however, they cannot protect against *Plasmodium* liver-stage infection. It is possible that the protein recognised by PbT-II cells, i.e. Hsp90, is sequestered in the vacuole formed by the parasite inside the hepatocyte or is insufficiently expressed for efficient presentation on the cell surface of infected hepatocytes or by local APC, which could explain the lack of protection mediated by PbT-II cells. This does not mean that all CD4 T cells would fail to mediate protection. Potentially, CD4 T cells of different specificities that recognise *Plasmodium*-derived epitopes that are highly expressed or more efficiently presented during the liver-stage, may mediate protection against sporozoite infection. It was therefore important to address this possibility. While no other *Plasmodium* derived MHC-II restricted epitopes for liver-stage infection were available to investigate, this question could be addressed using *Plasmodium* parasites expressing the model antigen OVA. In a first set of experiments, OT-II cells, specific for OVA, were *in vitro* differentiated into Th1 cells and  $5 \times 10^6$  cells were injected into mice one day prior to challenge. Mice were then either challenged with sporozoites expressing OVA (spz.OVA) or with WT sporozoites (spz.WT), not recognised by OT-II cells and thus serving as a negative control. Analysis of the liver parasite burden 42 h post-infection showed no differences between mice infected with spz.WT or spz.OVA in the presence of OVA-specific CD4 T cells (Figure 5.4A, B). While this suggested that specific CD4 T cells might not be protective, it was possible that larger numbers of OT-II cells were required to reduce parasite burden in the liver. Therefore,  $10^7$  naïve OT-II cells or *in vitro* activated OT-II Th1 or Th2 cells were injected into mice 3 days before challenge. In addition, as a positive control for protection, one group of mice was vaccinated with  $5 \times 10^4$  RAS, 7 days before sporozoite challenge. As one dose of RAS is known to induce only partial protection against liver-stage infection, this vaccination approach was used to determine if partial liver-stage protection could be detected with this system (Figure 5.4C, D). As seen in Figure 5.4D, RAS vaccinated or mice injected with OT-II Th1 or Th2 cells, but not naïve OT-II cells, showed reduced liver parasite burdens (Figure 5.4D). However, only

OT-II Th1 differentiated cells achieved a significant reduction in liver-parasite burden compared to naïve mice infected with spz.OVA. These results indicate that CD4 T cells are capable of decreasing the liver parasite burden. However, large numbers of these cells may be required to induce sterile-protection against sporozoite infection. These findings also suggest that the Hsp90 epitope recognised by PbT-II cells might not be an ideal target for elimination of *Plasmodium* infection of the liver and, therefore, might be unsuitable for liver-stage CD4 T cell-based vaccines.

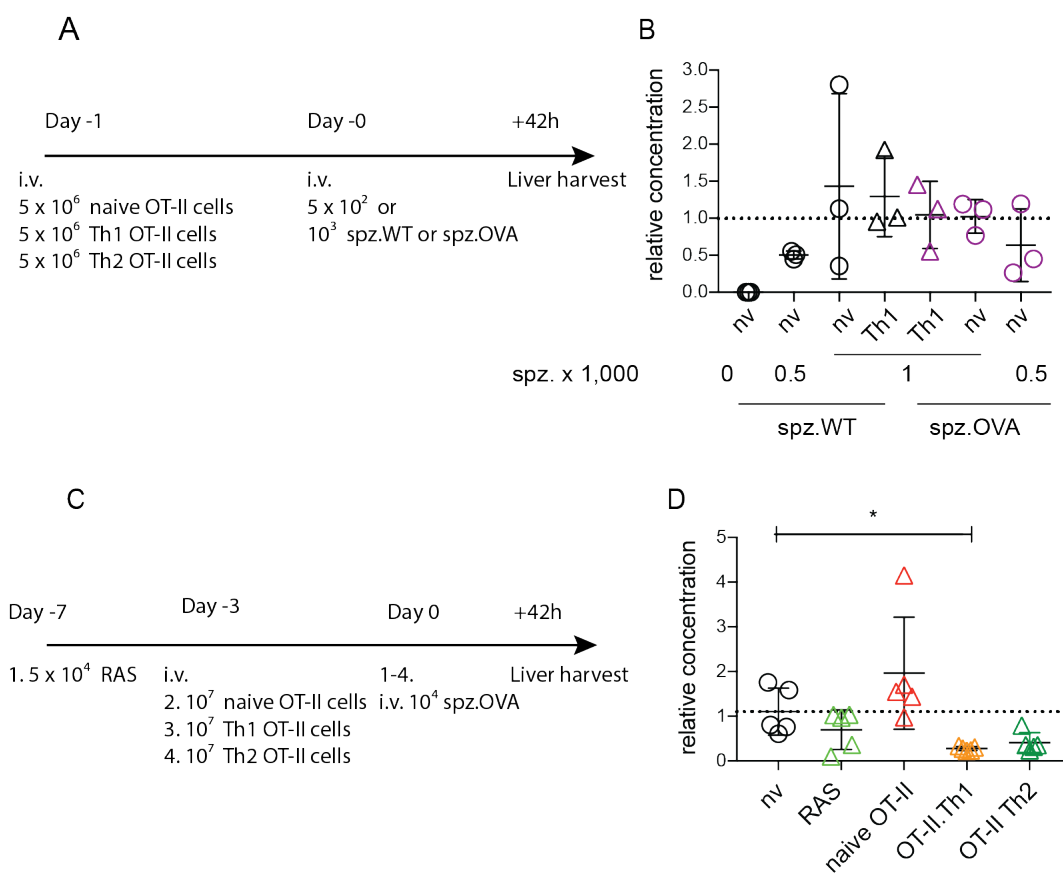


**Figure 5.4. OVA-specific CD4 T response to sporozoite infection determined by liver-parasite burden.**

Protective capacity of *in vitro* differentiated Th1, Th2 OT-II cells against PbA sporozoite infection. **A, C.** Experimental scheme.  $5 \times 10^6$  (**B**) or  $10^7$  (**D**) naïve or *in vitro* differentiated Th1 or Th2 OT-II cells were injected into mice. **B.** One day later, mice were challenged with  $5 \times 10^2$  or  $10^3$  wildtype (spz.WT) or OVA expressing (spz.OVA) sporozoites. **D.** Three-day post-transfer or 7 days post-vaccination with  $5 \times 10^4$  RAS, mice were challenged with  $10^4$  spz.OVA. Livers were harvest 42-43 h post sporozoite infection. Data represent a single

experiment with 3-5 mice per group. Data was normalized to the average of naïve mice challenged with  $10^3$  (B) or  $10^4$  (D) sporozoites. Relative concentration based on the mean of spz infected livers of untreated mice. Statistical comparison performed Kruskal-Wallis test followed by Dunn's multiple comparison test. \*, $P<0.05$ ; \*\*, $P<0.01$ ; \*\*\*,  $P<0.001$ ; \*\*\*\*,  $P<0.0001$ ; n.s., not significant.

### **5.2.2 Assessment of the protective capacity of Hsp90-specific CD4 T cells against *Plasmodium* blood-stage infection.**

As an alternative to a liver-stage vaccine, a CD4 T cell-based vaccine could also target the blood-stage of *Plasmodium* infection. Th1 cells are responsible for macrophage activation, which in turn can clear iRBCs (Su and Stevenson, 2000, Fontana et al., 2016). Furthermore, Tfh cells help B cells for their activation and antibody class switching, which are required for control of parasitaemia in the blood (Perez-Mazliah et al., 2017). While the protective function of CD4 T cells is better documented in the blood-stage than the liver-stage of infection, generating a blood-stage vaccine has other challenges as this stage is associated with pathology.

As seen in the previous section, PbT-II cells did not eliminate *Plasmodium* infected hepatocytes. However, the protective capacity of PbT-II cells in *Plasmodium* blood-stage infection was not dissected. To achieve this goal, naïve PbT-II cells or *in vitro* differentiated PbT-II Th1 or Th2 cells were injected into mice one day prior to challenge with PbA iRBCs. Injection of iRBCs bypasses the liver-stage and therefore differences in blood parasitaemia are directly related to the control of *Plasmodium* blood-stage infection. In all naïve mice, and mice that received naïve PbT-II, PbT-II Th1 or Th2 cells, iRBCs were detectable from day five post-infection (Figure 5.5A). However, mice injected either with PbT-II Th1 or Th2 cells had reduced parasitaemia compared to naïve mice or mice injected with naïve PbT-II cells. In addition, one mouse of the PbT-II Th2 cell injected group

did not develop ECM albeit high parasitaemia, while all other mice had to be euthanized between day 7 and 8 post-infection due to ECM (Figure 5.5B). This indicated that PbT-II cells can partially control PbA blood-stage infection and alter the development of malaria-associated pathology.

One possibility was that the protection seen above was due to release of cytokines from cells immediately upon transfer and that no real interaction with parasites was required. This was particularly concerning because mice were challenged with iRBCs only one day after transfer of Th cells. To determine if a longer interval could be left between transfer and challenge,  $10^7$  *in vitro* differentiated PbT-II Th1 or Th2 cells were injected into mice, which were then left 7 days before infection with  $10^4$  PbA iRBCs. Similar to the previous experiment, mice injected with either PbT-II Th1 or Th2 cells had reduced blood parasitaemia compared to naive mice (Figure 5.5C). Interestingly, Th1 and Th2 cells significantly reduced ECM development (Figure 5.5D). This shows that Hsp90-specific PbT-II CD4 T cells can reduce blood parasitaemia and the risk of ECM after blood-stage PbA infection.

As adoptive transfer of *in vitro* activated PbT-II cells could partially control parasitemia and reduce ECM rates, the next step was to investigate if a similar effect could be induced through vaccination. To address this question, mice were vaccinated with  $\alpha$ Clec9A-DIY one day after injection of naïve PbT-II cells. 14 days later, mice were challenged with  $10^4$  PbA iRBCs, and parasitaemia was evaluated from day five post-infection by flow cytometry analyses (Figure 5.5E, F). No differences in parasitemia or ECM were seen between vaccinated and naïve mice. Therefore,  $\alpha$ Clec9A-DIY vaccination was not effective at altering the course of a PbA blood-stage infection.

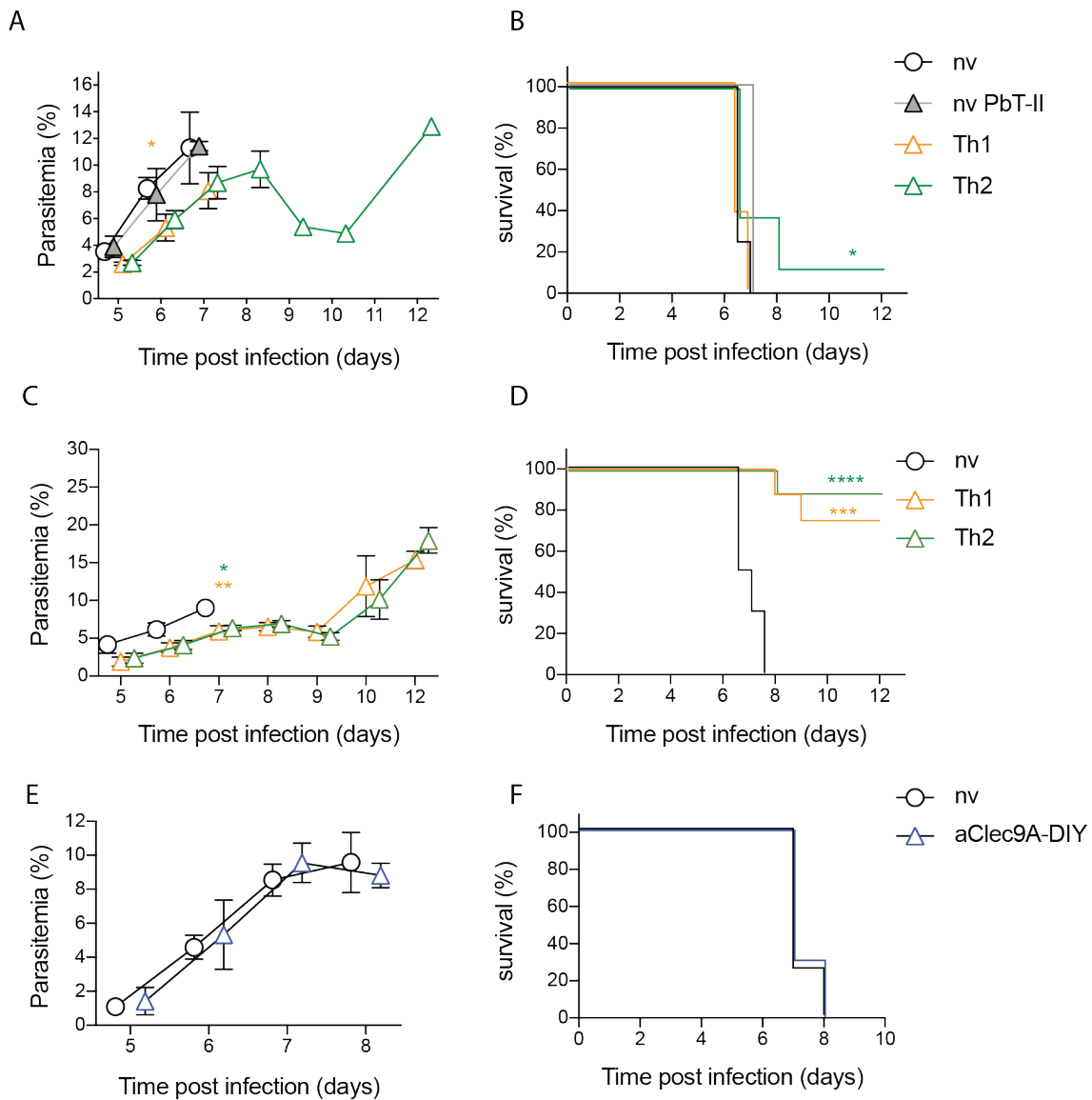


**Figure 5.5. Hsp90-specific CD4 T cells induce partial immunity to blood-stage PbA infection, and ECM protection at an effector stage.**

**A-D.** Protective capacity of *in vitro* differentiated Th1 or Th2 effector Hsp90-specific CD4 T cells against PbA blood-stage infection. Mice received  $2 \times 10^6$  (**A, B**) or  $10^7$  (**C, D**) *in vitro* activated Th1- or Th2-polarised PbT-II cells. One (**A, B**) or 7 (**C, D**) days later mice were infected with  $10^4$  PbA iRBC. **A, C.** Course of PbA parasitaemia. **B, D.** Survival. Data were pooled from 2 independent experiments with a total of 8-10 mice per group. **E, F.** Protective capacity of PbT-II cells after  $\alpha$ Clec9A-DIY vaccination. Mice received  $5 \times 10^4$  PbT-II.uGFP cells and were left untreated or vaccinated with  $2 \mu\text{g}$   $\alpha$ Clec9A-DIY + 5 nmol CpG one day later. 14 days later, mice were infected with  $10^4$  PbA iRBC. **E.** Course of PbA parasitaemia. **F.** Survival. Data were pooled from 2 independent experiments with a total of 20 mice per group. Statistical comparison performed Kruskal-Wallis test followed by Dunn's multiple comparison test. \*,  $P < 0.05$ ; \*\*,  $P < 0.01$ ; \*\*\*,  $P < 0.001$ ;

\*\*\*\*,  $P < 0.0001$ ; n.s., not significant. (**B, D, F**) Survival was analysed by performing pairwise comparisons between the different groups using log-rank.

The data generated so far were obtained using CD4 T cell effector phase T cells and therefore, the protective potential of memory T cells remained to be investigated. To assess this issue, mice were either adoptively transferred with naïve PbT-II cells and then vaccinated with  $\alpha$ Clec9A-DIY or injected with  $10^7$  *in vitro* differentiated PbT-II Th1 or Th2 cells. 35 days later, these mice were infected with 100 PbA iRBCs. As a control for antigen specificity, *Plasmodium* non-specific gDT-II Th1 cells were injected into an additional group of mice (Figure 5.6A). As seen in Figure 5.6B,  $\alpha$ Clec9A-DIY vaccination or transfer of PbT-II Th1 or Th2 cells reduced the blood parasite burden as early as day seven post-infection compared to naïve mice. In contrast, mice that received gDT-II Th1 cells had the same parasitaemia profile as naïve mice, which shows that the described reduction in parasitaemia in mice that received PbT-II cells was indeed antigen-specific. In contrast to the previous results using effector cells (Figure 5.5D), mice injected with *in vitro* differentiated PbT-II Th1 cells and left to form memory showed high ECM development (Figure 5.6C). However, Th2 PbT-II cells largely prevented ECM, suggesting these cells provide superior protection against ECM development than Th1 cells. Regarding  $\alpha$ Clec9A-DIY vaccination, most mice developed ECM (Figure 5.6C).

Mice primed with  $\alpha$ Clec9A-DIY or given *in vitro* polarized PbT-II cells showed reduced parasitaemia when challenged 35 days later. This prompted the question of how long memory cells may be protective. To address this question, mice were challenged with  $10^4$  PbA iRBCs 88 days post  $\alpha$ Clec9A-DIY vaccination or transfer of PbT-II Th1 or Th2 cells. In this case, neither  $\alpha$ Clec9A vaccinated mice nor those given PbT-II Th1 cells were able to significantly reduce parasitaemia compared to naïve mice or mice injected with gDT-II Th1 cells (Figure 5.6E, G). In contrast, mice that received PbT-II Th2 cells had significantly reduced parasite levels compared to naïve mice at various time points including day 7 post-infection (Figure 5.6E, G). In addition, none of the mice injected with

PbT-II Th2 cells developed any signs of ECM for at least 20 days, whereas  $\alpha$ Clec9A vaccination did not alter the onset of ECM symptoms and mice that received PbT-II Th1 cells showed a two day delay for ECM development (Figure 5.6F). In general, PbT-II Th2 memory cells were better at protecting mice against ECM development after PbA blood-stage infection than seen for  $\alpha$ CLec9A-DIY vaccination or PbT-II Th1 memory cells.

In summary, PbT-II cells are capable of modulating parasitaemia after PbA blood-stage infection but cannot fully control infection. While Hsp90-specific CD4 T cells prevented ECM in some mice, the reduced risk of developing pathology depended on the specific CD4 T cell activation method used. While PbT-II Th1 cells prevented ECM only in the effector phase after transfer of large numbers of cells, PbT-II Th2 polarized cells protected mice from ECM in both the effector and memory phases.

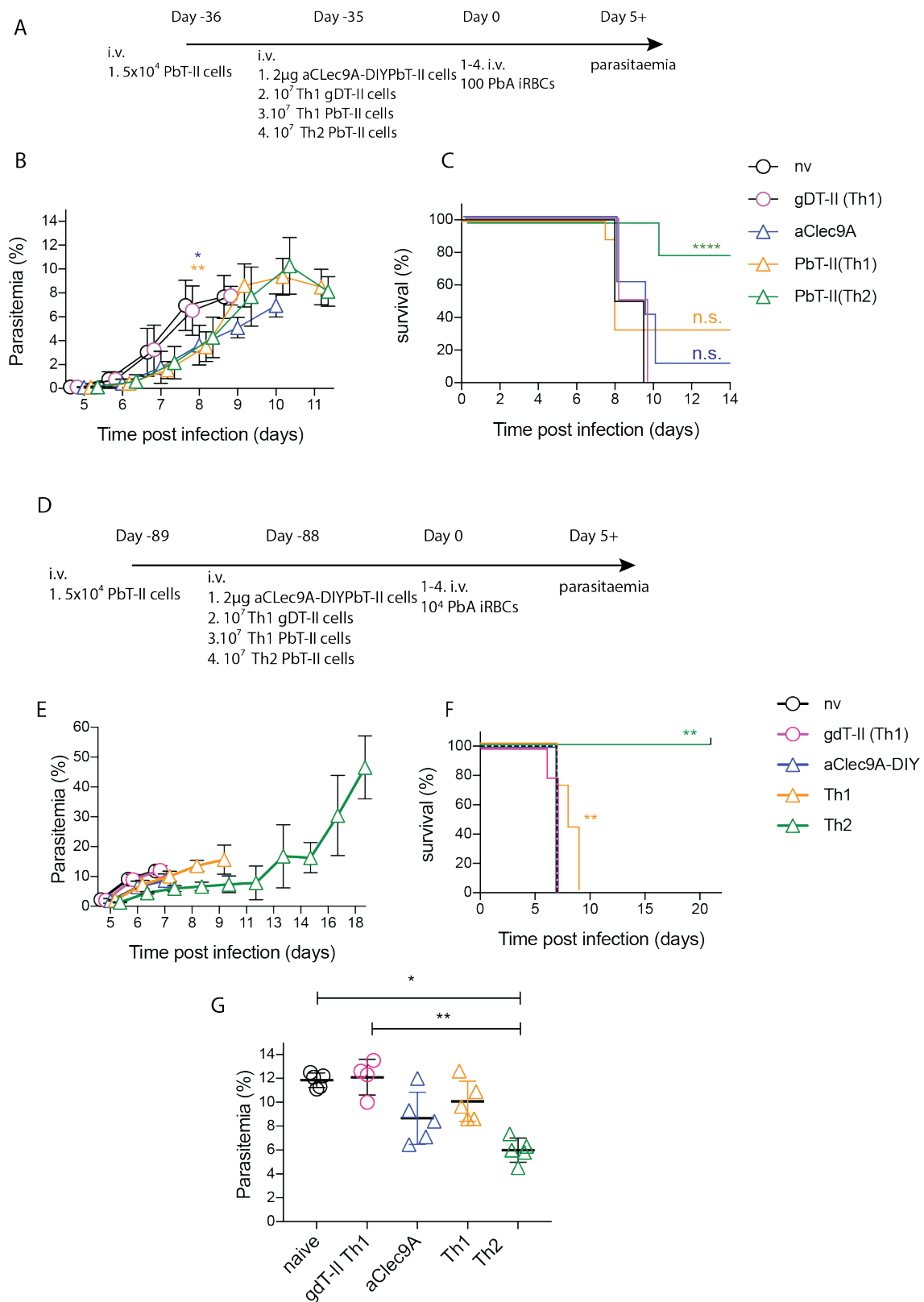


**Figure 5.6 Hsp90-specific PbT-II CD4 T cells induce partial immunity to blood stage PbA infection, and ECM protection at a memory stage.**

Protective capacity of  $\alpha$ Clec9A-DIY vaccinated or *in vitro* differentiated Th1 or Th2 Hsp90-specific PbT-II CD4 T cells on the course of PbA blood-stage infection. **A, D.** Experimental scheme. Mice received  $5 \times 10^4$  naïve PbT-II cells and one day later vaccinated with  $2 \mu\text{g}$   $\alpha$ Clec9A-DIY +  $5 \text{ nmol}$  CpG. Additional mice received  $10^7$  *in vitro* activated Th1- or Th2-polarised PbT-II cells or gDT-II Th1 cells. On day 35 (**B, C**) or 88 (**E-G**) post vaccination or cell transfer, mice were infected with 100 (**B, C**) or  $10^4$  (**C-G**) PbA iRBCs. **B, E.** Course of PbA parasitaemia. **C, F.** Survival. **G.** Parasitaemia at day 7 post infection. (**B, C**) Data were pooled from 2 independent experiments with total of 8-10 mice per group. (**E-G**) Data represents one experiment with 5 mice per group. Statistical comparison performed Kruskal-Wallis test followed by Dunn's multiple comparison test. \*,  $P < 0.05$ ; \*\*,  $P < 0.01$ ; \*\*\*,  $P < 0.001$ ; \*\*\*\*,  $P < 0.0001$ ; n.s., not significant. (**B, F**) Differences in survival between groups were analysed by performing pairwise comparisons using log-rank tests and adjusting for multiple comparisons by performing a Bonferroni correction for the total number of groups  $P < 0.01$ ; n.s.,  $P > 0.01$ ; \*\*\*\*,  $P < 0.0001$ .

So far, PbA parasites were used to investigate Hsp90-specific CD4 T cell responses. This *Plasmodium* species is lethal in B6 mice. As shown, in this acute infection model, PbT-II cells could partially reduce parasitemia and prevent ECM development in some mice. However, the role of CD4 T cells in chronic infection had not been examined. As chronic *Plasmodium* infections are described in humans repeatedly exposed to *Plasmodium* parasites, knowledge of whether Hsp90-specific PbT-II cells might control chronic infection was of interest. However, PbA infection is not an adequate model to study chronic *Plasmodium* infection, as B6 mice develop ECM within one week post infection (Hansen et al., 2003). To examine the protective value of PbT-II cells in a chronic model, Pch parasites were used, as this infection is characterised by a high peak of parasitaemia at around day 10 and a lower second peak between day 20 and 25 (van der Heyde et al., 1997). Low levels of iRBCs can be found up to approximately day 30 when infection is eventually cleared. In a previous study, the transfer of naïve PbT-II cells into CD40L<sup>-/-</sup> mice, which are susceptible to Pch infection, could prevent lethality (Fernandez-Ruiz et al., 2017). Here, we wanted to investigate if activated PbT-II Th1 cells can, firstly, rescue CD40L<sup>-/-</sup> mice from lethality and, secondly, reduce parasitaemia, similar to that observed in the PbA infection model. To investigate these questions, naïve PbT-II or *in vitro*

differentiated PbT-II Th1 cells were injected into CD40L<sup>-/-</sup> mice. 7 days later, these mice were challenged with 10<sup>3</sup> Pch iRBCs and monitored for parasitaemia from day six onwards. In agreement with published results, CD40L<sup>-/-</sup> mice that received naïve PbT-II cells could control Pch blood-stage infection while naïve CD40L<sup>-/-</sup> mice had to be euthanized due to severe body condition e.g. unresponsiveness to external stimuli around day 18 (Figure 5.7B) (Fernandez-Ruiz et al., 2017). As expected, PbT-II Th1 cells also protected CD40L<sup>-/-</sup> mice from death (Figure 5.7B). No significant differences in parasitaemia were observed between mice injected with naïve or Th1 PbT-II cells up to day 18, even though parasite levels seemed to decline slightly faster in mice injected with PbT-II Th1 cells in the following days (Figure 5.7A). Thus, pre-activated PbT-II cells did not have an advantage compared to naïve PbT-II cells in protecting CD40L<sup>-/-</sup> mice against Pch infection at the peak of infection.

The next step was to investigate the potential of PbT-II cells to reduce parasitemia in WT B6 mice, which can naturally control Pch blood-stage infection within about 30 days of infection. To address this question, mice were vaccinated with  $\alpha$ Clec9A-DIY or injected with either naïve PbT-II cells or *in vitro* differentiated PbT-II Th1 or Th2 cells. Also, one group of mice received PbT-II Th0 cells, which are *in vitro* activated cells that have not been exposed to further differentiation reagents. 7 days later, mice were infected with 10<sup>3</sup> Pch iRBCs, and parasitaemia was determined by flow-cytometry from 6 days post-infection. As seen in Figure 5.7C, all mice developed a peak of parasitaemia at around day 10-11. A smaller second peak was observed between days 20 and 24 (Figure 5.7C). A closer look at the difference in the first peak of parasitaemia (Figure 5.7D) revealed that mice that were vaccinated with  $\alpha$ Clec9A-DIY or received *in vitro* activated PbT-II cells had slightly reduced parasitaemia between days 10 and 14. However, only mice that received *in vitro* activated PbT-II Th2 cells or were vaccinated with  $\alpha$ Clec9A-DIY achieved significant reductions of the parasite burden between days 10 and 13, compared to naïve mice (Figure 5.7D). Nevertheless, the reduction was relatively small and did not change the overall course of Pch infection. These data suggest that Hsp90 may be a relatively poor target antigen for vaccines designed

to prevent blood-stage infection with Pch. It should be noted that only one experiment for the PbT-II Th2 experiment was performed and this therefore requires repeating. Furthermore, some mice infected with Pch iRBCs displayed such severe symptoms at the peak of parasitaemia or shortly after, that those mice had to be euthanised (Figure 5.7E). In contrast, none of the mice vaccinated with  $\alpha$ Clec9A-DIY or injected with Th2 cells prior to infection had to be euthanised. This supports the idea that reduced parasitaemia at the peak of the infection observed in those mice reduced disease severity in general.

In summary, the results presented in this chapter revealed that CD4 T cells specific for Hsp90 could reduce blood-parasite burden after PbA and Pch infection.  $\alpha$ Clec9A-DIY vaccination only had a limited ability to reduce PbA parasitaemia. *In vitro* differentiated PbT-II Th1 and Th2 cells could reduce PbA parasitaemia in both the effector and memory phases but could not fully control the establishment of *Plasmodium* blood-stage infection. Surprisingly, Th1 and even more so Th2 PbT-II cells significantly reduced ECM rates in B6 mice after PbA infection. Targeting exclusively CD4 T cells might not be an ideal strategy that induces a response capable of controlling *Plasmodium* blood-stage infection. However, the protection observed here against ECM development after transfer of PbT-II Th1 and Th2 cells should be further investigated and Hsp90 specific CD4 T cells are an ideal tool to identify the underlying mechanisms.

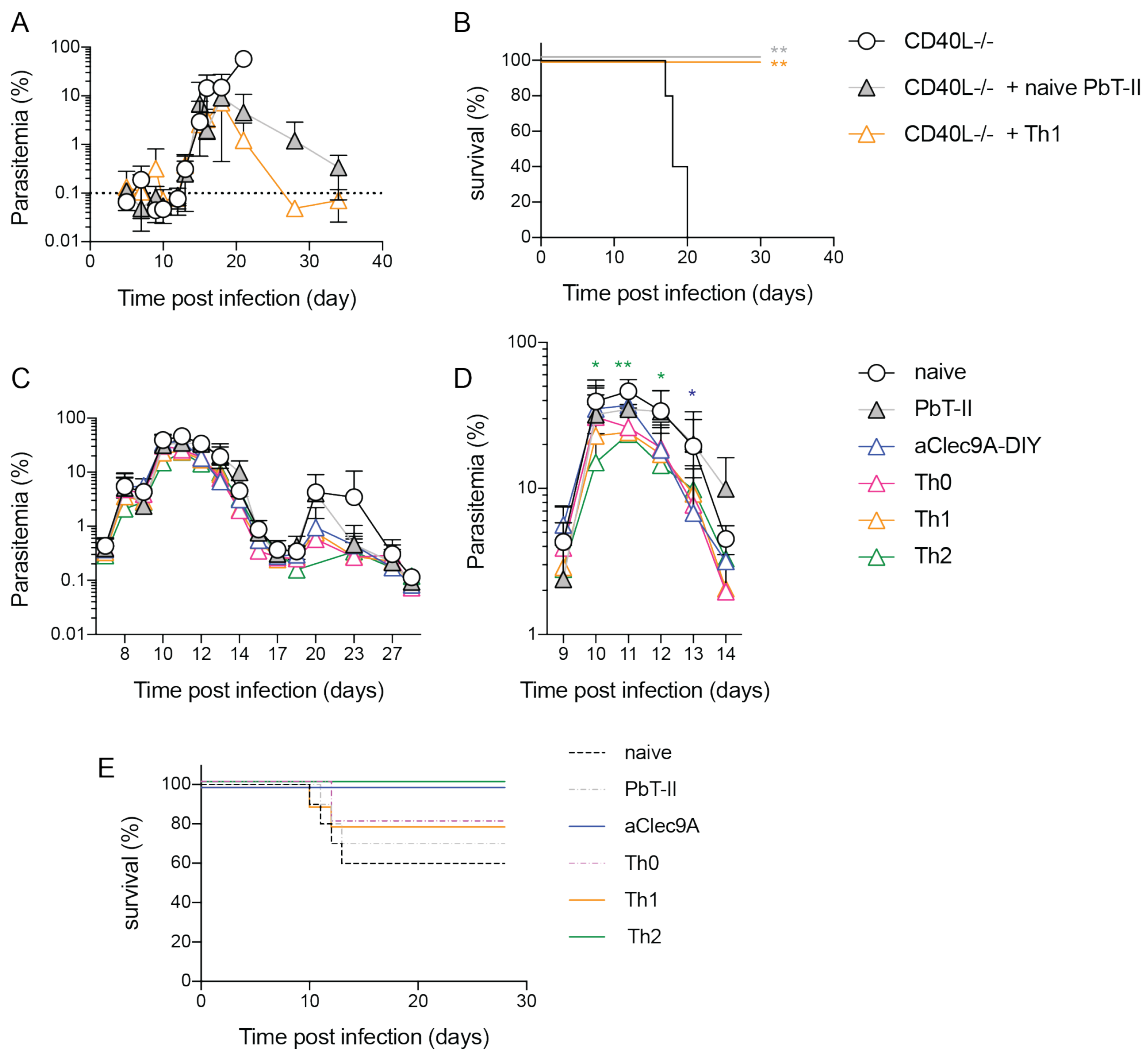


**Figure 5.7 Protective capacity of PbT-II cells on blood-stage Pch infection.** (A-B) CD40L<sup>-/-</sup> mice received  $2 \times 10^6$  *in vitro* activated, Th1- polarised or naïve PbT-II cells. 7 days later mice were challenged with  $10^3$  Pch iRBCs. (C-E) Mice received  $2 \times 10^6$  *in vitro* activated, Th1- or Th2-differentiated PbT-II cells, or  $5 \times 10^4$  PbT-II.uGFP cells and were left untreated or vaccinated with  $2 \mu\text{g}$   $\alpha\text{Clec9A-DIY}$  and  $5 \text{ nmol}$  CpG one day later. 7 days later, mice were infected with  $10^3$  Pch iRBC. **A,C.** Complete course of parasitaemia. **B.** Survival of CD40L<sup>-/-</sup> mice. **D.** Detailed representation of the first peak of Pch parasitaemia. **E.** Survival of B6 mice (**A, B**) Data represents one experiment with 5 mice per group. Statistical comparison performed Kruskal-Wallis test followed by Dunn's multiple comparison test. \*,  $P < 0.05$ ; \*\*,  $P < 0.01$ ; \*\*\*,  $P < 0.001$ ; \*\*\*\*,  $P < 0.0001$ ; n.s., not significant. (C-E) Data represents two independent experiments with 10 mice per group. Th2 group represent one experiment with 5 mice per group. (**A, D**) Statistical comparison performed Kruskal-Wallis test followed by Dunn's multiple comparison test. \*,  $P < 0.05$ ; \*\*,  $P < 0.01$ ; \*\*\*,  $P < 0.001$ ; \*\*\*\*,  $P < 0.0001$ ; n.s., not significant. (**B, E**) Differences in survival between groups were analysed by performing pairwise comparisons using log-rank tests and adjusting for multiple

comparisons by performing a Bonferroni correction for the total number of groups  
 $P < 0.01$ ; n.s.,  $P > 0.01$ ; \*\*\*,  $P < 0.0001$ .

### 5.3 Discussion

CD4 T cells are essential mediators of immunity against *Plasmodium* liver and blood-stage infection (Oliveira et al., 2008, Tsuji et al., 1990, Su and Stevenson, 2000, Perez-Mazliah et al., 2017, Oakley et al., 2013). However, their protective function has traditionally been considered indirect, mainly by providing help to DCs to induce efficient CD8 T cell activation, and to B cells to induce antibody class-switching (Carvalho et al., 2002, Perez-Mazliah et al., 2017, Langhorne, 1989). Current literature suggested that CD4 T cells can also directly mediate protection against *Plasmodium* liver-stage infection (Oliveira et al., 2008, Tsuji et al., 1990). Furthermore, a direct role for CD4 T cells in mediating protection against blood-stage infection after vaccination was shown (Xu et al., 2000, Pinzon-Charry et al., 2010, Pombo et al., 2002). However, less is known about their potential to mediate protection upon vaccination against the liver stage of infection. Here, we investigated the role of Hsp90-specific CD4 T cells in protection against *Plasmodium* liver and blood-stage infection after  $\alpha$ Clec9A-DIY vaccination. In addition, the protective capacities of Th1 and Th2 lineages were investigated by transfer of *in vitro* polarized PbT-II cells.

The use of transgenic PbT-II cells expressing GFP enabled us to investigate the behaviour of *Plasmodium*-specific CD4 T cells in the liver upon sporozoite challenge. Previous reports have revealed clustering of antigen-specific CD8 T cells in the liver around sporozoite infected hepatocytes (Cockburn et al., 2013, Kimura et al., 2013). Similar clustering was observed using PbT-II cells after  $\alpha$ Clec9A-DIY vaccination and sporozoite challenge (Figure 5.2). To determine whether these clusters were driven by specific antigen recognition, we tested cluster formation by gDT-II cells, unable to respond to malaria antigens, in the same system. gDT-II cells were found to co-cluster with PbT-II cells 24h post sporozoite infection. This is in line with a study by Akbari et al., where CD8 T cells of two specificities, i.e. a sporozoite epitope and an

irrelevant epitope, formed cell clusters around sporozoite infected hepatocytes (Akbari et al., 2018).

CD8 T cells not specific for *Plasmodium* were only recruited into the cell clusters in the presence of CD8 T cells specific to a *Plasmodium* epitope. In contrast, in the experiments presented here studying CD4 T cell responses, gDT-II cells clustered even in the absence of antigen-specific PbT-II cells. This indicated that CD4 T cell clustering in the liver upon sporozoite infection was driven in an antigen-independent manner. This result is likely due to the inflammatory environment elicited by sporozoite infection in the liver. Upon sporozoite encounter, infected hepatocytes can activate the MDA5 pathway resulting in the phosphorylation of transcription factor IRF3 and dimerization with IRF7, which finally results in the release of different chemokines, including CXCL10 (Liehl et al., 2014). As a result, cells expressing the corresponding chemokine receptors, e.g. CXCR3, can be recruited along a chemokine gradient in an antigen-independent manner. CXCR3 is known to be expressed by a variety of immune cells, including activated T cells (Groom and Luster, 2011). Thus, CXCR3<sup>+</sup> PbT-II and gDT-II cells might have been recruited around infected hepatocytes along a CXCL10 gradient and potentially through additional chemokines released by infected hepatocytes, all independent of antigen recognition.

Although CD4 T cell clustering seems to, at least in part, be driven independently of antigen, there is still the potential that PbT-II cell clustering in the liver after sporozoite challenge might also be promoted by antigen, as previously shown for CD8 T cells (Akbari et al., 2018). This antigen-dependent recruitment might have been promoted by CD11c<sup>+</sup> dendritic cells or macrophages. CD11c<sup>+</sup> cells were shown to contribute to the formation of *Plasmodium*-specific and non-specific CD8 T cell clusters after sporozoite infection. In the liver, CD11c<sup>+</sup> cells are mostly CD11c<sup>+</sup> F4/80<sup>-</sup> dendritic cells and CD11c<sup>+</sup> F4/80<sup>+</sup> KCs (David et al., 2016). PbT-II cells clustered around F4/80<sup>+</sup> cells, most likely KCs. KCs have been described as a potential portal for sporozoites to enter the liver parenchyma and infect hepatocytes (Baer et al.,

2007, Pradel and Frevert, 2001). KCs can express MHC-II molecules, and co-stimulatory molecules to support T cell proliferation and activation (Burgio et al., 1998). It is therefore possible that KC obtained parasite antigen (e.g. Hsp90) from traversing sporozoites or dying sporozoites and presented it to PbT-II cells to contribute to their recruitment, in an antigen-dependent manner. Also, a recent study showed the infiltration of CD11c<sup>+</sup>, CD11b<sup>int-hi</sup>, MHC-II<sup>+</sup>, F4/80<sup>+</sup> DCs into the liver tissue upon sporozoite infection (Kurup et al., 2019). These cells were found to capture sporozoites from dying hepatocytes and induce priming of *Plasmodium*-specific CD8 T cells (Kurup et al., 2019). These infiltrating CD11c<sup>+</sup> DCs expressed macrophage-associated markers such as F4/80 and CSF1R. It is, therefore, possible that the observed F4/80<sup>+</sup> cells inside a PbT-II cells cluster were not KCs but were these infiltrating cells, recruited to the liver after sporozoite infection. Perhaps, F4/80<sup>+</sup>, CSF1R<sup>+</sup>, CD11c<sup>+</sup> DCs captured sporozoites from apoptotic hepatocyte and presented the Hsp90-epitope via MHC-II molecules, which facilitated PbT-II cell clustering in the liver.

An important role for CD4 T cell-mediated immunity against the liver stage of *Plasmodium* infection in mice was demonstrated by repeated injection of large amounts of RAS (Doolan and Hoffman, 2000, Oliveira et al., 2008). While this induced a variety of CD4 T cell specificities potentially targeting infected hepatocytes, it was also shown that the transfer of CSP-specific CD4 T cells, obtained from RAS vaccinated BALB/c mice, conferred sterile protection to naïve BALB/c mice against challenge with 3 – 5 x 10<sup>3</sup> sporozoites (Tsuji et al., 1990). As a single CD4 T cell epitope specificity (CSP) induced sterile protection against *Plasmodium* sporozoite infection, we hypothesised that CD4 T cells specific for the MHC-II restricted epitope in PbA Hsp90 might be protective in B6 mice, too. However, targeting Hsp90-specific PbT-II cells with a  $\alpha$ Clec9A-DIY vaccination strategy did not lead to detectable protection against *Plasmodium* liver-stage infection. We hypothesised that this result could reflect insufficient generation of Th1 cells by  $\alpha$ Clec9A vaccination: in both experimental mouse studies and human RTS.S/AS02 vaccination studies, a correlation between IFN- $\gamma$  expressing CD4 T cells (hence Th1 cells) and protection was found (Reece et al., 2004, Tsuji

et al., 1990). While  $\alpha$ Clec9A vaccination induced Th1 cells, it also led to Tfh cell formation. It is thus possible that insufficient numbers of *Plasmodium-specific* Th1 T cells were induced by  $\alpha$ Clec9A-DIY immunisation (Lahoud et al., 2011). To investigate Th1 cell responses against sporozoite infection, *in vitro* polarization of PbT-II cells, which allowed for the generation of large numbers of pure Th1 cells, was performed to determine their protective capacity in a PbA sporozoite challenge model. However, the transfer of PbT-II Th1 cells did not alter the liver-parasite burden, suggesting that PbT-II Th1 cells are unable to eliminate sporozoite infected hepatocytes.

In addition to PbT-II Th1 cells, we also investigated the role of PbT-II Th2 cells against PbA liver-stage infection. So far, no correlation of Th2 cells in protection against sporozoite infection has been described in the literature. However, a previous study showed that IL-4 producing CD4 T cells (i.e. Th2 cells) were necessary to induce protective CD8 T cell responses after RAS vaccination, although they were not directly accountable for protection (Carvalho et al., 2002). In our experiments, PbT-II Th2 cells were not able to induce a detectable reduction of liver-parasite burden. The lack of PbT-II cell mediated protection against sporozoite infection, independent of the method of activation, suggested that Hsp90 might not represent an accessible liver-stage epitope. Hsp90 mRNA is expressed during the liver-stage of *Plasmodium* infection (Howick et al., 2019), however, compared to expression by the PbA ring form, Hsp90 is only expressed at an intermediate level at the liver stage. Furthermore, mRNA levels might not directly translate to Hsp90 protein levels expressed by the sporozoite. Hsp90 mRNA might be rapidly degraded before translation into peptide. Western blot analyses to determine the amount of the Hsp90 protein in the liver stage of *Plasmodium* infection could answer this question. Furthermore, sporozoites are encapsulated during the liver-stage in a parasitophorous vacuole, shielding the parasite from the host cells (Mota et al., 2001, Silvie et al., 2003). It is therefore possible, that the Hsp90 protein is also retained inside the parasite vacuole at the liver stage of infection and cannot be presented to CD4 T cells via MHC-II molecules by hepatocytes.

Based on these findings, we hypothesized that the PbT-II cell epitope was not presented efficiently enough during the liver stage of infection, leading to lack of protection. To address whether other antigens might be protective if presented to CD4 T cells during this stage, we examined protection with CD4 T cells of a different specificity. Indeed, the transfer of large numbers of OT-II Th1 or Th2 cells reduced the liver-parasite burden after infection with OVA expressing sporozoites, and this protection was similar to that seen after immunizing with one dose of RAS. This finding further supports the idea that the Hsp90 epitope is not a protective target antigen for the liver-stage of infection and might not be suitable as a liver-stage directed vaccine. However, the OT-II cell data in combination with a study that showed protection by transfer of CSP-specific CD4 T cells into BALB/c mice, demonstrates that at least partial protection against sporozoite infection can be achieved through CD4 T cell-mediated immunity (Tsuji et al., 1990). It should therefore be possible to generate protective CD4 T cells populations through vaccination, if more accessible MHC-II restricted epitopes can be identified. Thus, future research is required to identify additional MHC-II restricted epitopes that are protective against liver-stage *Plasmodium* infection.

CD4 T cells have been shown to be crucial for protective immunity against *Plasmodium* blood-stage infection (Oakley et al., 2013, Fontana et al., 2016). Thus, we wanted to investigate the protective potential of PbT-II cells at this stage of infection. Previous work has shown that injection of MSP-1 specific CD4 T cells (B5) promoted long-term survival in RAG1<sup>-/-</sup> mice after Pch infection (Stephens et al., 2005). Similar results were detected after transfer of naïve PbT-II cells in CD40L KO mice and RAG1 KO mice (Fernandez-Ruiz et al., 2016). Based on those results, we asked the question whether the presence of effector or memory PbT-II cells at the time of *Plasmodium* blood-stage infection could be protective.

In experimental PbA and Pch blood-stage infection models parasite-specific Th1 and Tfh CD4 T cell subpopulations are described to form early after infection (Lönnerberg et al., 2017, Fernandez-Ruiz et al., 2017). While Th1 cells have been shown to reduce PbA parasitaemia and contribute to the control of the

peak parasitaemia of an acute Pch infection, Tfh cells are crucial for the generation of efficient humoral responses enabling final clearance of Pch blood-stage parasites of persistent infection and non-lethal *P. yoelii* infections (Oakley et al., 2013, James et al., 2018, Perez-Mazliah et al., 2015, Perez-Mazliah et al., 2017, Wikenheiser et al., 2016). Therefore, Clec9A targeted vaccination, reflecting CD4 T cell lineages generated after blood-stage PbA and Pch infection (namely Th1 and Tfh), might be well suited to enhance protection against *Plasmodium* blood-stage infection (Lahoud et al., 2011, Fernandez-Ruiz et al., 2017, Lönnberg et al., 2017, Perez-Mazliah et al., 2015, Perez-Mazliah et al., 2017). However,  $\alpha$ Clec9A-DIY did not induce detectable reduction of PbA parasitaemia but did result in a moderate decrease of Pch parasitaemia (in the acute phase of infection) compared to unvaccinated control mice. This is seemingly in contrast to previous work showing that Th1 cells could mediate reduction of parasitaemia after PbA infection. However, Th1 cell numbers generated after  $\alpha$ Clec9A-DIY immunisation might simply be too low to mediate protection (Oakley et al., 2013). On the other hand, Pch parasite clearance in natural infection mainly correlates with efficient B cell activation and antibody production. (Perez-Mazliah et al., 2015, Perez-Mazliah et al., 2017). Therefore  $\alpha$ Clec9A-DIY generated Tfh cells might not have provided further help to B cell activation over the endogenous Tfh cells induced during the course of Pch infection. In addition,  $\alpha$ Clec9A-DIY vaccination was shown to induce CD4 T cells expressing higher levels of PD-1 compared to blood stage infection (Chapter 3). Previous work showed that PD-1 blockade can restrict parasite growth early after infection (Butler et al., 2011). Furthermore, a study found that PD-1 deficiency resulted in elevated malaria specific antibodies and better protection against blood-stage infection (Liu et al., 2015). This suggests that while Tfh cells and malaria-specific antibodies are crucial for protection against blood-stage infection, high PD-1 expression on CD4 T cells after  $\alpha$ Clec9A-DIY vaccination might hinder protective responses.

Next, *in vitro* polarization of PbT-II cells was used to evaluate the protective capacity of Th1 and Th2 PbT-II cell populations. Previous studies have

shown that the control of PbA and Pch infection correlated with IFN- $\gamma$  and TNF levels (Su and Stevenson, 2000, van der Heyde et al., 1997, Li and Langhorne, 2000). In line with these studies, the transfer of large numbers of Th1 cells, which expressed both cytokines, at least upon *in vitro* restimulation (Chapter 3), significantly reduced parasitaemia after PbA and moderately after Pch infection. Furthermore, the transfer of *in vitro* polarized PbT-II Th2 cells improved control of Pch parasitaemia and decreased PbA parasitaemia. While a protective role for Th2 cells in PbA infection is not documented, the relevance of Th2 cells in mediating parasitaemia control in Pch infection has been shown (Taylor-Robinson et al., 1993). Consistent with this observation, IL-4 KO mice developed a higher peak of parasitaemia and a prolonged chronic phase of infection than wild-type mice (von der Weid et al., 1994). At this stage it is not clear why and how Th2 cell protected mice better against PbA blood-stage infection compared to Th1 or  $\alpha$ Clec9A-DIY vaccination. Further research is required to investigate potential de-differentiation, cytokine milieu and cell numbers post blood-stage infection. However, during *in vitro* differentiation of PbT-II cells it could be observed that Th2 PbT-II cell proliferated more strongly compared to Th1 PbT-II cells upon activation. Thus, PbT-II Th2 memory cells might also have responded more strongly to PbA blood-stage infection, giving mice that received PbT-II Th2 cells the advantage to reduce of blood-stage parasite numbers early after infection. Additionally, it is possible that due to the strong Th1 bias upon PbA blood-stage infection (Chapter 3), a proportion of Th2 PbT-II cells de-differentiated into Th1 cells. This might result in a mixed population of IFN- $\gamma$  producing Th1 and IL-4, IL-13 producing Th2 cells. The existence of Th1 and Th2 cells in the early phase of *Plasmodium* blood-stage infection might then result in IFN- $\gamma$  and TNF activated macrophages, eliminating blood-stage parasites, and alternative activated macrophages, through IL-4 and IL-13, leading to the reduction of PbA blood-stage infection related pathology (Su and Stevenson, 2000; Fontana et al., 2016; Raes et al., 2007).

How is the clearance of iRBCs and therefore a reduction of parasitaemia mediated? T cells cannot directly recognise infected red blood cells, as mature

RBCs do not express MHC-I or MHC-II molecules. However, it is well documented that IFN- $\gamma$ , expressed by Th1 cells, activates macrophages to release reactive oxygen and nitrogen intermediates that result in the clearance of iRBCs (Jakobsen et al., 1995, Lutz et al., 1996, Su and Stevenson, 2000, Hoffman et al., 2002, Shear et al., 1989). While PbT-II Th1 cells are capable of secreting IFN- $\gamma$ , PbT-II Th2 cells do not express IFN- $\gamma$  (Chapter 3). However, TNF, also expressed by PbT-II Th2 cells (Chapter 3), has the potential to trigger reactive oxygen species synthesis in macrophages (Roca and Ramakrishnan, 2013). In addition, B cells and antibodies play a major role in the clearance of *Plasmodium* iRBCs. However, neither malaria specific B cells nor CD4 T cell are sufficient to clear a *Plasmodium* blood-stage infection on their own. For example, neither the transfer of B5 Tg cells or *Plasmodium* immune B cells into RAG<sup>-/-</sup> mice resulted in clearance of the infection (Stephens et al., 2005). Only the transfer of both cell types led to a fast resolution of the infection.

In B6 mice, PbA infection is accompanied by the development of lethal ECM and the role of CD4 T cells in the development of this severe symptom is not fully elucidated (Villegas-Mendez et al., 2012, Oakley et al., 2013, Haque et al., 2011b, Haque et al., 2014). Transfer of naïve PbT-II cells accelerated the onset of ECM after PbA infection in CD40L KO mice compared to CD40L KO mice that did not receive PbT-II cells, which indicated a pathology driving role of PbT-II cells (Fernandez-Ruiz et al., 2017). Furthermore, previous studies reported IFN- $\gamma$  producing CD4 T cells promote ECM by attracting CD8 T cells into the brain after PbA infection in B6 mice and Tbet<sup>-/-</sup> mice had a lower accumulation of CD4 and CD8 T cells in the brain and no ECM, despite reduced ability to control parasitaemia (Villegas-Mendez et al., 2012, Oakley et al., 2013). On the other hand, PbA infection of IFN $\alpha$ R<sup>-/-</sup> mice, which resulted in enhanced IFN- $\gamma$ <sup>+</sup>Tbet<sup>+</sup> CD4 T cells formation, did not lead to ECM development (Haque et al., 2011a, Haque et al., 2014). In contrast, here we found that the adoptive transfer of *in vitro* polarized PbT-II Th1 or Th2 cells did not aggravate but actually reduced the risk of ECM development. While the lack of IFN- $\gamma$  secretion by Th2 cells might explain the lack of ECM onset after transfer of PbT-II Th2 cells, it does not explain

why mice that received PbT-II Th1 cells did not develop ECM. Furthermore, in response to PbA blood-stage infection, endogenous CD4 and CD8 T cells will be activated and should in theory induce ECM, as observed in naïve mice (without Th1 and Th2 transfer). This suggests that PbT-II Th1 and Th2 might mediate regulatory functions after PbA blood-stage infection. One possible explanation is that PbT-II Th1 and Th2 cells could differentiate into T regulatory type 1 (Tr1) cells during PbA infection. Previous studies have shown that *P. yoellii* infection induced a type I interferon responses which led to secretion of IL-10 by DCs and resulted in further IL-10 secretion by CD4 T cells (Zander et al., 2016, Loevenich et al., 2017). Similar mechanisms might operate during PbA blood stage infection, which, inducing a regulatory phenotype in Th1 and Th2 cells. Indeed, it was demonstrated that Tr1 cells can directly derive from Th1 cells after Pch infection, while no such mechanisms are described for Th2 cells (Lönnberg et al., 2017). Tr1 cells are documented to suppress inflammatory cytokines including IFN- $\gamma$ , TNF, IL17 and IL-1 $\beta$  and Th1 and Th2 responses (Groux et al., 1997, Cottrez et al., 2000, Couper et al., 2008, Montes de Oca et al., 2016, Zander et al., 2016). Furthermore, IL-10 can directly inhibit CD8 T cells responses (Biswas et al., 2007). An inhibited inflammatory response and lower formation of *Plasmodium*-specific CD8 T cells could lead to a reduced accumulation of these cells in the brain which potentially preventing ECM development in these experiments. While this is still speculative, future work should investigate the cytokine profile of PbT-II Th1 and Th2 cells after PbA blood-stage infections and examine the existence of regulatory cytokine production by PbT-II cells.

Our results indicated that *Plasmodium*-specific Th2 cells might be the most suitable T cell subtype to protect against blood-stage *Plasmodium* infection and associated pathology. However, neither natural infection nor  $\alpha$ Clec9A-DIY immunisation induced Th2 CD4 T cells. Natural infection and  $\alpha$ Clec9A vaccination both favour Th1 and Tfh differentiation mostly via CD4 T cell priming by cDC1 (Fernandez-Ruiz et al., 2017, Lahoud et al., 2011). The transfer of *in vitro* activated and polarised PbT-II Th2 cells is so far the best strategy to study Hsp90-specific T helper cell responses to PbA infection. Targeting the Hsp90

epitope to cDC2, which favours Th2 cell differentiation, may enable a protective PbT-II Th2 population to be induced by vaccination (Sponaas et al., 2006, Kasahara and Clark, 2012).

# **Chapter 6**

## **General Discussion**

## Chapter 6: General Discussion

### 6.1 Context

Despite decades of effort, Malaria, caused by *Plasmodium* parasites, is still a global health burden with an estimated 409,000 (2019) deaths annually (WHO, WHO, 2019). Emerging drug or insecticide resistance of *Plasmodium* parasites and mosquitos, respectively, requires alternative methods to fight this disease. Efficient vaccination strategies, which provide sterile protection against *Plasmodium* infection will inevitably increase life expectancy and quality of individuals living in malaria endemic areas.

Current vaccine approaches, however, fail to provide long-lasting sterile immunity. A better understanding of the immune response induced by *Plasmodium* infection can potentially be used to improve current anti-malaria vaccine strategies or lead to the development of completely new approaches.

CD4 T cells are essential for a robust immune response against liver- or blood-stage malaria (Weiss et al., 1993, Fontana et al., 2016). However, tools to study *Plasmodium*-specific CD4 T cell immune responses are limited. Recently, our laboratory developed an MHC-II restricted TCR transgenic mouse line, termed PbT-II, that generates PbA reactive CD4 T cells (PbT-II cells) (Fernandez-Ruiz et al., 2017). PbT-II cells were also shown proliferate in response to *P. yoelii* 17XNL, *P. chabaudi* AS, *P. berghei* NK65 and *P. falciparum* iRBCs as well as to PbA RAS, indicating that these cells recognise an epitope conserved amongst different *Plasmodium* species and parasite stages. While the use of PbT-II T cells allowed for the study of CD4 T cell responses to *Plasmodium* infection, identification of the specific epitope recognised by these T cells would enable the study of the endogenous CD4 T cell response and the harnessing of these responses for the development of CD4 T cell-targeted vaccines.

## 6.2 Key findings

In chapter 3, the cognate antigen recognised by PbT-II cells was identified as Hsp90<sub>484-496</sub> (abbreviated as DIY). The identification of this epitope allowed us to deliver this specific antigen to CD8<sup>+</sup> DCs by targeting the Clec9A-receptor expressed primarily by cDC1 using a specific mAb fused to DIY. Administration of this  $\alpha$ Clec9A-DIY subunit vaccine induced PbT-II memory cell formation in the liver and spleen, exceeding memory formation observed after iRBCs infection or RAS vaccination. Furthermore,  $\alpha$ Clec9A-DIY vaccination induced endogenous Hsp90 reactive memory CD4 T cells in the liver and spleen. In addition, identification of the cognate antigen of PbT-II cells enabled us to establish an *in vitro* polarization protocol for the generation of large numbers of PbT-II Th1 and Th2 cells.

In chapter 4, we identified three different populations of memory CD4 T cells in the liver and spleen, which could be discriminated by their differential expression of CD69 and CD62L. CD69<sup>+</sup> cells in the liver resembled previously described CD69<sup>+</sup> CD8 memory T cells, which were demonstrated to be liver-resident (Fernandez-Ruiz et al., 2016). Therefore, we assessed the residency characteristics of CD69<sup>+</sup> PbT-II cells in the liver. Parabiosis experiments on RAS vaccinated mice confirmed that, unlike CD69<sup>-</sup> PbT-II T<sub>EM</sub> cells, which recirculated between parabionts, CD69<sup>+</sup> PbT-II cells were retained in the liver in which they originated and were thus resident (T<sub>RM</sub>). Furthermore, we identified PbT-II cells expressing similar surface markers to the RAS-generated PbT-II T<sub>RM</sub> cells after  $\alpha$ Clec9A-DIY immunisation or adoptive transfer of *in vitro* polarized PbT-II Th1 or Th2 cells. Further analysis revealed that these cells, independently of their activation method, were transcriptionally similar to RAS generated CD8 T<sub>RM</sub> cells in the liver and shared a transcriptional core signature expressed by liver resident immune cells (Mackay et al., 2016). We thus consider these cells to be T<sub>RM</sub> cells.

As it was previously shown that CD4 T<sub>RM</sub> cells in the lung promote CD8 T<sub>RM</sub> cell formation, we sought to define if this was also the case for *Plasmodium*

specific CD4 T<sub>RM</sub> cells in the liver (Son et al., 2021). This revealed that the presence of responding PbT-II cells during the priming phase of CD8 T cells did not result in the enhanced formation of *Plasmodium*-specific CD8 memory T cells after RAS or  $\alpha$ Clec9A immunisation.

In chapter 5, the protective capacity of PbT-II memory and effector T cells in response to PbA and Pch infection was investigated. While PbT-II cells formed clusters in the liver 24 h post sporozoite infection, neither effector nor memory PbT-II cells could reduce liver-parasite burden after PbA sporozoite infection. The factors driving cluster formation, and whether those clusters form in an antigen dependent manner, remain to be determined. In contrast to their failure to control the liver-stage of infection, *in vitro* polarized PbT-II Th1 and Th2 cells significantly reduced PbA parasitemia after blood-stage infection at an effector and memory time point. Moreover, mice that received high doses of PbT-II Th1 or Th2 cells were partially protected from ECM, although they could not fully control the infection. In contrast,  $\alpha$ Clec9A-DIY vaccination did not significantly change the course of PbA blood-stage infection.

Taken together, this study defined a previously unknown MHC-II restricted, highly conserved *Plasmodium* derived epitope and began characterisation of the CD4 T cell responses arising from vaccination or *Plasmodium* infection, with a specific focus on CD4 T<sub>RM</sub> cells. While CD4 T cells formed circulating and liver-resident memory populations after different vaccination methods, these cells did not protect from *Plasmodium* liver-stage infection and only partly protected against blood-stage infection. The following section will discuss potential reasons for the lack or limited protective capacity of CD4 T cells in this system and implications for vaccination strategies targeting CD4 T cells and specifically CD4 T<sub>RM</sub> cells.

## 6.3 Are anti-malaria vaccines aiming to induce protective CD4 T cells an appropriate immunisation strategy?

### 6.3.1 Targeting CD4 T cells against blood-stage infection

CD4 T cells are important mediators of immunity against multiple diseases. A lack of CD4 T cells results in an impaired immune response towards a variety of bacterial, viral, and parasitic infections, such as *Mycobacterium tuberculosis*, influenza, and *Plasmodium* respectively (Srivastava and Ernst, 2013, Valkenburg et al., 2018, Weiss et al., 1993). The role of CD4 T cells is often associated with helper functions, such as licensing of DCs to activate CD8 T cells or promoting B cell maturation and antibody production (Smith et al., 2004, Parker, 1993). Tfh cells, for example, are required for effective B cell activation and antibody maturation, as the lack of these cells led to impaired antibody formation and Pch blood-stage control (Perez-Mazliah et al., 2017). However, evidence of antibody independent control of *Plasmodium* blood-stage infection has also been described (Amante and Good, 1997, Kumar et al., 1989, Xu et al., 2000, Pombo et al., 2002). For example, depletion of CD4 T cells post-immunisation with Pch apical membrane antigen 1 reduces protection against Pch blood-stage infection (Xu et al., 2000). Interestingly, antibody titres were comparable in CD4-depleted and undepleted mice. An earlier study revealed that B cell-deficient mice developed a similar immunity to *P. vinckei* blood-stage infection compared to immunologically intact mice (Kumar et al., 1989). Furthermore, CD4 T cell depletion in mice immunised by *P. vinckei* blood-stage infection and drug cured, rendered BALB/c mice susceptible to re-infection. In line with these findings, a small study including four individuals repeatedly inoculated with approximately 30 *P. falciparum* iRBCs followed by drug treatment showed acquisition of sterile protection, which correlated with IFN- $\gamma$  producing CD4 and CD8 T cells (Pombo et al., 2002). Interestingly, parasite-specific antibodies, often accredited with parasitaemia reduction, were under the limit of

detection. The authors showed that repeated low dose inoculation induced Th1 and CD8 T cells that secreted IFN- $\gamma$ , which induced upregulation of nitric oxide synthase released by peripheral blood mononuclear cells. They suggested that this would then lead to enhanced nitric oxide production and death of the *Plasmodium* parasites. However, only four participants finished this study, and the final infection was 5 weeks after the last immunisation step or 3.5 weeks after the last drug administration (Pombo et al., 2002). Nevertheless, these results are in line with mouse studies, which revealed the importance of IFN- $\gamma$  and M-CSF secretion by Th1 cells for facilitating macrophage activation (Fontana et al., 2016). Furthermore, this macrophage activation led to the release of reactive oxygen and nitrogen intermediates, inducing iRBCs surface protein alteration and ultimately clearance of iRBCs by macrophages (Jakobsen et al., 1995, Lutz et al., 1996, Su and Stevenson, 2000, Shear et al., 1989, Fontana et al., 2016).

As RBCs do not express MHC-I or MHC-II molecules and can therefore not be directly targeted by T cells, the reduced parasitemia observed after the transfer of *in vitro* polarized PbT-II Th1 and Th2 cells and PbA iRBCs infection can most likely be attributed to activation of macrophages and B cells. However, we did not measure malaria specific antibody titers or reactive oxygen and nitrogen intermediates to formally prove that this was the mechanism reducing parasitaemia and further experiments are required to address this issue.

The design of an efficient anti-malaria blood-stage vaccine faces some challenges. Unlike the liver-stage, where only low numbers of locally restricted parasites are present, large numbers of merozoites are released even by a single infected hepatocyte (Sturm et al., 2006). Therefore, the immune response elicited by a blood-stage vaccine must eliminate large numbers of merozoites or iRBCs early after their release into the blood-circulation of the body. Furthermore, blood-stage parasites are well described to use a variety of immune escape mechanisms (Qari et al., 1998, Smith et al., 1995b). Antigen diversity or polymorphism can result in antibody responses which are effective against one expressed protein allele not being effective against another, as observed by antibody responses against MSP-1 (Qari et al., 1998, Burns et al., 1989, Urban

et al., 1999, Ocana-Morgner et al., 2003). Similar effects can be observed for proteins that are transported to the surface of the iRBCs. One such protein, PfEMP1, was shown to have around 50 loci on different chromosomes responsible for its coding (Smith et al., 1995a). The switch between expression of different PfEMP1 loci by the parasite in the blood-stage of infection leads to antigen variation between parasite clones, which can result in escape from the primary antibody response to PfEMP1. In addition to immune escape mechanisms by the parasites, *Plasmodium* blood-stage infection was shown to induce immune suppression in humans and mice (Urban et al., 1999, Ocana-Morgner et al., 2003). Binding of iRBCs to APCs was shown to repress APC maturation, resulting in impaired T cells responses and secretion of immune suppressive cytokines such as IL-10.

While CD4 T cells are important to generate anti-*Plasmodium* immune responses against the blood-stage of infection, high numbers of parasites in the blood-stage elevate the potential for immune escape mechanisms and development of pathology. In contrast, low numbers of parasites in a well-defined location and the lack of potential malaria associated pathology in the liver-stage of infection might render the liver a better target for anti-malaria vaccines to induce sterile protection against *Plasmodium* infection mediated by CD4 and CD8 T cell responses.

### **6.3.2 Targeting CD4 T cells against *Plasmodium* liver stage infection**

In the context of *Plasmodium* liver-stage infection, CD8 T cells have been described to be potent mediators of immunity against sporozoite infection, and thus these cells have become the focus of novel vaccine approaches (Mueller et al., 2007, Fernandez-Ruiz et al., 2016, Holz et al., 2020, Valencia-Hernandez et al., 2020). However, RAS vaccination induces not only CD8 memory T cell formation but also CD4 T cell responses (Doolan and Hoffman, 2000, Oliveira et al., 2008). Indeed, we detected memory PbT-II cells for at least 50 days after

RAS vaccination, although the numbers of these cells were relatively small. In contrast,  $\alpha$ Clec9A-DIY vaccination induced much stronger PbT-II memory cell formation in spleen and liver compared to RAS vaccination. Thus, it is possible to induce large numbers of *Plasmodium*-specific CD4 T cells through the right vaccination strategies.

While CD8 T cells are commonly described to have a high cytotoxic function, CD4 T cells can mediate apoptosis of infected target cells, as well. Three main mechanisms have been described to mediate elimination of target cells by T cells: the Fas-Fas-ligand interaction, induction of inflammatory cytokines, and perforin/granzyme have all been shown to mediate apoptosis. FasL (CD95L), expressed on T cells, binds to its cognate receptor Fas (CD95) on target cells. This binding results in the trimerization of Fas in the target cells and recruitment of intracellular death-inducing signalling complexes, which finally results in caspase 3-mediated cell death (Kischkel et al., 1995, Nagata and Golstein, 1995, Krammer, 2000). In addition, cytokines, such as IFN- $\gamma$  and TNF, expressed by CD4 T cells and other cell types, have been shown to induce upregulation of pro-apoptotic genes and proteins (Ossina et al., 1997, Wold et al., 1999, Perez and White, 2000). Of note, PbT-II cells were shown to express IFN- $\gamma$  and TNF after PbA blood-stage infection or  $\alpha$ -Clec9A-DIY vaccination. While these mechanisms are well explored in CD4 and CD8 T cells, perforin/granzyme mediated cytotoxicity is mainly attributed to CD8 T cells. However, in recent years cytotoxic CD4 T cells, releasing perforin and granzymes, were found after viral infection or vaccination in humans and mice (Marshall and Swain, 2011, van de Berg et al., 2008, Frevert et al., 2009). CD4 T cells, similar to CD8 T cells, can therefore be equipped to induce apoptosis in infected target cells. Here, we investigated the capacity of CD4 T<sub>RM</sub> generated by different vaccination and activation methods to mediate target cell killing by comparing mRNA expression of different effector molecules. Our RNAseq analysis of PbT-II liver T<sub>RM</sub> cells revealed that some CD4 T<sub>RM</sub> populations had the potential to mediate target cell killing via expression of key cytotoxic molecules, while other populations were less well equipped to do so. Clec9A-DIY generated PbT-II T<sub>RM</sub> cells expressed

higher levels of perforin (Prf1) than PbT-II Th2 T<sub>RM</sub>. Furthermore, granzyme K (Gzmk) also showed higher expression in PbT-II T<sub>RM</sub> cells generated after RAS,  $\alpha$ Clec9A or Th1 polarization compared to Th2 T<sub>RM</sub> cells. Thus, although we did not investigate protein levels of the above-mentioned mediators, it is likely that *Plasmodium*-specific CD4 T<sub>RM</sub> cells, depending on their activation method, have the potential to mediate cytotoxicity via perforin and granzyme K. Of note, while perforin/granzyme mediated cytotoxicity is mainly attributed to granzyme B, granzyme K induces DNA fragmentation that can lead to cell apoptosis in a caspase independent manner (Shi et al., 1992, Zhao et al., 2007). However, our data showed that PbT-II cells did not facilitate protection against sporozoite infection.

Interestingly, a study by Frevert et al. described cytotoxic CD4 T cells specific for a universal *P. falciparum* CSP epitope in humans after RAS or synthetic peptide immunisation (Frevert et al., 2009). These human CSP-specific CD4 T cells were able to induce apoptosis of peptide-pulsed target cells, potentially via perforin/granzyme cytotoxicity. However, the authors used peptide pulsed Epstein-Barr Virus (EBV) transformed human B cells as targets in their CD4 T cell killing assay and it was not investigated if CD4 T cells detected or lysed infected hepatocytes *in vitro* or *in vivo*. While this showed that cytotoxic *Plasmodium*-specific CD4 T cells form after RAS vaccination, one major question was left unanswered: do hepatocytes express MHC-II molecules and therefore recognised by CD4 T cells upon sporozoite infection? As mentioned previously, under steady state conditions, MHC-II molecules are not present on the cell-surface of hepatocytes, making them “invisible” for antigen directed recognition by CD4 T cells (Franco et al., 1988). However, strong IFN- $\gamma$  stimulation can lead to the induction of MHC-II molecules on hepatocytes (Franco et al., 1988). While sporozoite infection indeed induces IFN- $\gamma$  expression in the liver tissue, it has not been examined if these levels are sufficient to induce MHC-II expression on hepatocytes and therefore this matter requires further investigation (Liehl et al., 2015). Nevertheless, mouse studies showed partial protection against liver stage infection in the absence of B and CD8 T cells after RAS immunisation, indirectly

suggesting a role for CD4 T cells and thereby potentially implying that MHC-II molecules are expressed by hepatocytes upon sporozoite infection (Doolan and Hoffman, 2000, Oliveira et al., 2008). The idea that CD4 T cells can recognise infected hepatocytes is further supported by a study that showed sterile protection after adoptive transfer of *Plasmodium*-specific CD4 T cells in naïve BALB/c mice (Tsuji et al., 1990). Interestingly, this CD4 T cell clone was specific for an epitope within CSP, the same protein that human cytotoxic CD4 T cells were found to be reactive to (Tsuji et al., 1990, Frevet et al., 2009). Together, these studies suggest that CSP-reactive CD4 T cell can mediate protection against *Plasmodium* liver-stage infection. The fact that no protection against sporozoite infection using Hsp90-specific CD4 T cells (PbT-II cells) could be induced, suggests that the cognate antigen might not be accessible for PbT-II cells in the liver. One possible explanation is that Hsp90, highly expressed in the ring and oocyst stage on a transcriptional level (PBANKA\_080570), is only expressed at an intermediate level in the liver-stage (Howick et al., 2019). Supportive of this idea is the weak PbT-II cell proliferative response induced by RAS vaccination, compared to blood-stage infection. Thus, the Hsp90 epitope might not be expressed abundantly enough by sporozoites, or it may be contained inside the parasitophorous vacuole and therefore not be accessible to the peptide processing and presentation machinery of the hepatocyte. The potential lack of cognate antigen presentation in the liver after sporozoite infection might also explain why even high numbers of PbT-II cells were not able to reduce liver-parasite burden in our experiments. In contrast, preliminary data indicated that the transfer of high numbers of OT-II Th1 or Th2 cells, three days before infection with ovalbumin (OVA)-expressing sporozoites resulted in a decreased liver-parasite burden, suggesting that activated CD4 T cells may be able to recognize infected hepatocytes in this setting. These results strongly support the hypothesis that Hsp90 is not a suitable epitope for CD4 T cell immunity against *Plasmodium* liver stage infection. However, it is possible that the observed reduction in liver-parasite burden is not due to CD4 T cell recognizing infected hepatocytes. Previous work showed that IFN- $\gamma$  release, as observed for Th1 cells in response to sporozoite infection, lead to an induction of nitric oxide pathway in

infected hepatocytes (Nussler et al., 1993, Seguin et al., 1994, Wang et al., 1996). This activation would then lead to the elimination of the sporozoites without a direct interaction between CD4 T cells and infected hepatocytes. Further experiments utilizing OT-II cells and OVA expressing sporozoites will reveal whether CD4 T<sub>RM</sub> cells can indeed mediate protection against liver-stage parasites. However, the preliminary experiments strongly suggest that CD4 T cell immunity can be utilised for protection against liver stage infection.

The negative results obtained with PbT-II cells indicate that in order to fully investigate the protective potential of CD4 T<sub>RM</sub> cells, novel MHC-II restricted liver-stage epitopes must be identified. The method used here to identify *Plasmodium*-specific immunogenic epitopes, relied on *in vitro* incubation of DCs with PbA iRBCs, followed by elution of peptides bound to MHC-II molecules. While the similarity between blood and liver stage parasite proteome is 70 %, some proteins are only expressed in the liver-stage and were therefore excluded from our analyses (Tarun et al., 2008). While a similar approach using sporozoites instead of iRBCs might be possible and would give valuable insight into potential novel liver-stage antigen targets, billions of sporozoites would be required, which makes this approach non-viable at present (Fernandez-Ruiz et al., 2017). Instead, including epitope prediction software as well as RNA expression profiles of *Plasmodium* parasite stages may support the identification of immunogenic liver-stage target peptides (Vita et al., 2019, Howick et al., 2019).

In summary, in addition to CD8 T cells, CD4 T cells may be targeted by novel anti-malaria liver-stage vaccines for enhanced protection. Although Hsp90 is not the ideal epitope candidate, alternative MHC-II restricted epitopes are likely to induce protection against sporozoite infection. Combining such protective CD4 T cell epitopes with CD8 T cell epitopes will further enhance the efficiency of liver-stage malaria vaccines.

## 6.4 The importance of CD4 T<sub>RM</sub> cells in infectious diseases

### 6.4.1 CD4 T<sub>RM</sub> cells are involved in the defence mechanism against different pathogens

The discovery of T<sub>RM</sub> cells has fundamentally changed the view of tissue-specific adaptive immune responses towards infections. First defined in the context of skin CD8 T cells, T<sub>RM</sub> cells have now been described in most organs in humans and mice (Gebhardt et al., 2009, Sathaliyawala et al., 2013, Steinert et al., 2015, Casey et al., 2012). Their strategic location in tissues allows fast responses to re-infections and renders these cells perfectly situated to immediately perform effector functions. This is considered a major reason for the high protective potential of CD8 T<sub>RM</sub> cells against cancer or viral, bacterial and parasite infections (Park et al., 2019, Wakim et al., 2015, Sheridan et al., 2014, Fernandez-Ruiz et al., 2016).

Recent research has also focused on the development and function of CD4 T<sub>RM</sub> cells in various infection models (Iijima, 2014, Benoun et al., 2018, Thawer et al., 2014). In this work, it was shown that *Plasmodium*-specific CD4 T<sub>RM</sub> cells are induced in the liver by vaccination with RAS. Thus, *Plasmodium* parasites rank in a growing list of pathogens that induce tissue resident memory CD4 T cells. Unlike Hsp90-specific PbT-II T cells, which were not able to protect against sporozoite infection, CD4 T<sub>RM</sub> cells were shown to be crucial for protection against different pathogens including virus', bacteria and parasites (Iijima, 2014, Benoun et al., 2018, Thawer et al., 2014). For example, adoptive transfer of HA-specific CD4 T cells derived from the lung conferred protection against influenza infection, while HA-specific CD4 T cells from the spleen did not (Teijaro et al., 2011). Furthermore, herpes-simplex virus-2 (HSV-2), deficient for thymidine-kinase (TK<sup>-</sup>), which prevents neurovirulence, induced long-term protection against WT HSV-2 infection by promoting CD4 T<sub>RM</sub> cell formation in

the female reproductive tract (Iijima, 2014). It was further shown that non-circulatory CD69<sup>+</sup>CD103<sup>+/-</sup> CD4 T cells in the lung formed after *Bordetella pertussis* infection and adoptive transfer into naïve mice conferred protection against infection (Sakai et al., 2014).

These studies show that CD4 T<sub>RM</sub> cells can be highly protective in many different contexts and suggest that targeting these cells via vaccination could potentially induce protection. In addition, CD4 T<sub>RM</sub> cells have been shown to recruit other immune cells such as B cells or CD8 T<sub>RM</sub> cells into tissues to enhance immune responses (Son et al., 2021). Furthermore, local macrophages need to interact with CD4 T<sub>RM</sub> cells in genital mucosa in order to protect against HSV-2 infection (Iijima, 2014). The ability to either eliminate infected or altered cells as well as to recruit and activate other cells of the immune system makes CD4 T<sub>RM</sub> cells ideal candidates to induce a broad immune response against infections. While the importance of CD4 T<sub>RM</sub> cells to fight local infections is suggested, the question is, if CD4 T<sub>RM</sub> cells can be induced by vaccination.

#### **6.4.2 Can CD4 T<sub>RM</sub> cells be induced by vaccination?**

A recent study by Benoun and co-authors showed that IFN- $\gamma$  secreting liver homing Th1 T cells, presumably CD4 T<sub>RM</sub> cells, formed in response to a live vaccine *Salmonella* strain (LVS) in B6 mice (Benoun et al., 2018). Subsequent infection with a virulent *Salmonella* strain led to significantly reduced bacterial burdens in vaccinated compared to unvaccinated mice. Parabiosis experiments revealed that CD4 T<sub>RM</sub> cells were partially accountable for this reduction. In line with this study, it was further shown that liver-resident *Plasmodium*-specific CD4 T cells could be induced by two different vaccination approaches and by *in vitro* activation and cell transfer. While this clearly shows the potential of CD4 T<sub>RM</sub> cells

to form in the context of anti-malaria immunisation, one question remains unanswered: What is the optimal vaccination protocol to induce CD4 T<sub>RM</sub> cells?

### **6.4.3 What is the optimal vaccination protocol to induce CD4 T<sub>RM</sub> cells?**

#### **6.4.3.1 The route of vaccination influences the formation of CD4 T<sub>RM</sub> cell.**

Several factors are essential for efficient T<sub>RM</sub> cell induction. First, the route of vaccination is crucial. Subcutaneous immunisation of SARS-CoV-1 nucleocapsid protein failed to induce antigen-specific CD4 T<sub>RM</sub> cells in the lung, while intranasal (i.n.) administration of the same protein induced protective airway CD4 T<sub>RM</sub> cells (Zhao et al., 2016). Furthermore, i.n. vaccination with attenuated influenza vaccine (FluMist) generated CD4 T<sub>RM</sub> cells that mediated long-term protection against re-infection, while other parenteral routes (s.c., i.m. or i.v.) failed to do so (Zens et al., 2016). In the present study, RAS or  $\alpha$ Clec9A-DIY was i.v. injected. While mosquito bites and release of sporozoites occurs in the skin, which would suggest an intradermal (i.d.) or subcutaneous (s.c.) administration, we reasoned that i.v. delivery might be the superior route as sporozoites infiltrate hepatocytes from the bloodstream. Moreover, i.v. RAS injection induces potent T cell proliferation in the spleen (Lau et al., 2014), Chapter 4). In addition, it was shown that i.v. but not s.c. RAS inoculation in non-human primates led to detection of *Plasmodium*-specific CD4 and CD8 T cell responses (Epstein et al., 2011). In addition, our study in mice supports the notion that i.v. administration of RAS mainly induced CD4 and CD8 T<sub>RM</sub> cells in the liver (Chapter 4, (Fernandez-Ruiz et al., 2016)). Thus, the route of vaccine administration must be carefully considered to induce strong tissue-specific CD4 T<sub>RM</sub> cell responses.

### 6.4.3.2 Live attenuated versus inactivated pathogens vaccines

In addition to the route of administration, the nature of the vaccine is pivotal for the successful generation of  $T_{RM}$  cells. Live attenuated vaccines are found to be highly efficient in inducing large proportions of  $T_{RM}$  cells in the targeted tissues, compared to inactivated pathogens (Zens et al., 2016, Ghilas et al., 2021) Chapter 4). For example, i.n. administration of live attenuated influenza vaccine induced strong CD4  $T_{RM}$  cell responses, while a similar vaccine approach using an inactivated influenza virus vaccine induced neutralising antibodies, but no CD4  $T_{RM}$  cell responses (Zens et al., 2016). Similar observations were made using WSV strategies. Inoculation with radiation attenuated sporozoites induced strong CD8  $T_{RM}$  cell responses, while heat inactivated sporozoites only induced moderate numbers of *Plasmodium*-specific CD8  $T_{RM}$  cells in the liver (Ghilas et al., 2021). Therefore, the question remains, why is injection of inactive pathogens less robust at inducing  $T_{RM}$  cell responses and how can we improve  $T_{RM}$  cell formation in this circumstance.

### 6.4.3.3 Can non-live attenuated vaccination approaches be improved to induce stronger $T_{RM}$ cells responses?

It was previously shown that the use of specific adjuvants can boost  $T_{RM}$  cell formation after heat inactivated sporozoite vaccination (Ghilas et al., 2021). Administration of  $\alpha$ GalCer adjuvants significantly improved the formation of CD8  $T_{RM}$  cells in response to heat killed sporozoites. The presence of  $\alpha$ GalCer, which binds CD1d on APC, has been shown to induce NKT cell activation that results in DC maturation via IL-4 and CD40L-CD40 interactions and finally in CD4 and CD8 T cells responses (Hermans et al., 2003, Fujii et al., 2003, Wang and Zhang, 2019). Therefore, it is important to identify adjuvants facilitating potent CD4 T cell activation and  $T_{RM}$  cell formation in the target tissue, as seen for  $\alpha$ GalCer, which

leads to improved *Plasmodium*-specific liver CD8 T<sub>RM</sub> cell formation after inoculation of heat inactivated sporozoites.

Furthermore, different adjuvants do not only alter the quantity but can also influence the quality of induced CD4 T cell responses. Vaccination with UV-inactivated *Chlamydia trachomatis* favoured regulatory T cell differentiation, while co-administration of charge-switching synthetic adjuvant particles induced long-lasting protection mediated by Th1 CD4 T<sub>RM</sub> cells (Stary et al., 2015). Therefore, the choice of adjuvant in a CD4 T<sub>RM</sub> cell inducing vaccine will be crucial for the induction of protective CD4 T cell lineages.

An alternative to whole sporozoite vaccines are sub-unit vaccines such as  $\alpha$ Clec9A-DIY. We found that while RAS vaccination mostly induced CD4 T cells with a T<sub>RM</sub> cell phenotype,  $\alpha$ Clec9A vaccination favoured T<sub>EM</sub> cell formation. Previous work showed that  $\alpha$ Clec9A carrying a *Plasmodium* antigen, in combination with CpG (as an adjuvant) and recombinant adeno associated virus (rAAV), which induces liver inflammation and cognate antigen expression in the liver respectively, induced significantly higher numbers of *Plasmodium*-specific CD8 T<sub>RM</sub> cells in the liver compared to mice that only received  $\alpha$ Clec9A (Huang et al., 2013, Fernandez-Ruiz et al., 2016). It must be noted that, while local antigen expression in the targeted tissue favours T<sub>RM</sub> cell formation, it is not essential, at least for *Plasmodium*-specific CD4 and CD8 T<sub>RM</sub> cells in the liver (Chapter 4, (Holz et al., 2018). Taken together, adjuvants are a powerful tool that has the potential to significantly enhance the quantity as well as the quality of induced T<sub>RM</sub> cells in response to vaccination.

#### **6.4.3.4 Induction of specific cytokine responses might induce stronger CD4 T<sub>RM</sub> cell responses.**

In addition to adjuvants, CD4 and CD8 T<sub>RM</sub> cells are known to rely on specific cytokines. While IL-15 is important for CD4 T<sub>RM</sub> cells in the lung and CD8

$T_{RM}$  cells in the liver, it is not yet known which cytokines can improve CD4  $T_{RM}$  cell maintenance in the liver (Strutt et al., 2018, Holz et al., 2018). Interestingly, PbT-II  $T_{RM}$  cell formation was improved in mice injected with *in vitro* polarised PbT-II Th2 cells. While a combination of reagents are used, IL-4 is a key cytokine for Th2 polarization. Furthermore, RAS vaccinated mice favoured liver CD4  $T_{RM}$  formation. Interestingly, RNAseq. data showed that IL-4 is highly expressed in PbT-II  $T_{RM}$  cells generated by RAS immunization, compared to Th1 and  $\alpha$ Clec9A-DIY-generated PbT-II  $T_{RM}$  cells. Therefore, we sought to investigate the role of IL-4 in CD4  $T_{RM}$  cell formation. Preliminary data from the laboratory, where naïve PbT-II cell were *in vitro* polarized in the presences of IL-2, DIY and either with or without IL-4, showed that PbT-II cells activated in the presence of IL-4 formed elevated numbers and proportions of CD4  $T_{RM}$  cells in the liver compared to control cells after adoptive transfer (personal communication Dr. Daniel Fernandez-Ruiz). This finding supports a role for IL-4 in promoting  $T_{RM}$  cell formation in the liver. These results imply that specific cytokines induced by a vaccine might further support the formation or maintenance of CD4  $T_{RM}$  cells in specific tissues.

#### **6.4.3.5 Are there intrinsic mechanisms that facilitate tissue-residency?**

The induction of optimal  $T_{RM}$  cell responses requires migration of the precursors of these cells to the targeted tissue, such as the liver in *Plasmodium* sporozoite infection. While local antigen expression and inflammation might favour  $T_{RM}$  cell formation in specific tissues, it has been suggested that  $T_{RM}$  cells, once generated, can have imprinted mechanisms that lead to homing to specific tissues (Fernandez-Ruiz et al., 2016, Teijaro et al., 2011). HA-specific memory CD4 T cells isolated from lung tissue, for example, re-entered exclusively the lung when adoptively transferred into naïve mice, while splenic memory CD4 T cells in the same experiment homed to multiple tissues in naïve mice (Teijaro et al., 2011). Induction of such tissue-specific homing characteristics early in T cell

activation might induce stronger CD4 T<sub>RM</sub> cell formation in targeted tissues, while sparing other organs and potentially reducing adverse side effects. One group of markers associated with tissue specific homing are chemokine receptors, which aid recruitment of immune cells into specific organs (Mora et al., 2003, Uehara et al., 2002, Panina-Bordignon et al., 2001, Campbell et al., 1999). CCR4 expression, for example, is mainly found on T cells in the lung and the skin but not the gut (Campbell et al., 1999, Panina-Bordignon et al., 2001). It is therefore crucial to explore potent mechanisms to induce signalling pathways and expression of molecules (e.g. chemokine receptors) governing T cell homing to specific tissues. Based on previous studies, which showed IL-4 dependency for RAS generated CD8 T cells to protect against sporozoite infection, we hypothesised that IL-4 can induced potent liver CD8 liver T<sub>RM</sub> cell formation (Carvalho et al., 2002, Morrot et al., 2005). Preliminary data indicate that *in vitro* activated transgenic T cells specific for the HSV-derived glycoprotein gB (gBT-I cells), show improved CD8 T<sub>RM</sub> cell formation in the liver but not the lung, when cultured in the presence of IL-4 before transfer into mice (personal communication Dr. Daniel Fernandez-Ruiz). This result suggested that induction of specific cytokines early in T cell priming can favour formation of T<sub>RM</sub> cells in specific tissues. Future research should focus on additional cytokines or adjuvants resulting in enhanced CD4 T<sub>RM</sub> cells formation in different tissues. Furthermore, it should be investigated which surface marker/chemokine receptor combinations are responsible for guiding or retaining T<sub>RM</sub> cells in specific tissues. Such knowledge about tissue homing properties that favour T<sub>RM</sub> cell formation in particular tissues could potentially change how other diseases are treated.

One example where this may be relevant is in the use of chimeric antigen receptor-(CAR) T cell therapy. While CAR-T cell therapy has been successfully used to treat non-solid tumours, problems with tissue penetration in solid tumours limit their applications (Lee et al., 2015, Park et al., 2007, Whilding and Maher, 2015). Treatment of such CAR-T cells with cytokines or drugs inducing surface marker expression leading to an easier and more specific tissue infiltration could promote their effectiveness against solid tumours and furthermore reduce the

number of required cells and potentially limit off-target reactions in healthy organs, while efficiently removing cancerous cells.

Taken together, the identification of the mechanisms directing and retaining T<sub>RM</sub> cells in specific tissues will not only improve the development and specificity of vaccines inducing protective CD4 T<sub>RM</sub> cells. Such knowledge will also be adaptable to other fields of medical research.

## 6.5 Concluding remarks

409,000 (2019) annual deaths caused by *Plasmodium* infection emphasises the need for efficient malaria vaccines (WHO, 2019). Advances in the understanding of T cell-mediated immunity against *Plasmodium* infection have led to efficient experimental vaccine designs inducing strong memory T cell responses. Stimulation of CD4 T cells mediating effector functions against the blood-stage and potentially in the liver-stage of *Plasmodium* infection may be a promising strategy to lower the overall *Plasmodium* infection burden. Tissue resident CD4 T cells might represent an ideal target for anti-malaria liver-stage vaccines due to their permanent localisation within the liver. While no protection against sporozoite infection in vaccinated mice was achieved, preliminary data suggested that an alternative CD4 T cell epitope might have the capacity to reduce the liver parasite burden. Furthermore, Hsp90-specific CD4 T cells were able to reduce parasitaemia after blood-stage infection. New *Plasmodium*-specific MHC-II restricted epitopes, in combination with strategies that enhance CD4 T<sub>RM</sub> cell formation (e.g. IL-4 or inducing cognate antigen expression in the liver) may one day improve anti-malaria vaccines.

## References

<rudensky 1991.pdf>.

- ACHTMAN, A. H., STEPHENS, R., CADMAN, E. T., HARRISON, V. & LANGHORNE, J. 2007. Malaria-specific antibody responses and parasite persistence after infection of mice with *Plasmodium chabaudi chabaudi*. *Parasite Immunol*, 29, 435-44.
- ACKERMAN, A. L. & CRESSWELL, P. 2004. Cellular mechanisms governing cross-presentation of exogenous antigens. *Nat Immunol*, 5, 678-84.
- ADEMOKUN, A. A. & DUNN-WALTERS, D. 2010. Immune Responses: Primary and Secondary. *eLS*.
- AGARWAL, S. & RAO, A. 1998. Modulation of chromatin structure regulates cytokine gene expression during T cell differentiation. *Immunity*, 9, 765-75.
- AHMED, M. A. & COX-SINGH, J. 2015. *Plasmodium knowlesi* - an emerging pathogen. *ISBT Sci Ser*, 10, 134-140.
- AKBARI, M., KIMURA, K., BAYARSAIKHAN, G., KIMURA, D., MIYAKODA, M., JURIASINGANI, S., YUDA, M., AMINO, R. & YUI, K. 2018. Nonspecific CD8 +T Cells and Dendritic Cells/Macrophages Participate in Formation of CD8 +T Cell-Mediated Clusters against Malaria Liver-Stage Infection. *Infection and Immunity*, 86, e00717-17-11.
- ALOULO, M. & FAZILLEAU, N. 2019. Regulation of B cell responses by distinct populations of CD4 T cells. *Biomed J*, 42, 243-251.
- AMANTE, F. H. & GOOD, M. F. 1997. Prolonged Th1-like response generated by a *Plasmodium yoelii*-specific T cell clone allows complete clearance of infection in reconstituted mice. *Parasite Immunol*, 19, 111-26.
- AMANTE, F. H., STANLEY, A. C., RANDALL, L. M., ZHOU, Y., HAQUE, A., MCSWEENEY, K., WATERS, A. P., JANSE, C. J., GOOD, M. F., HILL, G. R. & ENGWERDA, C. R. 2007. A role for natural regulatory T cells in the pathogenesis of experimental cerebral malaria. *Am J Pathol*, 171, 548-59.
- AMINO, R., THIBERGE, S., MARTIN, B., CELLI, S., SHORTE, S., FRISCHKNECHT, F. & MÉNARD, R. 2006. Quantitative imaging of *Plasmodium* transmission from mosquito to mammal. *Nature Medicine*, 12, 220-224.
- ANSEL, K. M., GREENWALD, R. J., AGARWAL, S., BASSING, C. H., MONTICELLI, S., INTERLANDI, J., DJURETIC, I. M., LEE, D. U., SHARPE, A. H., ALT, F. W. & RAO, A. 2004. Deletion of a conserved *Il4* silencer impairs T helper type 1-mediated immunity. *Nat Immunol*, 5, 1251-9.
- ARROYO, E. N. & PEPPER, M. 2019. B cells are sufficient to prime the dominant CD4+Tfh response to *Plasmodium* infection. *The Journal of Experimental Medicine*, 162, jem.20190849-12.
- ARTAVANIS-TSAKONAS, K. & RILEY, E. M. 2002. Innate immune response to malaria: rapid induction of IFN-gamma from human NK cells by live *Plasmodium falciparum*-infected erythrocytes. *J Immunol*, 169, 2956-63.
- ATTRIDGE, K., WANG, C. J., WARDZINSKI, L., KENEFECK, R., CHAMBERLAIN, J. L., MANZOTTI, C., KOPF, M. & WALKER, L. S. 2012. IL-21 inhibits T cell IL-2 production and impairs Treg homeostasis. *Blood*, 119, 4656-64.

- AWASTHI, A., CARRIER, Y., PERON, J. P., BETTELLI, E., KAMANAKA, M., FLAVELL, R. A., KUCHROO, V. K., OUKKA, M. & WEINER, H. L. 2007. A dominant function for interleukin 27 in generating interleukin 10-producing anti-inflammatory T cells. *Nat Immunol*, 8, 1380-9.
- BAER, K., ROOSEVELT, M., CLARKSON, A. B., JR., VAN ROOIJEN, N., SCHNIEDER, T. & FREVERT, U. 2007. Kupffer cells are obligatory for Plasmodium yoelii sporozoite infection of the liver. *Cell Microbiol*, 9, 397-412.
- BAIRD, J. K., KRISIN, BARCUS, M. J., ELYAZAR, I. R., BANGS, M. J., MAGUIRE, J. D., FRYAUFF, D. J., RICHIE, T. L., SEKARTUTI & KALALO, W. 2003. Onset of clinical immunity to Plasmodium falciparum among Javanese migrants to Indonesian Papua. *Ann Trop Med Parasitol*, 97, 557-64.
- BAJENOFF, M., WURTZ, O. & GUERDER, S. 2002. Repeated antigen exposure is necessary for the differentiation, but not the initial proliferation, of naive CD4(+) T cells. *J Immunol*, 168, 1723-9.
- BALAM, S., ROMERO, J. F., BONGFEN, S. E., GUILLAUME, P. & CORRADIN, G. 2012. CSP-- a model for in vivo presentation of Plasmodium berghei sporozoite antigens by hepatocytes. *PLoS One*, 7, e51875.
- BANUMATHY, G., SINGH, V., PAVITHRA, S. R. & TATU, U. 2003. Heat shock protein 90 function is essential for Plasmodium falciparum growth in human erythrocytes. *J Biol Chem*, 278, 18336-45.
- BARRERA, V., HALEY, M. J., STRANGWARD, P., ATTREE, E., KAMIZA, S., SEYDEL, K. B., TAYLOR, T. E., MILNER, D. A., JR., CRAIG, A. G. & COUPER, K. N. 2019. Comparison of CD8(+) T Cell Accumulation in the Brain During Human and Murine Cerebral Malaria. *Front Immunol*, 10, 1747.
- BECKER, T. C., WHERRY, E. J., BOONE, D., MURALI-KRISHNA, K., ANTIA, R., MA, A. & AHMED, R. 2002. Interleukin 15 is required for proliferative renewal of virus-specific memory CD8 T cells. *J Exp Med*, 195, 1541-8.
- BEDOUI, S., WHITNEY, P. G., WAITHMAN, J., EIDSMO, L., WAKIM, L., CAMINSCHI, I., ALLAN, R. S., WOJTASIAK, M., SHORTMAN, K., CARBONE, F. R., BROOKS, A. G. & HEATH, W. R. 2009. Cross-presentation of viral and self antigens by skin-derived CD103+ dendritic cells. *Nat Immunol*, 10, 488-95.
- BELNOUE, E., KAYIBANDA, M., VIGARIO, A. M., DESCHEMIN, J. C., VAN ROOIJEN, N., VIGUIER, M., SNOUNOU, G. & RENIA, L. 2002. On the pathogenic role of brain-sequestered alphabeta CD8+ T cells in experimental cerebral malaria. *J Immunol*, 169, 6369-75.
- BELNOUE, E., POTTER, S. M., ROSA, D. S., MAUDUIT, M., GRUNER, A. C., KAYIBANDA, M., MITCHELL, A. J., HUNT, N. H. & RENIA, L. 2008. Control of pathogenic CD8+ T cell migration to the brain by IFN-gamma during experimental cerebral malaria. *Parasite Immunol*, 30, 544-53.
- BENDELAC, A., RIVERA, M. N., PARK, S. H. & ROARK, J. H. 1997. Mouse CD1-specific NK1 T cells: development, specificity, and function. *Annu Rev Immunol*, 15, 535-62.
- BENDING, D., DE LA PENA, H., VELDHOEN, M., PHILLIPS, J. M., UYTENHOVE, C., STOCKINGER, B. & COOKE, A. 2009. Highly purified Th17 cells from BDC2.5NOD mice convert into Th1-like cells in NOD/SCID recipient mice. *J Clin Invest*, 119, 565-72.

- BENNETT, C. L. & CLAUSEN, B. E. 2007. DC ablation in mice: promises, pitfalls, and challenges. *Trends Immunol*, 28, 525-31.
- BENOUN, J. M., PERES, N. G., WANG, N., PHAM, O. H., RUDISILL, V. L., FOGASSY, Z. N., WHITNEY, P. G., FERNANDEZ-RUIZ, D., GEBHARDT, T., PHAM, Q.-M., PUDDINGTON, L., BEDOUI, S., STRUGNELL, R. A. & MCSORLEY, S. J. 2018. Optimal protection against Salmonella infection requires noncirculating memory. *Proceedings of the National Academy of Sciences*, 145, 201808339-6.
- BERENZON, D., SCHWENK, R. J., LETELLIER, L., GUEBRE-XABIER, M., WILLIAMS, J. & KRZYCH, U. 2003. Protracted protection to Plasmodium berghei malaria is linked to functionally and phenotypically heterogeneous liver memory CD8+ T cells. *J Immunol*, 171, 2024-34.
- BERKOWITZ, F. E. 1991. Hemolysis and infection: categories and mechanisms of their interrelationship. *Rev Infect Dis*, 13, 1151-62.
- BHANOT, P., SCHAUER, K., COPPENS, I. & NUSSENZWEIG, V. 2005. A Surface Phospholipase Is Involved in the Migration of Plasmodium Sporozoites through Cells. *Journal of Biological Chemistry*, 280, 6752-6760.
- BHARDWAJ, D., KUSHWAHA, A., PURI, S. K., HERRERA, A., SINGH, N. & CHAUHAN, V. S. 2003. DNA prime-boost protein immunization in monkeys: efficacy of a novel construct containing functional domains of Plasmodium cynomolgi CS and TRAP. *FEMS Immunology & Medical Microbiology*, 39, 241-250.
- BISWAS, P. S., PEDICORD, V., PLOSS, A., MENET, E., LEINER, I. & PAMER, E. G. 2007. Pathogen-specific CD8 T cell responses are directly inhibited by IL-10. *J Immunol*, 179, 4520-8.
- BODDEY, J. A. & COWMAN, A. F. 2013. Plasmodium nesting: remaking the erythrocyte from the inside out. *Annu Rev Microbiol*, 67, 243-69.
- BORGES DA SILVA, H., FONSECA, R., CASSADO ADOS, A., MACHADO DE SALLES, E., DE MENEZES, M. N., LANGHORNE, J., PEREZ, K. R., CUCCOVIA, I. M., RYFFEL, B., BARRETO, V. M., MARINHO, C. R., BOSCARDIN, S. B., ALVAREZ, J. M., D'IMPERIO-LIMA, M. R. & TADOKORO, C. E. 2015. In vivo approaches reveal a key role for DCs in CD4+ T cell activation and parasite clearance during the acute phase of experimental blood-stage malaria. *PLoS Pathog*, 11, e1004598.
- BORSA, M., BARNSTORF, I., BAUMANN, N. S., PALLMER, K., YERMANOS, A., GRÄBNITZ, F., BARANDUN, N., HAUSMANN, A., SANDU, I., BARRAL, Y. & OXENIUS, A. 2019. Modulation of asymmetric cell division as a mechanism to boost CD8+ T cell memory. *Science Immunology*, 4, eaav1730.
- BOUBOU, M. I., COLLETTE, A., VOEGTLE, D., MAZIER, D., CAZENAVE, P. A. & PIED, S. 1999. T cell response in malaria pathogenesis: selective increase in T cells carrying the TCR V(beta)8 during experimental cerebral malaria. *Int Immunol*, 11, 1553-62.
- BOUVIER, M. & WILEY, D. C. 1994. Importance of peptide amino and carboxyl termini to the stability of MHC class I molecules. *Science*, 265, 398-402.
- BOYLE, M. J., JAGANNATHAN, P., BOWEN, K., MCINTYRE, T. I., VANCE, H. M., FARRINGTON, L. A., SCHWARTZ, A., NANKYA, F., NALUWU, K., WAMALA, S., SIKYOMU, E., REK, J., GREENHOUSE, B., ARINAITWE, E., DORSEY, G., KAMYA, M. R. & FEENEY, M. E. 2017. The Development of Plasmodium falciparum-Specific

- IL10 CD4 T Cells and Protection from Malaria in Children in an Area of High Malaria Transmission. *Front Immunol*, 8, 1329.
- BROWN, C. C., GUDJONSON, H., PRITYKIN, Y., DEEP, D., LAVALLEE, V. P., MENDOZA, A., FROMME, R., MAZUTIS, L., ARIYAN, C., LESLIE, C., PE'ER, D. & RUDENSKY, A. Y. 2019. Transcriptional Basis of Mouse and Human Dendritic Cell Heterogeneity. *Cell*, 179, 846-863 e24.
- BROWN, H., HIEN, T. T., DAY, N., MAI, N. T., CHUONG, L. V., CHAU, T. T., LOC, P. P., PHU, N. H., BETHELL, D., FARRAR, J., GATTER, K., WHITE, N. & TURNER, G. 1999. Evidence of blood-brain barrier dysfunction in human cerebral malaria. *Neuropathol Appl Neurobiol*, 25, 331-40.
- BROWN, M. G., DRISCOLL, J. & MONACO, J. J. 1993. MHC-linked low-molecular mass polypeptide subunits define distinct subsets of proteasomes. Implications for divergent function among distinct proteasome subsets. *The Journal of Immunology*, 151, 1193-1204.
- BRUCE-CHWATT, L. J. 1962. A longitudinal survey of natural malaria infection in a group of West African adults. *World Health Organization*, 1-14.
- BUENO, L. L., MORAIS, C. G., LACERDA, M. V., FUJIWARA, R. T. & BRAGA, E. M. 2012. Interleukin-17 producing T helper cells are increased during natural *Plasmodium vivax* infection. *Acta Trop*, 123, 53-7.
- BUFFET, P. A., SAFEUKUI, I., DEPLAINE, G., BROUSSE, V., PRENDKI, V., THELLIER, M., TURNER, G. D. & MERCEREAU-PUIJALON, O. 2011. The pathogenesis of *Plasmodium falciparum* malaria in humans: insights from splenic physiology. *Blood*, 117, 381-92.
- BUGGERT, M., NGUYEN, S., SALGADO-MONTES DE OCA, G., BENGSCH, B., DARKO, S., RANSIER, A., ROBERTS, E. R., DEL ALCAZAR, D., BRODY, I. B., VELLA, L. A., BEURA, L., WIJEYESINGHE, S., HERATI, R. S., DEL RIO ESTRADA, P. M., ABLANEDO-TERRAZAS, Y., KURI-CERVANTES, L., SADA JAPP, A., MANNE, S., VARTANIAN, S., HUFFMAN, A., SANDBERG, J. K., GOSTICK, E., NADOLSKI, G., SILVESTRI, G., CANADAY, D. H., PRICE, D. A., PETROVAS, C., SU, L. F., VAHEDI, G., DORI, Y., FRANK, I., ITKIN, M. G., WHERRY, E. J., DEEKS, S. G., NAJI, A., REYES-TERAN, G., MASOPIST, D., DOUEK, D. C. & BETTS, M. R. 2018. Identification and characterization of HIV-specific resident memory CD8(+) T cells in human lymphoid tissue. *Sci Immunol*, 3.
- BURGIO, V. L., BALLARDINI, G., ARTINI, M., CARATOZZOLO, M., BIANCHI, F. B. & LEVRERO, M. 1998. Expression of co-stimulatory molecules by Kupffer cells in chronic hepatitis of hepatitis C virus etiology. *Hepatology*, 27, 1600-6.
- BURNS, J. M., JR., PARKE, L. A., DALY, T. M., CAVACINI, L. A., WEIDANZ, W. P. & LONG, C. A. 1989. A protective monoclonal antibody recognizes a variant-specific epitope in the precursor of the major merozoite surface antigen of the rodent malarial parasite *Plasmodium yoelii*. *J Immunol*, 142, 2835-40.
- BUTLER, N. S., MOEBIUS, J., PEWE, L. L., TRAORE, B., DOUMBO, O. K., TYGRET, L. T., WALDSCHMIDT, T. J., CROMPTON, P. D. & HARTY, J. T. 2011. Therapeutic blockade of PD-L1 and LAG-3 rapidly clears established blood-stage *Plasmodium* infection. *Nat Immunol*, 13, 188-95.

- BUTLER, N. S., SCHMIDT, N. W. & HARTY, J. T. 2010. Differential effector pathways regulate memory CD8 T cell immunity against *Plasmodium berghei* versus *P. yoelii* sporozoites. *J Immunol*, 184, 2528-38.
- CAMINSCHI, I., PROIETTO, A. I., AHMET, F., KITSOULIS, S., SHIN TEH, J., LO, J. C. Y., RIZZITELLI, A., WU, L., VREMEC, D., VAN DOMMELEN, S. L. H., CAMPBELL, I. K., MARASKOVSKY, E., BRALEY, H., DAVEY, G. M., MOTTRAM, P., VAN DE VELDE, N., JENSEN, K., LEW, A. M., WRIGHT, M. D., HEATH, W. R., SHORTMAN, K. & LAHOUD, M. H. 2008. The dendritic cell subtype-restricted C-type lectin Clec9A is a target for vaccine enhancement. *Blood*, 112, 3264-3273.
- CAMPBELL, J. J., HARALDSEN, G., PAN, J., ROTTMAN, J., QIN, S., PONATH, P., ANDREW, D. P., WARNKE, R., RUFFING, N., KASSAM, N., WU, L. & BUTCHER, E. C. 1999. The chemokine receptor CCR4 in vascular recognition by cutaneous but not intestinal memory T cells. *Nature*, 400, 776-80.
- CARNEIRO, I., ROCA-FELTRER, A., GRIFFIN, J. T., SMITH, L., TANNER, M., SCHELLENBERG, J. A., GREENWOOD, B. & SCHELLENBERG, D. 2010. Age-patterns of malaria vary with severity, transmission intensity and seasonality in sub-Saharan Africa: a systematic review and pooled analysis. *PLoS One*, 5, e8988.
- CARPIO, V. H., AUSSÉNAC, F., PUEBLA-CLARK, L., WILSON, K. D., VILLARINO, A. V., DENT, A. L. & STEPHENS, R. 2020. T Helper Plasticity Is Orchestrated by STAT3, Bcl6, and Blimp-1 Balancing Pathology and Protection in Malaria. *iScience*, 23, 101310.
- CARPIO, V. H., OPATA, M. M., MONTANEZ, M. E., BANERJEE, P. P., DENT, A. L. & STEPHENS, R. 2015. IFN-gamma and IL-21 Double Producing T Cells Are Bcl6-Independent and Survive into the Memory Phase in *Plasmodium chabaudi* Infection. *PLoS One*, 10, e0144654.
- CARVALHO, L. H., SANO, G.-I., HAFALLA, J. C. R., MORROT, A., DE LAFAILLE, M. A. C. & ZAVALA, F. 2002. IL-4-secreting CD4 + T cells are crucial to the development of CD8 + T-cell responses against malaria liver stages. *Nature Medicine*, 8, 166-170.
- CASEY, K. A., FRASER, K. A., SCHENKEL, J. M., MORAN, A., ABT, M. C., BEURA, L. K., LUCAS, P. J., ARTIS, D., WHERRY, E. J., HOGQUIST, K., VEZYS, V. & MASOPIUST, D. 2012. Antigen-independent differentiation and maintenance of effector-like resident memory T cells in tissues. *J Immunol*, 188, 4866-75.
- CEPEK, K. L., SHAW, S. K., PARKER, C. M., RUSSELL, G. J., MORROW, J. S., RIMM, D. L. & BRENNER, M. B. 1994. Adhesion between epithelial cells and T lymphocytes mediated by E-cadherin and the alpha E beta 7 integrin. *Nature*, 372, 190-3.
- CERAMI, C., FREVERT, U., SINNIS, P., TAKACS, B., CLAVIJO, P., SANTOS, M. J. & NUSSENZWEIG, V. 1992. The basolateral domain of the hepatocyte plasma membrane bears receptors for the circumsporozoite protein of *Plasmodium falciparum* sporozoites. *Cell*, 70, 1021-33.
- CHAKRAVARTY, S., COCKBURN, I. A., KUK, S., OVERSTREET, M. G., SACCI, J. B. & ZAVALA, F. 2007. CD8+ T lymphocytes protective against malaria liver stages are primed in skin-draining lymph nodes. *Nat Med*, 13, 1035-41.
- CHAKRAVORTY, S. J. & CRAIG, A. 2005. The role of ICAM-1 in *Plasmodium falciparum* cytoadherence. *Eur J Cell Biol*, 84, 15-27.

- CHANDELE, A., MUKERJEE, P., DAS, G., AHMED, R. & CHAUHAN, V. S. 2011. Phenotypic and functional profiling of malaria-induced CD8 and CD4 T cells during blood-stage infection with *Plasmodium yoelii*. *Immunology*, 132, 273-86.
- CHANG, S. & AUNE, T. M. 2007. Dynamic changes in histone-methylation 'marks' across the locus encoding interferon-gamma during the differentiation of T helper type 2 cells. *Nat Immunol*, 8, 723-31.
- CHARPIAN, S. & PRZYBORSKI, J. M. 2008. Protein transport across the parasitophorous vacuole of *Plasmodium falciparum*: into the great wide open. *Traffic*, 9, 157-65.
- CHEN, G., DU, J. W., NIE, Q., DU, Y. T., LIU, S. C., LIU, D. H., ZHANG, H. M. & WANG, F. F. 2020. *Plasmodium yoelii* 17XL infection modified maturation and function of dendritic cells by skewing Tregs and amplifying Th17. *BMC Infect Dis*, 20, 266.
- CHEUK, S., SCHLUMS, H., GALLAIS SEREZAL, I., MARTINI, E., CHIANG, S. C., MARQUARDT, N., GIBBS, A., DETLOFSSON, E., INTROINI, A., FORKEL, M., HOOG, C., TJERNLUND, A., MICHAELSSON, J., FOLKERSEN, L., MJOSBERG, J., BLOMQVIST, L., EHRSTROM, M., STAHL, M., BRYCESON, Y. T. & EIDSMO, L. 2017. CD49a Expression Defines Tissue-Resident CD8(+) T Cells Poised for Cytotoxic Function in Human Skin. *Immunity*, 46, 287-300.
- CHIZZOLINI, C., TROTTEIN, F., BERNARD, F. X. & KAUFMANN, M. H. 1991. Isotypic analysis, antigen specificity, and inhibitory function of maternally transmitted *Plasmodium falciparum*-specific antibodies in Gabonese newborns. *Am J Trop Med Hyg*, 45, 57-64.
- CLYDE, D. F. 1990. Immunity to *falciparum* and *vivax* malaria induced by irradiated sporozoites: a review of the University of Maryland studies, 1971-75. *Bulletin of the World Health Organization*, 68, 9-12.
- COBAN, C., ISHII, K. J., SULLIVAN, D. J. & KUMAR, N. 2002. Purified malaria pigment (hemozoin) enhances dendritic cell maturation and modulates the isotype of antibodies induced by a DNA vaccine. *Infect Immun*, 70, 3939-43.
- COCKBURN, I. A., AMINO, R., KELEMEN, R. K., KUO, S. C., TSE, S. W., RADTKE, A., MACDANIEL, L., GANUSOV, V. V., ZAVALA, F. & MENARD, R. 2013. In vivo imaging of CD8+ T cell-mediated elimination of malaria liver stages. *Proc Natl Acad Sci U S A*, 110, 9090-5.
- COTTREZ, F., HURST, S. D., COFFMAN, R. L. & GROUX, H. 2000. T regulatory cells 1 inhibit a Th2-specific response in vivo. *J Immunol*, 165, 4848-53.
- COUPER, K. N., BLOUNT, D. G., WILSON, M. S., HAFALLA, J. C., BELKAID, Y., KAMANAKA, M., FLAVELL, R. A., DE SOUZA, J. B. & RILEY, E. M. 2008. IL-10 from CD4CD25Foxp3CD127 adaptive regulatory T cells modulates parasite clearance and pathology during malaria infection. *PLoS Pathog*, 4, e1000004.
- COWMAN, A. F., HEALER, J., MARAPANA, D. & MARSH, K. 2016. Malaria: Biology and Disease. *Cell*, 167, 610-624.
- CUI, G., STARON, M. M., GRAY, S. M., HO, P. C., AMEZQUITA, R. A., WU, J. & KAECH, S. M. 2015. IL-7-Induced Glycerol Transport and TAG Synthesis Promotes Memory CD8+ T Cell Longevity. *Cell*, 161, 750-61.
- DAVID, B. A., REZENDE, R. M., ANTUNES, M. M., SANTOS, M. M., FREITAS LOPES, M. A., DINIZ, A. B., SOUSA PEREIRA, R. V., MARCHESI, S. C., ALVARENGA, D. M., NAKAGAKI, B. N., ARAUJO, A. M., DOS REIS, D. S., ROCHA, R. M., MARQUES, P. E.,

- LEE, W. Y., DENISET, J., LIEW, P. X., RUBINO, S., COX, L., PINHO, V., CUNHA, T. M., FERNANDES, G. R., OLIVEIRA, A. G., TEIXEIRA, M. M., KUBES, P. & MENEZES, G. B. 2016. Combination of Mass Cytometry and Imaging Analysis Reveals Origin, Location, and Functional Repopulation of Liver Myeloid Cells in Mice. *Gastroenterology*, 151, 1176-1191.
- DAVISON, B. B., COGSWELL, F. B., BASKIN, G. B., FALKENSTEIN, K. P., HENSON, E. W. & KROGSTAD, D. J. 2000. Placental changes associated with fetal outcome in the *Plasmodium coatneyi*/rhesus monkey model of malaria in pregnancy. *Am J Trop Med Hyg*, 63, 158-73.
- DE LEEUW, A. M., MCCARTHY, S. P., GEERTS, A. & KNOOK, D. L. 1984. Purified rat liver fat-storing cells in culture divide and contain collagen. *Hepatology*, 4, 392-403.
- DE, S. L., STANISIC, D. I., VAN BREDA, K., BELLETE, B., HARRIS, I., MCCALLUM, F., EDSTEIN, M. D. & GOOD, M. F. 2016. Persistence and immunogenicity of chemically attenuated blood stage *Plasmodium falciparum* in Aotus monkeys. *Int J Parasitol*, 46, 581-91.
- DEN HAAN, J. M., LEHAR, S. M. & BEVAN, M. J. 2000. CD8(+) but not CD8(-) dendritic cells cross-prime cytotoxic T cells in vivo. *J Exp Med*, 192, 1685-96.
- DENGJEL, J., SCHOOR, O., FISCHER, R., REICH, M., KRAUS, M., MULLER, M., KREYMBORG, K., ALTENBEREND, F., BRANDENBURG, J., KALBACHER, H., BROCK, R., DRIESSEN, C., RAMMENSEE, H. G. & STEVANOVIC, S. 2005. Autophagy promotes MHC class II presentation of peptides from intracellular source proteins. *Proc Natl Acad Sci U S A*, 102, 7922-7.
- DENT, A. E., NAKAJIMA, R., LIANG, L., BAUM, E., MOORMANN, A. M., SUMBA, P. O., VULULE, J., BABINEAU, D., RANDALL, A., DAVIES, D. H., FELGNER, P. L. & KAZURA, J. W. 2015. *Plasmodium falciparum* Protein Microarray Antibody Profiles Correlate With Protection From Symptomatic Malaria in Kenya. *J Infect Dis*, 212, 1429-38.
- DJURETIC, I. M., LEVANON, D., NEGREANU, V., GRONER, Y., RAO, A. & ANSEL, K. M. 2007. Transcription factors T-bet and Runx3 cooperate to activate Irfng and silence Il4 in T helper type 1 cells. *Nat Immunol*, 8, 145-53.
- DODOO, D., STAALSOE, T., GIHA, H., KURTZHALS, J. A., AKANMORI, B. D., KORAM, K., DUNYO, S., NKRUHMAH, F. K., HVIID, L. & THEANDER, T. G. 2001. Antibodies to variant antigens on the surfaces of infected erythrocytes are associated with protection from malaria in Ghanaian children. *Infect Immun*, 69, 3713-8.
- DOOLAN, D. L., DOBANO, C. & BAIRD, J. K. 2009. Acquired immunity to malaria. *Clin Microbiol Rev*, 22, 13-36, Table of Contents.
- DOOLAN, D. L. & HOFFMAN, S. L. 2000. The complexity of protective immunity against liver-stage malaria. *J Immunol*, 165, 1453-62.
- DOROVINI-ZIS, K., SCHMIDT, K., HUYNH, H., FU, W., WHITTEN, R. O., MILNER, D., KAMIZA, S., MOLYNEUX, M. & TAYLOR, T. E. 2011. The neuropathology of fatal cerebral malaria in Malawian children. *Am J Pathol*, 178, 2146-58.
- DOUGLAS, A. D., BALDEVIANO, G. C., LUCAS, C. M., LUGO-ROMAN, L. A., CROSNIER, C., BARTHOLDSON, S. J., DIOUF, A., MIURA, K., LAMBERT, L. E., VENTOCILLA, J. A., LEIVA, K. P., MILNE, K. H., ILLINGWORTH, J. J., SPENCER, A. J., HJERRILD, K. A., ALANINE, D. G., TURNER, A. V., MOORHEAD, J. T., EDGEL, K. A., WU, Y., LONG, C.

- A., WRIGHT, G. J., LESCANO, A. G. & DRAPER, S. J. 2015. A PfRH5-based vaccine is efficacious against heterologous strain blood-stage Plasmodium falciparum infection in aotus monkeys. *Cell Host Microbe*, 17, 130-9.
- DOUGLAS, A. D., WILLIAMS, A. R., ILLINGWORTH, J. J., KAMUYU, G., BISWAS, S., GOODMAN, A. L., WYLLIE, D. H., CROSNIER, C., MIURA, K., WRIGHT, G. J., LONG, C. A., OSIER, F. H., MARSH, K., TURNER, A. V., HILL, A. V. & DRAPER, S. J. 2011. The blood-stage malaria antigen PfRH5 is susceptible to vaccine-inducible cross-strain neutralizing antibody. *Nat Commun*, 2, 601.
- DRAHEIM, M., WLODARCZYK, M. F., CROZAT, K., SALIOU, J. M., ALAYI, T. D., TOMAVO, S., HASSAN, A., SALVIONI, A., DEMARTA-GATSI, C., SIDNEY, J., SETTE, A., DALOD, M., BERRY, A., SILVIE, O. & BLANCHARD, N. 2017. Profiling MHC II immunopeptidome of blood-stage malaria reveals that cDC1 control the functionality of parasite-specific CD4 T cells. *EMBO Mol Med*, 9, 1605-1621.
- DUFFY, P. E. & FRIED, M. 2003. Antibodies that inhibit Plasmodium falciparum adhesion to chondroitin sulfate A are associated with increased birth weight and the gestational age of newborns. *Infect Immun*, 71, 6620-3.
- ECHVERRIA, P. C., MATRAJT, M., HARB, O. S., ZAPPIA, M. P., COSTAS, M. A., ROOS, D. S., DUBREMETZ, J. F. & ANGEL, S. O. 2005. Toxoplasma gondii Hsp90 is a potential drug target whose expression and subcellular localization are developmentally regulated. *J Mol Biol*, 350, 723-34.
- EIZENBERG-MAGAR, I., RIMER, J., ZARETSKY, I., LARA-ASTIASO, D., REICH-ZELIGER, S. & FRIEDMAN, N. 2017. Diverse continuum of CD4(+) T-cell states is determined by hierarchical additive integration of cytokine signals. *Proc Natl Acad Sci U S A*, 114, E6447-E6456.
- EL SAHLY, H. M., PATEL, S. M., ATMAR, R. L., LANFORD, T. A., DUBE, T., THOMPSON, D., SIM, B. K., LONG, C. & KEITEL, W. A. 2010. Safety and immunogenicity of a recombinant nonglycosylated erythrocyte binding antigen 175 Region II malaria vaccine in healthy adults living in an area where malaria is not endemic. *Clin Vaccine Immunol*, 17, 1552-9.
- ELLIOTT, S. R., SPURCK, T. P., DODIN, J. M., MAIER, A. G., VOSS, T. S., YOSAATMADJA, F., PAYNE, P. D., MCFADDEN, G. I., COWMAN, A. F., ROGERSON, S. J., SCHOFIELD, L. & BROWN, G. V. 2007. Inhibition of dendritic cell maturation by malaria is dose dependent and does not require Plasmodium falciparum erythrocyte membrane protein 1. *Infect Immun*, 75, 3621-32.
- ENDERS, M. H., BAYARSAIKHAN, G., GHILAS, S., CHUA, Y. C., MAY, R., DE MENEZES, M. N., GE, Z., TAN, P. S., COZIJNSEN, A., MOLLARD, V., YUI, K., MCFADDEN, G. I., LAHOUD, M. H., CAMINSCHI, I., PURCELL, A. W., SCHITTENHELM, R. B., BEATTIE, L., HEATH, W. R. & FERNANDEZ-RUIZ, D. 2021. Plasmodium berghei Hsp90 contains a natural immunogenic I-Ab-restricted antigen common to rodent and human Plasmodium species. *Current Research in Immunology*, 2, 79-92.
- ENGLISH, M., SAUERWEIN, R., WARUIRU, C., MOSOBO, M., OBIERO, J., LOWE, B. & MARSH, K. 1997. Acidosis in severe childhood malaria. *QJM*, 90, 263-70.
- EPSTEIN, J. E., TEWARI, K., LYKE, K. E., SIM, B. K., BILLINGSLEY, P. F., LAURENS, M. B., GUNASEKERA, A., CHAKRAVARTY, S., JAMES, E. R., SEDEGAH, M., RICHMAN, A., VELMURUGAN, S., REYES, S., LI, M., TUCKER, K., AHUMADA, A., RUBEN, A. J., LI,

- T., STAFFORD, R., EAPPEN, A. G., TAMMINGA, C., BENNETT, J. W., OCKENHOUSE, C. F., MURPHY, J. R., KOMISAR, J., THOMAS, N., LOYEVSKY, M., BIRKETT, A., PLOWE, C. V., LOUCQ, C., EDELMAN, R., RICHIE, T. L., SEDER, R. A. & HOFFMAN, S. L. 2011. Live attenuated malaria vaccine designed to protect through hepatic CD8(+) T cell immunity. *Science*, 334, 475-80.
- EWER, K. J., O'HARA, G. A., DUNCAN, C. J., COLLINS, K. A., SHEEHY, S. H., REYES-SANDOVAL, A., GOODMAN, A. L., EDWARDS, N. J., ELIAS, S. C., HALSTEAD, F. D., LONGLEY, R. J., ROWLAND, R., POULTON, I. D., DRAPER, S. J., BLAGBOROUGH, A. M., BERRIE, E., MOYLE, S., WILLIAMS, N., SIANI, L., FOLGORI, A., COLLOCA, S., SINDEN, R. E., LAWRIE, A. M., CORTESE, R., GILBERT, S. C., NICOSIA, A. & HILL, A. V. 2013. Protective CD8+ T-cell immunity to human malaria induced by chimpanzee adenovirus-MVA immunisation. *Nat Commun*, 4, 2836.
- EWER, K. J., SIERRA-DAVIDSON, K., SALMAN, A. M., ILLINGWORTH, J. J., DRAPER, S. J., BISWAS, S. & HILL, A. V. 2015. Progress with viral vectored malaria vaccines: A multi-stage approach involving "unnatural immunity". *Vaccine*, 33, 7444-51.
- FERNANDEZ-RUIZ, D., LAU, L. S., GHAZANFARI, N., JONES, C. M., NG, W. Y., DAVEY, G. M., BERTHOLD, D., HOLZ, L., KATO, Y., ENDERS, M. H., BAYARSAIKHAN, G., HENDRIKS, S. H., LANSINK, L. I. M., ENGEL, J. A., SOON, M. S. F., JAMES, K. R., COZIJNSEN, A., MOLLARD, V., UBOLDI, A. D., TONKIN, C. J., DE KONING-WARD, T. F., GILSON, P. R., KAISHO, T., HAQUE, A., CRABB, B. S., CARBONE, F. R., MCFADDEN, G. I. & HEATH, W. R. 2017. Development of a Novel CD4+ TCR Transgenic Line That Reveals a Dominant Role for CD8+ Dendritic Cells and CD40 Signaling in the Generation of Helper and CTL Responses to Blood-Stage Malaria. *Journal of immunology (Baltimore, Md. : 1950)*, 199, 4165-4179.
- FERNANDEZ-RUIZ, D., NG, W. Y., HOLZ, L. E., MA, J. Z., ZAID, A., WONG, Y. C., LAU, L. S., MOLLARD, V., COZIJNSEN, A., COLLINS, N., LI, J., DAVEY, G. M., KATO, Y., DEVI, S., SKANDARI, R., PAULEY, M., MANTON, J. H., GODFREY, D. I., BRAUN, A., TAY, S. S., TAN, P. S., BOWEN, D. G., KOCH-NOLTE, F., RISSIEK, B., CARBONE, F. R., CRABB, B. S., LAHOUD, M., COCKBURN, I. A., MUELLER, S. N., BERTOLINO, P., MCFADDEN, G. I., CAMINSCHI, I. & HEATH, W. R. 2016. Liver-Resident Memory CD8+ T Cells Form a Front-Line Defense against Malaria Liver-Stage Infection. *Immunity*, 45, 889-902.
- FONSECA, R., BEURA, L. K., QUARNSTROM, C. F., GHONEIM, H. E., FAN, Y., ZEBLEY, C. C., SCOTT, M. C., FARES-FREDERICKSON, N. J., WIJEYESINGHE, S., THOMPSON, E. A., BORGES DA SILVA, H., VEZYS, V., YOUNGBLOOD, B. & MASOPUST, D. 2020. Developmental plasticity allows outside-in immune responses by resident memory T cells. *Nat Immunol*, 21, 412-421.
- FONTANA, M. F., DE MELO, G. L., ANIDI, C., HAMBURGER, R., KIM, C. Y., LEE, S. Y., PHAM, J. & KIM, C. C. 2016. Macrophage Colony Stimulating Factor Derived from CD4+ T Cells Contributes to Control of a Blood-Borne Infection. *PLoS Pathog*, 12, e1006046.
- FOWKES, F. J., BOEUF, P. & BEESON, J. G. 2016. Immunity to malaria in an era of declining malaria transmission. *Parasitology*, 143, 139-53.

- FRANCO, A., BARNABA, V., NATALI, P., BALSANO, C., MUSCA, A. & BALSANO, F. 1988. Expression of class I and class II major histocompatibility complex antigens on human hepatocytes. *Hepatology*, 8, 449-54.
- FREITAS DO ROSARIO, A. P., LAMB, T., SPENCE, P., STEPHENS, R., LANG, A., ROERS, A., MULLER, W., O'GARRA, A. & LANGHORNE, J. 2012. IL-27 promotes IL-10 production by effector Th1 CD4+ T cells: a critical mechanism for protection from severe immunopathology during malaria infection. *J Immunol*, 188, 1178-90.
- FREMONT, D. H., CRAWFORD, F., MARRACK, P., HENDRICKSON, W. A. & KAPPLER, J. 1998. Crystal structure of mouse H2-M. *Immunity*, 9, 385-93.
- FREVERT, U., MORENO, A., CALVO-CALLE, J. M., KLOTZ, C. & NARDIN, E. 2009. Imaging effector functions of human cytotoxic CD4+ T cells specific for Plasmodium falciparum circumsporozoite protein. *Int J Parasitol*, 39, 119-32.
- FREVERT, U., SINNIS, P., CERAMI, C., SHREFFLER, W., TAKACS, B. & NUSSENZWEIG, V. 1993. Malaria circumsporozoite protein binds to heparan sulfate proteoglycans associated with the surface membrane of hepatocytes. *J Exp Med*, 177, 1287-98.
- FREVERT, U., USYNIN, I., BAER, K. & KLOTZ, C. 2006. Nomadic or sessile: can Kupffer cells function as portals for malaria sporozoites to the liver? *Cell Microbiol*, 8, 1537-46.
- FRIED, M., MUGA, R. O., MISORE, A. O. & DUFFY, P. E. 1998. Malaria elicits type 1 cytokines in the human placenta: IFN-gamma and TNF-alpha associated with pregnancy outcomes. *J Immunol*, 160, 2523-30.
- FUJII, S., SHIMIZU, K., SMITH, C., BONIFAZ, L. & STEINMAN, R. M. 2003. Activation of natural killer T cells by alpha-galactosylceramide rapidly induces the full maturation of dendritic cells in vivo and thereby acts as an adjuvant for combined CD4 and CD8 T cell immunity to a coadministered protein. *J Exp Med*, 198, 267-79.
- GAO, Y., NISH, S. A., JIANG, R., HOU, L., LICONA-LIMON, P., WEINSTEIN, J. S., ZHAO, H. & MEDZHITOV, R. 2013. Control of T helper 2 responses by transcription factor IRF4-dependent dendritic cells. *Immunity*, 39, 722-32.
- GATTINONI, L., LUGLI, E., JI, Y., POS, Z., PAULOS, C. M., QUIGLEY, M. F., ALMEIDA, J. R., GOSTICK, E., YU, Z., CARPENITO, C., WANG, E., DOUEK, D. C., PRICE, D. A., JUNE, C. H., MARINCOLA, F. M., ROEDERER, M. & RESTIFO, N. P. 2011. A human memory T cell subset with stem cell-like properties. *Nat Med*, 17, 1290-7.
- GATTINONI, L., ZHONG, X. S., PALMER, D. C., JI, Y., HINRICHS, C. S., YU, Z., WRZESINSKI, C., BONI, A., CASSARD, L., GARVIN, L. M., PAULOS, C. M., MURANSKI, P. & RESTIFO, N. P. 2009. Wnt signaling arrests effector T cell differentiation and generates CD8+ memory stem cells. *Nat Med*, 15, 808-13.
- GEBHARDT, T., WAKIM, L. M., EIDSMO, L., READING, P. C., HEATH, W. R. & CARBONE, F. R. 2009. Memory T cells in nonlymphoid tissue that provide enhanced local immunity during infection with herpes simplex virus. *Nat Immunol*, 10, 524-30.
- GERLACH, C., MOSEMAN, E. A., LOUGHHEAD, S. M., ALVAREZ, D., ZWIJNENBURG, A. J., WAANDERS, L., GARG, R., DE LA TORRE, J. C. & VON ANDRIAN, U. H. 2016. The Chemokine Receptor CX3CR1 Defines Three Antigen-Experienced CD8 T Cell Subsets with Distinct Roles in Immune Surveillance and Homeostasis. *Immunity*, 45, 1270-1284.

- GHAZANFARI, N., MUELLER, S. N. & HEATH, W. R. 2018. Cerebral Malaria in Mouse and Man. *Front Immunol*, 9, 2016.
- GHILAS, S., ENDERS, M. H., MAY, R., HOLZ, L. E., FERNANDEZ-RUIZ, D., COZIJNSEN, A., MOLLARD, V., COCKBURN, I. A., MCFADDEN, G. I., HEATH, W. R. & BEATTIE, L. 2021. Development of Plasmodium-specific liver-resident memory CD8(+) T cells after heat-killed sporozoite immunization in mice. *Eur J Immunol*, 51, 1153-1165.
- GILBERT, S. C., PLEBANSKI, M., HARRIS, S. J., ALLSOPP, C. E., THOMAS, R., LAYTON, G. T. & HILL, A. V. 1997. A protein particle vaccine containing multiple malaria epitopes. *Nat Biotechnol*, 15, 1280-4.
- GODFREY, D. I. & KRONENBERG, M. 2004. Going both ways: immune regulation via CD1d-dependent NKT cells. *J Clin Invest*, 114, 1379-88.
- GOLA, A., SILMAN, D., WALTERS, A. A., SRIDHAR, S., UDERHARDT, S., SALMAN, A. M., HALBROTH, B. R., BELLAMY, D., BOWYER, G., POWLSON, J., BAKER, M., VENKATRAMAN, N., POULTON, I., BERRIE, E., ROBERTS, R., LAWRIE, A. M., ANGUS, B., KHAN, S. M., JANSE, C. J., EWER, K. J., GERMAIN, R. N., SPENCER, A. J. & HILL, A. V. S. 2018. Prime and target immunization protects against liver-stage malaria in mice. *Sci Transl Med*, 10.
- GOLDRATH, A. W., SIVAKUMAR, P. V., GLACCUM, M., KENNEDY, M. K., BEVAN, M. J., BENOIST, C., MATHIS, D. & BUTZ, E. A. 2002. Cytokine requirements for acute and Basal homeostatic proliferation of naive and memory CD8+ T cells. *J Exp Med*, 195, 1515-22.
- GONZALEZ-ASEGUINOLAZA, G., DE OLIVEIRA, C., TOMASKA, M., HONG, S., BRUNAROMERO, O., NAKAYAMA, T., TANIGUCHI, M., BENDELAC, A., VAN KAER, L., KOEZUKA, Y. & TSUJI, M. 2000. alpha-galactosylceramide-activated Valpha 14 natural killer T cells mediate protection against murine malaria. *Proc Natl Acad Sci U S A*, 97, 8461-6.
- GOWDA, N. M., WU, X. & GOWDA, D. C. 2011. The nucleosome (histone-DNA complex) is the TLR9-specific immunostimulatory component of Plasmodium falciparum that activates DCs. *PLoS One*, 6, e20398.
- GRAU, G. E., MACKENZIE, C. D., CARR, R. A., REDARD, M., PIZZOLATO, G., ALLASIA, C., CATALDO, C., TAYLOR, T. E. & MOLYNEUX, M. E. 2003. Platelet accumulation in brain microvessels in fatal pediatric cerebral malaria. *J Infect Dis*, 187, 461-6.
- GREINER, J., DOROVINI-ZIS, K., TAYLOR, T. E., MOLYNEUX, M. E., BEARE, N. A., KAMIZA, S. & WHITE, V. A. 2015. Correlation of hemorrhage, axonal damage, and blood-tissue barrier disruption in brain and retina of Malawian children with fatal cerebral malaria. *Front Cell Infect Microbiol*, 5, 18.
- GROOM, J. R. & LUSTER, A. D. 2011. CXCR3 ligands: redundant, collaborative and antagonistic functions. *Immunology and Cell Biology*, 89, 207-215.
- GROUX, H., O'GARRA, A., BIGLER, M., ROULEAU, M., ANTONENKO, S., DE VRIES, J. E. & RONCAROLO, M. G. 1997. A CD4+ T-cell subset inhibits antigen-specific T-cell responses and prevents colitis. *Nature*, 389, 737-42.
- GRURING, C., HEIBER, A., KRUSE, F., FLEMMING, S., FRANCI, G., COLOMBO, S. F., FASANA, E., SCHOELER, H., BORGESSE, N., STUNNENBERG, H. G., PRZYBORSKI, J. M., GILBERGER, T. W. & SPIELMANN, T. 2012. Uncovering common principles in protein export of malaria parasites. *Cell Host Microbe*, 12, 717-29.

- HAFALLA, J. C., BAUZA, K., FRIESEN, J., GONZALEZ-ASEGUINOLAZA, G., HILL, A. V. & MATUSCHEWSKI, K. 2013. Identification of targets of CD8(+) T cell responses to malaria liver stages by genome-wide epitope profiling. *PLoS Pathog*, 9, e1003303.
- HALPERN, M. D., KURLANDER, R. J. & PISETSKY, D. S. 1996. Bacterial DNA induces murine interferon-gamma production by stimulation of interleukin-12 and tumor necrosis factor-alpha. *Cell Immunol*, 167, 72-8.
- HANNINEN, A., MAKSIMOW, M., ALAM, C., MORGAN, D. J. & JALKANEN, S. 2011. Ly6C supports preferential homing of central memory CD8+ T cells into lymph nodes. *Eur J Immunol*, 41, 634-44.
- HANSEN, D. S., BERNARD, N. J., NIE, C. Q. & SCHOFIELD, L. 2007. NK cells stimulate recruitment of CXCR3+ T cells to the brain during Plasmodium berghei-mediated cerebral malaria. *J Immunol*, 178, 5779-88.
- HANSEN, D. S., SIOMOS, M.-A., BUCKINGHAM, L., SCALZO, A. A. & SCHOFIELD, L. 2003. Regulation of Murine Cerebral Malaria Pathogenesis by CD1d-Restricted NKT Cells and the Natural Killer Complex. *Immunity*, 18, 391-402.
- HANSON, J., LEE, S. J., MOHANTY, S., FAIZ, M. A., ANSTEY, N. M., CHARUNWATTHANA, P., YUNUS, E. B., MISHRA, S. K., TJITRA, E., PRICE, R. N., RAHMAN, R., NOSTEN, F., HTUT, Y., HOQUE, G., HONG CHAU, T. T., HOAN PHU, N., HIEN, T. T., WHITE, N. J., DAY, N. P. & DONDORP, A. M. 2010. A simple score to predict the outcome of severe malaria in adults. *Clin Infect Dis*, 50, 679-85.
- HAQUE, A., BEST, S. E., AMANTE, F. H., MUSTAFAH, S., DESBARRIERES, L., DE LABASTIDA, F., SPARWASSER, T., HILL, G. R. & ENGWERDA, C. R. 2010. CD4+ natural regulatory T cells prevent experimental cerebral malaria via CTLA-4 when expanded in vivo. *PLoS Pathog*, 6, e1001221.
- HAQUE, A., BEST, S. E., AMMERDORFFER, A., DESBARRIERES, L., DE OCA, M. M., AMANTE, F. H., DE LABASTIDA RIVERA, F., HERTZOG, P., BOYLE, G. M., HILL, G. R. & ENGWERDA, C. R. 2011a. Type I interferons suppress CD4(+) T-cell-dependent parasite control during blood-stage Plasmodium infection. *Eur J Immunol*, 41, 2688-98.
- HAQUE, A., BEST, S. E., MONTES DE OCA, M., JAMES, K. R., AMMERDORFFER, A., EDWARDS, C. L., DE LABASTIDA RIVERA, F., AMANTE, F. H., BUNN, P. T., SHEEL, M., SEBINA, I., KOYAMA, M., VARELIAS, A., HERTZOG, P. J., KALINKE, U., GUN, S. Y., RENIA, L., RUEDL, C., MACDONALD, K. P., HILL, G. R. & ENGWERDA, C. R. 2014. Type I IFN signaling in CD8- DCs impairs Th1-dependent malaria immunity. *J Clin Invest*, 124, 2483-96.
- HAQUE, A., BEST, S. E., UNOSSON, K., AMANTE, F. H., DE LABASTIDA, F., ANSTEY, N. M., KARUPIAH, G., SMYTH, M. J., HEATH, W. R. & ENGWERDA, C. R. 2011b. Granzyme B expression by CD8+ T cells is required for the development of experimental cerebral malaria. *J Immunol*, 186, 6148-56.
- HARA, T., SHITARA, S., IMAI, K., MIYACHI, H., KITANO, S., YAO, H., TANI-ICHI, S. & IKUTA, K. 2012. Identification of IL-7-producing cells in primary and secondary lymphoid organs using IL-7-GFP knock-in mice. *J Immunol*, 189, 1577-84.
- HARPUR, C. M., KATO, Y., DEWI, S. T., STANKOVIC, S., JOHNSON, D. N., BEDOUI, S., WHITNEY, P. G., LAHOUD, M. H., CAMINSCHI, I., HEATH, W. R., BROOKS, A. G. &

- GEBHARDT, T. 2019. Classical Type 1 Dendritic Cells Dominate Priming of Th1 Responses to Herpes Simplex Virus Type 1 Skin Infection. *J Immunol*, 202, 653-663.
- HATZI, K., NANCE, J. P., KROENKE, M. A., BOTHWELL, M., HADDAD, E. K., MELNICK, A. & CROTTY, S. 2015. BCL6 orchestrates Tfh cell differentiation via multiple distinct mechanisms. *J Exp Med*, 212, 539-53.
- HAYAKAWA, Y., GODFREY, D. I. & SMYTH, M. J. 2004. Alpha-galactosylceramide: potential immunomodulatory activity and future application. *Curr Med Chem*, 11, 241-52.
- HEGAZY, A. N., PEINE, M., HELMSTETTER, C., PANSE, I., FROHLICH, A., BERGTHALER, A., FLATZ, L., PINSCHER, D. D., RADBRUCH, A. & LOHNING, M. 2010. Interferons direct Th2 cell reprogramming to generate a stable GATA-3(+)T-bet(+) cell subset with combined Th2 and Th1 cell functions. *Immunity*, 32, 116-28.
- HENN, V., SLUPSKY, J. R., GRAFE, M., ANAGNOSTOPOULOS, I., FORSTER, R., MULLER-BERGHAUS, G. & KROCZEK, R. A. 1998. CD40 ligand on activated platelets triggers an inflammatory reaction of endothelial cells. *Nature*, 391, 591-4.
- HERMANS, I. F., SILK, J. D., GILEADI, U., SALIO, M., MATHEW, B., RITTER, G., SCHMIDT, R., HARRIS, A. L., OLD, L. & CERUNDOLO, V. 2003. NKT cells enhance CD4+ and CD8+ T cell responses to soluble antigen in vivo through direct interaction with dendritic cells. *J Immunol*, 171, 5140-7.
- HERNDLER-BRANDSTETTER, D., ISHIGAME, H., SHINNAKASU, R., PLAJER, V., STECHER, C., ZHAO, J., LIETZENMAYER, M., KROEHLING, L., TAKUMI, A., KOMETANI, K., INOUE, T., KLUGER, Y., KAECH, S. M., KUROSAKI, T., OKADA, T. & FLAVELL, R. A. 2018. KLRG1(+) Effector CD8(+) T Cells Lose KLRG1, Differentiate into All Memory T Cell Lineages, and Convey Enhanced Protective Immunity. *Immunity*, 48, 716-729 e8.
- HILDEMAN, D. A., ZHU, Y., MITCHELL, T. C., BOUILLET, P., STRASSER, A., KAPPLER, J. & MARRACK, P. 2002. Activated T Cell Death In Vivo Mediated by Proapoptotic Bcl-2 Family Member Bim. *Immunity*, 16, 759-767.
- HOCHMAN, S. E., MADALINE, T. F., WASSMER, S. C., MCALE, E., CHOI, N., SEYDEL, K. B., WHITTEN, R. O., VARUGHESE, J., GRAU, G. E., KAMIZA, S., MOLYNEUX, M. E., TAYLOR, T. E., LEE, S., MILNER, D. A., JR. & KIM, K. 2015. Fatal Pediatric Cerebral Malaria Is Associated with Intravascular Monocytes and Platelets That Are Increased with HIV Coinfection. *mBio*, 6, e01390-15.
- HOFFMAN, S. L., GOH, L. & OF, T. L. T. J. 2002. Protection of Humans against Malaria by Immunization with Radiation-Attenuated Plasmodium falciparum Sporozoites. *academic.oup.com*.
- HOLDER, A. A. & BLACKMAN, M. J. 1994. What is the function of MSP-I on the malaria merozoite? *Parasitology Today*, 10.
- HOLLAND, C. J., COLE, D. K. & GODKIN, A. 2013. Re-Directing CD4(+) T Cell Responses with the Flanking Residues of MHC Class II-Bound Peptides: The Core is Not Enough. *Front Immunol*, 4, 172.
- HOLZ, L. E., CHUA, Y. C., DE MENEZES, M. N., ANDERSON, R. J., DRAPER, S. L., COMPTON, B. J., CHAN, S. T. S., MATHEW, J., LI, J., KEDZIERSKI, L., WANG, Z., BEATTIE, L., ENDERS, M. H., GHILAS, S., MAY, R., STEINER, T. M., LANGE, J., FERNANDEZ-RUIZ, D., VALENCIA-HERNANDEZ, A. M., OSMOND, T. L., FARRAND, K. J., SENEVIRATNA,

- R., ALMEIDA, C. F., TULLETT, K. M., BERTOLINO, P., BOWEN, D. G., COZIJNSEN, A., MOLLARD, V., MCFADDEN, G. I., CAMINSCHI, I., LAHOUD, M. H., KEDZIERSKA, K., TURNER, S. J., GODFREY, D. I., HERMANS, I. F., PAINTER, G. F. & HEATH, W. R. 2020. Glycolipid-peptide vaccination induces liver-resident memory CD8(+) T cells that protect against rodent malaria. *Sci Immunol*, 5.
- HOLZ, L. E., PRIER, J. E., FREESTONE, D., STEINER, T. M., ENGLISH, K., JOHNSON, D. N., MOLLARD, V., COZIJNSEN, A., DAVEY, G. M., GODFREY, D. I., YUI, K., MACKAY, L. K., LAHOUD, M. H., CAMINSCHI, I., MCFADDEN, G. I., BERTOLINO, P., FERNANDEZ-RUIZ, D. & HEATH, W. R. 2018. CD8(+) T Cell Activation Leads to Constitutive Formation of Liver Tissue-Resident Memory T Cells that Seed a Large and Flexible Niche in the Liver. *Cell Rep*, 25, 68-79 e4.
- HOMBRINK, P., HELBIG, C., BACKER, R. A., PIET, B., OJA, A. E., STARK, R., BRASSER, G., JONGEJAN, A., JONKERS, R. E., NOTA, B., BASAK, O., CLEVERS, H. C., MOERLAND, P. D., AMSEN, D. & VAN LIER, R. A. 2016. Programs for the persistence, vigilance and control of human CD8(+) lung-resident memory T cells. *Nat Immunol*, 17, 1467-1478.
- HORII, T., SHIRAI, H., JIE, L., ISHII, K. J., PALACPAC, N. Q., TOUGAN, T., HATO, M., OHTA, N., BOBOGARE, A., ARAKAKI, N., MATSUMOTO, Y., NAMAZUE, J., ISHIKAWA, T., UEDA, S. & TAKAHASHI, M. 2010. Evidences of protection against blood-stage infection of Plasmodium falciparum by the novel protein vaccine SE36. *Parasitol Int*, 59, 380-6.
- HOWICK, V. M., RUSSELL, A. J. C., ANDREWS, T., HEATON, H., REID, A. J., NATARAJAN, K., BUTUNGI, H., METCALF, T., VERZIER, L. H., RAYNER, J. C., BERRIMAN, M., HERREN, J. K., BILLKER, O., HEMBERG, M., TALMAN, A. M. & LAWNICZAK, M. K. N. 2019. The Malaria Cell Atlas: Single parasite transcriptomes across the complete Plasmodium life cycle. *Science*, 365.
- HOWLAND, S. W., POH, C. M. & RENIA, L. 2015. Activated Brain Endothelial Cells Cross-Present Malaria Antigen. *PLoS Pathog*, 11, e1004963.
- HUANG, L. R., WOHLLEBER, D., REISINGER, F., JENNE, C. N., CHENG, R. L., ABDULLAH, Z., SCHILDBERG, F. A., ODENTHAL, M., DIENES, H. P., VAN ROOIJEN, N., SCHMITT, E., GARBI, N., CROFT, M., KURTS, C., KUBES, P., PROTZER, U., HEIKENWALDER, M. & KNOLLE, P. A. 2013. Intrahepatic myeloid-cell aggregates enable local proliferation of CD8(+) T cells and successful immunotherapy against chronic viral liver infection. *Nat Immunol*, 14, 574-83.
- HUME, D. A. 2011. Applications of myeloid-specific promoters in transgenic mice support in vivo imaging and functional genomics but do not support the concept of distinct macrophage and dendritic cell lineages or roles in immunity. *J Leukoc Biol*, 89, 525-38.
- HUNT, D. F., HENDERSON, R. A., SHABANOWITZ, J., SAKAGUCHI, K., MICHEL, H., SEVILIR, N., COX, A. L., APPELLA, E. & ENGELHARD, V. H. 1992. Characterization of peptides bound to the class I MHC molecule HLA-A2.1 by mass spectrometry. *Science*, 255, 1261-3.
- HUTTEN, T. J., THORDARDOTTIR, S., FREDRIX, H., JANSSEN, L., WOESTENENK, R., TEL, J., JOOSTEN, B., CAMBI, A., HEEMSKERK, M. H., FRANSSSEN, G. M., BOERMAN, O. C., BAKKER, L. B., JANSEN, J. H., SCHAAP, N., DOLSTRA, H. & HOBBO, W. 2016.

- CLEC12A-Mediated Antigen Uptake and Cross-Presentation by Human Dendritic Cell Subsets Efficiently Boost Tumor-Reactive T Cell Responses. *J Immunol*, 197, 2715-25.
- HUYSAMEN, C., WILLMENT, J. A., DENNEHY, K. M. & BROWN, G. D. 2008. CLEC9A Is a Novel Activation C-type Lectin-like Receptor Expressed on BDCA3 +Dendritic Cells and a Subset of Monocytes. *Journal of Biological Chemistry*, 283, 16693-16701.
- HVIID, L., KURTZHALS, J. A., ADABAYERI, V., LOIZON, S., KEMP, K., GOKA, B. Q., LIM, A., MERCEREAU-PUJJALON, O., AKANMORI, B. D. & BEHR, C. 2001. Perturbation and proinflammatory type activation of V delta 1(+) gamma delta T cells in African children with Plasmodium falciparum malaria. *Infect Immun*, 69, 3190-6.
- IDOYAGA, J., LUBKIN, A., FIORESE, C., LAHOUD, M. H., CAMINSCHI, I., HUANG, Y., RODRIGUEZ, A., CLAUSEN, B. E., PARK, C. G., TRUMPFHELLER, C. & STEINMAN, R. M. 2011. Comparable T helper 1 (Th1) and CD8 T-cell immunity by targeting HIV gag p24 to CD8 dendritic cells within antibodies to Langerin, DEC205, and Clec9A. *Proceedings of the National Academy of Sciences of the United States of America*, 108, 2384-2389.
- IGYARTO, B. Z., HALEY, K., ORTNER, D., BOBR, A., GERAMI-NEJAD, M., EDELSON, B. T., ZURAWSKI, S. M., MALISSEN, B., ZURAWSKI, G., BERMAN, J. & KAPLAN, D. H. 2011. Skin-resident murine dendritic cell subsets promote distinct and opposing antigen-specific T helper cell responses. *Immunity*, 35, 260-72.
- IJIMA, N. 2014. A local Macrophage chemokine network sustains protective tissue-resident memory CD4 T cells. *Science*, 346, 89-93.
- ILLINGWORTH, J. J., ALANINE, D. G., BROWN, R., MARSHALL, J. M., BARTLETT, H. E., SILK, S. E., LABBE, G. M., QUINKERT, D., CHO, J. S., WENDLER, J. P., PATTINSON, D. J., BARFOD, L., DOUGLAS, A. D., SHEA, M. W., WRIGHT, K. E., DE CASSAN, S. C., HIGGINS, M. K. & DRAPER, S. J. 2019. Functional Comparison of Blood-Stage Plasmodium falciparum Malaria Vaccine Candidate Antigens. *Front Immunol*, 10, 1254.
- IMAI, T., SHEN, J., CHOU, B., DUAN, X., TU, L., TETSUTANI, K., MORIYA, C., ISHIDA, H., HAMANO, S., SHIMOKAWA, C., HISAEDA, H. & HIMENO, K. 2010. Involvement of CD8+ T cells in protective immunity against murine blood-stage infection with Plasmodium yoelii 17XL strain. *Eur J Immunol*, 40, 1053-61.
- ING, R., SEGURA, M., THAWANI, N., TAM, M. & STEVENSON, M. M. 2006. Interaction of mouse dendritic cells and malaria-infected erythrocytes: uptake, maturation, and antigen presentation. *J Immunol*, 176, 441-50.
- ISHINO, T., CHINZEI, Y. & YUDA, M. 2005. A Plasmodium sporozoite protein with a membrane attack complex domain is required for breaching the liver sinusoidal cell layer prior to hepatocyte infection. *Cell Microbiol*, 7, 199-208.
- ISHINO, T., YANO, K., CHINZEI, Y. & YUDA, M. 2004. Cell-passage activity is required for the malarial parasite to cross the liver sinusoidal cell layer. *PLoS Biol*, 2, E4.
- ISHIZUKA, A. S., LYKE, K. E., DEZURE, A., BERRY, A. A., RICHIE, T. L., MENDOZA, F. H., ENAMA, M. E., GORDON, I. J., CHANG, L. J., SARWAR, U. N., ZEPHIR, K. L., HOLMAN, L. A., JAMES, E. R., BILLINGSLEY, P. F., GUNASEKERA, A., CHAKRAVARTY, S., MANOJ, A., LI, M., RUBEN, A. J., LI, T., EAPPEN, A. G.,

- STAFFORD, R. E., K, C. N., MURSHEDKAR, T., DECEDERFELT, H., PLUMMER, S. H., HENDEL, C. S., NOVIK, L., COSTNER, P. J., SAUNDERS, J. G., LAURENS, M. B., PLOWE, C. V., FLYNN, B., WHALEN, W. R., TODD, J. P., NOOR, J., RAO, S., SIERRA-DAVIDSON, K., LYNN, G. M., EPSTEIN, J. E., KEMP, M. A., FAHLE, G. A., MIKOLAJCZAK, S. A., FISHBAUGHER, M., SACK, B. K., KAPPE, S. H., DAVIDSON, S. A., GARVER, L. S., BJORKSTROM, N. K., NASON, M. C., GRAHAM, B. S., ROEDERER, M., SIM, B. K., HOFFMAN, S. L., LEDGERWOOD, J. E. & SEDER, R. A. 2016. Protection against malaria at 1 year and immune correlates following PfSPZ vaccination. *Nat Med*, 22, 614-23.
- IVANOV, II, MCKENZIE, B. S., ZHOU, L., TADOKORO, C. E., LEPELLEY, A., LAFAILLE, J. J., CUA, D. J. & LITTMAN, D. R. 2006. The orphan nuclear receptor ROR $\gamma$  directs the differentiation program of proinflammatory IL-17+ T helper cells. *Cell*, 126, 1121-33.
- JAGANNATHAN, P., ECCLES-JAMES, I., BOWEN, K., NANKYA, F., AUMA, A., WAMALA, S., EBUSU, C., MUHINDO, M. K., ARINAITWE, E., BRIGGS, J., GREENHOUSE, B., TAPPERO, J. W., KAMYA, M. R., DORSEY, G. & FEENEY, M. E. 2014. IFN $\gamma$ /IL-10 co-producing cells dominate the CD4 response to malaria in highly exposed children. *PLoS Pathog*, 10, e1003864.
- JAKOBSEN, P. H., BATE, C. A., TAVERNE, J. & PLAYFAIR, J. H. 1995. Malaria: toxins, cytokines and disease. *Parasite Immunol*, 17, 223-31.
- JAMES, K. R., SOON, M. S. F., SEBINA, I., FERNANDEZ-RUIZ, D., DAVEY, G., LILIGETO, U. N., NAIR, A. S., FOGG, L. G., EDWARDS, C. L., BEST, S. E., LANSINK, L. I. M., SCHRODER, K., WILSON, J. A. C., AUSTIN, R., SUHRBIER, A., LANE, S. W., HILL, G. R., ENGWERDA, C. R., HEATH, W. R. & HAQUE, A. 2018. IFN Regulatory Factor 3 Balances Th1 and T Follicular Helper Immunity during Nonlethal Blood-Stage Plasmodium Infection. *J Immunol*, 200, 1443-1456.
- JARDETZKY, T. S., LANE, W. S., ROBINSON, R. A., MADDEN, D. R. & WILEY, D. C. 1991. Identification of self peptides bound to purified HLA-B27. *Nature*, 353, 326-9.
- JENNER, R. G., TOWNSEND, M. J., JACKSON, I., SUN, K., BOUWMAN, R. D., YOUNG, R. A., GLIMCHER, L. H. & LORD, G. M. 2009. The transcription factors T-bet and GATA-3 control alternative pathways of T-cell differentiation through a shared set of target genes. *Proc Natl Acad Sci U S A*, 106, 17876-81.
- JIANG, W., SWIGGARD, W. J., HEUFLER, C., PENG, M., MIRZA, A., STEINMAN, R. M. & NUSSENZWEIG, M. C. 1995. The receptor DEC-205 expressed by dendritic cells and thymic epithelial cells is involved in antigen processing. *Nature*, 375, 151-5.
- JIANG, X., CLARK, R. A., LIU, L., WAGERS, A. J., FUHLBRIGGE, R. C. & KUPPER, T. S. 2012. Skin infection generates non-migratory memory CD8+ T(RM) cells providing global skin immunity. *Nature*, 483, 227-31.
- JOBE, O., DONOFRIO, G., SUN, G., LIEPINSH, D., SCHWENK, R. & KRZYCH, U. 2009. Immunization with radiation-attenuated Plasmodium berghei sporozoites induces liver cCD8 $\alpha$ +DC that activate CD8+T cells against liver-stage malaria. *PLoS One*, 4, e5075.
- JOHNSTON, R. J., POHOLEK, A. C., DITORO, D., YUSUF, I., ETO, D., BARNETT, B., DENT, A. L., CRAFT, J. & CROTTY, S. 2009. Bcl6 and Blimp-1 are reciprocal and antagonistic regulators of T follicular helper cell differentiation. *Science*, 325, 1006-10.

- JOSHI, N. S., CUI, W., CHANDELE, A., LEE, H. K., URSO, D. R., HAGMAN, J., GAPIN, L. & KAECH, S. M. 2007. Inflammation directs memory precursor and short-lived effector CD8(+) T cell fates via the graded expression of T-bet transcription factor. *Immunity*, 27, 281-95.
- JOSLING, G. A. & LLINAS, M. 2015. Sexual development in Plasmodium parasites: knowing when it's time to commit. *Nat Rev Microbiol*, 13, 573-87.
- JUNG, Y. W., RUTISHAUSER, R. L., JOSHI, N. S., HABERMAN, A. M. & KAECH, S. M. 2010. Differential localization of effector and memory CD8 T cell subsets in lymphoid organs during acute viral infection. *J Immunol*, 185, 5315-25.
- KAECH, S. M., TAN, J. T., WHERRY, E. J., KONIECZNY, B. T., SURH, C. D. & AHMED, R. 2003. Selective expression of the interleukin 7 receptor identifies effector CD8 T cells that give rise to long-lived memory cells. *Nat Immunol*, 4, 1191-8.
- KARIU, T., ISHINO, T., YANO, K., CHINZEI, Y. & YUDA, M. 2006. CelTOS, a novel malarial protein that mediates transmission to mosquito and vertebrate hosts. *Mol Microbiol*, 59, 1369-79.
- KASAHARA, S. & CLARK, E. A. 2012. Dendritic cell-associated lectin 2 (DCAL2) defines a distinct CD8alpha- dendritic cell subset. *J Leukoc Biol*, 91, 437-48.
- KASSIM, O. O., AKO-ANAI, K. A., TORIMIRO, S. E., HOLLOWELL, G. P., OKOYE, V. C. & MARTIN, S. K. 2000. Inhibitory factors in breastmilk, maternal and infant sera against in vitro growth of Plasmodium falciparum malaria parasite. *J Trop Pediatr*, 46, 92-6.
- KATO, Y., ZAID, A., DAVEY, G. M., MUELLER, S. N., NUTT, S. L., ZOTOS, D., TARLINTON, D. M., SHORTMAN, K., LAHOUD, M. H., HEATH, W. R. & CAMINSCHI, I. 2015. Targeting Antigen to Clec9A Primes Follicular Th Cell Memory Responses Capable of Robust Recall. *J Immunol*, 195, 1006-14.
- KAWABE, T., NAKA, T., YOSHIDA, K., TANAKA, T., FUJIWARA, H., SUEMATSU, S., YOSHIDA, N., KISHIMOTO, T. & KIKUTANI, H. 1994. The immune responses in CD40-deficient mice: Impaired immunoglobulin class switching and germinal center formation. *Immunity*, 1, 167-178.
- KAZMIN, D., NAKAYA, H. I., LEE, E. K., JOHNSON, M. J., VAN DER MOST, R., VAN DEN BERG, R. A., BALLOU, W. R., JONGERT, E., WILLE-REECE, U., OCKENHOUSE, C., ADEREM, A., ZAK, D. E., SADOFF, J., HENDRIKS, J., WRAMMERT, J., AHMED, R. & PULENDRAN, B. 2017. Systems analysis of protective immune responses to RTS,S malaria vaccination in humans. *Proc Natl Acad Sci U S A*, 114, 2425-2430.
- KEBAIER, C., VOZA, T. & VANDERBERG, J. 2009. Kinetics of mosquito-injected Plasmodium sporozoites in mice: fewer sporozoites are injected into sporozoite-immunized mice. *PLoS Pathog*, 5, e1000399.
- KEEGAN, L. T. & DUSHOFF, J. 2013. Population-level effects of clinical immunity to malaria. *BMC Infect Dis*, 13, 428.
- KELLY, E., WON, A., REFAELI, Y. & VAN PARIJS, L. 2002. IL-2 and related cytokines can promote T cell survival by activating AKT. *J Immunol*, 168, 597-603.
- KESTER, K. E., CUMMINGS, J. F., OFORI-ANYINAM, O., OCKENHOUSE, C. F., KRZYCH, U., MORIS, P., SCHWENK, R., NIELSEN, R. A., DEBEBE, Z., PINELIS, E., JUOMPAN, L., WILLIAMS, J., DOWLER, M., STEWART, V. A., WIRTZ, R. A., DUBOIS, M. C., LIEVENS, M., COHEN, J., BALLOU, W. R., HEPPNER, D. G., JR. & RTS, S. V. E. G.

2009. Randomized, double-blind, phase 2a trial of falciparum malaria vaccines RTS,S/AS01B and RTS,S/AS02A in malaria-naive adults: safety, efficacy, and immunologic associates of protection. *J Infect Dis*, 200, 337-46.
- KESWANI, T. & BHATTACHARYYA, A. 2014. Differential role of T regulatory and Th17 in Swiss mice infected with Plasmodium berghei ANKA and Plasmodium yoelii. *Exp Parasitol*, 141, 82-92.
- KIMURA, D., MIYAKODA, M., KIMURA, K., HONMA, K., HARA, H., YOSHIDA, H. & YUI, K. 2016. Interleukin-27-Producing CD4+ T Cells Regulate Protective Immunity during Malaria Parasite Infection. *Immunity*, 44, 672-682.
- KIMURA, K., KIMURA, D., MATSUSHIMA, Y., MIYAKODA, M., HONMA, K., YUDA, M. & YUI, K. 2013. CD8+ T cells specific for a malaria cytoplasmic antigen form clusters around infected hepatocytes and are protective at the liver stage of infection. *Infect Immun*, 81, 3825-34.
- KISCHKEL, F. C., HELLBARDT, S., BEHRMANN, I., GERMER, M., PAWLITA, M., KRAMMER, P. H. & PETER, M. E. 1995. Cytotoxicity-dependent APO-1 (Fas/CD95)-associated proteins form a death-inducing signaling complex (DISC) with the receptor. *The EMBO Journal*, 14, 5579-5588.
- KISHIKAWA, H., SUN, J., CHOI, A., MIAW, S. C. & HO, I. C. 2001. The cell type-specific expression of the murine IL-13 gene is regulated by GATA-3. *J Immunol*, 167, 4414-20.
- KONDRACK, R. M., HARBERTSON, J., TAN, J. T., MCBREEN, M. E., SURH, C. D. & BRADLEY, L. M. 2003. Interleukin 7 regulates the survival and generation of memory CD4 cells. *J Exp Med*, 198, 1797-806.
- KRAMMER, P. H. 2000. CD95's deadly mission in the immune system. *Nature*, 407, 789-95.
- KRIEG, A. M., LOVE-HOMAN, L., YI, A. K. & HARTY, J. T. 1998. CpG DNA induces sustained IL-12 expression in vivo and resistance to Listeria monocytogenes challenge. *J Immunol*, 161, 2428-34.
- KUBLER-KIELB, J., MAJADLY, F., WU, Y., NARUM, D. L., GUO, C., MILLER, L. H., SHILOACH, J., ROBBINS, J. B. & SCHNEERSON, R. 2007. Long-lasting and transmission-blocking activity of antibodies to Plasmodium falciparum elicited in mice by protein conjugates of Pfs25. *Proc Natl Acad Sci U S A*, 104, 293-8.
- KUBLIN, J. G., MIKOLAJCZAK, S. A., SACK, B. K., FISHBAUGHER, M. E., SEILIE, A., SHELTON, L., VONGOEDERT, T., FIRAT, M., MAGEE, S., FRITZEN, E., BETZ, W., KAIN, H. S., DANKWA, D. A., STEEL, R. W., VAUGHAN, A. M., NOAH SATHER, D., MURPHY, S. C. & KAPPE, S. H. 2017. Complete attenuation of genetically engineered Plasmodium falciparum sporozoites in human subjects. *Sci Transl Med*, 9.
- KUMAR, B. V., KRATCHMAROV, R., MIRON, M., CARPENTER, D. J., SENDA, T., LERNER, H., FRIEDMAN, A., REINER, S. L. & FARBER, D. L. 2018. Functional heterogeneity of human tissue-resident memory T cells based on dye efflux capacities. *JCI Insight*, 3.
- KUMAR, B. V., MA, W., MIRON, M., GRANOT, T., GUYER, R. S., CARPENTER, D. J., SENDA, T., SUN, X., HO, S.-H., LERNER, H., FRIEDMAN, A. L., SHEN, Y. & FARBER, D. L. 2017. Human Tissue-Resident Memory T Cells Are Defined by Core

- Transcriptional and Functional Signatures in Lymphoid and Mucosal Sites. *CellReports*, 20, 2921-2934.
- KUMAR, R., LOUGHLAND, J. R., NG, S. S., BOYLE, M. J. & ENGWERDA, C. R. 2019. The regulation of CD4 +T cells during malaria. *Immunological Reviews*, 22, 13-18.
- KUMAR, S., GOOD, M. F., DONTFRAID, F., VINETZ, J. M. & MILLER, L. H. 1989. Interdependence of CD4+ T cells and malarial spleen in immunity to Plasmodium vinckei vinckei. Relevance to vaccine development. *The Journal of Immunology*, 143, 2017-2023.
- KURUP, S. P., ANTHONY, S. M., HANCOX, L. S., VIJAY, R., PEWE, L. L., MOIOFFER, S. J., SOMPALLAE, R., JANSE, C. J., KHAN, S. M. & HARTY, J. T. 2019. Monocyte-Derived CD11c+ Cells Acquire Plasmodium from Hepatocytes to Prime CD8 T Cell Immunity to Liver-Stage Malaria. *Cell Host & Microbe*, 25, 565-577.e6.
- KURUP, S. P., OBENG-ADJEI, N., ANTHONY, S. M., TRAORE, B., DOUMBO, O. K., BUTLER, N. S., CROMPTON, P. D. & HARTY, J. T. 2017. Regulatory T cells impede acute and long-term immunity to blood-stage malaria through CTLA-4. *Nature Medicine*, 23, 1220-1225.
- KWOK, W. W., TAN, V., GILLETTE, L., LITTELL, C. T., SOLTIS, M. A., LAFOND, R. B., YANG, J., JAMES, E. A. & DELONG, J. H. 2012. Frequency of epitope-specific naive CD4(+) T cells correlates with immunodominance in the human memory repertoire. *J Immunol*, 188, 2537-44.
- LACOMBE, M. H., HARDY, M. P., ROONEY, J. & LABRECQUE, N. 2005. IL-7 receptor expression levels do not identify CD8+ memory T lymphocyte precursors following peptide immunization. *J Immunol*, 175, 4400-7.
- LAHOUD, M. H., AHMET, F., KITSOULIS, S., WAN, S. S., VREMEC, D., LEE, C. N., PHIPSON, B., SHI, W., SMYTH, G. K., LEW, A. M., KATO, Y., MUELLER, S. N., DAVEY, G. M., HEATH, W. R., SHORTMAN, K. & CAMINSCHI, I. 2011. Targeting Antigen to Mouse Dendritic Cells via Clec9A Induces Potent CD4 T Cell Responses Biased toward a Follicular Helper Phenotype. *The Journal of Immunology*, 187, 842-850.
- LAHOUD, M. H., PROIETTO, A. I., AHMET, F., KITSOULIS, S., EIDSMO, L., WU, L., SATHE, P., PIETERSZ, S., CHANG, H. W., WALKER, I. D., MARASKOVSKY, E., BRALEY, H., LEW, A. M., WRIGHT, M. D., HEATH, W. R., SHORTMAN, K. & CAMINSCHI, I. 2009. The C-type lectin Clec12A present on mouse and human dendritic cells can serve as a target for antigen delivery and enhancement of antibody responses. *J Immunol*, 182, 7587-94.
- LAIDLAW, B. J., ZHANG, N., MARSHALL, H. D., STARON, M. M., GUAN, T., HU, Y., CAULEY, L. S., CRAFT, J. & KAECH, S. M. 2014. CD4+ T cell help guides formation of CD103+ lung-resident memory CD8+ T cells during influenza viral infection. *Immunity*, 41, 633-45.
- LALVANI, A., BROOKES, R., HAMBLETON, S., BRITTON, W. J., HILL, A. V. & MCMICHAEL, A. J. 1997. Rapid effector function in CD8+ memory T cells. *J Exp Med*, 186, 859-65.
- LANDAIS, E., ROMAGNOLI, P. A., CORPER, A. L., SHIRES, J., ALTMAN, J. D., WILSON, I. A., GARCIA, K. C. & TEYTON, L. 2009. New design of MHC class II tetramers to accommodate fundamental principles of antigen presentation. *J Immunol*, 183, 7949-57.

- LANGHORNE, J. 1989. The role of CD4+ T-cells in the immune response to *Plasmodium chabaudi*. *Parasitology Today*, 5, 362-364.
- LANGHORNE, J., NDUNGU, F. M., SPONAAS, A.-M. & MARSH, K. 2008. Immunity to malaria: more questions than answers. *Nature Immunology*, 9, 725-732.
- LANIER, L. L. 2005. NK cell recognition. *Annu Rev Immunol*, 23, 225-74.
- LAU, L. S., FERNANDEZ-RUIZ, D., MOLLARD, V., STURM, A., NELLER, M. A., COZIJNSEN, A., GREGORY, J. L., DAVEY, G. M., JONES, C. M., LIN, Y.-H., HAQUE, A., ENGWERDA, C. R., NIE, C. Q., HANSEN, D. S., MURPHY, K. M., PAPENFUSS, A. T., MILES, J. J., BURROWS, S. R., DE KONING-WARD, T., MCFADDEN, G. I., CARBONE, F. R., CRABB, B. S. & HEATH, W. R. 2014. CD8+ T Cells from a Novel T Cell Receptor Transgenic Mouse Induce Liver-Stage Immunity That Can Be Boosted by Blood-Stage Infection in Rodent Malaria. *PLoS Pathogens*, 10, e1004135-16.
- LEE, D. U., AVNI, O., CHEN, L. & RAO, A. 2004. A distal enhancer in the interferon-gamma (IFN-gamma) locus revealed by genome sequence comparison. *J Biol Chem*, 279, 4802-10.
- LEE, D. W., KOCHENDERFER, J. N., STETLER-STEVENSON, M., CUI, Y. K., DELBROOK, C., FELDMAN, S. A., FRY, T. J., ORENTAS, R., SABATINO, M., SHAH, N. N., STEINBERG, S. M., STRONCEK, D., TSCHERNIA, N., YUAN, C., ZHANG, H., ZHANG, L., ROSENBERG, S. A., WAYNE, A. S. & MACKALL, C. L. 2015. T cells expressing CD19 chimeric antigen receptors for acute lymphoblastic leukaemia in children and young adults: a phase 1 dose-escalation trial. *The Lancet*, 385, 517-528.
- LEE, W. & LEE, G. R. 2018. Transcriptional regulation and development of regulatory T cells. *Exp Mol Med*, 50, e456.
- LEVINGS, M. K., GREGORI, S., TRESOLDI, E., CAZZANIGA, S., BONINI, C. & RONCAROLO, M. G. 2005. Differentiation of Tr1 cells by immature dendritic cells requires IL-10 but not CD25+CD4+ Tr cells. *Blood*, 105, 1162-9.
- LI, C. & LANGHORNE, J. 2000. Tumor necrosis factor alpha p55 receptor is important for development of memory responses to blood-stage malaria infection. *Infect Immun*, 68, 5724-30.
- LI, J., AHMET, F., SULLIVAN, L. C., BROOKS, A. G., KENT, S. J., DE ROSE, R., SALAZAR, A. M., REIS E SOUSA, C., SHORTMAN, K., LAHOUD, M. H., HEATH, W. R. & CAMINSCHI, I. 2015. Antibodies targeting Clec9A promote strong humoral immunity without adjuvant in mice and non-human primates. *European Journal of Immunology*, 45, 854-864.
- LIANG, S. C., TAN, X. Y., LUXENBERG, D. P., KARIM, R., DUNUSSI-JOANNOPOULOS, K., COLLINS, M. & FOUSER, L. A. 2006. Interleukin (IL)-22 and IL-17 are coexpressed by Th17 cells and cooperatively enhance expression of antimicrobial peptides. *J Exp Med*, 203, 2271-9.
- LIEHL, P., MEIRELES, P., ALBUQUERQUE, I. S., PINKEVYCH, M., BAPTISTA, F., MOTA, M. M., DAVENPORT, M. P. & PRUDENCIO, M. 2015. Innate immunity induced by *Plasmodium* liver infection inhibits malaria reinfections. *Infect Immun*, 83, 1172-80.
- LIEHL, P., S, V. Z.-L. I., CHAN, J., ZILLINGER, T., BAPTISTA, F., CARAPAU, D., KONERT, M., HANSON, K. K., CARRET, C. E. L., LASSNIG, C., LLER, M. M. U., KALINKE, U., SAEED, M., CHORA, A. F., GOLENBOCK, D. T., STROBL, B., NCIO, M. P. E., COELHO, L. P.,

- KAPPE, S. H., SUPERTI-FURGA, G., PICHLMAIR, A., RIO, A. M. V. A., RICE, C. M., FITZGERALD, K. A., BARCHET, W. & MOTA, M. M. 2014. Host-cell sensors for Plasmodium activate innate immunity against liver-stage infection. *Nature Medicine*, 20, 1-9.
- LIU, T., LU, X., ZHAO, C., FU, X., ZHAO, T. & XU, W. 2015. PD-1 deficiency enhances humoral immunity of malaria infection treatment vaccine. *Infect Immun*, 83, 2011-7.
- LJUNGGREN, H.-G. & KÄRRE, K. 1990. In search of the 'missing self': MHC molecules and NK cell recognition. *Immunology Today*, 11, 237-244.
- LODISH, H., BERK, A., ZIPURSKY, S. L., MATSUDAIRA, P., BALTIMORE, D. & DARNELL, J. 2000. Cellular energetics: glycolysis, aerobic oxidation, and photosynthesis. *Molecular cell biology*, 4th ed.
- LOEVENICH, K., UEFFING, K., ABEL, S., HOSE, M., MATUSCHEWSKI, K., WESTENDORF, A. M., BUER, J. & HANSEN, W. 2017. DC-Derived IL-10 Modulates Pro-inflammatory Cytokine Production and Promotes Induction of CD4(+)IL-10(+) Regulatory T Cells during Plasmodium yoelii Infection. *Front Immunol*, 8, 152.
- LUNDIE, R. J., DE KONING-WARD, T. F., DAVEY, G. M., NIE, C. Q., HANSEN, D. S., LAU, L. S., MINTER, J. D., BELZ, G. T., SCHOFIELD, L., CARBONE, F. R., VILLADANGOS, J. A., CRABB, B. S. & HEATH, W. R. 2008. Blood-stage Plasmodium infection induces CD8+ T lymphocytes to parasite-expressed antigens, largely regulated by CD8alpha+ dendritic cells. *Proc Natl Acad Sci U S A*, 105, 14509-14.
- LUTZ, M. B., GIROLOMONI, G. & RICCIARDI-CASTAGNOLI, P. 1996. The Role of Cytokines in Functional Regulation and Differentiation of Dendritic Cells. *Immunobiology*, 195, 431-455.
- LÖNNBERG, T., SVENSSON, V., JAMES, K. R., FERNANDEZ-RUIZ, D., SEBINA, I., MONTANDON, R., SOON, M. S. F., FOGG, L. G., NAIR, A. S., LILIGETO, U., STUBBINGTON, M. J. T., LY, L.-H., BAGGER, F. O., ZWIESSELE, M., LAWRENCE, N. D., SOUZA-FONSECA-GUIMARAES, F., BUNN, P. T., ENGWERDA, C. R., HEATH, W. R., BILLKER, O., STEGLE, O., HAQUE, A. & TEICHMANN, S. A. 2017. Single-cell RNA-seq and computational analysis using temporal mixture modelling resolves Th1/Tfh fate bifurcation in malaria. *Science Immunology*, 2, eaal2192-26.
- MACKAY, L. K., BRAUN, A., MACLEOD, B. L., COLLINS, N., TEBARTZ, C., BEDOUI, S., CARBONE, F. R. & GEBHARDT, T. 2015a. Cutting edge: CD69 interference with sphingosine-1-phosphate receptor function regulates peripheral T cell retention. *J Immunol*, 194, 2059-63.
- MACKAY, L. K., MINNICH, M., KRAGTEN, N., LIAO, Y. & 2016 2016. Hobit and Blimp1 instruct a universal transcriptional program of tissue residency in lymphocytes. *science.sciencemag.org*, 352, 453-459.
- MACKAY, L. K., RAHIMPOUR, A., MA, J. Z., COLLINS, N., STOCK, A. T., HAFON, M.-L., VEGA-RAMOS, J., LAUZURICA, P., MUELLER, S. N., STEFANOVIC, T., TSCHARKE, D. C., HEATH, W. R., INOUE, M., CARBONE, F. R. & GEBHARDT, T. 2013. The developmental pathway for CD103+CD8+ tissue-resident memory T cells of skin. *Nature Immunology*, 14, 1294-1301.
- MACKAY, L. K., WAKIM, L., VAN VLIET, C. J., JONES, C. M., MUELLER, S. N., BANNARD, O., FEARON, D. T., HEATH, W. R. & CARBONE, F. R. 2012. Maintenance of T cell

- function in the face of chronic antigen stimulation and repeated reactivation for a latent virus infection. *J Immunol*, 188, 2173-8.
- MACKAY, L. K., WYNNE-JONES, E., FREESTONE, D., PELLICCI, D. G., MIELKE, L. A., NEWMAN, D. M., BRAUN, A., MASSON, F., KALLIES, A., BELZ, G. T. & CARBONE, F. R. 2015b. T-box Transcription Factors Combine with the Cytokines TGF-beta and IL-15 to Control Tissue-Resident Memory T Cell Fate. *Immunity*, 43, 1101-11.
- MACKINTOSH, C. L., BEESON, J. G. & MARSH, K. 2004. Clinical features and pathogenesis of severe malaria. *Trends Parasitol*, 20, 597-603.
- MACPHEE, P. J., SCHMIDT, E. E. & GROOM, A. C. 1995. Intermittence of blood flow in liver sinusoids, studied by high-resolution in vivo microscopy. *Am J Physiol*, 269, G692-8.
- MACPHERSON, G. G., WARRELL, M. J., WHITE, N. J., LOOAREESUWAN, S. & WARRELL, D. A. 1985. Human cerebral malaria. A quantitative ultrastructural analysis of parasitized erythrocyte sequestration. *Am J Pathol*, 119, 385-401.
- MAGISTRADO, P. A., LUSINGU, J., VESTERGAARD, L. S., LEMNGE, M., LAVSTSEN, T., TURNER, L., HVIID, L., JENSEN, A. T. & THEANDER, T. G. 2007. Immunoglobulin G antibody reactivity to a group A Plasmodium falciparum erythrocyte membrane protein 1 and protection from P. falciparum malaria. *Infect Immun*, 75, 2415-20.
- MAIER, A. G., COOKE, B. M., COWMAN, A. F. & TILLEY, L. 2009. Malaria parasite proteins that remodel the host erythrocyte. *Nat Rev Microbiol*, 7, 341-54.
- MAITLAND, K. & NEWTON, C. R. 2005. Acidosis of severe falciparum malaria: heading for a shock? *Trends Parasitol*, 21, 11-6.
- MAMEDOV, M. R., SCHOLZEN, A., NAIR, R. V., CUMNOCK, K., KENKEL, J. A., OLIVEIRA, J. H. M., TRUJILLO, D. L., SALIGRAMA, N., ZHANG, Y., RUBELT, F., SCHNEIDER, D. S., CHIEN, Y.-H., SAUERWEIN, R. W. & DAVIS, M. M. 2018. A Macrophage Colony-Stimulating-Factor-Producing  $\gamma\delta$  T Cell Subset Prevents Malarial Parasitemic Recurrence. *Immunity*, 48, 350-363.e7.
- MARSH, K., FORSTER, D., WARUIRU, C., MWANGI, I., WINSTANLEY, M., MARSH, V., NEWTON, C., WINSTANLEY, P., WARN, P., PESHU, N., PASVOL, G. & SNOW, R. 1995. Indicators of Life-Threatening Malaria in African Children. *New England Journal of Medicine*, 332, 1399-1404.
- MARSH, K. & KINYANJUI, S. 2006. Immune effector mechanisms in malaria. *Parasite Immunol*, 28, 51-60.
- MARSHALL, N. B. & SWAIN, S. L. 2011. Cytotoxic CD4 T cells in antiviral immunity. *Journal of Biomedicine and Biotechnology*, 2011, 954602-8.
- MARTIN, M. D., KIM, M. T., SHAN, Q., SOMPALLAE, R., XUE, H. H., HARTY, J. T. & BADOVINAC, V. P. 2015. Phenotypic and Functional Alterations in Circulating Memory CD8 T Cells with Time after Primary Infection. *PLoS Pathog*, 11, e1005219.
- MASOPIST, D., VEZYS, V., MARZO, A. L. & LEFRANCOIS, L. 2001. Preferential localization of effector memory cells in nonlymphoid tissue. *Science*, 291, 2413-7.
- MASTELIC, B., DO ROSARIO, A. P., VELDHONEN, M., RENAULD, J. C., JARRA, W., SPONAAS, A. M., ROETYNCK, S., STOCKINGER, B. & LANGHORNE, J. 2012. IL-22 Protects Against Liver Pathology and Lethality of an Experimental Blood-Stage Malaria Infection. *Front Immunol*, 3, 85.

- MATUSCHEWSKI, K., NUNES, A., NUSSENZWEIG, V. & MÉNARD, R. 2002. Plasmodium sporozoite invasion into insect and mammalian cells is directed by the same dual binding system. *EMBO*, 21.
- MCCUSKEY, R. S. & REILLY, F. D. 1993. Hepatic microvasculature: dynamic structure and its regulation. *Semin Liver Dis*, 13, 1-12.
- MCFARLAND, B. J., BEESON, C. & SANT, A. J. 1999. Cutting Edge: A Single, Essential Hydrogen Bond Controls the Stability of Peptide-MHC Class II Complexes. *The Journal of Immunology*, 163, 3567-3571.
- MCGREGOR, I. A., ROWE, D. S., WILSON, M. E. & BILLEWICZ, W. Z. 1970. Plasma immunoglobulin concentrations in an African (Gambian) community in relation to season, malaria and other infections and pregnancy. *Clin Exp Immunol*, 7, 51-74.
- MCGREGOR, I. A., TURNER, M. W., WILLIAMS, K. & HALL, P. 1968. Soluble Antigens in the Blood of African Patients with Severe Plasmodium Falciparum Malaria. *The Lancet*, 291, 881-884.
- MCLEAN, A. R., ATAIDE, R., SIMPSON, J. A., BEESON, J. G. & FOWKES, F. J. 2015. Malaria and immunity during pregnancy and postpartum: a tale of two species. *Parasitology*, 142, 999-1015.
- MEDICA, D. L. & SINNIS, P. 2005. Quantitative dynamics of Plasmodium yoelii sporozoite transmission by infected anopheline mosquitoes. *Infect Immun*, 73, 4363-9.
- MEDZHITOV, R. & JANEWAY, C. A., JR. 1997. Innate immunity: the virtues of a nonclonal system of recognition. *Cell*, 91, 295-8.
- MEIS, J. F., VERHAVE, J. P., JAP, P. H., SINDEN, R. E. & MEUWISSEN, J. H. 1983. Ultrastructural observations on the infection of rat liver by Plasmodium berghei sporozoites in vivo. *J Protozool*, 30, 361-6.
- MENSAH, V. A., GUEYE, A., NDIAYE, M., EDWARDS, N. J., WRIGHT, D., ANAGNOSTOU, N. A., SYLL, M., NDAW, A., ABIOLA, A., BLISS, C., GOMIS, J. F., PETERSEN, I., OGWANG, C., DIEYE, T., VIEBIG, N. K., LAWRIE, A. M., ROBERTS, R., NICOSIA, A., FAYE, B., GAYE, O., LEROY, O., IMOUKHUEDE, E. B., EWER, K. J., BEJON, P., HILL, A. V., CISSE, B. & GROUP, M. 2016. Safety, Immunogenicity and Efficacy of Prime-Boost Vaccination with ChAd63 and MVA Encoding ME-TRAP against Plasmodium falciparum Infection in Adults in Senegal. *PLoS One*, 11, e0167951.
- MIKOLAJCZAK, S. A., LAKSHMANAN, V., FISHBAUGHER, M., CAMARGO, N., HARUPA, A., KAUSHANSKY, A., DOUGLASS, A. N., BALDWIN, M., HEALER, J., O'NEILL, M., PHUONG, T., COWMAN, A. & KAPPE, S. H. 2014. A next-generation genetically attenuated Plasmodium falciparum parasite created by triple gene deletion. *Mol Ther*, 22, 1707-15.
- MILLER, J. L., SACK, B. K., BALDWIN, M., VAUGHAN, A. M. & KAPPE, S. H. I. 2014. Interferon-Mediated Innate Immune Responses against Malaria Parasite Liver Stages. *CellReports*, 7, 436-447.
- MIURA, K., KEISTER, D. B., MURATOVA, O. V., SATTABONGKOT, J., LONG, C. A. & SAUL, A. 2007. Transmission-blocking activity induced by malaria vaccine candidates Pfs25/Pvs25 is a direct and predictable function of antibody titer. *Malar J*, 6, 107.

- MIYAKODA, M., KIMURA, D., YUDA, M., CHINZEI, Y., SHIBATA, Y., HONMA, K. & YUI, K. 2008. Malaria-specific and nonspecific activation of CD8+ T cells during blood stage of *Plasmodium berghei* infection. *J Immunol*, 181, 1420-8.
- MOHAN K, MOULIN P & MM., S. 1997. Natural killer cell cytokine production, not cytotoxicity, contributes to resistance against blood-stage *Plasmodium chabaudi* AS infection. *J Immunol.*, 77.
- MONSO-HINARD, C., LOU, J. N., BEHR, C., JUILLARD, P. & GRAU, G. E. 1997. Expression of major histocompatibility complex antigens on mouse brain microvascular endothelial cells in relation to susceptibility to cerebral malaria. *Immunology*, 92, 53-9.
- MONTES DE OCA, M., KUMAR, R., DE LABASTIDA RIVERA, F., AMANTE, F. H., SHEEL, M., FALEIRO, R. J., BUNN, P. T., BEST, S. E., BEATTIE, L., NG, S. S., EDWARDS, C. L., MULLER, W., CRETNEY, E., NUTT, S. L., SMYTH, M. J., HAQUE, A., HILL, G. R., SUNDAR, S., KALLIES, A. & ENGWERDA, C. R. 2016. Blimp-1-Dependent IL-10 Production by Tr1 Cells Regulates TNF-Mediated Tissue Pathology. *PLoS Pathog*, 12, e1005398.
- MOON, J. J., CHU, H. H., PEPPER, M., MCSORLEY, S. J., JAMESON, S. C., KEDL, R. M. & JENKINS, M. K. 2007. Naive CD4+ T Cell Frequency Varies for Different Epitopes and Predicts Repertoire Diversity and Response Magnitude. *Immunity*, 27, 203-213.
- MORA, J. R., BONO, M. R., MANJUNATH, N., WENINGER, W., CAVANAGH, L. L., ROSEMBLATT, M. & VON ANDRIAN, U. H. 2003. Selective imprinting of gut-homing T cells by Peyer's patch dendritic cells. *Nature*, 424, 88-93.
- MORDMULLER, B., SURAT, G., LAGLER, H., CHAKRAVARTY, S., ISHIZUKA, A. S., LALREMRUATA, A., GMEINER, M., CAMPO, J. J., ESEN, M., RUBEN, A. J., HELD, J., CALLE, C. L., MENGUE, J. B., GEBRU, T., IBANEZ, J., SULYOK, M., JAMES, E. R., BILLINGSLEY, P. F., NATASHA, K. C., MANOJ, A., MURSHEDKAR, T., GUNASEKERA, A., EAPPEN, A. G., LI, T., STAFFORD, R. E., LI, M., FELGNER, P. L., SEDER, R. A., RICHIE, T. L., SIM, B. K., HOFFMAN, S. L. & KREMSNER, P. G. 2017. Sterile protection against human malaria by chemoattenuated PfSPZ vaccine. *Nature*, 542, 445-449.
- MORENO, A., CLAVIJO, P., EDELMAN, R., DAVIS, J., SZTEIN, M., HERRINGTON, D. & NARDIN, E. 1991. Cytotoxic CD4+ T cells from a sporozoite-immunized volunteer recognize the *Plasmodium falciparum* CS protein. *Int Immunol*, 3, 997-1003.
- MORROT, A., HAFALLA, J. C., COCKBURN, I. A., CARVALHO, L. H. & ZAVALA, F. 2005. IL-4 receptor expression on CD8+ T cells is required for the development of protective memory responses against liver stages of malaria parasites. *J Exp Med*, 202, 551-60.
- MOTA, M. M., BROWN, K. N., HOLDER, A. A. & JARRA, W. 1998. Acute *Plasmodium chabaudi chabaudi* malaria infection induces antibodies which bind to the surfaces of parasitized erythrocytes and promote their phagocytosis by macrophages in vitro. *Infect Immun*, 66, 4080-6.
- MOTA, M. M., HAFALLA, J. C. & RODRIGUEZ, A. 2002. Migration through host cells activates *Plasmodium* sporozoites for infection. *Nat Med*, 8, 1318-22.

- MOTA, M. M., PRADEL, G., VANDERBERG, J. P., HAFALLA, J. C. R., FREVERT, U., NUSSENZWEIG, R. S., NUSSENZWEIG, V. & RODRÍGUEZ, A. 2001. Migration of Plasmodium Sporozoites Through Cells Before Infection. *Science*, 291, 141-144.
- MOU, Z., LI, J., BOUSSOFFARA, T., KISHI, H., HAMANA, H., EZZATI, P., HU, C., YI, W., LIU, D., KHADEM, F., OKWOR, I., JIA, P., SHITAOKA, K., WANG, S., NDAO, M., PETERSEN, C., CHEN, J., RAFATI, S., LOUZIR, H., MURAGUCHI, A., WILKINS, J. A. & UZONNA, J. E. 2015. Identification of broadly conserved cross-species protective Leishmania antigen and its responding CD4+ T cells. *Sci Transl Med*, 7, 310ra167.
- MUELLER, A. K., DECKERT, M., HEISS, K., GOETZ, K., MATUSCHEWSKI, K. & SCHLUTER, D. 2007. Genetically attenuated Plasmodium berghei liver stages persist and elicit sterile protection primarily via CD8 T cells. *Am J Pathol*, 171, 107-15.
- NACER, A., MOVILA, A., BAER, K., MIKOLAJCZAK, S. A., KAPPE, S. H. & FREVERT, U. 2012. Neuroimmunological blood brain barrier opening in experimental cerebral malaria. *PLoS Pathog*, 8, e1002982.
- NAGATA, S. & GOLSTEIN, P. 1995. The Fas death factor. *Science*, 267, 1449-56.
- NAKAGAWA, R., MOTOKI, K., UENO, H., IJIMA, R., NAKAMURA, H., KOBAYASHI, E., SHIMOSAKA, A. & KOEZUKA, Y. 1998. Treatment of hepatic metastasis of the colon26 adenocarcinoma with an alpha-galactosylceramide, KRN7000. *Cancer Res*, 58, 1202-7.
- NDAM, N. T. & DELORON, P. 2007. Molecular aspects of Plasmodium falciparum Infection during pregnancy. *J Biomed Biotechnol*, 2007, 43785.
- NEBIE, I., DIARRA, A., OUEDRAOGO, A., TIONO, A. B., KONATE, A. T., GANSANE, A., SOULAMA, I., COUSENS, S., LEROY, O. & SIRIMA, S. B. 2009. Humoral and cell-mediated immunity to MSP3 peptides in adults immunized with MSP3 in malaria endemic area, Burkina Faso. *Parasite Immunol*, 31, 474-80.
- NELSON, C. A., PETZOLD, S. J. & UNANUE, E. R. 1994. Peptides determine the lifespan of MHC class II molecules in the antigen-presenting cell. *Nature*, 371, 250-2.
- NIE, C. Q., BERNARD, N. J., SCHOFIELD, L. & HANSEN, D. S. 2007. CD4+ CD25+ regulatory T cells suppress CD4+ T-cell function and inhibit the development of Plasmodium berghei-specific TH1 responses involved in cerebral malaria pathogenesis. *Infect Immun*, 75, 2275-82.
- NITCHEU, J., BONDUELLE, O., COMBADIÈRE, C., TEFIT, M., SEILHEAN, D., MAZIER, D. & COMBADIÈRE, B. 2003. Perforin-dependent brain-infiltrating cytotoxic CD8+ T lymphocytes mediate experimental cerebral malaria pathogenesis. *J Immunol*, 170, 2221-8.
- NUNES-SILVA, S., DECHAVANNE, S., MOUSSILIOU, A., PSTRAG, N., SEMBLAT, J. P., GANGNARD, S., TUIKUE-NDAM, N., DELORON, P., CHENE, A. & GAMAIN, B. 2015. Beninese children with cerebral malaria do not develop humoral immunity against the IT4-VAR19-DC8 PfEMP1 variant linked to EPCR and brain endothelial binding. *Malar J*, 14, 493.
- NURIEVA, R. I., CHUNG, Y., HWANG, D., YANG, X. O., KANG, H. S., MA, L., WANG, Y. H., WATOWICH, S. S., JETTEN, A. M., TIAN, Q. & DONG, C. 2008. Generation of T follicular helper cells is mediated by interleukin-21 but independent of T helper 1, 2, or 17 cell lineages. *Immunity*, 29, 138-49.

- NUSSENZWEIG, R. S., VANDERBERG, J., MOST, H. & ORTON, C. 1967. Protective immunity produced by the injection of x-irradiated sporozoites of plasmodium berghei. *Nature*, 216, 160-2.
- NUSSLER, A. K., RENIA, L., PASQUETTO, V., MILTGEN, F., MATILE, H. & MAZIER, D. 1993. In vivo induction of the nitric oxide pathway in hepatocytes after injection with irradiated malaria sporozoites, malaria blood parasites or adjuvants. *Eur J Immunol*, 23, 882-7.
- OAKLEY, M. S., SAHU, B. R., LOTSPEICH-COLE, L., SOLANKI, N. R., MAJAM, V., PHAM, P. T., BANERJEE, R., KOZAKAI, Y., DERRICK, S. C., KUMAR, S. & MORRIS, S. L. 2013. The transcription factor T-bet regulates parasitemia and promotes pathogenesis during Plasmodium berghei ANKA murine malaria. *J Immunol*, 191, 4699-708.
- OBENG-ADJEI, N., PORTUGAL, S., TRAN, T. M., YAZEWE, T. B., SKINNER, J., LI, S., JAIN, A., FELGNER, P. L., DOUMBO, O. K., KAYENTAO, K., ONGOIBA, A., TRAORE, B. & CROMPTON, P. D. 2015. Circulating Th1-Cell-type Tfh Cells that Exhibit Impaired B Cell Help Are Preferentially Activated during Acute Malaria in Children. *Cell Rep*, 13, 425-39.
- OCANA-MORGNER, C., MOTA, M. M. & RODRIGUEZ, A. 2003. Malaria blood stage suppression of liver stage immunity by dendritic cells. *J Exp Med*, 197, 143-51.
- OFORI, M. F., DODOO, D., STAALSOE, T., KURTZHALS, J. A., KORAM, K., THEANDER, T. G., AKANMORI, B. D. & HVIID, L. 2002. Malaria-induced acquisition of antibodies to Plasmodium falciparum variant surface antigens. *Infect Immun*, 70, 2982-8.
- OGWANG, C., KIMANI, D., EDWARDS, N. J., ROBERTS, R., MWACHARO, J., BOWYER, G., BLISS, C., HODGSON, S. H., NJUGUNA, P., VIEBIG, N. K., NICOSIA, A., GITAU, E., DOUGLAS, S., ILLINGWORTH, J., MARSH, K., LAWRIE, A., IMOUKHUEDE, E. B., EWER, K., URBAN, B. C., HILL, A. V. S., BEJON, P. & GROUP, M. 2015. Prime-boost vaccination with chimpanzee adenovirus and modified vaccinia Ankara encoding TRAP provides partial protection against Plasmodium falciparum infection in Kenyan adults. *Sci Transl Med*, 7, 286re5.
- OLIVEIRA, G. A., KUMAR, K. A., CALVO-CALLE, J. M., OTHORO, C., ALTSZULER, D., NUSSENZWEIG, V. & NARDIN, E. H. 2008. Class II-Restricted Protective Immunity Induced by Malaria Sporozoites. *Infection and Immunity*, 76, 1200-1206.
- LOTU, A., FEGAN, G., WAMBUA, J., NYANGWESO, G., LEACH, A., LIEVENS, M., KASLOW, D. C., NJUGUNA, P., MARSH, K. & BEJON, P. 2016. Seven-Year Efficacy of RTS,S/AS01 Malaria Vaccine among Young African Children. *N Engl J Med*, 374, 2519-29.
- OLSON, J. A., MCDONALD-HYMAN, C., JAMESON, S. C. & HAMILTON, S. E. 2013. Effector-like CD8(+) T cells in the memory population mediate potent protective immunity. *Immunity*, 38, 1250-60.
- OPFERMAN, J. T., LETAI, A., BEARD, C., SORCINELLI, M. D., ONG, C. C. & KORSMEYER, S. J. 2003. Development and maintenance of B and T lymphocytes requires antiapoptotic MCL-1. *Nature*, 426, 671-6.
- OSSINA, N. K., CANNAS, A., POWERS, V. C., FITZPATRICK, P. A., KNIGHT, J. D., GILBERT, J. R., SHEKHTMAN, E. M., TOMEI, L. D., UMANSKY, S. R. & KIEFER, M. C. 1997. Interferon-gamma modulates a p53-independent apoptotic pathway and apoptosis-related gene expression. *J Biol Chem*, 272, 16351-7.

- OWUSU-AGYEI, S., KORAM, K. A., BAIRD, J. K., UTZ, G. C., BINKA, F. N., NKRUMAH, F. K., FRYAUFF, D. J. & HOFFMAN, S. L. 2001. Incidence of symptomatic and asymptomatic *Plasmodium falciparum* infection following curative therapy in adult residents of northern Ghana. *Am J Trop Med Hyg*, 65, 197-203.
- PAI, S., QIN, J., CAVANAGH, L., MITCHELL, A., EL-ASSAAD, F., JAIN, R., COMBES, V., HUNT, N. H., GRAU, G. E. & WENINGER, W. 2014. Real-time imaging reveals the dynamics of leukocyte behaviour during experimental cerebral malaria pathogenesis. *PLoS Pathog*, 10, e1004236.
- PALLAVI, R., ROY, N., NAGESHAN, R. K., TALUKDAR, P., PAVITHRA, S. R., REDDY, R., VENKETESH, S., KUMAR, R., GUPTA, A. K., SINGH, R. K., YADAV, S. C. & TATU, U. 2010. Heat shock protein 90 as a drug target against protozoan infections: biochemical characterization of HSP90 from *Plasmodium falciparum* and *Trypanosoma evansi* and evaluation of its inhibitor as a candidate drug. *J Biol Chem*, 285, 37964-75.
- PANINA-BORDIGNON, P., PAPI, A., MARIANI, M., DI LUCIA, P., CASONI, G., BELLETTATO, C., BUONSANTI, C., MIOTTO, D., MAPP, C., VILLA, A., ARRIGONI, G., FABBRI, L. M. & SINIGAGLIA, F. 2001. The C-C chemokine receptors CCR4 and CCR8 identify airway T cells of allergen-challenged atopic asthmatics. *J Clin Invest*, 107, 1357-64.
- PARK, B., LEE, S., KIM, E. & AHN, K. 2003. A single polymorphic residue within the peptide-binding cleft of MHC class I molecules determines spectrum of tapasin dependence. *J Immunol*, 170, 961-8.
- PARK, J. R., DIGIUSTO, D. L., SLOVAK, M., WRIGHT, C., NARANJO, A., WAGNER, J., MEECHOOVET, H. B., BAUTISTA, C., CHANG, W. C., OSTBERG, J. R. & JENSEN, M. C. 2007. Adoptive transfer of chimeric antigen receptor re-directed cytolytic T lymphocyte clones in patients with neuroblastoma. *Mol Ther*, 15, 825-33.
- PARK, S. L., BUZZAI, A., RAUTELA, J., HOR, J. L., HOCHHEISER, K., EFFERN, M., MCBAIN, N., WAGNER, T., EDWARDS, J., MCCONVILLE, R., WILMOTT, J. S., SCOLYER, R. A., TUTING, T., PALENDIRA, U., GYORKI, D., MUELLER, S. N., HUNTINGTON, N. D., BEDOUI, S., HOLZEL, M., MACKAY, L. K., WAITHMAN, J. & GEBHARDT, T. 2019. Tissue-resident memory CD8(+) T cells promote melanoma-immune equilibrium in skin. *Nature*, 565, 366-371.
- PARK, S. L., ZAID, A., HOR, J. L., CHRISTO, S. N., PRIER, J. E., DAVIES, B., ALEXANDRE, Y. O., GREGORY, J. L., RUSSELL, T. A., GEBHARDT, T., CARBONE, F. R., TSCHARKE, D. C., HEATH, W. R., MUELLER, S. N. & MACKAY, L. K. 2018. Local proliferation maintains a stable pool of tissue-resident memory T cells after antiviral recall responses. *Nat Immunol*, 19, 183-191.
- PARKER, D. C. 1993. T cell-dependent B cell activation. *Annu Rev Immunol*, 11, 331-60.
- PARTNERSHIP, R. C. T. 2015. Articles Efficacy and safety of RTS,S/AS01 malaria vaccine with or without a booster dose in infants and children in Africa: final results of a phase 3, individually randomised, controlled trial. *The Lancet*, 386, 31-45.
- PAYNE, R. O., SILK, S. E., ELIAS, S. C., MIURA, K., DIOUF, A., GALAWAY, F., DE GRAAF, H., BRENDISH, N. J., POULTON, I. D., GRIFFITHS, O. J., EDWARDS, N. J., JIN, J., LABBE, G. M., ALANINE, D. G., SIANI, L., DI MARCO, S., ROBERTS, R., GREEN, N., BERRIE, E., ISHIZUKA, A. S., NIELSEN, C. M., BARDELLI, M., PARTEY, F. D., OFORI, M. F.,

- BARFOD, L., WAMBUA, J., MURUNGI, L. M., OSIER, F. H., BISWAS, S., MCCARTHY, J. S., MINASSIAN, A. M., ASHFIELD, R., VIEBIG, N. K., NUGENT, F. L., DOUGLAS, A. D., VEKEMANS, J., WRIGHT, G. J., FAUST, S. N., HILL, A. V., LONG, C. A., LAWRIE, A. M. & DRAPER, S. J. 2017. Human vaccination against RH5 induces neutralizing antimalarial antibodies that inhibit RH5 invasion complex interactions. *JCI Insight*, 2.
- PEARCE, E. L., WALSH, M. C., CEJAS, P. J., HARMS, G. M., SHEN, H., WANG, L. S., JONES, R. G. & CHOI, Y. 2009. Enhancing CD8 T-cell memory by modulating fatty acid metabolism. *Nature*, 460, 103-7.
- PEREZ, D. & WHITE, E. 2000. TNF- $\alpha$  Signals Apoptosis through a Bid-Dependent Conformational Change in Bax that Is Inhibited by E1B 19K. *Molecular Cell*, 6, 53-63.
- PEREZ-MAZLIAH, D., NG, D. H., FREITAS DO ROSARIO, A. P., MCLAUGHLIN, S., MASTELIC-GAVILLET, B., SODENKAMP, J., KUSHINGA, G. & LANGHORNE, J. 2015. Disruption of IL-21 signaling affects T cell-B cell interactions and abrogates protective humoral immunity to malaria. *PLoS Pathog*, 11, e1004715.
- PEREZ-MAZLIAH, D., NGUYEN, M. P., HOSKING, C., MCLAUGHLIN, S., LEWIS, M. D., TUMWINE, I., LEVY, P. & LANGHORNE, J. 2017. Follicular Helper T Cells are Essential for the Elimination of Plasmodium Infection. *EBioMedicine*, 24, 216-230.
- PERKINS, D. J., WERE, T., DAVENPORT, G. C., KEMPAIAH, P., HITTNER, J. B. & ONG'ECHA, J. M. 2011. Severe malarial anemia: innate immunity and pathogenesis. *Int J Biol Sci*, 7, 1427-42.
- PERRY, J. A., RUSH, A., WILSON, R. J., OLVER, C. S. & AVERY, A. C. 2004. Dendritic cells from malaria-infected mice are fully functional APC. *J Immunol*, 172, 475-82.
- PHILLIPS, M. A., BURROWS, J. N., MANYANDO, C., VAN HUIJSDUIJNEN, R. H., VAN VOORHIS, W. C. & WELLS, T. N. C. 2017. Malaria. *Nat Rev Dis Primers*, 3, 17050.
- PICHUGIN, A., ZARLING, S., PERAZZO, L., DUFFY, P. E., PLOEGH, H. L. & KRZYCH, U. 2018. Identification of a Novel CD8 T Cell Epitope Derived from Plasmodium berghei Protective Liver-Stage Antigen. *Front Immunol*, 9, 91.
- PINZON-CHARRY, A., MCPHUN, V., KIENZLE, V., HIRUNPETCHARAT, C., ENGWERDA, C., MCCARTHY, J. & GOOD, M. F. 2010. Low doses of killed parasite in CpG elicit vigorous CD4+ T cell responses against blood-stage malaria in mice. *J Clin Invest*, 120, 2967-78.
- PINZON-ORTIZ, C., FRIEDMAN, J., ESKO, J. & SINNIS, P. 2001. The binding of the circumsporozoite protein to cell surface heparan sulfate proteoglycans is required for plasmodium sporozoite attachment to target cells. *J Biol Chem*, 276, 26784-91.
- POLLIZZI, K. N., SUN, I. H., PATEL, C. H., LO, Y. C., OH, M. H., WAICKMAN, A. T., TAM, A. J., BLOSSER, R. L., WEN, J., DELGOFFE, G. M. & POWELL, J. D. 2016. Asymmetric inheritance of mTORC1 kinase activity during division dictates CD8(+) T cell differentiation. *Nat Immunol*, 17, 704-11.
- POMBO, D. J., LAWRENCE, G., HIRUNPETCHARAT, C., RZEPczyk, C., BRYDEN, M., CLOONAN, N., ANDERSON, K., MAHAKUNKIJCHAROEN, Y., MARTIN, L. B., WILSON, D., ELLIOTT, S., ELLIOTT, S., EISEN, D. P., WEINBERG, J. B., SAUL, A. &

- GOOD, M. F. 2002. Immunity to malaria after administration of ultra-low doses of red cells infected with *Plasmodium falciparum*. *The Lancet*, 360, 610-617.
- PONGPONRATN, E., TURNER, G. D., DAY, N. P., PHU, N. H., SIMPSON, J. A., STEPNIEWSKA, K., MAI, N. T. H., VIRIYAVEJAKUL, P., LOOAREESUWAN, S. & HIEN, T. T. 2003. An ultrastructural study of the brain in fatal *Plasmodium falciparum* malaria. *The American journal of tropical medicine and hygiene*, 69, 345-359.
- PRADEL, G. & FREVERT, U. 2001. Malaria sporozoites actively enter and pass through rat Kupffer cells prior to hepatocyte invasion. *Hepatology*, 33, 1154-65.
- PULENDRAN, B., SMITH, J. L., CASPARY, G., BRASEL, K., PETTIT, D., MARASKOVSKY, E. & MALISZEWSKI, C. R. 1999. Distinct dendritic cell subsets differentially regulate the class of immune response in vivo. *Proc Natl Acad Sci U S A*, 96, 1036-41.
- PURCELL, A. W. & ELLIOTT, T. 2008. Molecular machinations of the MHC-I peptide loading complex. *Curr Opin Immunol*, 20, 75-81.
- QARI, S. H., SHI, Y.-P., GOLDMAN, I. F., NAHLEN, B. L., TIBAYRENC, M. & LAL, A. A. 1998. Predicted and observed alleles of *Plasmodium falciparum* merozoite surface protein-1 (MSP-1), a potential malaria vaccine antigen. *Molecular and Biochemical Parasitology*, 92, 241-252.
- RADTKE, A. J., ANDERSON, C. F., RITEAU, N., RAUSCH, K., SCARIA, P., KELNHOFER, E. R., HOWARD, R. F., SHER, A., GERMAIN, R. N. & DUFFY, P. 2017. Adjuvant and carrier protein-dependent T-cell priming promotes a robust antibody response against the *Plasmodium falciparum* Pfs25 vaccine candidate. *Sci Rep*, 7, 40312.
- RADTKE, A. J., KASTENMULLER, W., ESPINOSA, D. A., GERNER, M. Y., TSE, S. W., SINNIS, P., GERMAIN, R. N., ZAVALA, F. P. & COCKBURN, I. A. 2015. Lymph-node resident CD8alpha+ dendritic cells capture antigens from migratory malaria sporozoites and induce CD8+ T cell responses. *PLoS Pathog*, 11, e1004637.
- RAES, G., BESCHIN, A., GHASSABEH, G. H. & DE BAETSELIER, P. 2007. Alternatively activated macrophages in protozoan infections. *Curr Opin Immunol*, 19, 454-9.
- RATHMELL, J. C., FARKASH, E. A., GAO, W. & THOMPSON, C. B. 2001. IL-7 enhances the survival and maintains the size of naive T cells. *J Immunol*, 167, 6869-76.
- RAULET, D. H., VANCE, R. E. & MCMAHON, C. W. 2001. Regulation of the natural killer cell receptor repertoire. *Annu Rev Immunol*, 19, 291-330.
- RAY, S. J., FRANKI, S. N., PIERCE, R. H., DIMITROVA, S., KOTELIANSKY, V., SPRAGUE, A. G., DOHERTY, P. C., DE FOUGEROLLES, A. R. & TOPHAM, D. J. 2004. The collagen binding alpha1beta1 integrin VLA-1 regulates CD8 T cell-mediated immune protection against heterologous influenza infection. *Immunity*, 20, 167-79.
- REECE, W. H. H., PINDER, M., GOTHARD, P. K., MILLIGAN, P., BOJANG, K., DOHERTY, T., PLEBANSKI, M., AKINWUNMI, P., EVERAERE, S., WATKINS, K. R., VOSS, G., TORNIEPORTH, N., ALLOUECHE, A., GREENWOOD, B. M., KESTER, K. E., MCADAM, K. P. W. J., COHEN, J. & HILL, A. V. S. 2004. A CD4+ T-cell immune response to a conserved epitope in the circumsporozoite protein correlates with protection from natural *Plasmodium falciparum* infection and disease. *Nature Medicine*, 10, 406-410.
- REEDER, J. C., COWMAN, A. F., DAVERN, K. M., BEESON, J. G., THOMPSON, J. K., ROGERSON, S. J. & BROWN, G. V. 1999. The adhesion of *Plasmodium falciparum*-

- infected erythrocytes to chondroitin sulfate A is mediated by P. falciparum erythrocyte membrane protein 1. *Proc Natl Acad Sci U S A*, 96, 5198-202.
- RICHTER, J., FRANKEN, G., MEHLHORN, H., LABISCH, A. & HAUSSINGER, D. 2010. What is the evidence for the existence of Plasmodium ovale hypnozoites? *Parasitol Res*, 107, 1285-90.
- RIGGLE, B. A., MANGLANI, M., MARIC, D., JOHNSON, K. R., LEE, M. H., NETO, O. L. A., TAYLOR, T. E., SEYDEL, K. B., NATH, A., MILLER, L. H., MCGAVERN, D. B. & PIERCE, S. K. 2020. CD8+ T cells target cerebrovasculature in children with cerebral malaria. *J Clin Invest*, 130, 1128-1138.
- RIGLAR, D. T., RICHARD, D., WILSON, D. W., BOYLE, M. J., DEKIWADIA, C., TURNBULL, L., ANGRISANO, F., MARAPANA, D. S., ROGERS, K. L., WHITCHURCH, C. B., BEESON, J. G., COWMAN, A. F., RALPH, S. A. & BAUM, J. 2011. Super-resolution dissection of coordinated events during malaria parasite invasion of the human erythrocyte. *Cell Host Microbe*, 9, 9-20.
- ROCA, F. J. & RAMAKRISHNAN, L. 2013. TNF dually mediates resistance and susceptibility to mycobacteria via mitochondrial reactive oxygen species. *Cell*, 153, 521-34.
- ROESTENBERG, M., TEIRLINCK, A. C., MCCALL, M. B. B., TEELEN, K., MAKAMDOP, K. N., WIERSMA, J., ARENS, T., BECKERS, P., VAN GEMERT, G., VAN DE VEGTE-BOLMER, M., VAN DER VEN, A. J. A. M., LUTY, A. J. F., HERMSEN, C. C. & SAUERWEIN, R. W. 2011. Long-term protection against malaria after experimental sporozoite inoculation: an open-label follow-up study. *The Lancet*, 377, 1770-1776.
- ROGERSON, S. J., BROWN, H. C., POLLINA, E., ABRAMS, E. T., TADESSE, E., LEMA, V. M. & MOLYNEUX, M. E. 2003a. Placental tumor necrosis factor alpha but not gamma interferon is associated with placental malaria and low birth weight in Malawian women. *Infect Immun*, 71, 267-70.
- ROGERSON, S. J., DESAI, M., MAYOR, A., SICURI, E., TAYLOR, S. M. & VAN EIJK, A. M. 2018. Burden, pathology, and costs of malaria in pregnancy: new developments for an old problem. *The Lancet Infectious Diseases*, 18, e107-e118.
- ROGERSON, S. J., MOLYNEUX, M. E., LEMA, V. M., POLLINA, E., TADESSE, E. & GETACHEW, A. 2003b. Placental Monocyte Infiltrates in Response to Plasmodium Falciparum Malaria Infection and Their Association with Adverse Pregnancy Outcomes. *The American Journal of Tropical Medicine and Hygiene*, 68, 115-119.
- ROLAND, J., SOULARD, V., SELLIER, C., DRAPIER, A. M., DI SANTO, J. P., CAZENAVE, P. A. & PIED, S. 2006. NK Cell Responses to Plasmodium Infection and Control of Intrahepatic Parasite Development. *The Journal of Immunology*, 177, 1229-1239.
- ROMAGNOLI, P. A., FU, H. H., QIU, Z., KHAIRALLAH, C., PHAM, Q. M., PUDDINGTON, L., KHANNA, K. M., LEFRANCOIS, L. & SHERIDAN, B. S. 2017. Differentiation of distinct long-lived memory CD4 T cells in intestinal tissues after oral Listeria monocytogenes infection. *Mucosal Immunol*, 10, 520-530.
- ROMERO, J. F., EBERL, G., ROBSON MACDONALD, H. & CORRADIN, G. 2001. CD1d-restricted NK T cells are dispensable for specific antibody responses and protective immunity against liver stage malaria infection in mice. Research note. *Parasite immunology*, 23, 267-269.

- RONET, C., DARCHE, S., LEITE DE MORAES, M., MIYAKE, S., YAMAMURA, T., LOUIS, J. A., KASPER, L. H. & BUZONI-GATEL, D. 2005. NKT cells are critical for the initiation of an inflammatory bowel response against *Toxoplasma gondii*. *J Immunol*, 175, 899-908.
- RTS, S. C. T. P. 2015. Articles Efficacy and safety of RTS,S/AS01 malaria vaccine with or without a booster dose in infants and children in Africa: final results of a phase 3, individually randomised, controlled trial. *The Lancet*, 386, 31-45.
- RUBTSOV, A. V., RUBTSOVA, K., FISCHER, A., MEEHAN, R. T., GILLIS, J. Z., KAPPLER, J. W. & MARRACK, P. 2011. Toll-like receptor 7 (TLR7)-driven accumulation of a novel CD11c(+) B-cell population is important for the development of autoimmunity. *Blood*, 118, 1305-15.
- RUDENSKY, Y., PRESTON-HURLBURT, P., HONG, S. C., BARLOW, A. & JANEWAY, C. A., JR. 1991. Sequence analysis of peptides bound to MHC class II molecules. *Nature*, 353, 622-7.
- RYG-CORNEJO, V., NIE, C. Q., BERNARD, N. J., LUNDIE, R. J., EVANS, K. J., CRABB, B. S., SCHOFIELD, L. & HANSEN, D. S. 2013. NK cells and conventional dendritic cells engage in reciprocal activation for the induction of inflammatory responses during *Plasmodium berghei* ANKA infection. *Immunobiology*, 218, 263-71.
- SABA, N., SULTANA, A. & I., M. 2008. OUTCOME AND COMPLICATIONS OF MALARIA IN PREGNANCY. *Gomal Journal of Medical Sciences*, 6, 98-101.
- SAKAI, S., KAUFFMAN, K. D., SCHENKEL, J. M., MCBERRY, C. C., MAYER-BARBER, K. D., MASOPIUST, D. & BARBER, D. L. 2014. Cutting edge: control of *Mycobacterium tuberculosis* infection by a subset of lung parenchyma-homing CD4 T cells. *J Immunol*, 192, 2965-9.
- SALLUSTO, F., LENIG, D., FORSTER, R., LIPP, M. & LANZAVECCHIA, A. 1999. Two subsets of memory T lymphocytes with distinct homing potentials and effector functions. *Nature*, 401, 708-12.
- SANO, G., HAFALLA, J. C., MORROT, A., ABE, R., LAFAILLE, J. J. & ZAVALA, F. 2001. Swift development of protective effector functions in naive CD8(+) T cells against malaria liver stages. *J Exp Med*, 194, 173-80.
- SARGEANT, T. J., MARTI, M., CALER, E., CARLTON, J. M., SIMPSON, K., SPEED, T. P. & COWMAN, A. F. 2006. Lineage-specific expansion of proteins exported to erythrocytes in malaria parasites. *Genome Biol*, 7, R12.
- SARKAR, S., KALIA, V., HAINING, W. N., KONIECZNY, B. T., SUBRAMANIAM, S. & AHMED, R. 2008. Functional and genomic profiling of effector CD8 T cell subsets with distinct memory fates. *J Exp Med*, 205, 625-40.
- SATHALIYAWALA, T., KUBOTA, M., YUDANIN, N., TURNER, D., CAMP, P., THOME, J. J., BICKHAM, K. L., LERNER, H., GOLDSTEIN, M., SYKES, M., KATO, T. & FARBER, D. L. 2013. Distribution and compartmentalization of human circulating and tissue-resident memory T cell subsets. *Immunity*, 38, 187-97.
- SCHAERLI, P., WILLIMANN, K., LANG, A. B., LIPP, M., LOETSCHER, P. & MOSER, B. 2000. CXC chemokine receptor 5 expression defines follicular homing T cells with B cell helper function. *J Exp Med*, 192, 1553-62.

- SCHENKEL, J. M., FRASER, K. A., CASEY, K. A., BEURA, L. K., PAUKEN, K. E., VEZYS, V. & MASOPIUST, D. 2016. IL-15-Independent Maintenance of Tissue-Resident and Boosted Effector Memory CD8 T Cells. *J Immunol*, 196, 3920-6.
- SCHENKEL, J. M. & MASOPIUST, D. 2014a. Tissue-resident memory T cells. *Immunity*, 41, 886-97.
- SCHENKEL, J. M. & MASOPIUST, D. 2014b. Tissue-Resident Memory T Cells. *Immunity*, 41, 886-897.
- SCHLUNS, K. S., KIEPER, W. C., JAMESON, S. C. & LEFRANCOIS, L. 2000. Interleukin-7 mediates the homeostasis of naive and memory CD8 T cells in vivo. *Nat Immunol*, 1, 426-32.
- SCHMIDT, A., OBERLE, N. & KRAMMER, P. H. 2012. Molecular mechanisms of treg-mediated T cell suppression. *Front Immunol*, 3, 51.
- SCHMIDT, N. W., BUTLER, N. S., BADOVINAC, V. P. & HARTY, J. T. 2010. Extreme CD8 T cell requirements for anti-malarial liver-stage immunity following immunization with radiation attenuated sporozoites. *PLoS Pathog*, 6, e1000998.
- SCHMIDT, N. W., BUTLER, N. S. & HARTY, J. T. 2011. Plasmodium-host interactions directly influence the threshold of memory CD8 T cells required for protective immunity. *J Immunol*, 186, 5873-84.
- SCHMIDT, N. W., PODYMINOGIN, R. L., BUTLER, N. S., BADOVINAC, V. P., TUCKER, B. J., BAHJAT, K. S., LAUER, P., REYES-SANDOVAL, A., HUTCHINGS, C. L., MOORE, A. C., GILBERT, S. C., HILL, A. V., BARTHOLOMAY, L. C. & HARTY, J. T. 2008. Memory CD8 T cell responses exceeding a large but definable threshold provide long-term immunity to malaria. *Proc Natl Acad Sci U S A*, 105, 14017-22.
- SCHNORRER, P., BEHRENS, G. M., WILSON, N. S., POOLEY, J. L., SMITH, C. M., EL-SUKKARI, D., DAVEY, G., KUPRESANIN, F., LI, M., MARASKOVSKY, E., BELZ, G. T., CARBONE, F. R., SHORTMAN, K., HEATH, W. R. & VILLADANGOS, J. A. 2006. The dominant role of CD8+ dendritic cells in cross-presentation is not dictated by antigen capture. *Proc Natl Acad Sci U S A*, 103, 10729-34.
- SCHOFIELD, L., VILLAQUIRAN, J., FERREIRA, A., SCHELLEKENS, H., NUSSENZWEIG, R. & NUSSENZWEIG, V. 1987. Gamma interferon, CD8+ T cells and antibodies required for immunity to malaria sporozoites. *Nature*, 330, 664-6.
- SEDER, R. A., CHANG, L. J., ENAMA, M. E., ZEPHIR, K. L., SARWAR, U. N., GORDON, I. J., HOLMAN, L. A., JAMES, E. R., BILLINGSLEY, P. F., GUNASEKERA, A., RICHMAN, A., CHAKRAVARTY, S., MANOJ, A., VELMURUGAN, S., LI, M., RUBEN, A. J., LI, T., EAPPEN, A. G., STAFFORD, R. E., PLUMMER, S. H., HENDEL, C. S., NOVIK, L., COSTNER, P. J., MENDOZA, F. H., SAUNDERS, J. G., NASON, M. C., RICHARDSON, J. H., MURPHY, J., DAVIDSON, S. A., RICHIE, T. L., SEDEGAH, M., SUTAMIHARDJA, A., FAHLE, G. A., LYKE, K. E., LAURENS, M. B., ROEDERER, M., TEWARI, K., EPSTEIN, J. E., SIM, B. K., LEDGERWOOD, J. E., GRAHAM, B. S., HOFFMAN, S. L. & TEAM, V. R. C. S. 2013. Protection against malaria by intravenous immunization with a nonreplicating sporozoite vaccine. *Science*, 341, 1359-65.
- SEGUIN, M. C., KLOTZ, F. W., SCHNEIDER, I., WEIR, J. P., GOODBARY, M., SLAYTER, M., RANEY, J. J., ANIAGOLU, J. U. & GREEN, S. J. 1994. Induction of nitric oxide synthase protects against malaria in mice exposed to irradiated Plasmodium

- berghei infected mosquitoes: involvement of interferon gamma and CD8+ T cells. *J Exp Med*, 180, 353-8.
- SERGHIDES, L., SMITH, T. G., PATEL, S. N. & KAIN, K. C. 2003. CD36 and malaria: friends or foes? *Trends Parasitol*, 19, 461-9.
- SEYDEL, K. B., KAMPONDENI, S. D., VALIM, C., POTCHEN, M. J., MILNER, D. A., MUWALO, F. W., BIRBECK, G. L., BRADLEY, W. G., FOX, L. L., GLOVER, S. J., HAMMOND, C. A., HEYDERMAN, R. S., CHILINGULO, C. A., MOLYNEUX, M. E. & TAYLOR, T. E. 2015. Brain swelling and death in children with cerebral malaria. *N Engl J Med*, 372, 1126-37.
- SHEAR, H. L., SRINIVASAN, R., NOLAN, T. & NG, C. 1989. Role of IFN-gamma in lethal and nonlethal malaria in susceptible and resistant murine hosts. *J Immunol*, 143, 2038-44.
- SHERIDAN, B. S., PHAM, Q. M., LEE, Y. T., CAULEY, L. S., PUDDINGTON, L. & LEFRANCOIS, L. 2014. Oral infection drives a distinct population of intestinal resident memory CD8(+) T cells with enhanced protective function. *Immunity*, 40, 747-57.
- SHI, L., KAM, C. M., POWERS, J. C., AEBERSOLD, R. & GREENBERG, A. H. 1992. Purification of three cytotoxic lymphocyte granule serine proteases that induce apoptosis through distinct substrate and target cell interactions. *J Exp Med*, 176, 1521-9.
- SHIN, H. & IWASAKI, A. 2012. A vaccine strategy that protects against genital herpes by establishing local memory T cells. *Nature*, 491, 463-7.
- SHIOW, L. R., ROSEN, D. B., BRDICKOVA, N., XU, Y., AN, J., LANIER, L. L., CYSTER, J. G. & MATLOUBIAN, M. 2006. CD69 acts downstream of interferon-alpha/beta to inhibit S1P1 and lymphocyte egress from lymphoid organs. *Nature*, 440, 540-4.
- SHNYREVA, M., WEAVER, W. M., BLANCHETTE, M., TAYLOR, S. L., TOMPA, M., FITZPATRICK, D. R. & WILSON, C. B. 2004. Evolutionarily conserved sequence elements that positively regulate IFN-gamma expression in T cells. *Proc Natl Acad Sci U S A*, 101, 12622-7.
- SIDOBRE, S., NAIDENKO, O. V., SIM, B. C., GASCOIGNE, N. R., GARCIA, K. C. & KRONENBERG, M. 2002. The V alpha 14 NKT cell TCR exhibits high-affinity binding to a glycolipid/CD1d complex. *J Immunol*, 169, 1340-8.
- SILVIE, O., RUBINSTEIN, E., FRANETICH, J. F., PRENANT, M., BELNOUE, E., RENIA, L., HANNOUN, L., ELING, W., LEVY, S., BOUCHEIX, C. & MAZIER, D. 2003. Hepatocyte CD81 is required for Plasmodium falciparum and Plasmodium yoelii sporozoite infectivity. *Nat Med*, 9, 93-6.
- SINDEN, R. E. 1983. Sexual Development of Malarial Parasites. *Advances in Parasitology Volume 22*.
- SIRIMA, S. B., DURIER, C., KARA, L., HOUARD, S., GANSANE, A., LOULERGUE, P., BAHUAUD, M., BENHAMOUDA, N., NEBIE, I., FABER, B., REMARQUE, E., LAUNAY, O. & GROUP, A. M.-D. S. 2017. Safety and immunogenicity of a recombinant Plasmodium falciparum AMA1-DiCo malaria vaccine adjuvanted with GLA-SE or Alhydrogel(R) in European and African adults: A phase 1a/1b, randomized, double-blind multi-centre trial. *Vaccine*, 35, 6218-6227.
- SIRIMA, S. B., NEBIE, I., OUEDRAOGO, A., TIONO, A. B., KONATE, A. T., GANSANE, A., DERME, A. I., DIARRA, A., OUEDRAOGO, A., SOULAMA, I., CUZZIN-OUATTARA, N., COUSENS, S. & LEROY, O. 2007. Safety and immunogenicity of the Plasmodium

- falciparum merozoite surface protein-3 long synthetic peptide (MSP3-LSP) malaria vaccine in healthy, semi-immune adult males in Burkina Faso, West Africa. *Vaccine*, 25, 2723-32.
- SISSOKO, M. S., HEALY, S. A., KATILE, A., OMASWA, F., ZAIDI, I., GABRIEL, E. E., KAMATE, B., SAMAKE, Y., GUINDO, M. A., DOLO, A., NIANGALY, A., NIARÉ, K., ZEGUIME, A., SISSOKO, K., DIALLO, H., THERA, I., DING, K., FAY, M. P., O'CONNELL, E. M., NUTMAN, T. B., WONG-MADDEN, S., MURSHEDKAR, T., RUBEN, A. J., LI, M., ABEBE, Y., MANOJ, A., GUNASEKERA, A., CHAKRAVARTY, S., SIM, B. K. L., BILLINGSLEY, P. F., JAMES, E. R., WALTHER, M., RICHIE, T. L., HOFFMAN, S. L., DOUMBO, O. & DUFFY, P. E. 2017. Safety and efficacy of PfSPZ Vaccine against Plasmodium falciparum via direct venous inoculation in healthy malaria-exposed adults in Mali: a randomised, double-blind phase 1 trial. *The Lancet Infectious Diseases*, 17, 498-509.
- SMITH, C. M., WILSON, N. S., WAITHMAN, J., VILLADANGOS, J. A., CARBONE, F. R., HEATH, W. R. & BELZ, G. T. 2004. Cognate CD4+ T cell licensing of dendritic cells in CD8+ T cell immunity. *Nature Immunology*, 5, 1143-1148.
- SMITH, J. D., CHITNIS, C. E., CRAIG, A. G., ROBERTS, D. J., HUDSON-TAYLOR, D. E., PETERSON, D. S., PINCHES, R., NEWBOLD, C. I. & MILLER, L. H. 1995a. Switches in expression of Plasmodium falciparum var genes correlate with changes in antigenic and cytoadherent phenotypes of infected erythrocytes. *Cell*, 82, 101-110.
- SMITH, J. D., CHITNIS, C. E., CRAIG, A. G., ROBERTS, D. J., HUDSON-TAYLOR, D. E., PETERSON, D. S., PINCHES, R., NEWBOLD, C. I. & MILLER, L. H. 1995b. Switches in expression of plasmodium falciparum var genes correlate with changes in antigenic and cytoadherent phenotypes of infected erythrocytes. *Cell*, 82, 101-110.
- SMITH, N. M., WASSERMAN, G. A., COLEMAN, F. T., HILLIARD, K. L., YAMAMOTO, K., LIPSITZ, E., MALLEY, R., DOOMS, H., JONES, M. R., QUINTON, L. J. & MIZGERD, J. P. 2018. Regionally compartmentalized resident memory T cells mediate naturally acquired protection against pneumococcal pneumonia. *Mucosal Immunol*, 11, 220-235.
- SMOLDERS, J., HEUTINCK, K. M., FRANSEN, N. L., REMMERSWAAL, E. B. M., HOMBRINK, P., TEN BERGE, I. J. M., VAN LIER, R. A. W., HUITINGA, I. & HAMANN, J. 2018. Tissue-resident memory T cells populate the human brain. *Nat Commun*, 9, 4593.
- SNOW, R. W., NAHLEN, B., PALMER, A., DONNELLY, C. A., GUPTA, S. & MARSH, K. 1998. Risk of severe malaria among African infants: direct evidence of clinical protection during early infancy. *J Infect Dis*, 177, 819-22.
- SOKOLOVSKA, A., HEM, S. L. & HOGENESCH, H. 2007. Activation of dendritic cells and induction of CD4(+) T cell differentiation by aluminum-containing adjuvants. *Vaccine*, 25, 4575-85.
- SON, Y. M., CHEON, I. S., WU, Y., LI, C., WANG, Z., GAO, X., CHEN, Y., TAKAHASHI, Y., FU, Y. X., DENT, A. L., KAPLAN, M. H., TAYLOR, J. J., CUI, W. & SUN, J. 2021. Tissue-resident CD4(+) T helper cells assist the development of protective respiratory B and CD8(+) T cell memory responses. *Sci Immunol*, 6.

- SPARWASSER, T., KOCH, E. S., VABULAS, R. M., HEEG, K., LIPFORD, G. B., ELLWART, J. W. & WAGNER, H. 1998. Bacterial DNA and immunostimulatory CpG oligonucleotides trigger maturation and activation of murine dendritic cells. *Eur J Immunol*, 28, 2045-54.
- SPENCE, P. J., JARRA, W., LEVY, P., REID, A. J., CHAPPELL, L., BRUGAT, T., SANDERS, M., BERRIMAN, M. & LANGHORNE, J. 2013. Vector transmission regulates immune control of Plasmodium virulence. *Nature*, 498, 228-31.
- SPIEGEL, S. & MILSTIEN, S. 2011. The outs and the ins of sphingosine-1-phosphate in immunity. *Nat Rev Immunol*, 11, 403-15.
- SPONAAS, A. M., CADMAN, E. T., VOISINE, C., HARRISON, V., BOONSTRA, A., O'GARRA, A. & LANGHORNE, J. 2006. Malaria infection changes the ability of splenic dendritic cell populations to stimulate antigen-specific T cells. *J Exp Med*, 203, 1427-33.
- SRIVASTAVA, S. & ERNST, J. D. 2013. Cutting edge: Direct recognition of infected cells by CD4 T cells is required for control of intracellular Mycobacterium tuberculosis in vivo. *J Immunol*, 191, 1016-20.
- STAALSOE, T., SHULMAN, C. E., BULMER, J. N., KAWUONDO, K., MARSH, K. & HVIID, L. 2004. Variant surface antigen-specific IgG and protection against clinical consequences of pregnancy-associated Plasmodium falciparum malaria. *The Lancet*, 363, 283-289.
- STANISIC, D. I., FINK, J., MAYER, J., COGHILL, S., GORE, L., LIU, X. Q., EL-DEEB, I., RODRIGUEZ, I. B., POWELL, J., WILLEMSSEN, N. M., DE, S. L., HO, M. F., HOFFMAN, S. L., GERRARD, J. & GOOD, M. F. 2018. Vaccination with chemically attenuated Plasmodium falciparum asexual blood-stage parasites induces parasite-specific cellular immune responses in malaria-naive volunteers: a pilot study. *BMC Med*, 16, 184.
- STARY, G., OLIVE, A., RADOVIC-MORENO, A. F., GONDEK, D., ALVAREZ, D., BASTO, P. A., PERRO, M., VRBANAC, V. D., TAGER, A. M., SHI, J., YETHON, J. A., FAROKHZAD, O. C., LANGER, R., STARNBACH, M. N. & VON ANDRIAN, U. H. 2015. VACCINES. A mucosal vaccine against Chlamydia trachomatis generates two waves of protective memory T cells. *Science*, 348, aaa8205.
- STEINER-MONARD, V., KAMAKA, K., KAROUI, O., ROETHLISBERGER, S., AUDRAN, R., DAUBENBERGER, C., FAYET-MELLO, A., ERDMANN-VOISIN, A., FELGER, I., GEIGER, K., GOVENDER, L., HOUARD, S., HUBER, E., MAYOR, C., MKINDI, C., PORTEVIN, D., RUSCH, S., SCHMIDLIN, S., TIENDREBEOGO, R. W., THEISEN, M., THIERRY, A. C., VALLOTTON, L., CORRADIN, G., LEROY, O., ABDULLA, S., SHEKALAGHE, S., GENTON, B., SPERTINI, F. & JONGO, S. A. 2019. The Candidate Blood-stage Malaria Vaccine P27A Induces a Robust Humoral Response in a Fast Track to the Field Phase 1 Trial in Exposed and Nonexposed Volunteers. *Clin Infect Dis*, 68, 466-474.
- STEINERT, E. M., SCHENKEL, J. M., FRASER, K. A., BEURA, L. K., MANLOVE, L. S., IGYARTO, B. Z., SOUTHERN, P. J. & MASOPUST, D. 2015. Quantifying Memory CD8 T Cells Reveals Regionalization of Immunosurveillance. *Cell*, 161, 737-49.
- STEPHENS, R., ALBANO, F. R., QUIN, S., PASCAL, B. J., HARRISON, V., STOCKINGER, B., KIOUSSIS, D., WELTZIEN, H. U. & LANGHORNE, J. 2005. Malaria-specific

- transgenic CD4(+) T cells protect immunodeficient mice from lethal infection and demonstrate requirement for a protective threshold of antibody production for parasite clearance. *Blood*, 106, 1676-84.
- STEPHENS, R. & LANGHORNE, J. 2010. Effector Memory Th1 CD4 T Cells Are Maintained in a Mouse Model of Chronic Malaria. *PLoS Pathogens*, 6, e1001208-13.
- STEVENSON, M. M. & RILEY, E. M. 2004. Innate immunity to malaria. *Nat Rev Immunol*, 4, 169-80.
- STEVENSON, M. M., SU, Z., SAM, H. & MOHAN, K. 2001. Modulation of host responses to blood-stage malaria by interleukin-12: from therapy to adjuvant activity. *Microbes Infect*, 3, 49-59.
- STEVENSON, M. M., TAM, M. F., BELOSEVIC, M., VAN DER MEIDE, P. H. & PODOBA, J. E. 1990. Role of endogenous gamma interferon in host response to infection with blood-stage Plasmodium chabaudi AS. *Infect Immun*, 58, 3225-32.
- STRUTT, T. M., DHUME, K., FINN, C. M., HWANG, J. H., CASTONGUAY, C., SWAIN, S. L. & MCKINSTRY, K. K. 2018. IL-15 supports the generation of protective lung-resident memory CD4 T cells. *Mucosal Immunol*, 11, 668-680.
- STUMHOFER, J. S., SILVER, J. S., LAURENCE, A., PORRETT, P. M., HARRIS, T. H., TURKA, L. A., ERNST, M., SARIS, C. J., O'SHEA, J. J. & HUNTER, C. A. 2007. Interleukins 27 and 6 induce STAT3-mediated T cell production of interleukin 10. *Nat Immunol*, 8, 1363-71.
- STURM, A. 2006. Manipulation of Host Hepatocytes by the Malaria Parasite for Delivery into Liver Sinusoids. *Science*, 313, 1287-1290.
- STURM, A., AMINO, R., VAN DE SAND, C., REGEN, T., RETZLAFF, S., RENNENBERG, A., KRUEGER, A., POLLOK, J. M., MENARD, R. & HEUSSLER, V. T. 2006. Manipulation of host hepatocytes by the malaria parasite for delivery into liver sinusoids. *Science*, 313, 1287-90.
- SU, Z. & STEVENSON, M. M. 2000. Central role of endogenous gamma interferon in protective immunity against blood-stage Plasmodium chabaudi AS infection. *Infect Immun*, 68, 4399-406.
- SUGUITAN, A. L., JR., LEKE, R. G., FOUA, G., ZHOU, A., THUITA, L., METENOU, S., FOGAKO, J., MEGNEKOU, R. & TAYLOR, D. W. 2003. Changes in the levels of chemokines and cytokines in the placentas of women with Plasmodium falciparum malaria. *J Infect Dis*, 188, 1074-82.
- SUKHBAATAR, O., KIMURA, D., MIYAKODA, M., NAKAMAE, S., KIMURA, K., HARA, H., YOSHIDA, H., INOUE, S. I. & YUI, K. 2020. Activation and IL-10 production of specific CD4(+) T cells are regulated by IL-27 during chronic infection with Plasmodium chabaudi. *Parasitol Int*, 74, 101994.
- SUNDARARAJAN, Z., KNOLL, R., HOMBACH, P., BECKER, M., SCHULTZE, J. L. & ULAS, T. 2019. Shiny-Seq: advanced guided transcriptome analysis. *BMC Res Notes*, 12, 432.
- SURH, C. D. & SPRENT, J. 2008. Homeostasis of naive and memory T cells. *Immunity*, 29, 848-62.
- SWANSON, P. A., 2ND, HART, G. T., RUSSO, M. V., NAYAK, D., YAZEWE, T., PENA, M., KHAN, S. M., JANSE, C. J., PIERCE, S. K. & MCGAVERN, D. B. 2016. CD8+ T Cells

- Induce Fatal Brainstem Pathology during Cerebral Malaria via Luminal Antigen-Specific Engagement of Brain Vasculature. *PLoS Pathog*, 12, e1006022.
- SZABO, S. J., KIM, S. T., COSTA, G. L., ZHANG, X., FATHMAN, C. G. & GLIMCHER, L. H. 2000. A Novel Transcription Factor, T-bet, Directs Th1 Lineage Commitment. *Cell*, 100, 655-669.
- TAKAMURA, S., YAGI, H., HAKATA, Y., MOTOZONO, C., MCMASTER, S. R., MASUMOTO, T., FUJISAWA, M., CHIKAISHI, T., KOMEDA, J., ITOH, J., UMEMURA, M., KYUSAI, A., TOMURA, M., NAKAYAMA, T., WOODLAND, D. L., KOHLMEIER, J. E. & MIYAZAWA, M. 2016. Specific niches for lung-resident memory CD8+ T cells at the site of tissue regeneration enable CD69-independent maintenance. *J Exp Med*, 213, 3057-3073.
- TAKEMOTO, N., INTLEKOFER, A. M., NORTHRUP, J. T., WHERRY, E. J. & REINER, S. L. 2006. Cutting Edge: IL-12 inversely regulates T-bet and eomesodermin expression during pathogen-induced CD8+ T cell differentiation. *J Immunol*, 177, 7515-9.
- TALAAAT, K. R., ELLIS, R. D., HURD, J., HENTRICH, A., GABRIEL, E., HYNES, N. A., RAUSCH, K. M., ZHU, D., MURATOVA, O., HERRERA, R., ANDERSON, C., JONES, D., AEBIG, J., BROCKLEY, S., MACDONALD, N. J., WANG, X., FAY, M. P., HEALY, S. A., DURBIN, A. P., NARUM, D. L., WU, Y. & DUFFY, P. E. 2016. Safety and Immunogenicity of Pfs25-EPA/Alhydrogel(R), a Transmission Blocking Vaccine against Plasmodium falciparum: An Open Label Study in Malaria Naive Adults. *PLoS One*, 11, e0163144.
- TAM, J. P., CLAVIJO, P., LU, Y. A., NUSSENZWEIG, V., NUSSENZWEIG, R. & ZAVALA, F. 1990. Incorporation of T and B epitopes of the circumsporozoite protein in a chemically defined synthetic vaccine against malaria. *J Exp Med*, 171, 299-306.
- TARUN, A. S., PENG, X., DUMPIT, R. F., OGATA, Y., SILVA-RIVERA, H., CAMARGO, N., DALY, T. M., BERGMAN, L. W. & KAPPE, S. H. 2008. A combined transcriptome and proteome survey of malaria parasite liver stages. *Proc Natl Acad Sci U S A*, 105, 305-10.
- TAYLOR, T. E. & MOLYNEUX, M. E. 2015. The pathogenesis of pediatric cerebral malaria: eye exams, autopsies, and neuroimaging. *Ann N Y Acad Sci*, 1342, 44-52.
- TAYLOR-ROBINSON, A. W., PHILLIPS, R. S., SEVERN, A., MONCADA, S. & LIEW, F. Y. 1993. The role of TH1 and TH2 cells in a rodent malaria infection. *Science*, 260, 1931-4.
- TEIJARO, J. R., TURNER, D., PHAM, Q., WHERRY, E. J., LEFRANCOIS, L. & FARBER, D. L. 2011. Cutting Edge: Tissue-Retentive Lung Memory CD4 T Cells Mediate Optimal Protection to Respiratory Virus Infection. *The Journal of Immunology*, 187, 5510-5514.
- THAM, W. H., HEALER, J. & COWMAN, A. F. 2012. Erythrocyte and reticulocyte binding-like proteins of Plasmodium falciparum. *Trends Parasitol*, 28, 23-30.
- THAWER, S. G., HORSNELL, W. G., DARBY, M., HOVING, J. C., DEWALS, B., CUTLER, A. J., LANG, D. & BROMBACHER, F. 2014. Lung-resident CD4(+) T cells are sufficient for IL-4Ralpha-dependent recall immunity to Nippostrongylus brasiliensis infection. *Mucosal Immunol*, 7, 239-48.
- THUMWOOD, C. M., HUNT, N. H., CLARK, I. A. & COWDEN, W. B. 1988. Breakdown of the blood-brain barrier in murine cerebral malaria. *Parasitology*, 96 ( Pt 3), 579-89.

- TOWNSEND, A., OHLEN, C., BASTIN, J., LJUNGGREN, H. G., FOSTER, L. & KARRE, K. 1989. Association of class I major histocompatibility heavy and light chains induced by viral peptides. *Nature*, 340, 443-8.
- TROYE-BLOMBERG, M., RILEY, E. M., KABILAN, L., HOLMBERG, M., PERLMANN, H., ANDERSSON, U., HEUSSER, C. H. & PERLMANN, P. 1990. Production by activated human T cells of interleukin 4 but not interferon-gamma is associated with elevated levels of serum antibodies to activating malaria antigens. *Proc Natl Acad Sci U S A*, 87, 5484-8.
- TSE, S. W., COCKBURN, I. A., ZHANG, H., SCOTT, A. L. & ZAVALA, F. 2013. Unique transcriptional profile of liver-resident memory CD8+ T cells induced by immunization with malaria sporozoites. *Genes Immun*, 14, 302-9.
- TSE, S. W., RADTKE, A. J., ESPINOSA, D. A., COCKBURN, I. A. & ZAVALA, F. 2014. The chemokine receptor CXCR6 is required for the maintenance of liver memory CD8(+) T cells specific for infectious pathogens. *J Infect Dis*, 210, 1508-16.
- TSUJI, M., ROMERO, P., NUSSENZWEIG, R. S. & ZAVALA, F. 1990. CD4+ cytolytic T cell clone confers protection against murine malaria. *The Journal of Experimental Medicine*, 172, 1353-1357.
- TUBO, N. J., PAGAN, A. J., TAYLOR, J. J., NELSON, R. W., LINEHAN, J. L., ERTELT, J. M., HUSEBY, E. S., WAY, S. S. & JENKINS, M. K. 2013. Single naive CD4+ T cells from a diverse repertoire produce different effector cell types during infection. *Cell*, 153, 785-96.
- UEHARA, S., GRINBERG, A., FARBER, J. M. & LOVE, P. E. 2002. A role for CCR9 in T lymphocyte development and migration. *J Immunol*, 168, 2811-9.
- URBAN, B. C., FERGUSON, D. J., PAIN, A., WILLCOX, N., PLEBANSKI, M., AUSTYN, J. M. & ROBERTS, D. J. 1999. Plasmodium falciparum-infected erythrocytes modulate the maturation of dendritic cells. *Nature*, 400, 73-7.
- VALENCIA-HERNANDEZ, A. M., NG, W. Y., GHAZANFARI, N., GHILAS, S., DE MENEZES, M. N., HOLZ, L. E., HUANG, C., ENGLISH, K., NAUNG, M., TAN, P. S., TULLETT, K. M., STEINER, T. M., ENDERS, M. H., BEATTIE, L., CHUA, Y. C., JONES, C. M., COZIJNSEN, A., MOLLARD, V., CAI, Y., BOWEN, D. G., PURCELL, A. W., LA GRUTA, N. L., VILLADANGOS, J. A., DE KONING-WARD, T., BARRY, A. E., BARCHET, W., COCKBURN, I. A., MCFADDEN, G. I., GRAS, S., LAHOUD, M. H., BERTOLINO, P., SCHITTENHELM, R. B., CAMINSCHI, I., HEATH, W. R. & FERNANDEZ-RUIZ, D. 2020. A Natural Peptide Antigen within the Plasmodium Ribosomal Protein RPL6 Confers Liver TRM Cell-Mediated Immunity against Malaria in Mice. *Cell Host Microbe*, 27, 950-962 e7.
- VALKENBURG, S. A., LI, O. T. W., LI, A., BULL, M., WALDMANN, T. A., PERERA, L. P., PEIRIS, M. & POON, L. L. M. 2018. Protection by universal influenza vaccine is mediated by memory CD4 T cells. *Vaccine*, 36, 4198-4206.
- VAN BLEEK, G. M. & NATHENSON, S. G. 1990. Isolation of an endogenously processed immunodominant viral peptide from the class I H-2Kb molecule. *Nature*, 348, 213-6.
- VAN DE BERG, P. J., VAN LEEUWEN, E. M., TEN BERGE, I. J. & VAN LIER, R. 2008. Cytotoxic human CD4(+) T cells. *Curr Opin Immunol*, 20, 339-43.

- VAN DER HEYDE, H. C., PEPPER, B., BATCHELDER, J., CIGEL, F. & WEIDANZ, W. P. 1997. The time course of selected malarial infections in cytokine-deficient mice. *Exp Parasitol*, 85, 206-13.
- VAN DER WINDT, G. J., EVERTS, B., CHANG, C. H., CURTIS, J. D., FREITAS, T. C., AMIEL, E., PEARCE, E. J. & PEARCE, E. L. 2012. Mitochondrial respiratory capacity is a critical regulator of CD8+ T cell memory development. *Immunity*, 36, 68-78.
- VAN RIJT, L. S., JUNG, S., KLEINJAN, A., VOS, N., WILLART, M., DUEZ, C., HOOGSTEDEN, H. C. & LAMBRECHT, B. N. 2005. In vivo depletion of lung CD11c+ dendritic cells during allergen challenge abrogates the characteristic features of asthma. *J Exp Med*, 201, 981-91.
- VANDERBERG, J. P. & FREVERT, U. 2004. Intravital microscopy demonstrating antibody-mediated immobilisation of Plasmodium berghei sporozoites injected into skin by mosquitoes. *Int J Parasitol*, 34, 991-6.
- VAUGHAN, A. M., SACK, B. K., DANKWA, D., MINKAH, N., NGUYEN, T., CARDAMONE, H. & KAPPE, S. H. I. 2018. A Plasmodium Parasite with Complete Late Liver Stage Arrest Protects against Preerythrocytic and Erythrocytic Stage Infection in Mice. *Infect Immun*, 86.
- VAUGHAN, J. A., SCHELLER, L. F., WIRTZ, R. A. & AZAD, A. F. 1999. Infectivity of Plasmodium berghei sporozoites delivered by intravenous inoculation versus mosquito bite: implications for sporozoite vaccine trials. *Infect Immun*, 67, 4285-9.
- VERBIST, K. C., FIELD, M. B. & KLONOWSKI, K. D. 2011. Cutting edge: IL-15-independent maintenance of mucosally generated memory CD8 T cells. *J Immunol*, 186, 6667-71.
- VERBIST, K. C., GUY, C. S., MILASTA, S., LIEDMANN, S., KAMINSKI, M. M., WANG, R. & GREEN, D. R. 2016. Metabolic maintenance of cell asymmetry following division in activated T lymphocytes. *Nature*, 532, 389-93.
- VILLEGAS-MENDEZ, A., GREIG, R., SHAW, T. N., DE SOUZA, J. B., GWYER FINDLAY, E., STUMHOFER, J. S., HAFALLA, J. C., BLOUNT, D. G., HUNTER, C. A., RILEY, E. M. & COUPER, K. N. 2012. IFN-gamma-producing CD4+ T cells promote experimental cerebral malaria by modulating CD8+ T cell accumulation within the brain. *J Immunol*, 189, 968-79.
- VITA, R., MAHAJAN, S., OVERTON, J. A., DHANDA, S. K., MARTINI, S., CANTRELL, J. R., WHEELER, D. K., SETTE, A. & PETERS, B. 2019. The Immune Epitope Database (IEDB): 2018 update. *Nucleic Acids Res*, 47, D339-D343.
- VLACHOU, D., SCHLEGELMILCH, T., RUNN, E., MENDES, A. & KAFATOS, F. C. 2006. The developmental migration of Plasmodium in mosquitoes. *Curr Opin Genet Dev*, 16, 384-91.
- VOISINE, C., MASTELIC, B., SPONAAS, A. M. & LANGHORNE, J. 2010. Classical CD11c+ dendritic cells, not plasmacytoid dendritic cells, induce T cell responses to Plasmodium chabaudi malaria. *Int J Parasitol*, 40, 711-9.
- VON DER WEID, T., KOPF, M., KOHLER, G. & LANGHORNE, J. 1994. The immune response to Plasmodium chabaudi malaria in interleukin-4-deficient mice. *Eur J Immunol*, 24, 2285-93.

- WAITUMBI, J. N., OPOLLO, M. O., MUGA, R. O., MISORE, A. O. & STOUTE, J. A. 2000. Red cell surface changes and erythrophagocytosis in children with severe *Plasmodium falciparum* anemia. *Blood*, 95, 1481-1486.
- WAKE, K. 1971. "Sternzellen" in the liver: perisinusoidal cells with special reference to storage of vitamin A. *Am J Anat*, 132, 429-62.
- WAKIM, L. M., SMITH, J., CAMINSCHI, I., LAHOUD, M. H. & VILLADANGOS, J. A. 2015. Antibody-targeted vaccination to lung dendritic cells generates tissue-resident memory CD8 T cells that are highly protective against influenza virus infection. *Mucosal Immunol*, 8, 1060-71.
- WAKIM, L. M., WOODWARD-DAVIS, A. & BEVAN, M. J. 2010. Memory T cells persisting within the brain after local infection show functional adaptations to their tissue of residence. *Proc Natl Acad Sci U S A*, 107, 17872-9.
- WALK, J., REULING, I. J., BEHET, M. C., MEERSTEIN-KESSEL, L., GRAUMANS, W., VAN GEMERT, G. J., SIEBELINK-STOTER, R., VAN DE VEGTE-BOLMER, M., JANSSEN, T., TEELLEN, K., DE WILT, J. H. W., DE MAST, Q., VAN DER VEN, A. J., DIEZ BENAVENTE, E., CAMPINO, S., CLARK, T. G., HUYNEN, M. A., HERMSEN, C. C., BIJKER, E. M., SCHOLZEN, A. & SAUERWEIN, R. W. 2017. Modest heterologous protection after *Plasmodium falciparum* sporozoite immunization: a double-blind randomized controlled clinical trial. *BMC Med*, 15, 168.
- WANG, R., CHAROENVIT, Y., CORRADIN, G., DE LA VEGA, P., FRANKE, E. D. & HOFFMAN, S. L. 1996. Protection against malaria by *Plasmodium yoelii* sporozoite surface protein 2 linear peptide induction of CD4+ T cell- and IFN-gamma-dependent elimination of infected hepatocytes. *The Journal of Immunology*, 157, 4061-4067.
- WANG, Y. & ZHANG, C. 2019. The Roles of Liver-Resident Lymphocytes in Liver Diseases. *Frontiers in Immunology*, 10, 1198-13.
- WARRELL, D. A., VEALL, N., CHANTHAVANICH, P., KARBWANG, J., WHITE, N. J., LOOAREESUWAN, S., PHILLIPS, R. E. & PONGPAEW, P. 1988. Cerebral Anaerobic Glycolysis and Reduced Cerebral Oxygen Transport in Human Cerebral Malaria. *The Lancet*, 332, 534-538.
- WARREN, A., LE COUTEUR, D. G., FRASER, R., BOWEN, D. G., MCCAUGHAN, G. W. & BERTOLINO, P. 2006. T lymphocytes interact with hepatocytes through fenestrations in murine liver sinusoidal endothelial cells. *Hepatology*, 44, 1182-90.
- WASSMER, S. C., TAYLOR, T. E., RATHOD, P. K., MISHRA, S. K., MOHANTY, S., AREVALO-HERRERA, M., DURASINGH, M. T. & SMITH, J. D. 2015. Investigating the Pathogenesis of Severe Malaria: A Multidisciplinary and Cross-Geographical Approach. *Am J Trop Med Hyg*, 93, 42-56.
- WATTS, C. 1997. Capture and processing of exogenous antigens for presentation on MHC molecules. *Annu Rev Immunol*, 15, 821-50.
- WEISS, G. E., GILSON, P. R., TAECHALERTPAISARN, T., THAM, W. H., DE JONG, N. W., HARVEY, K. L., FOWKES, F. J., BARLOW, P. N., RAYNER, J. C., WRIGHT, G. J., COWMAN, A. F. & CRABB, B. S. 2015. Revealing the sequence and resulting cellular morphology of receptor-ligand interactions during *Plasmodium falciparum* invasion of erythrocytes. *PLoS Pathog*, 11, e1004670.

- WEISS, W. R., SEDEGAH, M., BERZOFKY, J. A. & HOFFMAN, S. L. 1993. The role of CD4+ T cells in immunity to malaria sporozoites. *The Journal of Immunology*, 151, 2690-2698.
- WHILDING, L. M. & MAHER, J. 2015. CAR T-cell immunotherapy: The path from the by-road to the freeway? *Mol Oncol*, 9, 1994-2018.
- WHITE, M. T., BEJON, P., OLOTU, A., GRIFFIN, J. T., RILEY, E. M., KESTER, K. E., OCKENHOUSE, C. F. & GHANI, A. C. 2013. The relationship between RTS,S vaccine-induced antibodies, CD4(+) T cell responses and protection against Plasmodium falciparum infection. *PLoS One*, 8, e61395.
- WHITE, N. J. 2011. Determinants of relapse periodicity in Plasmodium vivax malaria. *Malar J*, 10, 297.
- WHITE, N. J., PUKRITTAYAKAMEE, S., HIEN, T. T., FAIZ, M. A., MOKUOLU, O. A. & DONDORP, A. M. 2014. Malaria. *The Lancet*, 383, 723-735.
- WHO WHO Malaria report 2018.
- WHO 2015. Global Technical Strategy for Malaria 2016-2030.
- WHO 2019. World Malaria Report 2019. <https://www.who.int/publications-detail/world-malaria-report-2019>.
- WICK, M. J., LEITHAUSER, F. & REIMANN, J. 2002. The hepatic immune system. *Crit Rev Immunol*, 22, 47-103.
- WIKENHEISER, D. J., GHOSH, D., KENNEDY, B. & STUMHOFER, J. S. 2016. The Costimulatory Molecule ICOS Regulates Host Th1 and Follicular Th Cell Differentiation in Response to Plasmodium chabaudi chabaudi AS Infection. *J Immunol*, 196, 778-91.
- WILSON, C. B., ROWELL, E. & SEKIMATA, M. 2009. Epigenetic control of T-helper-cell differentiation. *Nat Rev Immunol*, 9, 91-105.
- WISSE, E., DE ZANGER, R. B., CHARELS, K., VAN DER SMISSEN, P. & MCCUSKEY, R. S. 1985. The liver sieve: considerations concerning the structure and function of endothelial fenestrae, the sinusoidal wall and the space of Disse. *Hepatology*, 5, 683-92.
- WOLD, W. S. M., DORONIN, K., TOTH, K., KUPPUSWAMY, M., LICHTENSTEIN, D. L. & TOLLEFSON, A. E. 1999. Immune responses to adenoviruses: viral evasion mechanisms and their implications for the clinic. *Current Opinion in Immunology*, 11, 380-386.
- WU, X., GOWDA, N. M., KUMAR, S. & GOWDA, D. C. 2010. Protein-DNA complex is the exclusive malaria parasite component that activates dendritic cells and triggers innate immune responses. *J Immunol*, 184, 4338-48.
- WU, Y., ELLIS, R. D., SHAFFER, D., FONTES, E., MALKIN, E. M., MAHANTY, S., FAY, M. P., NARUM, D., RAUSCH, K., MILES, A. P., AEBIG, J., ORCUTT, A., MURATOVA, O., SONG, G., LAMBERT, L., ZHU, D., MIURA, K., LONG, C., SAUL, A., MILLER, L. H. & DURBIN, A. P. 2008. Phase 1 trial of malaria transmission blocking vaccine candidates Pfs25 and Pvs25 formulated with montanide ISA 51. *PLoS One*, 3, e2636.
- XU, H., HODDER, A. N., YAN, H., CREWETHER, P. E., ANDERS, R. F. & GOOD, M. F. 2000. CD4+ T cells acting independently of antibody contribute to protective immunity

- to *Plasmodium chabaudi* infection after apical membrane antigen 1 immunization. *J Immunol*, 165, 389-96.
- YAJIMA, T., YOSHIHARA, K., NAKAZATO, K., KUMABE, S., KOYASU, S., SAD, S., SHEN, H., KUWANO, H. & YOSHIKAI, Y. 2006. IL-15 regulates CD8+ T cell contraction during primary infection. *J Immunol*, 176, 507-15.
- YANEZ, D. M., MANNING, D. D., COOLEY, A. J., WEIDANZ, W. P. & VAN DER HEYDE, H. C. 1996. Participation of lymphocyte subpopulations in the pathogenesis of experimental murine cerebral malaria. *J Immunol*, 157, 1620-4.
- YAÑEZ, D., BATCHELDER, J., VAN DER HEYDE, H., MANNING, D. & WEIDANZ, W. 1999.  $\gamma\delta$  T-Cell Function in Pathogenesis of Cerebral Malaria in Mice Infected with *Plasmodium berghei* ANKA. *Infection and Immunity*, 67, 446-448.
- YONE, C. L., KREMSNER, P. G. & LUTY, A. J. 2005. Immunoglobulin G isotype responses to erythrocyte surface-expressed variant antigens of *Plasmodium falciparum* predict protection from malaria in African children. *Infect Immun*, 73, 2281-7.
- YONETO, T., YOSHIMOTO, T., WANG, C. R., TAKAHAMA, Y., TSUJI, M., WAKI, S. & NARIUCHI, H. 1999. Gamma interferon production is critical for protective immunity to infection with blood-stage *Plasmodium berghei* XAT but neither NO production nor NK cell activation is critical. *Infect Immun*, 67, 2349-56.
- ZANDER, R. A., GUTHMILLER, J. J., GRAHAM, A. C., POPE, R. L., BURKE, B. E., CARR, D. J. & BUTLER, N. S. 2016. Type I Interferons Induce T Regulatory 1 Responses and Restrict Humoral Immunity during Experimental Malaria. *PLoS Pathog*, 12, e1005945.
- ZENS, K. D., CHEN, J. K. & FARBER, D. L. 2016. Vaccine-generated lung tissue-resident memory T cells provide heterosubtypic protection to influenza infection. *JCI Insight*, 1.
- ZHANG, Y., JOE, G., HEXNER, E., ZHU, J. & EMERSON, S. G. 2005. Host-reactive CD8+ memory stem cells in graft-versus-host disease. *Nat Med*, 11, 1299-305.
- ZHAO, J., ZHAO, J., MANGALAM, A. K., CHANNAPPANAVAR, R., FETT, C., MEYERHOLZ, D. K., AGNIHOTHRAM, S., BARIC, R. S., DAVID, C. S. & PERLMAN, S. 2016. Airway Memory CD4(+) T Cells Mediate Protective Immunity against Emerging Respiratory Coronaviruses. *Immunity*, 44, 1379-91.
- ZHAO, T., ZHANG, H., GUO, Y., ZHANG, Q., HUA, G., LU, H., HOU, Q., LIU, H. & FAN, Z. 2007. Granzyme K cleaves the nucleosome assembly protein SET to induce single-stranded DNA nicks of target cells. *Cell Death Differ*, 14, 489-99.
- ZHENG, W.-P. & FLAVELL, R. A. 1997. The Transcription Factor GATA-3 Is Necessary and Sufficient for Th2 Cytokine Gene Expression in CD4 T Cells. *Cell*, 89, 587-596.
- ZONCU, R., EFEYAN, A. & SABATINI, D. M. 2011. mTOR: from growth signal integration to cancer, diabetes and ageing. *Nat Rev Mol Cell Biol*, 12, 21-35.

# Appendix

## Appendix

**Appendix Table 8.1. DEGs list of genes up or down-regulated in RAS generated liver PbT-II T<sub>RM</sub> cells versus RAS generated PbT-II T<sub>EM</sub> cells**

Symbol	Regulation	FoldChange	Symbol	Regulation	FoldChange
Nacc1	up	1.476	Tasp1	up	1.362
Slc25a1	up	2.094	Fam102a	up	1.345
Il27ra	up	1.221	Rbpj	up	1.927
Susd2	up	2.660	Sec24d	up	1.253
Zdhhc24	up	2.247	Tnfsf10	up	1.417
Gmnn	up	1.307	Mrps6	up	1.601
Bmp7	up	2.072	Fgl2	up	1.090
Podn1	up	3.198	Slc26a11	up	1.582
Pam16	up	2.242	Ptger4	up	1.521
Slamf1	up	1.272	Dtx4	up	1.599
Arnt2	up	2.665	Gm11639	up	1.745
Fcrls	up	2.572	Sntb2	up	1.257
Ttll12	up	1.735	Meis3	up	1.415
Eya2	up	2.176	Serpina3g	up	1.556
Dusp6	up	1.173	Tmtc4	up	2.015
Socs2	up	1.547	Bicdl1	up	1.897
Cry1	up	1.151	Tnfrsf18	up	1.060
Itk	up	1.290	Ccr8	up	3.259
Id2	up	1.229	Ubash3a	up	1.767
Ccl1	up	5.356	Gzmk	up	2.100
Mink1	up	1.313	Adprhl2	up	1.087
Snx11	up	1.668	Pla2g6	up	2.788
Susd3	up	1.272	Hic1	up	1.790
Glrx	up	1.456	Lrrn4	up	4.459
Atp8a2	up	2.084	Unc5cl	up	1.565
Rcbtb2	up	1.936	Ly6g5b	up	2.168
Sqle	up	1.455	Gimap7	up	1.381
Hsf1	up	2.241	Bex3	up	1.851
Slc52a2	up	1.732	Rpsa-ps10	up	2.151
Cd200r1	up	2.186	Bcl11b	up	1.148
Nagpa	up	1.537	Pskh1	up	1.697
Mut	up	1.170	Cxcr6	up	1.530
Slc29a1	up	1.008	Vps37c	up	1.933

Slc39a6	up	1.380		Tmem121	up	3.343
Gnl1	up	1.192		Zfp683	up	2.671
Cd6	up	1.187		Zfpm1	up	1.134
Lpxn	up	1.041		Zfp280b	up	1.983
Scyl1	up	1.446		Cxcr3	up	1.922
Men1	up	1.635		B3galt6	up	1.624
Nabp2	up	1.104		Insl6	up	1.031
Icos	up	1.309		Ercc6l	up	1.949
Tmem63a	up	1.884		Gimap4	up	1.071
Usp20	up	1.068		Zscan22	up	2.218
Notch1	up	1.677		Tmem154	up	1.104
Med19	up	1.462		Itpk1	up	1.684
Fahd2a	up	1.732		Dhcr7	up	1.279
Acox1	up	2.608		Gtf2i	up	1.004
Sdcbp2	up	1.894		Pla2g16	up	1.152
Nfatc2	up	1.041		Cd200r4	up	1.210
Il2	up	2.744		Tlr12	up	2.594
Dennd2d	up	1.069		3300002I08Rik	up	2.339
Coro2a	up	1.258		Trerf1	up	1.534
Nol6	up	1.530		Plcx1	up	2.787
Sit1	up	1.633		Serpina3f	up	2.353
Sytl1	up	1.428		Il2rb	up	1.610
Wrap73	up	1.573		Gm10240	up	3.051
Tnfrsf4	up	2.852		Clec16a	up	1.674
Gfi1	up	1.191		Irgm2	up	1.397
Abcg3	up	1.255		Rabepk	up	1.107
Tesc	up	2.170		Tigit	up	1.829
Pitpnm2	up	1.449		Apol7e	up	1.367
Abcb9	up	1.460		Lym9	up	1.330
P2rx7	up	2.054		Cep170b	up	2.776
Acads	up	1.403		H2-T-ps	up	1.409
Ccdc136	up	2.445		Gm10505	up	2.097
Wbp1	up	1.503		Klhl21	up	1.240
Plxna1	up	1.338		Btbd19	up	1.293
Fam234b	up	2.300		Plekhf1	up	2.207
D6Wsu163e	up	1.118		Ly6a	up	1.063
Furin	up	1.091		Trac	up	1.852
Sytl2	up	1.320		AW011738	up	2.146
Art2b	up	1.628		Igtp	up	1.059

Trat1	up	1.640	Zfp931	up	1.795
Dkk1	up	2.885	Gm14326	up	1.932
Eri2	up	1.801	Tgtp2	up	1.603
Slc9a9	up	1.106	lfit1bl1	up	1.041
Cd40lg	up	1.980	Gbp4	up	1.420
Leprotl1	up	1.065	Fam71f2	up	1.015
Cog8	up	1.442	Gm12250	up	1.391
Acad8	up	1.507	Gm13370	up	3.051
Cd3e	up	1.196	Gm14718	up	1.507
Cd3d	up	1.105	Gm15423	up	1.075
Acsbg1	up	1.795	Bcl2a1b	up	1.107
Ptpn9	up	1.166	Lime1	up	1.028
Trip4	up	1.139	2010016118Rik	up	1.244
Parp16	up	1.453	Gm21847	up	2.516
Cish	up	2.046	Gm3468	up	1.304
Micall1	up	1.335	Gm10359	up	3.333
Chst2	up	2.116	Gm20069	up	2.475
Mapkbp1	up	2.123	Gm12671	up	3.333
Faah	up	1.638	Trav9-4	up	2.682
Gbp8	up	1.721	Gm28373	up	3.426
Dhrs11	up	1.489	Gm26614	up	3.074
Rundc1	up	1.641	AU020206	up	1.066
Galm	up	1.761	Lppos	up	1.925
Cnot3	up	1.080	Bcl2a1d	up	1.454
Tdp2	up	1.920	Gm28347	up	2.253
Fam69b	up	3.039	Gm38194	up	1.063
Tfb1m	up	2.468	Gm37488	up	1.814
Zfyve28	up	1.734	Gm38249	up	1.567
Mxd4	up	1.024	Gbp6	up	1.330
Arid5a	up	1.242	AY036118	up	1.640
Asxl2	up	1.016	Gm43126	up	1.547
Kcnh3	up	4.364	Particl	up	2.649
Camk4	up	1.257	Gm44631	up	2.362
Cd160	up	1.296	Pvrig	up	1.736
Mesdc2	up	1.110	Gm18860	up	3.999
Samd10	up	1.683			
As3mt	down	-1.933	1110059E24Rik	down	-1.311
St3gal1	down	-1.315	Gramd4	down	-1.494
Ttpal	down	-1.049	Tmem177	down	-1.668
Atp2b1	down	-1.151	Tmprss13	down	-3.226

Tns3	down	-2.970		Btbd10	down	-1.435
Polm	down	-1.096		Zc3h12d	down	-1.149
Pecam1	down	-1.173		Pogk	down	-1.179
Spns3	down	-2.037		Rfx3	down	-1.705
Klhdc2	down	-1.443		Inpp5f	down	-1.186
Cinp	down	-2.642		Spice1	down	-1.459
Ripk1	down	-1.640		Olf975	down	-1.699
Lats2	down	-1.128		Hexim2	down	-1.388
Sidt1	down	-1.246		S1pr5	down	-3.048
Slc17a9	down	-1.044		S1pr1	down	-1.709
Ms4a7	down	-3.001		Insm2	down	-1.381
Slc6a20b	down	-1.310		Klre1	down	-2.369
Il18rap	down	-1.462		Ncald	down	-2.518
Epha4	down	-3.484		Sox12	down	-1.392
Atp2b4	down	-1.538		A630001G21Ri k	down	-1.329
Coq8a	down	-1.490		Nebi	down	-2.938
Zeb2	down	-2.087		Txk	down	-1.854
Creb3l1	down	-2.244		Smyd1	down	-2.761
Cdc25b	down	-1.190		Klf2	down	-2.005
Snx30	down	-1.962		Atp8b4	down	-1.444
Cd72	down	-1.482		Tmem65	down	-1.939
Osbpl9	down	-1.025		Rnls	down	-1.847
Ptpn12	down	-1.134		D330041H03Ri k	down	-1.461
Klf3	down	-1.745		Wdfy1	down	-1.045
Klrg1	down	-2.098		Aoc2	down	-2.157
Klrd1	down	-2.584		Cdc20b	down	-3.681
Klra13-ps	down	-2.531		Gm15807	down	-1.711
Kcnj8	down	-3.524		Mir142hg	down	-1.095
Klrb1c	down	-1.817		Gm11346	down	-1.102
Avpr2	down	-1.991		Klra8	down	-2.552
Mpp1	down	-1.022		Bend4	down	-2.548
Rasa3	down	-1.181		A430046D13Ri k	down	-1.788
Atp1b3	down	-1.054		Gm10522	down	-2.191
Stt3b	down	-1.466		Gm44834	down	-2.522
Trmt13	down	-1.362		Gm18959	down	-2.301
Tagap	down	-1.475		RP24-340L11.5	down	-1.753

**Appendix Table 8.2. DEGs list of genes up or down-regulated in  $\alpha$ Clec9A generated PbT-II T<sub>RM</sub> cells versus RAS generated PbT-II T<sub>RM</sub> cells from the liver.**

Symbol	Regulation	FoldChange	Symbol	Regulation	FoldChange
Angptl2	up	3.249	Emp1	up	2.318
Csf1	up	3.318	Gpm6b	up	1.899
Cinp	up	1.800	Tbc1d4	up	2.056
Tjp2	up	3.125	Vax2	up	2.265
Nrp1	up	2.478	Csgalnact1	up	2.913
Ctla4	up	2.534	Spry1	up	3.487
Il1rl1	up	2.140	Plcl1	up	3.160
Il18r1	up	2.786	Tox	up	3.185
Pdcd1	up	3.877	Trim46	up	1.886
Galnt3	up	2.536	Olf432	up	1.341
Itga4	up	1.660	5830411N06Rik	up	2.789
Il21	up	3.881	Gm28942	up	3.329
Tnfsf8	up	1.854	Gm10997	up	2.756
Lag3	up	3.168			
Il4	down	-5.218	Stard9	down	-2.669
Cpa3	down	-1.470	Tlr13	down	-2.020
St8sia6	down	-1.300	Arl4d	down	-1.830
Ccl9	down	-2.841	Filip1l	down	-1.554
Ahr	down	-3.649	Ccr4	down	-4.883
Socs2	down	-2.820	Clec4a1	down	-2.608
Ccl1	down	-3.212	Ifi205	down	-2.084
St6gal1	down	-2.765	Nfe2	down	-2.976
Pros1	down	-2.549	H2-Ab1	down	-2.383
Satb1	down	-1.539	Ttc30a1	down	-1.480
Gm4956	down	-2.608	Klra1	down	-2.228
Ell3	down	-1.683	Gm12112	down	-1.096
Csf3r	down	-3.246	Klra8	down	-2.647
Lrig1	down	-2.131	3110045C21Rik	down	-1.897
Tyrobp	down	-2.604	Gm36949	down	-1.107
Trat1	down	-2.874	Gm44631	down	-2.985
Aqp9	down	-2.889			

**Appendix Table 8.3. DEGs list of genes up or down-regulated in PbT-II Th1 T<sub>RM</sub> cells versus RAS generated PbT-II T<sub>RM</sub> cells from the liver.**

Symbol	Regulation	FoldChange		Symbol	Regulation	FoldChange
Uhrf1	up	2.033		Gpm6b	up	2.218
Angptl2	up	1.677		Mvb12a	up	1.659
Slc30a4	up	2.268		Ccnb2	up	2.083
Stx1a	up	1.852		Car12	up	2.501
Ptprs	up	2.171		Plod2	up	2.640
Csf1	up	3.197		Vipr1	up	2.207
Cinp	up	1.907		Tbc1d4	up	1.802
Ly6c2	up	2.730		AA467197	up	3.617
Qpct	up	2.180		Zdhhc15	up	1.824
Lta	up	2.395		Igsf9b	up	2.374
Psat1	up	2.167		Zc3h12c	up	2.199
Ms4a7	up	2.597		Rnf39	up	2.110
Ms4a4c	up	2.532		Spry1	up	1.847
Stambpl1	up	1.455		Ccdc138	up	1.759
Tjp2	up	2.261		Mrps6	up	1.905
Gsto1	up	2.065		Spsb1	up	2.235
Nrp1	up	1.796		Igsf3	up	2.165
Ctla4	up	2.036		Trim46	up	1.628
Il18r1	up	1.708		Chil5	up	2.628
Pdcd1	up	1.855		Tnfaip8l1	up	1.827
Ifi211	up	2.027		Onecut2	up	2.639
Galnt3	up	2.122		Gpr15	up	3.078
Bcl2l11	up	1.849		Utf1	up	2.572
Slc52a3	up	2.440		Tdrp	up	2.184
Dclk1	up	2.263		Klrc2	up	1.578
Lmna	up	1.923		Atp8b4	up	2.125
Hemgn	up	2.542		Tcrg-V4	up	2.315
Tnfsf8	up	1.808		Tcrg-C2	up	2.964
Mfsd2a	up	2.062		Trgv2	up	2.678
Rcc1	up	1.736		Trdv5	up	2.447
Tnfrsf9	up	2.560		Ly6c1	up	3.565
Rasl11a	up	1.893		Gm11725	up	1.675
Asns	up	2.590		Gm12505	up	2.106

Klrk1	up	2.733	Gm26083	up	2.289
Klrd1	up	2.357	Zfp966	up	1.944
Klrc1	up	2.134	Galnt4	up	1.840
Bcat1	up	2.446	Gm26513	up	1.437
Il4	down	-3.920	C5ar1	down	-1.682
Fcer2a	down	-2.149	Armcx6	down	-1.272
Ccl6	down	-3.022	Mest	down	-2.419
Ccl9	down	-3.598	Pbx1	down	-2.984
Arg2	down	-3.023	S100a8	down	-3.767
Pla2g7	down	-3.543	S100a9	down	-4.492
Cd74	down	-2.080	Fcer1g	down	-2.413
Cd7	down	-2.119	Alox5ap	down	-3.202
Alox5	down	-1.186	H2-Eb1	down	-2.190
F5	down	-3.915	Trerf1	down	-2.038
Ccr9	down	-2.574	Lyz2	down	-3.472
Tyrobp	down	-2.635	Skint3	down	-1.097
Nupr1	down	-1.112	H2-Ab1	down	-2.215
Trat1	down	-1.410	Igkv8-27	down	-2.375
Tlr13	down	-2.331	Igkc	down	-2.493
Cpne7	down	-2.483	Gm12112	down	-1.242
Ttc16	down	-1.656	H2-Q2	down	-2.249
Saa3	down	-2.913	Igkv6-15	down	-2.183
C130050018Rik	down	-2.028	Sirpb1b	down	-3.193
1700001022Rik	down	-1.911	Igkv6-23	down	-3.550
Tifa	down	-3.057	Ighv9-3	down	-2.346
Ccr4	down	-2.304	Igkv4-55	down	-2.656

**Appendix Table 8.4. DEGs list of genes up or down-regulated in PbT-II Th2 T<sub>RM</sub> cells versus RAS generated PbT-II T<sub>RM</sub> cells from the liver.**

Symbol	Regulation	FoldChange	Symbol	Regulation	FoldChange
Pparg	up	2.710	Csgalnact1	up	2.159
Vipr2	up	2.845	Hrh4	up	3.048
Csf1	up	4.852	Plcl1	up	3.429
Serinc3	up	1.167	Tbc1d19	up	2.559

Itgb3	up	1.817		Tex2	up	1.507
Ccl1	up	2.725		D330045A20Rik	up	3.075
Deptor	up	2.618		Trim46	up	1.610
Cpox	up	1.931		Ptgir	up	2.647
Cldnd1	up	2.503		Penk	up	3.726
Lmln	up	2.312		Ankle1	up	2.507
Qpct	up	1.734		Ltb4r1	up	2.928
Il1rl1	up	3.925		Gpr15	up	3.510
Lpcat4	up	2.376		Cysltr1	up	2.739
Kcnq5	up	1.989		Map6	up	2.700
Lrriq3	up	2.117		Khdc1a	up	2.669
Tnfrsf9	up	2.161		B630019A10Rik	up	2.763
Tnfrsf4	up	2.233		Gm5127	up	3.417
Ccdc184	up	2.462		Olfr1224-ps1	up	1.066
Bcat1	up	1.344		Ly6c1	up	2.942
Gpm6b	up	1.398		Ctsf	up	3.401
Rnf128	up	2.596		Gm14233	up	2.862
Vegfc	up	2.807		Zfp966	up	2.684
Olfm2	up	1.071		Gm37309	up	2.873
Car12	up	2.154		Gm36930	up	2.082
Tbc1d4	up	1.973		Gm38228	up	1.747
AA467197	up	1.883		Gm43949	up	1.616
Ankmy1	up	1.774		Gm17745	up	2.826
Ptpn13	up	2.566		RP23-411J14.3	up	1.282
Il5	up	4.005				
Ccl3	down	-2.898		Lat2	down	-2.237
Hck	down	-2.758		Coro2b	down	-2.285
Nkg7	down	-1.530		Rassf4	down	-2.687
Adgre1	down	-1.925		Gzmk	down	-3.135
G0s2	down	-2.170		Flt3	down	-2.521
Cybb	down	-2.917		Unc5cl	down	-2.072
Ncf1	down	-2.183		Clec4a3	down	-1.727
Ikzf3	down	-2.360		C130050O18Rik	down	-2.078
Ccl6	down	-3.167		Slc16a5	down	-1.707
Ccl4	down	-3.287		Baiap3	down	-2.757
Ccl9	down	-4.004		Jaml	down	-3.474
Plek	down	-3.025		Cx3cr1	down	-2.983
Cma1	down	-1.701		Rab7b	down	-2.595

Ttc39c	down	-2.094		Txk	down	-1.667
Cd74	down	-2.188		S100a8	down	-4.326
Cd7	down	-4.108		S100a9	down	-4.610
Alox5	down	-1.191		Fcer1g	down	-2.544
Rassf3	down	-1.722		Alox5ap	down	-2.874
F5	down	-3.921		Adgrg5	down	-1.919
Sell	down	-2.528		Lyz2	down	-2.744
Pkp4	down	-1.679		Rbm44	down	-2.134
Cers6	down	-2.477		H2-Ab1	down	-2.242
Il1b	down	-2.167		Ceacam1	down	-2.693
Csf3r	down	-2.972		Mafb	down	-3.456
Spp1	down	-2.581		Igkc	down	-2.431
Dtx1	down	-1.716		Iglc2	down	-2.320
Clec4a2	down	-3.363		Klra1	down	-2.574
Clec1b	down	-2.305		BC064078	down	-1.568
Plbd1	down	-4.305		Klra8	down	-2.828
Ptpro	down	-2.986		Adh6-ps1	down	-2.147
Slco1b2	down	-2.689		Igkv6-15	down	-2.599
Tyrobp	down	-2.701		Igkv6-25	down	-2.541
Pou2af1	down	-2.478		Sirpb1b	down	-3.636
Eomes	down	-2.588		Igkv4-55	down	-3.292
Tlr13	down	-2.305		6720427I07Rik	down	-2.684
Caskin2	down	-2.805		BE692007	down	-1.367
Ly6d	down	-2.291		1810041H14Rik	down	-1.840
Ccl5	down	-2.210		Gm44066	down	-2.513
Ccdc180	down	-2.883		Gm44631	down	-2.153

**Appendix Table 8.5. DEGs list of genes up or down-regulated in PbT-II Th1 T<sub>RM</sub> cells versus  $\alpha$ Clec9A-DIY generated PbT-II T<sub>RM</sub> cells from the liver.**

Symbol	Regulation	FoldChange		Symbol	Regulation	FoldChange
Cpa3	up	2.081		Aqp9	up	3.528
St8sia6	up	2.040		Ccnb2	up	3.241
Ggt1	up	2.632		Lif	up	1.768

Birc5	up	2.362	Bbs9	up	2.156
Ahr	up	2.725	Hrh4	up	1.417
Lama4	up	2.414	Pclaf	up	2.170
Socs2	up	2.402	E2f8	up	2.984
Aifm2	up	1.959	Ltb4r1	up	3.235
Hmmr	up	2.148	Gpr15	up	2.238
Ccl1	up	4.568	Ccr4	up	2.348
Aurkb	up	2.339	Samd13	up	1.840
Nefl	up	3.007	Enthd1	up	2.323
Ly6c2	up	2.447	Clec12a	up	2.274
Pros1	up	2.043	Ifitm2	up	2.755
Satb1	up	2.372	Zfp600	up	1.345
Anxa1	up	2.428	Spc24	up	1.950
Ms4a4c	up	2.298	Ttc30a1	up	1.045
Gm4956	up	3.134	Ly6c1	up	5.206
Gatm	up	1.474	Klra1	up	1.825
Bcl2l11	up	1.550	Gm13461	up	1.710
Tpx2	up	2.847	Gm15518	up	2.613
Cks1b	up	2.229	Gm20659	up	1.950
Lmna	up	2.481	Hist1h2ap	up	2.457
Hemgn	up	3.097	C230085N15Rik	up	2.365
Stmn1	up	2.321	5830444F18Rik	up	2.615
Klrk1	up	3.460	E430014B02Rik	up	2.562
Klrd1	up	2.349	Gm37248	up	2.455
Klrc1	up	2.050	Gm36931	up	1.045
Trat1	up	1.500	Pde2a	up	2.210
Plag1	down	-1.999	Ttc16	down	-1.610
Timp2	down	-2.423	Foxp3	down	-2.774
Ikzf3	down	-2.067	Tox	down	-2.815
Il1rl1	down	-2.235	Coro2b	down	-3.340
Itga4	down	-1.399	1700001O22Rik	down	-2.338
Lag3	down	-2.121	Olfir527	down	-1.412
Gpr83	down	-1.422	Phactr2	down	-2.011
Ubash3b	down	-1.563	Tigit	down	-2.132
Vax2	down	-1.987	Tox2	down	-2.674

**Appendix Table 8.6. DEGs list of genes up or down-regulated in PbT-II Th2 T<sub>RM</sub> cells versus  $\alpha$ Clec9A-DIY generated PbT-II T<sub>RM</sub> cells from the liver.**

Symbol	Regulation	FoldChange	Symbol	Regulation	FoldChange
Scmh1	up	2.637	Il5	up	3.504
Pparg	up	3.463	Krt80	up	2.100
Gm2a	up	1.704	Hrh4	up	3.856
Il4	up	5.980	Nme1	up	1.415
Cpa3	up	4.717	Cd81	up	2.633
St8sia6	up	1.837	Sesn1	up	1.639
Rcn1	up	1.606	Irs2	up	2.655
Ggt1	up	1.379	Arhgap18	up	1.591
Bmp7	up	3.027	Rbpj	up	1.594
Gata3	up	1.488	Gpr34	up	2.314
Rxra	up	2.791	Bach2	up	2.343
Fcrls	up	3.165	D330045A20Rik	up	3.995
Mmp9	up	2.784	Ptgir	up	4.693
Sept8	up	2.269	Tmem64	up	1.997
Csf2	up	3.404	Sptssa	up	1.455
Scn1b	up	1.884	Penk	up	3.747
Ahr	up	4.470	Ltb4r1	up	4.448
Socs2	up	3.403	Gpr15	up	2.676
Rnf130	up	2.698	Ccr4	up	5.255
Ccl1	up	5.939	Samd13	up	2.717
Gadd45g	up	2.483	Ccr2	up	1.590
Fam213a	up	3.144	Enthd1	up	2.356
Deptor	up	3.447	Ffar2	up	3.745
Cpox	up	1.862	Cysltr1	up	4.591
Cldnd1	up	3.114	Tusc1	up	2.399
Samsn1	up	1.647	Map6	up	2.756
St6gal1	up	3.229	Nfe2	up	2.141
Pros1	up	3.069	Ifitm2	up	3.725
Satb1	up	2.603	Cd200r4	up	1.651
Epas1	up	2.765	Gm22063	up	1.370
Nr3c1	up	1.168	Gm23971	up	2.328
Anxa1	up	3.526	Zfp600	up	1.095
Itih5	up	1.987	Nck2	up	1.779

Gm4956	up	4.325	B630019A10Rik	up	2.876
Atf3	up	1.926	Marcks	up	2.892
Tmem141	up	1.578	Ccdc153	up	2.371
Lpcat4	up	1.980	Trem12	up	2.311
Kcnq5	up	2.385	Gm5127	up	2.721
Ecm1	up	4.195	Olfr1224-ps1	up	1.664
Stmn1	up	1.722	Ttc30a1	up	1.311
Lrig1	up	2.179	Ly6c1	up	4.554
Trat1	up	1.555	Ctsf	up	4.045
Ctrb1	up	1.530	Gm15356	up	1.023
Aqp9	up	4.761	A530032D15Rik	up	2.334
Nedd4	up	1.485	Cd200r2	up	3.125
Ccnb2	up	2.134	Gm20659	up	1.815
Sh3bgrl2	up	2.722	Gm19585	up	1.328
Fam46a	up	1.858	C230085N15Rik	up	2.580
Cyp11a1	up	2.556	5830444F18Rik	up	2.650
Alpk2	up	2.207	E430014B02Rik	up	2.646
Stard9	up	2.003	Gm37248	up	2.623
Pkd2	up	3.243	Gm37357	up	2.049
Cpne7	up	2.041	Gm36949	up	2.135
Arl4d	up	2.134	4732496C06Rik	up	2.345
Ccr3	up	2.316	RP23-394M6.4	up	2.390
Bbs9	up	3.183			
Ccl3	down	-2.942	Adrb1	down	-1.831
S100a4	down	-1.820	Mcoln3	down	-1.987
Angptl2	down	-3.309	Prf1	down	-3.499
Nkg7	down	-2.095	Spry1	down	-3.472
Stx1a	down	-2.165	Themis2	down	-2.601
G0s2	down	-1.761	Smim3	down	-2.620
Mcoln2	down	-2.185	Snx10	down	-2.116
Slamf6	down	-1.982	Trps1	down	-2.347
Ikzf3	down	-3.177	Runx2	down	-1.864
6330403K07Rik	down	-2.065	Etfbkmt	down	-1.556
Dusp14	down	-2.348	Zc3h12d	down	-2.200
Heatr9	down	-2.248	Cdk6	down	-2.167

Ccl4	down	-4.129	Efhd2	down	-1.504
Plek	down	-3.027	Tox	down	-2.680
Nsg2	down	-2.947	Coro2b	down	-3.804
Enpp2	down	-2.658	Gzmk	down	-4.624
Ttc39c	down	-2.165	Lancl3	down	-1.943
Cd7	down	-3.378	Baiap3	down	-3.894
Il18r1	down	-1.882	Jaml	down	-3.512
Pdcd1	down	-2.741	Lax1	down	-1.512
Pkp4	down	-2.561	Txk	down	-2.222
Itga4	down	-2.689	Cyp3a11	down	-2.981
Cers6	down	-2.481	Gm8369	down	-2.370
Creb3l1	down	-2.727	Phactr2	down	-1.693
Il21	down	-3.877	Cst7	down	-1.867
Cd1d1	down	-1.775	Syt11	down	-1.927
Dtx1	down	-2.145	Rbm44	down	-1.684
Osbp13	down	-1.849	Tigit	down	-2.573
Lag3	down	-3.614	Runx2os1	down	-2.837
Plbd1	down	-2.326	Tox2	down	-2.498
Ldhb	down	-2.329	Cerkl	down	-1.660
Ubash3b	down	-1.626	Rab26	down	-2.946
Eomes	down	-4.084	Adh6-ps1	down	-2.745
Hsf4	down	-2.211	6720427I07Rik	down	-3.159
Tagap	down	-1.518	Mirt1	down	-1.894
Caskin2	down	-2.736	BE692007	down	-1.707
Ttyh2	down	-2.447	Gm28942	down	-4.056
Vax2	down	-1.679	Gm17764	down	-3.342
Dpp4	down	-2.041	Gm37004	down	-2.514
Ccl5	down	-2.623	Gm44066	down	-2.302

**Appendix Table 8.7. DEGs list of genes up or down-regulated in PbT-II Th2 T<sub>RM</sub> cells versus PbT-II Th1 T<sub>RM</sub> cells from the liver**

Symbol	Regulation	FoldChange	Symbol	Regulation	FoldChange
Pparg	up	3.725	Ccr3	up	2.566
Il4	up	4.790	Il5	up	3.672
Bmp7	up	2.366	Ppfibp2	up	2.073
Gata3	up	1.610	Socs5	up	1.762
Serinc3	up	1.091	Cd81	up	2.333

Fam213a	up	2.890	Plcl1	up	2.358
Deptor	up	3.595	D330045A20Ri k	up	3.261
Cpox	up	1.712	Ptgir	up	4.882
Cldnd1	up	2.080	Tmem64	up	1.537
Samsn1	up	1.256	Ccr4	up	2.907
Epas1	up	2.638	Ffar2	up	3.792
Pip5k1b	up	3.037	Acvr2a	up	2.260
Il6	up	2.104	Cysltr1	up	3.308
Il1rl1	up	4.097	Lgals7	up	3.112
Ecm1	up	3.315	Cd200r4	up	1.501
Cd38	up	1.254	Olfr527	up	2.872
Ccr9	up	2.201	Gm5127	up	3.959
Alpk2	up	1.647	Ctsf	up	4.267
Myo6	up	1.408	0610040F04Ri k	up	2.714
Ptpn13	up	2.699	BC049352	up	2.321
Cpne7	up	2.755	Gm38228	up	1.598
Myo1d	up	1.957			
Ccl3	down	-1.989	Caskin2	down	-3.010
Nkg7	down	-1.077	Ccl5	down	-1.689
Stx1a	down	-2.520	Ccdc180	down	-2.664
G0s2	down	-1.179	Mcoln3	down	-1.411
Ptprs	down	-1.746	Slc9a7	down	-2.174
Slamf6	down	-2.011	Esm1	down	-1.756
Ncf1	down	-2.399	Gzmk	down	-3.440
6330403K07Ri k	down	-1.783	Onecut2	down	-2.633
Dusp14	down	-1.507	E2f8	down	-3.358
Heatr9	down	-1.953	Lancl3	down	-1.319
Ccl4	down	-3.613	Baiap3	down	-2.219
Nsg2	down	-3.467	Jaml	down	-3.521
Nefl	down	-3.179	Tmem171	down	-2.218
Ly6c2	down	-2.839	Clec12a	down	-2.144
Sidt1	down	-1.793	Gm8369	down	-1.720
Fetub	down	-1.775	Atp8b4	down	-1.922
Ttc39c	down	-1.982	Adgrg5	down	-1.713
Cd6	down	-1.638	4933406P04Ri k	down	-2.447
Doc2g	down	-2.652	Ctcf1	down	-2.311
Cd7	down	-1.986	Rbm44	down	-1.819

Ifi211	down	-2.463	Runx2os1	down	-2.836
Lypd6b	down	-2.119	Selenom	down	-2.379
Pkp4	down	-1.970	Tcrg-V4	down	-2.902
Itga4	down	-1.290	Tcrg-C2	down	-2.237
Creb3l1	down	-2.992	Trgv2	down	-2.300
Smpdl3b	down	-1.835	Gm16602	down	-2.496
Klrk1	down	-2.345	Tcrg-C4	down	-2.674
Clec1b	down	-2.031	Rab26	down	-2.546
Klrd1	down	-3.298	Klra1	down	-2.202
Klrc1	down	-3.517	Stamos	down	-1.153
Plbd1	down	-1.872	Adh6-ps1	down	-2.424
Kcnj8	down	-2.424	Gm20712	down	-2.221
Klrb1c	down	-1.876	4831440E17Ri k	down	-1.683
Plxna3	down	-1.842	Gm26614	down	-2.771
Eomes	down	-2.536	Gm26732	down	-2.098
Tagap	down	-1.767	Gm44066	down	-2.494

2-photon intravital imaging Dataset (Video 8.1 to 8.7) is accessible via <https://doi.org/10.22000/471> (The University of Bonn) or <https://cloudstor.aarnet.edu.au/plus/s/jf7sdvY4nYxpTvn> (The University of Melbourne).

#### **Appendix Video 8.1 Visualisation of PbT-II cells in the liver after $\alpha$ -Clec9A-DIY priming.**

$5 \times 10^4$  PbT-II.uGFP cells were transferred into dtTomato mice one day prior to administration of  $2\mu\text{g}$   $\alpha$ Clec9A-DIY and 5 nmol CpG-combo. 14 days later mice underwent surgical procedure to gain access to the liver and 2 photon-intravital imaging was performed. Video of liver structure (red) and PbT-II cells (green) 14 days post priming. (<https://cloudstor.aarnet.edu.au/plus/s/Rlf43CySI9vPKn9>)

#### **Appendix Video 8.2 Visualisation of PbT-II cells in the liver after $\alpha$ -Clec9A-DIY priming and 24 h post sporozoite infection.**

$5 \times 10^4$  PbT-II.uGFP cells were transferred into dtTomato mice one day prior to administration of  $2\mu\text{g}$   $\alpha$ Clec9A-DIY and 5 nmol CpG-combo. 14 days later mice were challenged with  $1.5 \times 10^4$  spz. 24 post challenge mice underwent surgical procedure to gain access to the liver and 2 photon-intravital imaging was performed. Video of liver structure (red) and PbT-II cells (green) 14 days post priming. (<https://cloudstor.aarnet.edu.au/plus/s/uXVIIIG1geKI7ory>)

**Appendix Video 8.3 Visualisation of PbT-II cells in the liver after  $\alpha$ -Clec9A-DIY priming and 48 h post sporozoite infection.**

$5 \times 10^4$  PbT-II.uGFP cells were transferred into dtTomato mice one day prior to administration of  $2 \mu\text{g}$   $\alpha$ Clec9A-DIY and 5 nmol CpG-combo. 14 days later mice were challenged with  $1.5 \times 10^4$  spz. 48 post challenge mice underwent surgical procedure to gain access to the liver and 2 photon-intravital imaging was performed. Video of liver structure (red) and PbT-II cells (green) 14 days post priming. (<https://cloudstor.aarnet.edu.au/plus/s/XZhmaK8rG1SoMsm>)

**Appendix Video 8.4 Visualisation of gDT-II cells in the liver after  $\alpha$ -Clec9A-D3 priming.**

Mice received  $5 \times 10^4$  gDT-II.uGFP cells and were vaccinated with  $2 \mu\text{g}$   $\alpha$ Clec9A-D3 + 5 nmol CpG. 14 days later mice underwent surgical procedure to gain access to the liver and 2 photon-intravital imaging was performed. Video of liver gDT-II cells (green) 14 days post priming. (<https://cloudstor.aarnet.edu.au/plus/s/tWYOgs1m3TXQLaa>)

**Appendix Video 8.5 Visualisation of gDT-II cells in the liver after  $\alpha$ -Clec9A-D3 priming and 24 h post sporozoite infection.**

Mice received  $5 \times 10^4$  gDT-II.uGFP cells and were vaccinated with  $2 \mu\text{g}$   $\alpha$ Clec9A-D3 + 5 nmol CpG. 14 days later mice were challenged with  $10^4$  spz. 24 post challenge mice underwent surgical procedure to gain access to the liver and 2 photon-intravital imaging was performed. Video of gDT-II cells (green) 14 days post priming. (<https://cloudstor.aarnet.edu.au/plus/s/vkKfoCqImwft6Uf>)

**Appendix Video 8.6 Visualisation of LysM.GFP cells in the liver.**

LysM.GFP mice received  $5 \times 10^4$  PbT-II.ubTomato cells and were vaccinated with  $2 \mu\text{g}$   $\alpha$ Cle9A-DIY + 5 nmol CpG one day later. 14 days later mice underwent surgery to gain access to the liver and 2-photon intravital imaging was performed. (<https://cloudstor.aarnet.edu.au/plus/s/JQwsYZhBBDJiRGc>)

**Appendix Video 8.7 Visualisation of LysM.GFP cells in the liver 24 h post spz challenge.**

LysM.GFP mice received  $5 \times 10^4$  PbT-II.ubTomato cells and were vaccinated with  $2 \mu\text{g}$   $\alpha$ Cle9A-DIY + 5 nmol CpG one day later. 14 days later mice were challenged with  $10^4$  sporozoites. 24 h later mice underwent surgery to gain access to the liver and 2-photon intravital imaging was performed. (<https://cloudstor.aarnet.edu.au/plus/s/xwMtlS83aOJEgIZ>)